UNIVERSIDADE FEDERAL DE MINAS GERAIS
Escola de Engenharia
Programa de Pós-Graduação em Engenharia Elétrica

Iury Valente de Bessa

RECONFIGURATION BLOCKS FOR FAULT-TOLERANT CONTROL OF NONLINEAR SYSTEMS

Belo Horizonte
2022

Iury Valente de Bessa

RECONFIGURATION BLOCKS FOR FAULT-TOLERANT CONTROL OF NONLINEAR SYSTEMS

A thesis presented to the Graduate Program in Electrical Engineering (PPGEE) of the Federal Univesity of Minas Gerais (UFMG) in partial fullfillment of the requirements to obtain the degree of Doctor in Electrical Engineering.

Supervisor: Reinaldo Martínez Palhares

Belo Horizonte
2022

Bessa, Iury Valente de.
B557r Reconfiguration blocks for fault-tolerant control of nonlinear systems [recurso eletrônico] / Iury Valente de Bessa. - 2022.
1 recurso online (214 f. : il., color.) : pdf.

Orientador: Reinaldo Martinez Palhares.

Tese (doutorado) - Universidade Federal de Minas Gerais, Escola de Engenharia.

Bibliografia: f. 182-214.
Exigências do sistema: Adobe Acrobat Reader.

1. Engenharia elétrica - Teses. 2. Falha de sistema (Engenharia) - Teses. 3. Desigualdades matriciais lineares - Teses. 4. Sistemas não lineares - Teses. I. Palhares, Reinaldo Martinez. II. Universidade Federal de Minas Gerais. Escola de Engenharia. III. Título.

CDU: 621.3(043)

Ficha catalográfica elaborada pela Bibliotecária Roseli Alves de Oliveira CRB/6 2121
Biblioteca Prof. Mário Werneck, Escola de Engenharia da UFMG

UNIVERSIDADE FEDERAL DE MINAS GERAIS
ESCOLA DE ENGENHARIA
COLEGIADO DO CURSO DE PÓS-GRADUAÇÃO EM ENGENHARIA ELÉTRICA

FOLHA DE APROVAÇÃO

"Reconfiguration Blocks for Fault-tolerant Control of Nonlinear Systems"

IURY VALENTE DE BESSA

Tese de Doutorado defendida e aprovada, no dia 01 de junho de 2022, pela Banca Examinadora designada pelo Colegiado do Programa de Pós-Graduação Engenharia Elétrica da Universidade Federal de Minas Gerais constituída pelos seguintes professores:

Prof. Dr. Alexandre Sanfelice Bazanella (UFRGS)

Prof. Dr. Diego de Sousa Madeira (UFC)

Prof. Dr. Marcelo Carvalho Minhoto Teixeira (UNESP/IS)

Prof. Dr. Roberto Kawakami Harrop Galvão (ITA)

Prof. Dr. Tiago Roux de Oliveira (UERJ)

Prof. Dr. Reinaldo Martínez Palhares (DELT (UFMG)) - Orientador

Belo Horizonte, 1o. de junho 2022.

Documento assinado eletronicamente por **Reinaldo Martinez Palhares**, **Professor do Magistério Superior**, em 01/06/2022, às 18:17, conforme horário oficial de Brasília, com fundamento no art. 5º do Decreto nº 10.543, de 13 de novembro de 2020.

A autenticidade deste documento pode ser conferida no site https://sei.ufmg.br/sei/controlador_externo.php?acao=documento_conferir&id_orgao_acesso_externo=0, informando o código verificador **1494801** e o código CRC **916C4997**.

Referência: Processo nº 23072.231649/2022-46 SEI nº 1494801

TESE DE DOUTORADO Nº 397

RECONFIGURATION BLOCKS FOR FAULT-TOLERANT CONTROL OF NONLINEAR SYSTEMS

Iury Valente de Bessa

DATA DA DEFESA: 01/06/2022

To my beloved wife Danielli.

AGRADECIMENTOS

Foremost, I would like to express my sincere gratitude to my advisor Professor Reinaldo Martínez Palhares for the broadest support dedicated throughout these years in addition to everything I could learn from him. I would to thank him for the opportunity of being part of his team since my master's course. He provided me with a fruitful environment for developing ideas and research and was fully available with the best ideas whenever things got more complicated. I would also like to thank him for every discussion, advice, and instruction during this time. His words and actions will always be guidelines in my professional career.

Besides my thesis advisor, I would like to greatly thank Professor Vicenç Puig Cayuela who received me with great attention, availability, patience, and solicitude in the doctoral internship I did at the Universitat Politècnica de Catalunya. Even before the internship, he collaborated with us helping to build the results of this thesis, sharing his experience and diverse teachings and advice. Although it was never formally agreed, in every way, he played the role of co-supervisor for this thesis, and I am convinced I could not have had a better co-advisor. I also express my gratitude to other members of the SAC (Sistemes Avançats de Control) group, including Boutrous Khoury and Carlos Trapiello, that made my experience in this doctoral internship more pleasant and profitable.

I would also like to thank two people who have always inspired me to become a better professional and researcher: João Edgar Chaves Filho and Lucas Carvalho Cordeiro. Together with professors Reinaldo and Vicenç, two have certainly helped in my professional development and are also people I look up to as I climb new steps.

I reserve a special thanks to my fellow labmates in D!FCOM. I could never be surrounded by such a brilliant and special team anywhere else. With this team, I learned a lot and I hope to continue learning. In particular, I would like to thank my friends Pedro Henrique, Murilo, Luiz, Márcia, and Rodrigo who helped make the doctoral experience easier. I extend my thanks to the PPGEE/UFMG's professors that helped me in this graduation, in particular, to Professor Leonardo Torres, with whom I learned a lot.

I would like to thank my family: my wife Danielli, who always inspired me with her willingness in making me take the correct way, for her patience, care, and company; my parents, who always taught me the importance of my education and qualification, for which they made many sacrifices; Solange and Raimundo for the support they always gave us; my brother Isaías for the partnership and collaboration with some thesis' results; and my sisters Isabela and Irla.

I would also like to thank my colleagues from the Department of Electricity, which guaranteed the institutional support of my doctoral studies. In particular, I would like to thank Renan, Florindo, and Luiz Eduardo for their support and friendship.

My sincere thanks to my thesis committee which provided valuable comments to improve this document. Last but not the least, I would like to thank all the agencies and institutions that supported my doctoral studies, in particular, the agencies FAPEAM, CAPES, UFAM, and CNPq which directly financed the doctoral studies.

"Faz escuro mas eu canto,
porque a manhã vai chegar.
Vem ver comigo, companheiro,
a cor do mundo mudar.
Vale a pena não dormir para esperar
a cor do mundo mudar."

(Thiago de Mello)

RESUMO

Os processos industriais estão se tornando cada vez mais autônomos e complexos. Consequentemente, a demanda por segurança e confiabilidade desses processos é crescente. Nesse contexto, técnicas de controle tolerante a falhas (FTC, do inglês *Fault-Tolerant Control*) têm recebido bastante atenção ao longo das últimas décadas buscando fornecer redundância analítica e aumentar a confiabilidade desses sistemas. Esta tese aborda o problema de FTC para sistemas não-lineares baseado na abordagem de ocultação de falhas. A ocultação de falhas consiste na inserção de um bloco de reconfiguração (RB, do inglês *Reconfiguration Block*) entre a planta com falhas e o controlador. O RB mitiga os efeitos das falhas sem exigir reprojeto do controlador, do qual as falhas são ocultadas. Embora eficazes, a maioria das abordagens de ocultação de falhas na literatura não cobrem todas as classes de sistemas não-lineares, além de serem sensíveis a imprecisões na estimativa das falhas devido à dependência das estruturas canônicas de RB, conhecidas como sensores e atuadores virtuais, em relação ao princípio do modelo interno. Nesse sentido, esta tese aborda a ocultação de falhas para sistemas não-lineares baseada em novos RBs cujos parâmetros não dependem explicitamente do modelo de falhas. Para tal, condições suficientes baseadas em desigualdades matriciais lineares (LMIs, do inglês *Linear Matrix Inequalities*) são apresentadas para o projeto de RBs que garantam a recuperação da estabilidade. Para obter essas condições, três novas classes de abordagens são propostas, a saber: uma abordagem baseada em Lyapunov em que uma função de Lyapunov é obtida em uma etapa de análise do sistema nominal e, em seguida, é usada para projetar os RBs para recuperação de estabilidade do sistema reconfigurado em uma etapa de síntese; uma abordagem baseada em dissipatividade na qual as desigualdades de dissipação são obtidas em uma etapa de análise para o sistema nominal e, em seguida, são usadas para projetar os RBs para recuperação de dissipatividade do sistema reconfigurado em uma etapa de síntese; finalmente, uma abordagem baseada em passivação é proposta para obter RBs cuja dissipatividade compensem a falta de passividade devido à ocorrência de falhas.

Palavras-chave: Controle tolerante a falhas. Ocultação de falhas. Sistemas não-lineares. Desigualdades matriciais lineares. Inclusões diferenciais politópicas. Teoria da dissipatividade. Passivação.

ABSTRACT

Industrial processes and technological systems are becoming more and more autonomous and complex. Consequently, the demand for the safety and reliability of these systems is increasing. In this context, process monitoring and fault-tolerant control (FTC) have received a lot of attention during the last decades to provide analytical redundancy to these processes and improve their reliability. This thesis addresses the problem of FTC for nonlinear systems based on the fault hiding approach. Fault hiding consists in inserting a reconfiguration block (RB) between the faulty plant and the controller. The RB mitigates the fault effects by dispensing with the controller redesign, through recovering sensor measurements and reallocation of the control effort required by a controller that does not receive the information about the fault occurrence. Although effective, most of the fault hiding approaches available in the literature do not cover all classes of nonlinear systems, and they are sensitive to fault estimation inaccuracy because the canonical RB structures, known as virtual sensors and actuators, rely on the internal model principle. In this sense, this thesis addresses the problem of fault hiding for nonlinear systems based on novel RB structures whose parameters do not exhibit explicit dependence on the fault model. This thesis presents a novel constructive design with sufficient conditions based on linear matrix inequalities (LMIs) for guaranteeing stability recovery by fault hiding. For obtaining those conditions, three novel classes of approaches are proposed, namely: a Lyapunov-based approach wherein a Lyapunov function is obtained in a stability analysis step for the nominal system, then it is used to design the RBs for stability recovery of the reconfigured system in a synthesis step; a dissipativity based approach wherein dissipation inequalities are obtained in an analysis step for the nominal system, then they are used to design the RBs for dissipativity recovery of the reconfigured system in a synthesis step; finally, a passivation-based fault hiding approach is proposed to compute RBs with dissipativity properties which compensate for the lack of passivity of the closed-loop system due to the fault occurrence.

Keywords: Fault-tolerant control. Fault hiding. Nonlinear system. Linear matrix inequalities. Polytopic differential inclusions. Dissipativity theory. Passivation.

LIST OF FIGURES

LIST OF TABLES

LIST OF ABBREVIATIONS

FTC	Fault-tolerant control
AFTC	Active Fault Tolerant Control
PFTC	Passive Fault Tolerant Control
FDI	Fault Diagnosis and Isolation
VS	Virtual Sensor
VA	Virtual Actuator
T-S fuzzy	Takagi-Sugeno fuzzy
NT-S fuzzy model	Takagi-Sugeno fuzzy model with nonlinear consequent
LPV	Linear Parameter-varying
LMI	Linear Matrix Inequality
PWA	Piecewise Affine
KYP Lemma	Kalman-Yakubovich-Popov Lemma
RB	Reconfiguration Block
SRB	Static Reconfiguration Block
DRB	Dynamic Reconfiguration Block
TSRB	Takagi-Sugeno Fuzzy Reconfiguration Block
LSM	Least Squares Method
LSS	Large-Scale System
MPC	Model Predictive Control
MAS	Multi-Agent System
NCS	Networked Control System
SVS	Static Virtual Sensor
DVS	Dynamic Virtual Sensor
SVA	Static Virtual Actuator

DVA Dynamic Virtual Actuator

PB Passivation Block

DPB Dynamic Passivation Block

OF-PDC Output Feedback Parallel Distributed Compensator

MSIF Multisensor Integration and Fusion

SAFEPROCESS Symposium on Fault Detection, Supervision and Safety for Technical Processes

LTI Linear Time-invariant

ISS Input-to-State Stability

PI Proportional-Integral

MISO Multiple-Input Single-Output

UIO Unknown Input Observer

CPL Constant Power Load

ETC Event-triggered Control

PHM Prognostic and Health Maintanence

SOF Static Output-Feedback

ZSD Zero-State Detectable

IF-OFP Input Feedforward Output Feedback Passive

OFP Output Feedback Passive

IFP Input Feedforward Passive

VSP Very Strictly Passive

CONTENTS

1 INTRODUCTION

1.1 Fault Tolerant Control

Faults, failures and malfunctions are unavoidable in modern technical processes, although their increasing autonomy and complexity require higher levels of safety, reliability and availability. In this context, process monitoring [1, 2, 3, 4, 5, 6] and FTC [7, 8, 9, 10] have been receiving a lot of attention during the last decades in order to provide analytical redundancy to these processes and consequently improve their reliability. The fault occurrence in these modern technological processes particularly entails higher costs due to growing resilience requirements and increased processes complexity. FTC aims to ensure the maintenance of stability and required performance of closed-loop control systems overcoming their complexities and improving the reliability and availability of these processes. However, FTC techniques try to find the trade-off between stability and performance recovery conditions usually based on complex and imperfect models dealing with the computational costs demanded by these solutions.

Indeed the increasing of profits and productivity of industrial processes is usually achieved by means of actions to improve the reliability, availability, and maintainability of these processes. On the other hand, the safety and security issues are also indispensable properties to the new technological processes although they might be conflicting with respect to profitability and reliability, under penalty of severe legal and social sanctions in the case of violations.

The application of FDI and fault prognostics techniques aims to improve the reliability, safety and availability by generating alarms about the fault occurrences and the remaining useful life of the process parts. However, even when one relies on diagnosing and predicting failures, the process may remain out of operation while a maintenance task is not finished and, in some scenarios, such maintenance is simply impossible. In this sense, FTC systems require physical and analytical redundancy to maintain the safe operation of processes despite the fault occurrence, also improving their availability.

The origin and popularization of process supervision and FTC evidence their

complementarity: nuclear and chemical accidents motivated the early researches on process supervision and FDI; and aircraft accidents motivated the development of fault tolerance strategies; certainly, the early fault detection could avoid some of the chemical and nuclear disasters, but it would not be enough to avoid an flight disaster after a fault detection on air, in this case, FTC solutions are important to ensure the safety until some maintenance action can be done.

FTC techniques can be divided into two main groups, namely PFTC [11, 12] and AFTC [13, 14]. PFTC usually handles the fault occurrence as an unknown disturbance that must be rejected by the nominal controller to maintain acceptable operation. In this sense, the PFTC consists in designing a controller that is robust with respect to the fault occurrence, without changing the control law or the loop due to the fault detection. The inherent simplicity of PFTC systems makes them a common component in the most practical applications, however, they are conservative solutions that often produce poor performance even for the nominal operation [10]. Otherwise, the AFTC performs modifications on the control law or the loop after an estimation of the fault magnitude and its location provided by an imperative FDI module. There are three main classes of AFTC techniques: the fault accommodation [15] that adapts the controller parameters based on the fault estimation and without changing the control loop; the control reconfiguration [16] that modifies the control loop after a fault detection by redesigning a novel controller that deals only with the healthy part of the system; and the fault hiding [17, 18] that modifies the control loop by inserting a RB between the faulty plant and the nominal controller (which remains unaltered).

The overview of PFTC operation is depicted in Figure 1.1. In Figure 1.1a, the nominal closed-loop system is depicted with a nominal controller Σ_{C} connected to the healthy (nominal) plant Σ_{P}. Such controller computes the control signal to drive some of the m actuators based on some of the p sensors. In Figure 1.1b, a fault occurs affecting (red-colored) actuators and sensors. Notice that no further fault detection or management action is required in the PFTC strategy, since there are no modifications on the control loop neither on the nominal controller after the fault occurrence. This is so because the PFTC design methodologies are used to synthesize a Σ_{C} that must be able to maintain the control requirements for every faulty scenario. Obviously, the more fault scenarios are considered to design Σ_{C}, the more conservative

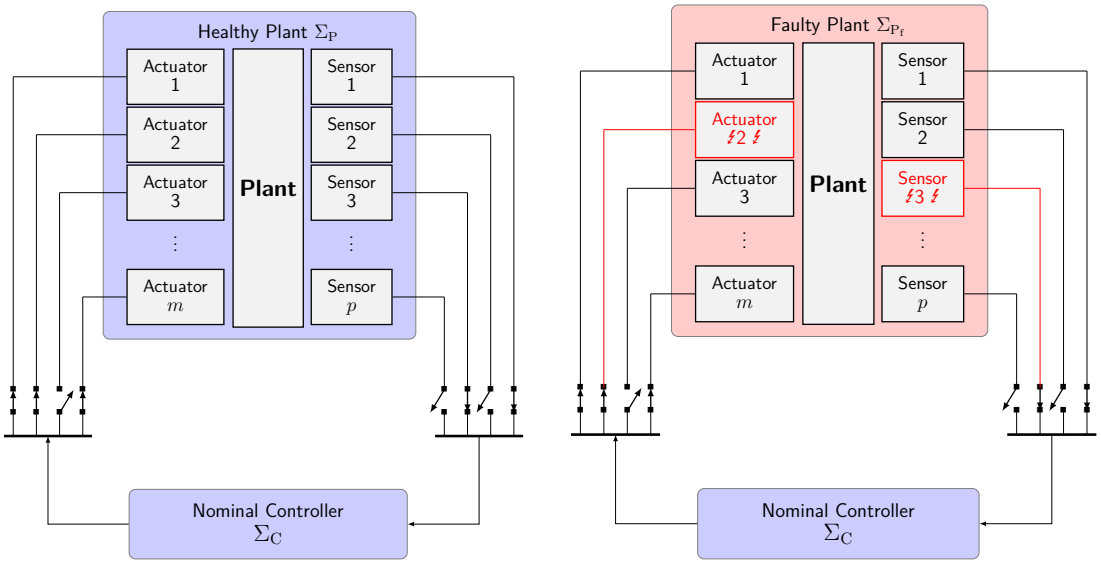

(a) Nominal (fault-free) closed-loop system. **(b)** Faulty closed-loop system with PFTC.

Figure 1.1 – The scheme of a PFTC strategy.

are the conditions for obtaining it, and consequently, they may become infeasible or the closed-loop performance can be severely degraded.

Thus, the AFTC strategies are proposed to provide stability guarantees and some performance recovery after the fault occurrence. Naturally, some conditions must be met to allow the success of the AFTC goals. For example, if one requires stability recovery, it is still necessary that the faulty system maintains the stabilizability despite of the operation under faulty conditions. Similarly, it is not possible find a modified control loop or design a novel controller if the controlability is lost due to actuators fault, and some measurements cannot be substituted or estimated after sensor faults if the observability and detectability is affected. Moreover, the exact performance recovery after the fault occurrence is unlikely, except if significant physical redundancy is available. However, it is usual to weaken the performance requirements after a fault. In this sense, although the expression performance recovery is used sometimes in this text, it usually does not denote the exact performance recovery, i.e., the post-fault performance requirements are usually weaker than the nominal performance requirements.

An overview of the three AFTC strategies are illustrated in Figure 1.2. Differently from PFTC in Figure 1.1b, every AFTC strategy requires an FDI system for providing

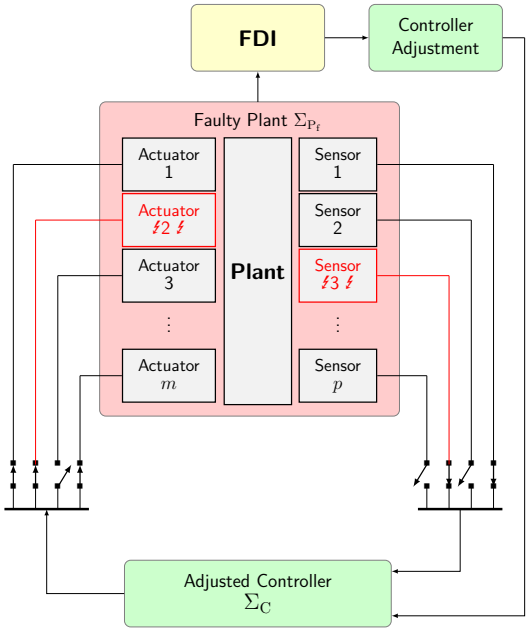

(a) AFTC scheme with fault accommodation.

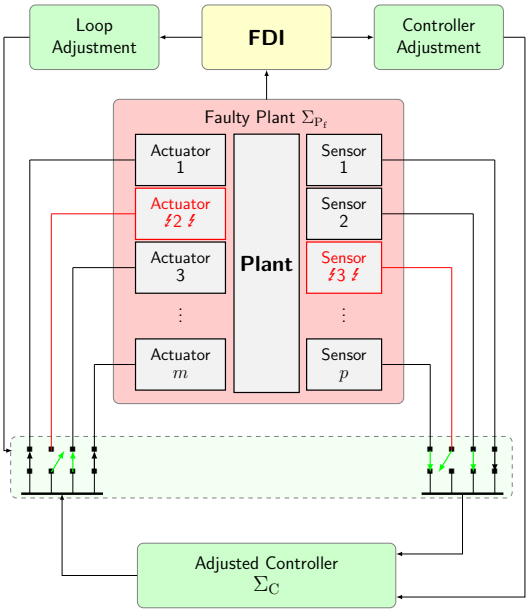

(b) AFTC scheme with control reconfiguration.

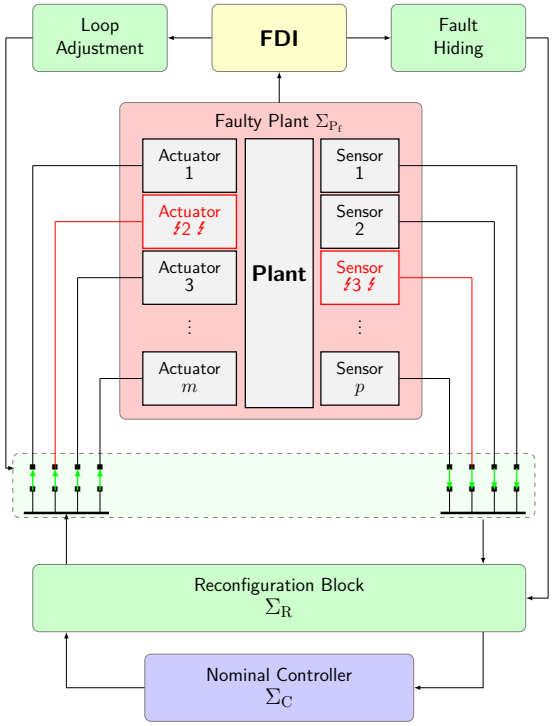

(c) AFTC scheme with fault hiding.

Figure 1.2 – AFTC strategies.

fault localization and estimation, which accuracy and readiness are key issues in achieving effective fault management procedures. In Figure 1.2a, an overview of fault accommodation strategy is depicted. In this case, the FDI system supervises the faulty plant $\Sigma_{\mathrm{P_f}}$ and provides the fault estimate and location for a controller redesign procedure to achieve an adjusted controller Σ_{C}. The adjusted controller Σ_{C} is able to recover the closed-loop system properties (e.g., stability and performance) by using the same group of actuators and sensors (including the faulty ones), i.e., without performing loop changes. Although, the fault accommodation allows to re-design a controller that recovers the required performance, it still produces conservative solutions since it does not take advantage of all the available redundancy related to maintaining the loop configuration.

In this sense, the control reconfiguration approach allows to re-design the controller for a reconfigured loop that explore all the (physical and analytical) redundancy. The control reconfiguration paradigm is illustrated in Figure 1.2b. As in fault accommodation, the control reconfiguration also requires the information from the FDI system, but the fault management is not performed by using the same actuators and sensors used before the fault occurrence. In this case, it is performed a loop adjustment for including the remaining actuators and sensors that are healthy, and then a different controller is designed for the novel control loop. Although effective, the control reconfiguration is too invasive since the controller and the control loop must be changed at every different status indicated by the FDI system.

The fault hiding approach allows to reconfigure the control and sensor signals that drive the plant actuators and the nominal controller, and also to explore the whole sensor and actuator redundancy without maintaining the nominal (fault ignorant) controller. On the one hand, the fault hiding procedure can be seen as a control adjustments (as in the fault accommodation case), wherein the reconfigured controller, i.e. the combination of the nominal controller with the RB, has a fixed part (nominal controller) and an adjustable part (reconfiguration block) which is designed to compensate for the fault effects by using the available redundancy. On the other hand, this approach provides minimum-invasive changes since all the control and sensor signals and loop changes are virtually performed by modifying the gains of a third subsystem, denominated RB, which is inserted between $\Sigma_{\mathrm{P_f}}$ and Σ_{C}. Figure 1.2c provides an overview about the fault hiding

based AFTC. Most of the fault hiding approaches described in the literature are based on the RBs known as Virtual Actuators (VAs) and Virtual Sensors (VSs) for dealing with actuator and sensor faults, respectively. Those blocks, the VAs and VSs, are based on the internal model principle, i.e., the blocks' parameters are based on the plant's nominal and faulty models. Although the internal model principle is convenient to guarantee the recovery after the reconfiguration by finding gains which ensure the stabilization of dynamics of the errors between the blocks and nominal plant dynamics, those blocks become too dependent on the accuracy of the plant models and the FDI systems. Moreover, the extension of the fault hiding approaches based on the traditional VAs and VSs to general classes of nonlinear systems is also challenging. In this sense, novel RBs structures and effective design techniques for fault hiding of nonlinear systems are welcome.

1.2 Thesis Overview

This thesis tackles the problem of stability and dissipativity recovery by fault hiding for nonlinear systems. In particular, this thesis aims to propose novel RBs structures without using the internal model principle, and to obtain constructive design conditions for those RBs. The proposed solutions are divided into two complementary classes: the first class uses polytopic differential inclusions, such as T-S fuzzy models, for representing nonlinear systems and design RBs based on those models; and the second class consists of novel design methodologies for RBs based on dissipativity theory. Figure 1.3 summarizes the novel blocks and design methods for fault hiding of nonlinear systems that are presented in this thesis.

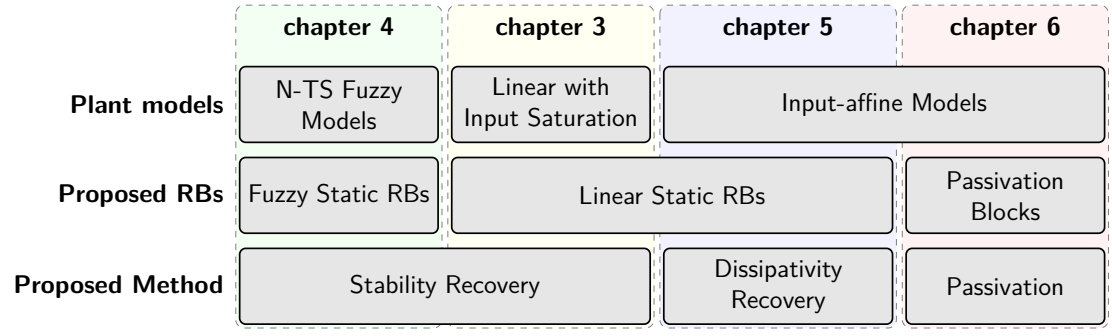

Figure 1.3 – Overview of the thesis content.

The following novel RBs are presented in this thesis: a static RB structure is presented in chapter 3 for fault hiding of linear systems with input saturation; a fuzzy version of that static RBs is presented in chapter 4; and the static and dynamic Passivation Blocks (PBs) are presented in chapter 6 for fault hiding. All those novel RB structures are able to deal with both sensor and actuator faults and their parameters do not include any parameter from the plant faulty model. To design those blocks for fault hiding purpose, novel design techniques are also presented in this thesis. A two-steps stability recovery by fault hiding methodology is proposed and used for LTI, linear with input saturation, T-S fuzzy, and distributed T-S fuzzy models in chapter 3 and chapter 4. That methodology is based on Lyapunov theory that proves the stability of the nominal system and also designs RBs that guarantee that the reconfigured system is stable using the same Lyapunov function. To deal with the nonlinear systems, we take advantage of the properties of differential polytopic inclusions, such as that obtained by using T-S fuzzy and sector nonlinearity methods, to obtain LMI-based sufficient conditions for stability recovery by fault hiding according to that methodology.

A similar idea is used for dissipativity recovery of input-affine systems in chapter 5, wherein storage and supply rate functions are obtained for the nominal system and used to design blocks that guarantee the same dissipation property. Finally, a passivation-based fault hiding approach for input-affine systems is presented in chapter 6. In this case, the RBs are designed to guarantee that the reconfigured system exhibits some desired dissipation property. In this case, only the passivity indices of the faulty plant and the controller are required to design the RBs, which is an additional step towards the independence on the accurate fault models. The design method provided in this thesis are achieved by means of constructive LMI-based conditions.

1.3 Objectives and scope

1.3.1 Objectives

The main objective of this thesis is to develop novel fault hiding strategies for nonlinear systems using RBs structures that do not depend on the faulty system parameters. In short, this thesis proposal aims to:

a) develop novel RB suitable for fault hiding of nonlinear systems whose struc-

tures do not depend on the faulty system parameters;

b) provide constructive LMI-based conditions to design RBs for fault hiding of nonlinear systems;

c) develop dissipativity-based methods for fault hiding of nonlinear systems;

d) formulate the problem of stability recovery by fault hiding as a passivation problem such that the RBs are designed to guarantee the desired dissipation behavior of the reconfigured system.

1.3.2 Scope of this thesis

The fault hiding of nonlinear system is a very broad topic that this thesis does not intend to exhaust. Thus this subsection aims at specify the scope of this thesis. Different fault hiding problems are proposed in the literature, for example, the stability recovery, setpoint tracking recovery and performance recovery. This thesis addresses only the problem of asymptotic stability recovery by fault hiding. Moreover, the results provided in this thesis cover multiplicative faults whose parameters are assumed to be accurately and timely known.

Regarding the guarantees for nonlinear systems, the classes of nonlinear systems supported by the methodologies presented in this thesis can be generically represented as follows

$$\Sigma : \begin{cases} \dot{\boldsymbol{x}}(t) = \boldsymbol{f}\left(\boldsymbol{x}(t)\right) + \boldsymbol{g}\left(\boldsymbol{x}(t), \boldsymbol{u}(t)\right), \\ \boldsymbol{y}(t) = \boldsymbol{h}\left(\boldsymbol{x}(t)\right) + \boldsymbol{j}\left(\boldsymbol{x}(t), \boldsymbol{u}(t)\right), \end{cases} \tag{1.1}$$

where $\boldsymbol{x}(t) \in \mathbb{R}^n$, $\boldsymbol{u}(t) \in \mathbb{R}^m$, and $\boldsymbol{y}(t) \in \mathbb{R}^m$ are, respectively, the state, input and output vectors, $t \in \mathbb{R}_{\geq 0}$, and the maps $\boldsymbol{f}$, $\boldsymbol{g}$, $\boldsymbol{h}$, and $\boldsymbol{j}$ are sufficiently smooth, i.e., for any $x\left(t_0\right)$, $t_0 \in \mathbb{R}_{\geq 0}$, and admissible $\boldsymbol{u}(t)$, the solutions of Σ satisfies to existence and uniqueness conditions for all $t \geq t_0$ and $\boldsymbol{y}(t)$ is locally integrable. Furthermore, $\boldsymbol{f}(0) = 0$ and $\boldsymbol{h}(0) = 0$. Moreover, Σ is ZSD [19].

The formulation in (1.1) includes a broad class of systems with different nonlinearities, e.g., polynomials, saturation, and dead zone. However, it is not able to cover some nonlinear phenomena, for example, finite escape time cannot be addressed by the results of this thesis. In particular, the methodologies presented in chapter 3 and chapter 4 are applied to LTI, input saturating, and Takagi-Sugeno fuzzy mod-

els with nonlinear consequent (NT-S fuzzy models) based on the sector-nonlinearity method [20, 21] which allows to build polytopic differential inclusions to represent Σ (cf. (1.1)) if the nonlinear maps are sufficiently smooth. In fact, the general ideas behind those methodologies could be applied to any nonlinear system like (1.1) through local exact representation of it by polytopic differential inclusions, which include but is not limited to LPV, differential-algebraic, and Takagi-Sugeno fuzzys (T-S fuzzys). One may notice that the guarantees become only locally valid if the polytopic differential inclusions are able to represent (1.1) only within a compact set. However, this issue will not be discussed in this thesis.

Regarding the methodologies presented in chapter 5 and chapter 6 are based on dissipativity theory whose concepts are suitable for nonlinear systems represented by the formulation in (1.1). However, those approaches require the obtaining of valid supply rates related to their dissipativity properties, which can be challenging for some nonlinear systems. Moreover, the computationally efficient methods for obtaining supply rates, e.g., using sum-of-squares programming, produce only local dissipativity results. In this case, the validity of the guarantees will be also local.

1.4 Thesis Outline

The thesis' organization and contributions, in each chapter, are:

a) chapter 2 provides a detailed revision on the origin and applications of RBs, the fault hiding approach, the main RB design methodologies and the open challenges related to fault hiding and RBs. Although it can be an informative reading to find out more details on the fault hiding approach, which is the focus of this thesis, that chapter can be skipped if the reader feels comfortable about the subject.

b) chapter 3 presents the proposed static RB structure and describes a general methodology to design that block by inducing the stability recovery based on the same Lyapunov function obtained by analyzing the nominal closed-loop system stability. In particular, this chapter provides LMI-based sufficient conditions for stability recovery by fault hiding of linear systems with input saturation.

c) chapter 4 extends the approach of chapter 3 to NT-S fuzzy model. For this purpose, fuzzy static RBs are proposed and LMI-based conditions are provided to design them. Moreover, it is considered the problem of fault hiding for distributed nonlinear plants by using both centralized and distributed RBs.

d) chapter 5 uses the SRB presented in chapter 2 and establishes the relation between the traditional stability recovery by fault hiding problem, already addressed in the literature and in chapter 2 and chapter 3, and the dissipativity recovery by fault hiding defined in that chapter. Then the dissipativity-based stability recovery by fault hiding is achieved for nonlinear system without requiring polytopic differential inclusions as used in chapter 2 and chapter 3. For linear systems, LMI-based constructive conditions are presented to design the SRB and guarantee the stability, passivity, and dissipativity after a fault occurrence.

e) chapter 6 presents a passivation-based fault hiding approach for nonlinear systems based on a novel dynamic RB structure named as PB. It is shown that the proposed PB generalizes the canonical RBs, i.e., VSs and VAs, and it can be used for both sensor and actuator faults simultaneously. It does not require the knowledge on the system and controller models. The LMI-based design condition only requires the knowledge on the passivity indices of the faulty system and controller to guarantee the passivation based stability recovery by fault hiding.

f) chapter 7 draws the main conclusions of this work and indicates further research directions.

1.5 Notations

The math variables adopted in this paper are written as lower case bold letters ($\boldsymbol{v}$) to denote vectors or matrix-valued functions, capital bold letters ($\boldsymbol{V}$) to denote matrices, non-bold letters (v or V) to denote scalars or scalar-valued functions, script capital letters ($\mathscr{V}$) to denote spaces or set-valued functions.

$\mathbb{N}$ denotes the set of natural numbers and $\mathbb{N}_{\leq m}$ is the set of natural numbers less than or equal to m; $\mathbb{R}^n$ and $\mathbb{R}_{\geq 0}$ denote respectively the Euclidean space of

n-dimensional real numbers and non-negative real numbers. $\mathscr{L}_1^{\mathrm{loc}}$ denotes the space of locally integrable signals. $\mathbb{R}^{m\times n}$ is the set of all $m \times n$ real matrices.

$\boldsymbol{I}_n$ and $\mathbf{0}_{n\times m}$ denote, respectively, the n-th order identity matrix and the null matrix of order $n \times m$, however, if the dimensions of both identity and null matrices are straightforwardly deduced, they are omitted. For a vector $\boldsymbol{v} \in \mathbb{R}^n$, $\|\boldsymbol{v}\|_2$ denotes its 2-norm, and $\boldsymbol{v}_{(l)}$ denotes the l-th entry of $\boldsymbol{v}$ with $l \in \mathbb{N}_{\leq n}$. For a matrix $\boldsymbol{V}$, $\boldsymbol{V} \succ (\prec)\, 0$ means that $\boldsymbol{V}$ is a positive (negative) definite matrix; $\boldsymbol{V}^\top$ is its transpose; $\boldsymbol{V}^\dagger$ is its Moore–Penrose pseudoinverse; ; $\mathrm{He}\{\boldsymbol{V}\}$ denotes $\mathrm{He}\{\boldsymbol{V}\} = \boldsymbol{V} + \boldsymbol{V}^\top$. For a matrix $\boldsymbol{V} \in \mathbb{R}^{m\times n}$, $\|\boldsymbol{V}\|_2$ denotes the induced matrix 2-norm of $\boldsymbol{V}$, and $\boldsymbol{V}_{(l)}$ denotes the l-th line of $\boldsymbol{V}$ with $l \in \mathbb{N}_{\leq n}$. The notation $\boldsymbol{V} \in \mathrm{Co}\{\boldsymbol{V}_1, \ldots, \boldsymbol{V}_{n_v}\}$ means that there exists a set of n_v scalars $\{\theta_1, \ldots, \theta_{n_v}\} \subset \mathbb{R}_{\geq 0}$ such that

$$\sum_{i=1}^{n_v} \theta_i = 1, \qquad \boldsymbol{V} = \sum_{i=1}^{n_v} \theta_i \boldsymbol{V}_i.$$

In a symmetric block matrix, '$\star$' is the term deduced by symmetry; $\mathrm{diag}\{\boldsymbol{d}_1, \ldots, \boldsymbol{d}_n\}$ is a diagonal matrix with the elements/blocks $d_1, \ldots, d_n$ in the main diagonal. The notation $(\Sigma_1, \ldots, \Sigma_n)$ represents the system obtained through the interconnection of the subsystems Σ_1, Σ_2, ..., and Σ_n.

2 RECONFIGURATION BLOCKS AND FAULT HIDING: DESIGN, APPLICATIONS, AND CHALLENGES

This chapter presents a review of the fault hiding approach and RBs. The review aims to provide a historic perspective to understand the roots and key milestones of fault hiding advances and their applications. Moreover, it presents the main RBs which have been proposed to solve the fault hiding approach. Finally, the review indicates open challenges and emerging applications for RBs, which can be also out of the FTC scope. The remainder of this chapter is organized as follows: section 2.1 presents the philosophy behind the use of RBs and the origins of the fault hiding approach; section 2.2 presents the fault hiding problem; section 2.3 discusses the main milestones of the fault hiding advances; section 2.4 describes the main structures for RBs; section 2.5 provides an overview on the design methodologies for RBs found in literature; and section 2.6 presents the main applications for RBs in the literature.

2.1 Philosophy of Reconfiguration Blocks

The general concept of using RBs is the possibility of achieving control objectives without modifying a controller which is already inserted in the loop. The term "reconfiguration block" was proposed by [17] for fault-tolerant control to designate an alternative to the most common reconfigurable control approaches where the controller used to be redesigned when a fault was detected. In this alternative, the key idea is inserting the RB between the nominal controller (which remains unchanged) and the faulty plant. Since then, the fault-tolerant control based on the insertion of RBs for recovering system properties after the fault detection and estimation is called fault hiding or fault masking. However, conceiving the design of additional blocks in the control loops to achieve control goals that were not initially considered when the baseline controller was designed is prior to the concept of RB and fault hiding. Indeed, the applications of such idea can be found within or without the fault-tolerant control body of knowledge.

The canonical RBs used for fault hiding are the VSs for dealing with sensor faults and the VAs for dealing with actuator faults [16, 18, 17]. The VSs are inspired by

the Luenberger observer design and aim at estimating fault system states and outputs despite the sensor faults. This concept has already inspired several fault-tolerant sensor control approaches prior to the emergence of fault hiding approaches. Indeed, it is well-known that the recovery of systems with sensor faults can be performed by observers or filters which use the analytical or physical redundancies [8]. For example, MSIF [22, 23, 24, 25] are techniques proposed to improve the accuracy of observations by combining the measurements from different sensors. The problem of integrating the information of fusion of individual sensor technologies to obtain a more accurate observation was first proposed in the seminal paper [25] concerning tactical warfare situations. However, solutions for this problem were only presented some years later by several researchers [24, 26, 27, 28] using mainly stochastic and fuzzy techniques. Currently, most of the guidance and navigation control systems employ some kind of MSIF technique. In this context, the term "virtual sensor" was first used in one of the earliest papers [28] on MSIF. The multisensor integration is extended to the problem of sensor fault-tolerant control [29, 30, 31, 32, 33, 34] for estimating the correct observations despite of the sensor faults by combining the measurements of the remaining healthy sensors, as performed in fault hiding. In the data-driven context, some soft-sensors to estimate the correct measurements after sensor faults are also proposed. They are built in the same spirit of VSs, however, they are based on machine learning structures, e.g., the neural networks [35, 36]. The core idea of using VSs for fault hiding is the ability to hide the fault effects from the nominal controller, which is probably borrowed from the sensor fault masking approaches [37, 38, 39]. In particular, the nonlinear sensor fault masking blocks presented in [38, 39] are designed to work in the same manner as the fault hiding VSs, by correcting the faulty measurements for injecting in a fault-ignorant controller. Another similar technique is the sensor data reconciliation [40, 41] which usually employs constrained optimization (typically, least squares methods [42]) to handle two kinds of errors in sensor data: random and gross errors [41]. Under some assumptions, the faults can be modeled as errors and the sensor reconciliation can be effectively employed for sensor fault-tolerant control in schemes that already integrate the fault estimation [43, 44, 45, 46]. In [44, 46], the relation between the sensor reconciliation blocks and VSs used for fault hiding is established. Indeed, the recent adaptive VAs are also proposed in frameworks which integrate fault estimation and fault-tolerant control which resembles the sensor

reconciliation [47, 48, 49, 50, 51, 52, 52, 53, 54].

Otherwise, the VAs are used to translate the nominal control signals into reconfigured ones which can recover the system performance by using the healthy actuators. In [55], the VAs are described as the dual Luenberger observer which was presented in[56]. However, the fault hiding by means of VAs is also closely related to other control approaches. For example, motivated by the airplane flight control, since the 1990s the control allocation problem is investigated for over-actuated system [57, 58, 59]. The control allocation aims at determining how to distribute a commanded virtual control between several (redundant) actuators while considering some issues which are ignored by the virtual control law [60], e.g.: input saturation, rate constraints, and tear-and-wear minimization [60, 61, 62, 63]. Based on the control allocation problem, it is proposed the use of a control mixer [64], also for flight control systems, to exploit the actuator redundancy in fault-tolerant control problems. The use of control allocation for fault-tolerant control purposes is usually named as control re-allocation [65, 66]. For this purpose, the most basic idea is to manipulate a weighting matrix that produces a reconfigured control signal by linearly transforming the original control signal computed through the nominal controller [67, 68, 69, 70, 71, 72]. A general solution for computing such matrix is the use of pseudo-inverse methods. However, this solution is too sensitive to uncertainties and numerical issues. A more complex version of this idea consists in inserting various (possibly dynamic) control mixer blocks to obtain the robust control reconfiguration for different kinds of faults [73]. In both cases, the information of FDI systems is used to reconfigure the control mixer blocks and achieve the fault tolerance. The relation between control reallocation and VAs is evidenced by the virtual thrusters [74, 75, 72], which are not physically existent but can be obtained by control reallocation based on the synthesis of control mixers that combine the remaining healthy actuators. In [76, 77], VAs are employed as control mixers to solve the control reallocation problem.

Probably, the embryonic idea of fault hiding is the control retrofit approach initially proposed for fault-tolerant flight control. The retrofit control consists in performing the control reconfiguration by inserting a supplementary control loop without replacing any nominal control element [78]. In that proposal, the fault-tolerant controller should be inactive during nominal operation and should be activated only

when a fault is detected. Indeed the peculiarities of the aviation industry motivated this kind of solution. Although the requirements for safety in the aviation sector are strict, the certification costs for a new control architecture are complex and expensive. In this sense, the proposed retrofit module could be aircraft independent, which allows certifying the module once for being used in various aircraft. Moreover, the certification process for the retrofit module should be easier than certifying a novel baseline controller [79, 80, 81, 82]. Therefore, the fault-tolerant control by using a retrofit module reduces both cost and complexity. [1] Although the aviation industry provides particular motivations for installing a supplementary control loop, the advantages of employing that kind of strategy are also valid for other systems with long life-cycle and strict regulation for providing performance improvement or fault tolerance, for example, power systems [84, 85, 86, 87, 88], transportation systems [78, 89], and internet congestion control [90]. As a matter of fact, the use of supplementary loops and virtual elements to improve the robustness and oscillation damping is usual in power grids [91, 92, 93, 94, 95, 96], where the local controllers are not easily modified. Moreover, the retrofit fault-tolerant control approach was extended to other applications such as for generic mechanical systems represented by Newton-Euler models [97]. Recently, the control retrofit approach has been proposed for improving the control performance or providing additional guarantees in a single subsystem of a networked system without affecting the other subsystems of the network [78, 98, 99].

Therefore, the philosophy behind using RBs is closely related to the control mixing and control retrofit for dealing with actuator faults and to soft sensors and sensor reconciliation for dealing with sensor faults. In particular, the RBs are generally designed to be inactive in nominal conditions and for achieving novel control goals (e.g., fault tolerance) without modifying the baseline controller. The main advantages of adopting RBs are listed as follows:

a) RBs are usually inactive when the system operates in the nominal conditions;

b) RBs can be designed independently of the controller design, which means that the nominal closed-loop properties and goals may be unknown for its

[1] Lessons learned from recent Boeing 737 MAX accidents [83] indicate that certification of supplementary control modules must require scrutiny of the conditions for activating these modules as well as training pilots in these technologies.

design;

c) RBs can be combined with any kind of controller, which includes: a human controller in human-in-the-loop control systems [18, 16][2]; "black-box" controllers whose only signals are available [17];

d) the fault-tolerance obtained by preserving the nominal controller also preserves some implicit knowledge of the process and desired performance usually contained in the original closed-loop system [7];

e) the insertion of RBs results in minimally invasive changes in the control system when compared to other control reconfiguration approaches, which allows, for instance plug-and-play approaches for control reconfiguration based on RBs [100];

f) the design of the RB may take advantage of the properties guaranteed by the nominal controller (e.g., stability, passivity, and dissipativity);

g) it is convenient for large-scale and interconnected systems because it allows to maintain overall process operation and handle the control reconfiguration of only specific components or subsystems.

2.2 Fault hiding

The main application of RBs is undoubtedly fault-tolerant control. In this sense, the fault hiding approach is proposed for fault-tolerant control of systems subject to sensors and actuators' faults. The fault hiding approach is an alternative to the classic model-matching control reconfiguration that requires the complete redesign of the nominal controller after a fault occurrence. In contrast, the fault hiding approach aims to hide the fault effects from the controller while mitigating them for recovering the nominal behavior. Thus, the nominal controller is maintained in the loop and a different component is inserted: the RB. The fault hiding approach inserts an RB between the plant and controller to mitigate the fault effects. The RB uses all the available (physical and analytical) redundancy to reallocate the control signals for the healthy actuators and compensate for the faults in the output measurements.

[2] Although the fault hiding in human-in-the-loop control systems is useful to improve the operation experience under critical circumstances, the fault alarm must be sent to the human operator, who must be trained to deal with the reconfigured system.

Figure 2.1 depicts the general idea of fault hiding. This figure illustrates that the nominal control system consists of the interconnection between the plant Σ_{P} and the controller Σ_{C}, if a fault occurs in the plant (modeled by its faulty model $\Sigma_{\mathrm{P_f}}$), then the RB Σ_{R} is inserted into the control loop without any modification in the nominal controller Σ_{C}.

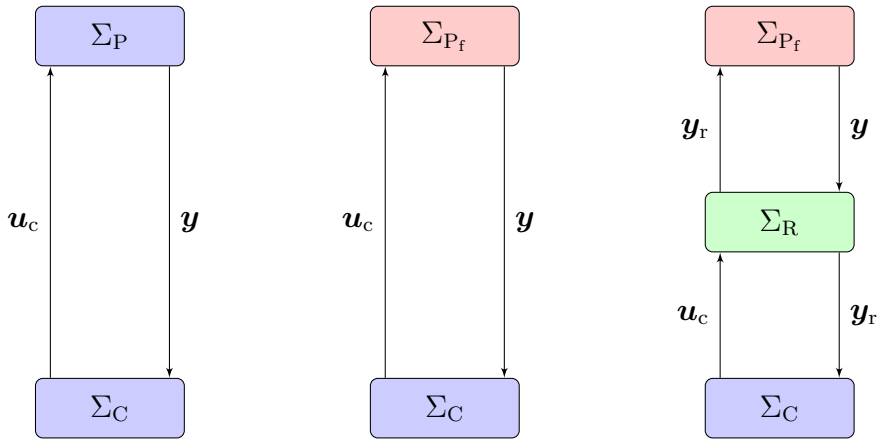

Nominal system Faulty system Reconfigured system

Figure 2.1 – Control reconfiguration by fault hiding. In this figure, the exogenous signals $\boldsymbol{w}_1$ and $\boldsymbol{w}_2$ are disregarded.

2.2.1 Fault hiding Problem

Let a fault-free plant be represented by the following nominal model Σ_{P}:

$$\Sigma_{\mathrm{P}} : \begin{cases} \dot{\boldsymbol{x}}(t) = \boldsymbol{f}\left(\boldsymbol{x}(t)\right) + \boldsymbol{g}\left(\boldsymbol{x}(t), \boldsymbol{u}_{\mathrm{p}}(t)\right), \\ \boldsymbol{y}_{\mathrm{p}}(t) = \boldsymbol{h}\left(\boldsymbol{x}(t)\right) + \boldsymbol{j}\left(\boldsymbol{x}(t), \boldsymbol{u}_{\mathrm{p}}(t)\right), \end{cases} \tag{2.1}$$

associated to the operator $\Sigma_{\mathrm{P}} : (\boldsymbol{y}_{\mathrm{p}}(\cdot), \boldsymbol{x}(t)) = \Omega\left(\boldsymbol{u}_{\mathrm{p}}(\cdot), \boldsymbol{x}_0\right)$. Notice that $\boldsymbol{x}(t) \in \mathbb{R}^n$, $\boldsymbol{u}(t) \in \mathbb{R}^m$, and $\boldsymbol{y}(t) \in \mathbb{R}^p$ are, respectively, the vectors of state, input, and output variables; $t \in \mathbb{R}_{\geq 0}$; the initial condition is $\boldsymbol{x}_0 = \boldsymbol{x}\left(0\right)$; and the matrix-valued maps $\boldsymbol{f}$, $\boldsymbol{g}$, $\boldsymbol{h}$, and $\boldsymbol{j}$ are sufficiently smooth with appropriate dimensions. The same model plant under faulty operation is represented by the following faulty model $\Sigma_{\mathrm{P_f}}$:

$$\Sigma_{\mathrm{P_f}} : \begin{cases} \dot{\boldsymbol{x}}(t) = \boldsymbol{f}_{\mathrm{f}}\left(\boldsymbol{x}(t)\right) + \boldsymbol{g}_{\mathrm{f}}\left(\boldsymbol{x}(t), \boldsymbol{u}_{\mathrm{p}}(t)\right), \\ \boldsymbol{y}_{\mathrm{p}}(t) = \boldsymbol{h}_{\mathrm{f}}\left(\boldsymbol{x}(t)\right) + \boldsymbol{j}_{\mathrm{f}}\left(\boldsymbol{x}(t), \boldsymbol{u}_{\mathrm{p}}(t)\right), \end{cases} \tag{2.2}$$

associated to the operator $\Sigma_{\mathrm{P_f}} : (\boldsymbol{y}_{\mathrm{p}}(\cdot), \boldsymbol{x}(\cdot)) = \Omega_{\mathrm{f}} (\boldsymbol{u}_{\mathrm{p}}(\cdot), \boldsymbol{x}_{\mathrm{f},0})$. Notice that $\boldsymbol{x}_{\mathrm{f},0} = \boldsymbol{x}(t_{\mathrm{f}})$, $t_{\mathrm{f}} \in \mathbb{R}_{\geq 0}$ is the time when the fault begins, $\boldsymbol{x}_{\mathrm{f}}(t) \in \mathbb{R}^n$, $\boldsymbol{u}_{\mathrm{f}}(t) \in \mathbb{R}^m$, and $\boldsymbol{y}(t) \in \mathbb{R}^p$ are, respectively, the vectors of state, input, and output variables; the matrix-valued maps $\boldsymbol{f}_{\mathrm{f}}$, $\boldsymbol{g}_{\mathrm{f}}$, $\boldsymbol{h}_{\mathrm{f}}$, and $\boldsymbol{j}_{\mathrm{f}}$ are sufficiently smooth with appropriate dimensions.

As depicted in Figure 2.2, the plant is interconnected by feedback to a dynamic output feedback controller Σ_{C} described as follows:

$$\Sigma_{\mathrm{C}} : \begin{cases} \dot{\boldsymbol{x}}_{\mathrm{c}}(t) = \boldsymbol{f}_{\mathrm{c}} (\boldsymbol{x}_{\mathrm{c}}(t)) + \boldsymbol{g}_{\mathrm{c}} (\boldsymbol{x}(t)) \boldsymbol{y}_{\mathrm{c}}(t), \\ \boldsymbol{u}_{\mathrm{c}}(t) = \boldsymbol{h}_{\mathrm{c}} (\boldsymbol{x}(t)) + \boldsymbol{j}_{\mathrm{c}} (\boldsymbol{x}_{\mathrm{c}}(t)) \boldsymbol{y}_{\mathrm{c}}(t). \end{cases} \tag{2.3}$$

The output feedback controller (5.6) is associated to the operator $\Sigma_{\mathrm{C}} : (\boldsymbol{u}_{\mathrm{c}}(\cdot), \boldsymbol{x}_{\mathrm{c}}(\cdot)) = \Omega_{\mathrm{C}} (\boldsymbol{y}_{\mathrm{c}}(\cdot), \boldsymbol{x}_{\mathrm{c},0})$, where $\boldsymbol{x}_{\mathrm{c},0} = \boldsymbol{x}_{\mathrm{c}}(0)$.

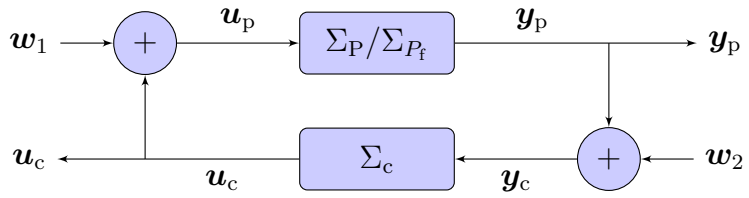

Figure 2.2 – Control loop with $\Sigma_{\mathrm{P}}/\Sigma_{\mathrm{P_f}}$ and Σ_{C} and without reconfiguration.

In Figure 2.2, $\boldsymbol{w}_1 \in \mathbb{R}^m$ and $\boldsymbol{w}_2 \in \mathbb{R}^p$ denote exogenous signals, e.g., disturbances or reference signals. After the fault diagnosis, the fault hiding mechanism inserts an RB Σ_{R}, designed according to the fault estimates, between the faulty plant $\Sigma_{\mathrm{P_f}}$ and the nominal controller Σ_{C}, as depicted in Figure 2.1, in order to recover the nominal performance or stability. Generically, Σ_{R} is described as follows

$$\Sigma_{\mathrm{R}} : \begin{cases} \dot{\boldsymbol{x}}_{\mathrm{r}}(t) = \boldsymbol{f}_{\mathrm{r}} (\boldsymbol{x}_{\mathrm{r}}(t), \boldsymbol{y}(t), \boldsymbol{u}_{\mathrm{c}}(t)), \\ \boldsymbol{y}_{\mathrm{r}}(t) = \boldsymbol{g}_{\mathrm{r}} (\boldsymbol{x}_{\mathrm{r}}(t), \boldsymbol{y}(t), \boldsymbol{u}_{\mathrm{c}}(t)), \\ \boldsymbol{u}_{\mathrm{r}}(t) = \boldsymbol{h}_{\mathrm{r}} (\boldsymbol{x}_{\mathrm{r}}(t), \boldsymbol{y}(t), \boldsymbol{u}_{\mathrm{c}}(t)), \end{cases} \tag{2.4}$$

where the matrix-valued maps $\boldsymbol{f}_{\mathrm{r}}$, $\boldsymbol{g}_{\mathrm{r}}$, and $\boldsymbol{h}_{\mathrm{r}}$ are sufficiently smooth with appropriate dimensions. The RB Σ_{R} (2.4) is associated to the operator $\Sigma_{\mathrm{R}} : (\boldsymbol{y}_{\mathrm{r}}(\cdot), \boldsymbol{u}_{\mathrm{r}}(\cdot), \boldsymbol{x}_{\mathrm{r}}(\cdot)) = \Omega_{\mathrm{R}} (\boldsymbol{y}_{\mathrm{f}}(\cdot), \boldsymbol{u}_{\mathrm{c}}(\cdot), \boldsymbol{x}_{\mathrm{r},0})$, where $\boldsymbol{x}_{\mathrm{r},0} = \boldsymbol{x}_{\mathrm{r}}(t_{\mathrm{r}})$, and $t_{\mathrm{r}} \in \mathbb{R}_{\geq 0}$ is the reconfiguration instant when Σ_{R} is inserted in the control loop.

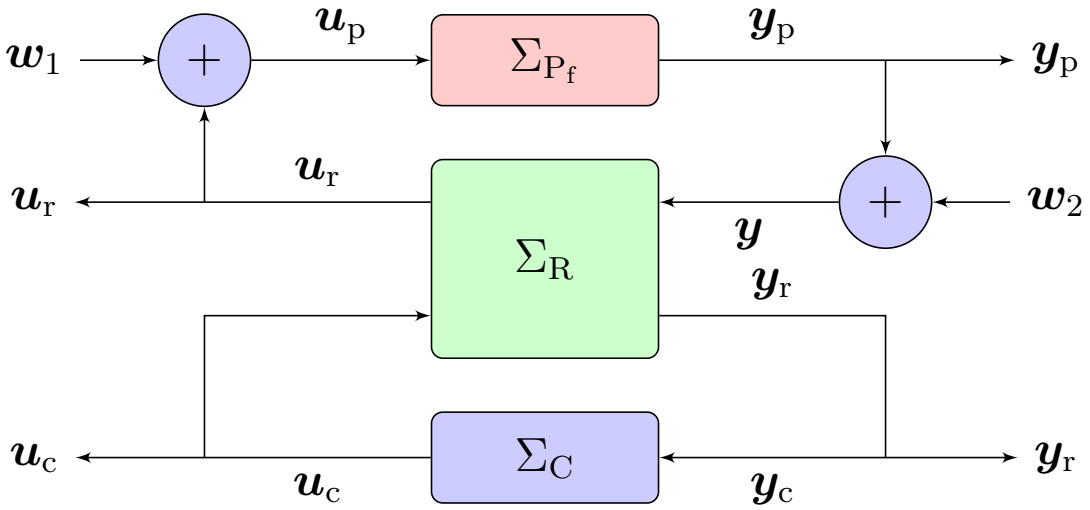

Figure 2.3 – Control loop with RB Σ_{R} inserted between the faulty plant $\Sigma_{\mathrm{P_f}}$ and the nominal controller Σ_{C}.

Notice that the insertion of the RB in the loop performs the following modifications in the signals injected in the controller and the plant as indicated by Figure 2.3:

$$\boldsymbol{y} = \boldsymbol{y}_p + \boldsymbol{w}_2 \tag{2.5}$$

$$\boldsymbol{u}_{\mathrm{p}} = \begin{cases} \boldsymbol{w}_1 + \boldsymbol{u}_{\mathrm{c}}, & \text{if the reconfiguration does not occur,} \\ \boldsymbol{w}_1 + \boldsymbol{u}_{\mathrm{r}}, & \text{if the RB is inserted,} \end{cases} \tag{2.6}$$

$$\boldsymbol{y}_{\mathrm{c}} = \begin{cases} \boldsymbol{w}_2 + \boldsymbol{y}_{\mathrm{p}}, & \text{if the reconfiguration does not occur,} \\ \boldsymbol{y}_{\mathrm{r}}, & \text{if the RB is inserted.} \end{cases} \tag{2.7}$$

The fault hiding problem is related to the design of Σ_{R} aiming at recovering some closed-loop property after the fault occurrence without changing the nominal controller Σ_{C}. Different problems and solutions can be formulated and obtained, respectively, depending on the property to be recovered. In the earliest research related to fault hiding [17, 16, 18], three generic fault-hiding problems are usually addressed: asymptotic stability, tracking, and trajectory recovery. Those problems are described as follows:

Problem 2.1. ***Asymptotic stability recovery by fault hiding.*** *Consider the plant whose nominal model is described in* (2.1)*, subject to faults represented by the faulty*

model $\Sigma_{\mathrm{P_f}}$ *described in* (2.2)*. The nominal plant* Σ_{P} *is connected to an output feedback controller* Σ_{C} *described in* (5.6) *such that* $(\Sigma_{\mathrm{P}}, \Sigma_{\mathrm{C}})$ *is asymptotically stable. Find an RB* Σ_{R} *of the form* (2.4) *such that the equilibrium of the reconfigured system* $(\Sigma_{\mathrm{P_f}}, \Sigma_{\mathrm{R}}, \Sigma_{\mathrm{C}})$ *is asymptotically stable.*

Problem 2.2. ***Asymptotic reference tracking recovery by fault hiding.*** *Consider the plant whose nominal model* $\Sigma_{\mathrm{P}} : (\boldsymbol{y}_{\mathrm{p}}(t), \boldsymbol{x}(t)) = \Omega\left(\boldsymbol{u}_{\mathrm{p}}(t), \boldsymbol{x}_0\right)$ *is described in* (2.1)*, subject to faults represented by the faulty model* $\Sigma_{\mathrm{P_f}} : (\boldsymbol{y}_{\mathrm{f}}(t), \boldsymbol{x}_{\mathrm{f}}(t)) = \Omega_{\mathrm{f}}\left(\boldsymbol{u}_{\mathrm{p}}(t), \boldsymbol{x}_{\mathrm{f},0}\right)$ *described in* (2.2)*. The nominal plant* Σ_{P} *is connected to an output feedback controller* Σ_{C} *described in* (5.6)*. Find an RB* Σ_{R} *of the form* (2.4) *such that the reconfigured system* $(\Sigma_{\mathrm{P_f}}, \Sigma_{\mathrm{R}}, \Sigma_{\mathrm{C}})$ *ensures*

$$\lim_{t\to\infty} \left(\boldsymbol{y}_{\mathrm{f}}(t) - \boldsymbol{y}_{\mathrm{p}}(t)\right) = 0, \quad \forall \boldsymbol{x}_{\mathrm{f},0}, \boldsymbol{x}_0. \tag{2.8}$$

Problem 2.3. ***Asymptotic trajectory recovery by fault hiding.*** *Consider the plant whose nominal model* $\Sigma_{\mathrm{P}} : (\boldsymbol{y}_{\mathrm{p}}(t), \boldsymbol{x}(t)) = \Omega\left(\boldsymbol{u}_{\mathrm{p}}(t), \boldsymbol{x}_0\right)$ *is described in* (2.1)*, subject to faults represented by the faulty model* $\Sigma_{\mathrm{P_f}} : (\boldsymbol{y}_{\mathrm{f}}(t), \boldsymbol{x}_{\mathrm{f}}(t)) = \Omega_{\mathrm{f}}\left(\boldsymbol{u}_{\mathrm{p}}(t), \boldsymbol{x}_{\mathrm{f},0}\right)$ *described in* (2.2)*. The nominal plant* Σ_{P} *is connected to an output feedback controller* Σ_{C} *described in* (5.6)*. Find an RB* Σ_{R} *of the form* (2.4) *such that the reconfigured system* $(\Sigma_{\mathrm{P_f}}, \Sigma_{\mathrm{R}}, \Sigma_{\mathrm{C}})$ *ensures*

$$\lim_{t\to\infty} \left(\boldsymbol{x}_{\mathrm{f}}(t) - \boldsymbol{x}(t)\right) = 0, \quad \forall \boldsymbol{x}_{\mathrm{f},0}, \boldsymbol{x}_0. \tag{2.9}$$

Most of the fault hiding literature solves those problems or some variations of them. For example, in the context of fault-tolerant control of Multi-Agent Systems (MASs), the problem of consensus recovery is also proposed [101]. Moreover, in systems subject to exogenous disturbances, the stability recovery problem with guaranteed $\mathcal{L}_2$ performance had also been handled [18, 102, 103, 104, 105]. More recently, novel fault hiding problems related to dissipativity and passivity recovery by fault hiding have been proposed [106]. They are described as follows:

Problem 2.4. ***Passivity recovery by fault hiding.*** *Consider the plant whose nominal model is described in* (2.1)*, subject to faults represented by the faulty model* $\Sigma_{\mathrm{P_f}}$ *described in* (2.2)*. The nominal plant* Σ_{P} *is connected to an output feedback controller* Σ_{C} *described in* (5.6) *such that* $(\Sigma_{\mathrm{P}}, \Sigma_{\mathrm{C}})$ *is passive. Find an RB* Σ_{R} *of the form* (2.4) *such that the reconfigured system* $(\Sigma_{\mathrm{P_f}}, \Sigma_{\mathrm{R}}, \Sigma_{\mathrm{C}})$ *is also passive.*

Problem 2.5. ***Dissipativity recovery by fault hiding.*** *Consider the plant whose nominal model is described in* (2.1)*, subject to faults represented by the faulty model* $\Sigma_{\mathrm{P_f}}$ *described in* (2.2)*. The nominal plant* Σ_{P} *is connected to an output feedback controller* Σ_{C} *described in* (5.6) *such that* $(\Sigma_{\mathrm{P}}, \Sigma_{\mathrm{C}})$ *is dissipative with respect to a supply rate* $S : \mathbb{R}^m \times \mathbb{R}^p \to \mathbb{R}$*. Find an RB* Σ_{R} *of the form* (2.4) *such that the reconfigured system* $(\Sigma_{\mathrm{P_f}}, \Sigma_{\mathrm{R}}, \Sigma_{\mathrm{C}})$ *is also dissipative with respect to* S*.*

Remark 2.1. *Relevant part of the literature on reconfiguration deals with quasi-LPV systems. Notice that if the nonlinear models used to describe* Σ_{P} *and* $\Sigma_{\mathrm{P_f}}$ *in* (2.1) *and* (2.2) *are input-affine models, then they can be exactly represented by quasi-LPV models using nonlinearity embedding methods described in [20, 21, 107]. For example, the following quasi-LPV models can be used to describe* Σ_{P} *and* $\Sigma_{\mathrm{P_f}}$*, respectively:*

$$\Sigma_{\mathrm{P}} : \begin{cases} \dot{\boldsymbol{x}}(t) = \boldsymbol{A}\left(\boldsymbol{z}(\boldsymbol{x}(t))\right)\boldsymbol{x}(t) + \boldsymbol{B}\left(\boldsymbol{z}(\boldsymbol{x}(t))\right)\boldsymbol{u}_{\mathrm{p}}(t), \\ \boldsymbol{y}_{\mathrm{p}}(t) = \boldsymbol{C}\left(\boldsymbol{z}(\boldsymbol{x}(t))\right)\boldsymbol{x}(t) + \boldsymbol{D}\left(\boldsymbol{z}(\boldsymbol{x}(t))\right)\boldsymbol{u}_{\mathrm{p}}(t), \end{cases} \tag{2.10}$$

$$\Sigma_{\mathrm{P_f}} : \begin{cases} \dot{\boldsymbol{x}}(t) = \boldsymbol{A}_{\mathrm{f}}\left(\boldsymbol{z}(\boldsymbol{x}(t))\right)\boldsymbol{x}(t) + \boldsymbol{B}_{\mathrm{f}}\left(\boldsymbol{z}(\boldsymbol{x}(t))\right)\boldsymbol{u}_{\mathrm{p}}(t), \\ \boldsymbol{y}_{\mathrm{p}}(t) = \boldsymbol{C}_{\mathrm{f}}\left(\boldsymbol{z}(\boldsymbol{x}(t))\right)\boldsymbol{x}(t) + \boldsymbol{D}_{\mathrm{f}}\left(\boldsymbol{z}(\boldsymbol{x}(t))\right)\boldsymbol{u}_{\mathrm{p}}(t), \end{cases} \tag{2.11}$$

where the matrix-valued maps $\boldsymbol{A}$*,* $\boldsymbol{B}$ $\boldsymbol{C}$*,* $\boldsymbol{D}$*,* $\boldsymbol{A}_{\mathrm{f}}$*,* $\boldsymbol{B}_{\mathrm{f}}$ $\boldsymbol{C}_{\mathrm{f}}$*, and* $\boldsymbol{D}_{\mathrm{f}}$ *are sufficiently smooth with appropriate dimensions and depending on the time-varying scheduling parameters (or premise variables in T-S fuzzy models)* $\boldsymbol{z}(\boldsymbol{x}(t)) = (z_1(\boldsymbol{x}(t)), \ldots, z_p(\boldsymbol{x}(t)))$ *used to embed nonlinear terms of* (2.1) *and* (2.2)*. In this case, the models* (2.10) *and* (2.11) *are defined within a domain of validity, which is usually a convex polytope on the state-space containing the equlibirum of interest. It follows that the image of* $\boldsymbol{z}(\boldsymbol{x}(t))$ *and the state-space matrix-valued maps are also convex polytopes for sufficiently smooth nonlinear maps in* (2.1) *and* (2.2)*. Therefore,* (2.10) *and* (2.11) *are differential polytopic inclusions. For example, the following inclusion is valid for the nominal model* (2.10)*:*

$$\begin{bmatrix} \boldsymbol{A}\left(\boldsymbol{z}(\boldsymbol{x}(t))\right) & \boldsymbol{B}\left(\boldsymbol{z}(\boldsymbol{x}(t))\right) \\ \boldsymbol{C}\left(\boldsymbol{z}(\boldsymbol{x}(t))\right) & \boldsymbol{D}\left(\boldsymbol{z}(\boldsymbol{x}(t))\right) \end{bmatrix} \in \mathrm{Co}\left\{ \begin{bmatrix} \boldsymbol{A}_i & \boldsymbol{B}_i \\ \boldsymbol{C}_i & \boldsymbol{D}_i \end{bmatrix} \right\}, \quad i \in \mathbb{N}_{\leq r}, \tag{2.12}$$

where matrices with appropriate dimensions $\boldsymbol{A}_i$*,* $\boldsymbol{B}_i$*,* $\boldsymbol{C}_i$*, and* $\boldsymbol{D}_i$ *represent the* i*-th vertex of a polytopic differential inclusion with* r *vertices. The same reasoning can be extended to* $\Sigma_{\mathrm{P_f}}$*.*

It is worthy to mention that $\boldsymbol{z}(\boldsymbol{x}(t))$ may be partially or totally unmeasured or compromised by sensor faults. Notice that if the matrix-valued maps $\boldsymbol{A}$, $\boldsymbol{B}$ $\boldsymbol{C}$, $\boldsymbol{D}$, $\boldsymbol{A}_{\mathrm{f}}$, $\boldsymbol{B}_{\mathrm{f}}$ $\boldsymbol{C}_{\mathrm{f}}$, and $\boldsymbol{D}_{\mathrm{f}}$ are constant, then Σ_{P} and $\Sigma_{\mathrm{P}_{\mathrm{f}}}$ are LTI models.

2.3 Brief history

Section 2.1 showed the connection between fault hiding ideas and other concepts in the literature. As discussed, the virtual blocks, VA and VS, have been consolidated before the fault hiding approach: the VAs are connected to retrofit and reallocation control techniques, while VSs combine concepts of MSIF and sensor conciliation. Those blocks have been used to solve fault hiding (fault masking) problems since the 5th SAFEPROCESS in 2003, when the papers [108] and [38] presented solutions for, respectively, the control reconfiguration by means of VAs, and the sensor fault masking problem. Those ideas are consolidated in the fault hiding approach whose first milestone should be the books [17, 7] in which the use of such a terminology begins and also solve the Problems 2.1, 2.2, and 2.3 for LTI systems. Since then, several advances were achieved to extend that idea to nonlinear systems, to develop novel design methods, to propose novel virtual blocks, and to integrate them to FDI systems. The main milestones in the development of fault hiding approaches are depicted in Figure 2.4.

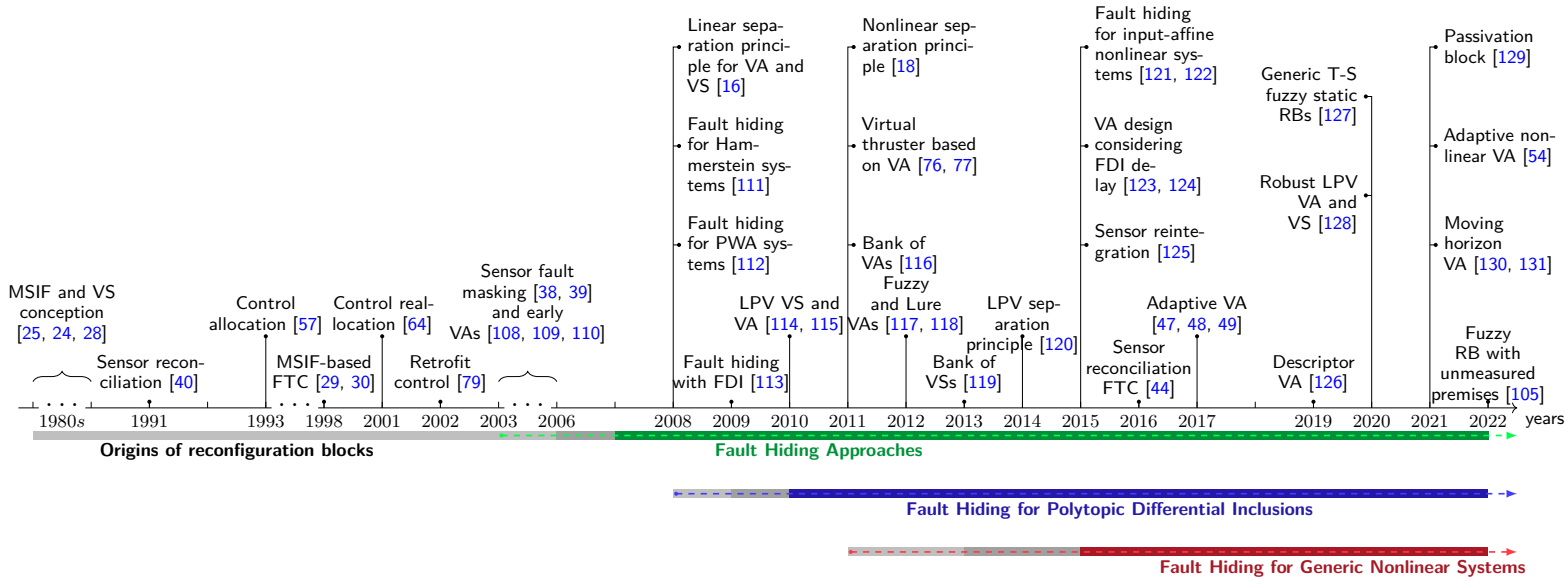

Figure 2.4 – Key advances of fault hiding literature.

2.3.1 Linear Fault Hiding

For systems with both sensors and actuator faults the VS and VA blocks can be used together to recover the system when actuator and sensor faults occur simultaneously. For this purpose, an important property is the separation principle that allows to design the VS and VA independently. This result is firstly presented in [16] for LTI systems. Indeed, the early results for fault hiding deal only with LTI systems [109, 110, 17, 7, 132, 133, 103, 134]. As discussed in [17, 7], the VS for LTI systems is a kind of Luenberguer observer. Based on that analogy, the paper [55] demonstrates that the VA for LTI systems is the dual observer based on the concepts proposed by [56] for perfect pole-assignment by means of state-feedback control. In [135], predictive VAs are proposed to deal with network-induced delays in networked LTI systems.

Most of those results for LTI systems are based on exact model-matching design conditions for solving the Problems 2.1–2.3. Although exact model-matching conditions are effective to recover the exact nominal dynamics, they tend to be conservative. An effective alternative to the model-matching conditions is the convex optimization approaches with LMI constraints. LMI-based conditions for optimal stability recovery are proposed in [103]. In [103], VAs are designed to minimize the $\mathcal{H}_\infty$ performance from the nominal controller input to the deviations and input gain due to the reconfiguration. Similarly, to guarantee some $\mathcal{H}_\infty$ robust performance, a PI VA structure and its LMI-based design conditions are provided for fault hiding of LTI systems.

Recently, MPC is used to design moving horizon VAs in [130, 131] aiming at minimizing the divergence between the reconfigured and nominal trajectories while guaranteeing input constraints.

2.3.2 Fault Hiding for Polytopic Differential Inclusions

The first application of fault hiding for nonlinear systems is presented in [111] which uses the KYP Lemma to design VA for Hammerstein nonlinear systems with Lipschitzian nonlinearities. However, the key milestone to achieve fault hiding for nonlinear systems are the results presented in [103, 112]. The main contribution of those works is that they indicate a way to solve the fault hiding problems using Linear Matrix Inequalities (LMIs). One of the advantages of the LMI-based control design

is the ease provided by these methods for dealing with nonlinear systems which can be represented by polytopic differential inclusions, e.g., LPV, L'ure, T-S fuzzy, PWA, and Lipschitzian systems. Indeed, in the next years, most of the fault hiding results are developed for those classes of systems.

Initially, the stability recovery by fault hiding problem for PWA systems with actuator faults is solved in [112] by means of PWA VAs designed through LMI-based conditions. In [136], that result is also extended to solve the reference tracking and trajectory recovery by fault hiding. Similarly, in [102], LMI-based conditions are used to design Hammerstein VAs which solve the Problems 2.1–2.3 for Hammerstein systems with Lipschitzian nonlinearities and include, for example, systems with input saturation. Both PWA systems and Hammerstein systems with Lipschitzian nonlinearities are examples of polytopic differential inclusions which are handled in different ways. The analysis or control design for polytopic differential inclusions can be performed vertex-wise (which results in one LMI for each vertex) considering all the possible combinations of the subsystems, e.g., plant, and controllers, vertices [137, 20], or applying some relaxation technique, e.g., Pólya Theorem [138]. This is the idea behind the design of VAs for PWA systems which is presented in [112], and it is also valid for LPV and T-S fuzzy models. Otherwise, the paper [111] deals with Lipschitzian nonlinearities as sector bounded nonlinearities [139] that allows obtaining robust LMI-based conditions taking into account the sector nonlinearity inequality. In addition to Hammerstein systems, this approach can be employed for fault hiding of any nonlinear system with Lipschitzian nonlinearities [140, 141] and L'ure systems [118, 142, 143]. Based on those ideas, the Problems 2.1–2.3 are solved for PWA and Hammerstein-Wiener systems in [18] using ISS concepts. The book [18] also presents a relevant result for designing simultaneously nonlinear VAs and VSs, which is the nonlinear separation principle based in the cascaded interconnection of ISS systems.

Among the polytopic differential inclusions, LPV and T-S fuzzy models stand out due to their ability to provide exact representations of input-affine nonlinear systems by embedding the nonlinearities into their time-varying or state-dependent parameters (or membership degrees). Indeed, most of the fault hiding approaches for nonlinear systems deal with T-S fuzzy, LPV and quasi-LPV models, which are LPV models whose parameters depend on the system states. For LPV systems, LPV VSs ([114])

and VA ([115]) are proposed to solve the stability recovery by fault hiding problem. The design of those LPV RBs is achieved by means of LMI-based conditions for $\mathcal{D}$-stabilization of the reconfigured dynamics. Moreover, the separability principle for gain-scheduled state-feedback controllers and VAs is obtained in [115]; and the separability principle for gain-scheduled state-feedback controllers, state observers, and VSs in [114]. The fault hiding for LPV systems with simultaneous sensor and actuator faults is addressed in [120], which also provides the separation principle for the design of LPV VAs and VSs. The simultaneous design of discrete-time LPV VAs and VSs is also addressed in [144, 145] in which the ISS property is used to guarantee the design separability as proposed by [18]. In [146], reference tracking recovery by fault hiding is presented for a four-wheeled omnidirectional mobile robot represented by switched quasi-LPV using a switching LPV VA. Other fault hiding applications to LPV systems can be found in [147, 148, 149, 119, 150, 151, 152, 153, 154, 125, 155, 156, 157, 44, 158, 159, 128, 160, 161].

In the same spirit, fault hiding approaches for T-S fuzzy fuzzy systems are also proposed in the literature [117, 162, 163, 164, 165, 166, 127, 105, 167]. Indeed, the control method for LPV systems can be easily adapted to T-S fuzzy systems since they are particular cases of quasi-LPV systems [21], whose fault hiding was already addressed in [154, 146]. The first fuzzy approach is proposed in [117] which proposes a T-S fuzzy VA for fault hiding of nonlinear systems represented by T-S fuzzy models. However, in the paper [117], the solution is based on the assumption that state-space matrix $\boldsymbol{B}$ is constant, which may be unable to represent some classes of nonlinear systems. Such a constraint is surpassed in subsequent researches on fuzzy fault hiding [162, 165, 164]. In [163], the result presented in [168] for LTI systems is extended to T-S fuzzy systems subject to unknown disturbances and the robust stability recovery by fault hiding with guaranteed $\mathcal{L}_2$ performance is obtained based on PI fuzzy VAs.

Although there are several papers proposing the use of fuzzy and LPV RBs for fault hiding of nonlinear systems represented by quasi-LPV models, as discussed before, most of them ignore the relevant problem: the existence of unmeasured parameters or premise variables. For state-observers, filters, and fuzzy controllers, the problem of unmeasured premise variables is well-known and investigated by several works [169, 170, 171, 172]. In sensor FTC, it becomes more relevant, since even the

measurable premise variables may become unavailable due to the sensor fault occurrence. Therefore, some fuzzy sensor FTC approaches are proposed to deal with unmeasured premises [173, 174]. However, most of the fuzzy and LPV fault hiding approaches do not consider unmeasured parameters even when they are affected by sensor faults. In this regard, the very recent work [105] presents a first complete solution using LMI-based design conditions for VSs and VAs considering unmeasured premises and premise variables affected by sensor faults. Moreover, [151] also considers errors in the scheduling parameters to design LPV VAs while guaranteeing stability recovery by fault hiding.

It is worth mentioning that there are a few works [175, 176, 177] that use fuzzy RBs for fault hiding which is applied to nonlinear systems without representing them as T-S fuzzy systems. Instead of designing the fuzzy RBs with fault hiding formal guarantees, they are used as expert systems whose fuzzy rule base and membership degrees are empirically tuned to compensate for faults.

2.3.3 Fault Hiding for Input-affine Nonlinear Systems

As mentioned before, most of the results on fault hiding for nonlinear systems are valid for systems that can be represented by polytopic differential inclusions. However, some few fault hiding approaches deal with more general nonlinear systems [121, 122, 106, 129].

In [145], it is proposed a nonlinear VA for fault hiding of a class of input-affine nonlinear systems as described in (2.1) with constant input map and linear output, i.e., $\boldsymbol{g}\left(\boldsymbol{x}(t)\right) = \boldsymbol{B}$ and $\boldsymbol{y}_{\mathrm{p}}(t) = \boldsymbol{C}\boldsymbol{x}(t)$. In that paper, it is shown that if the nominal closed-loop system $(\Sigma_{\mathrm{P}}, \Sigma_{\mathrm{C}})$ is ISS and the residual dynamics (between the states of VA and faulty plant $\Sigma_{\mathrm{P_f}}$) is also ISS, then the proposed nonlinear VA solves the Problem 2.1. Thus [121] presents a backstepping design methodology for the nonlinear VA which guarantees the ISS of the residual dynamics. In [122], the fault hiding problem is posed for input affine full-state linearizable MISO systems in a feedback linearization scheme. For this purpose, re-linearizing terms and a nonlinear static VA are inserted in the loop after the fault occurrence to guarantee trajectory recovery by fault hiding.

In [106], it is presented a two-step methodology for passivity and $(\boldsymbol{Q}, \boldsymbol{S}, \boldsymbol{R})$

dissipativity recovery by fault hiding (Problems 2.1, 2.4 and 2.5) for dissipative systems. Firstly, a dissipativity (passivity) analysis is performed for obtaining valid storage and supply rate functions which satisfy the dissipation inequality. Second, the RB is designed to guarantee that the same dissipation inequality holds for the reconfigured system. Moreover, it is shown that solving Problem 2.1 can be a consequence of solving Problems 2.4 and 2.5, since the nominal closed-loop system $(\Sigma_{\mathrm{P}}, \Sigma_{\mathrm{C}})$ is stable. Finally, the KYP Lemma and the linear $(\boldsymbol{Q}, \boldsymbol{S}, \boldsymbol{R})$ disipativity condition [178] are used to obtain constructive LMI-based conditions for the particular case of linear fault hiding. More recently, in [129], a novel RB, denominated PB, is presented for stability recovery by fault hiding for input-affine systems. PBs perform passivation of the faulty system to guarantee some dissipativity properties for the reconfigured systems.

In [54, 47], an adaptive VA is proposed for fault hiding of nonlinear MASs. That paper extends to input-affine nonlinear systems with constant input map the results of [47, 48, 49, 53, 52, 50], which present adaptive update laws for the VA parameters such that the trajectories are asymptotically recovered by fault hiding.

2.3.4 Fault Hiding for Distributed and Networked Control Systems

One of the advantages of the fault hiding FTC approach is the plug-and-play application of RBs. Such a property is particularly interesting in distributed or LSS, since distributed blocks can be used for reconfiguration of only a part of the network. In this sense, there are several fault hiding results for distributed systems [179, 142, 143, 180, 181, 100, 182, 48, 183, 127, 52, 50, 54]. In [179], a cooperative fault-hiding approach is proposed for Large-Scale Systems (LSSs), in which an admissibility criteria (related to stabilizability or controllability) is used to select a subset of subsystems of the LSS for which a VA is designed to recover the stability of the LSS.

In [181], the FTC of collaborating underwater robots is addressed by means of centralized and decentralized static VAs. The results indicated that both centralized and decentralized VAs can effectively hide the fault occurrence and recover trajectory tracking after the reconfiguration. For linear LSSs, a distributed fault hiding approach is presented in [180], which designs local linear VA for stability recovering by fault hiding of the network performing reconfiguration only for the local subsystem. Similarly, distribute VAs and Luenberger observer are proposed for FTC of MASs in [184].

Moreover, in [142, 143], the distributed fault hiding is proposed for power systems whose electric machines dynamics are represented by L'ure systems. In that case, a L'ure VA is connected to a specific faulty machine which guarantees the network stability. Still, for power systems, the fault-tolerant wide-area damping control is addressed in [185], which designs a bank of VAs for voltage stability by fault hiding after actuator faults.

In [182], a two-layer distributed fault-hiding approach for linear LSSs subject to both sensor and actuator faults is designed. The first layer consists of decentralized VAs and VSs which guarantees the stability recovery by fault hiding. The second layer uses a different block, the virtual reference generator, which is responsible for modifying the reference signals and ensuring the reference tracking recovery by fault hiding with disturbance rejection. In [127], the stability recovery by fault hiding for distributed T-S fuzzy systems is achieved by means of fuzzy Static Reconfiguration Blocks (SRBs) which can be used equally for faults in sensors, actuators, or both, i.e., it is not necessary different RBs for sensor (VS) and actuator (VA) fault recovery.

For MASs, adaptive VAs are proposed in [48, 52, 50, 54]. All those papers present the guarantees for asymptotic trajectory recovery by fault hiding with decentralized VAs whose parameters are updated online based on adaptive rules. An advantage provided by the proposed decentralized fault hiding approach over other distributed FTC approaches in the literature is the recovery of the nominal performance independently of the mission (e.g., consensus, coverage, and formation). In this spirit, the fault hiding problem is solved for MASs with identical linear agents in [48], heterogeneous linear agents in [52, 50], and heterogeneous nonlinear agents in [54].

Some fault hiding approaches are also aware of the phenomenons which affect Networked Control Systems (NCSs) [135, 186, 187, 188], where a communication network is used in the data exchange between the system's elements (e.g., actuators, sensors, RBs, and controllers). Among the phenomenons which affect NCSs, the aperiodic sampling and network-induced delay can be highlighted. In particular, a predictive VA structure is proposed in [135] for stability and trajectory recovery by fault hiding for NCSs subject to network-induced delays. Moreover, the reference tracking recovery by fault hiding for NCSs with varying sampling rate VAs and controllers is addressed in [187, 188].

2.3.5 Integration between Fault Hiding and FDI systems

Like any other AFTC approach, the fault hiding approaches require an FDI system to provide fault estimations which are used for designing or choosing the correct RB. However, most of the results on fault hiding assume the existence of an ideal FDI and address exclusively the FTC problem. But it is worthy to mention the relevant advances in the integration between fault hiding and FDI systems.

The earliest result which considers both fault hiding and FDI problems is provided by [113]. In that paper, there is no fault estimation, but only a fault isolation (classification) approach and a set-membership FDI system is proposed based on the separation of invariant sets which characterize the nominal and each faulty operation, assumed to be binary, i.e., each actuator is assumed to be totally healthy or lost. Thus, the VA is designed to recover the isolated fault. In [189], the integration between set-membership fault diagnosis, estimation, and hiding is proposed. For this purpose, an algorithm to check the correctness of fault classification is proposed and positively invariant sets are computed for the closed-loop stability for an interval of fault indicators.

A similar set-membership FDI mechanism is also integrated to VA for fault hiding in NCSs with aperiodic sampling in [188]. In [160], an FDI system based on an LPV interval predictor is integrated to VAs and VSs is used for fault hiding of wind turbines. In the integration with fault isolation systems, the online design of RBs may be inconvenient due to the computational costs for online design. For this reason, banks of RBs are proposed to aid the integration between fault hiding and FDI, since it allows to simply select the corresponding RB of the bank after the fault isolation. In this sense, the literature presents results for designing banks of linear VAs [116], linear VSs [190], LPV VAs [152], and LPV VSs [119, 153]. It is worthy to mention that the switching between RBs of the same bank is performed according to the FDI results. If the faults are intermittent or the FDI temporarily provides a wrong fault isolation, the reconfigured system may lose performance or even become unstable due to the excessive switching. For this purpose, in [191], dwell-time conditions for the reconfiguration mechanism are provided to guarantee the stability of the reconfigured system. An alternative to banks of RBs is presented in [128, 105], robust LPV VAs and VSs are proposed, where the fault estimates are also embedded as scheduling parameters.

In [149], an integrated fault estimation and hiding framework is proposed to design VA for LTI systems. In this case, recursive LSM is used for providing the estimation of fault parameters. Similarly, in [146], the online fault estimation based on windowed LSM is performed for obtaining switching LPV VAs for fault hiding of quasi-LPV systems. However, those papers do not analyze the impacts of fault estimation errors in the fault hiding performance nor provide convergence guarantees for the integrated system. In [148], another integrated fault estimation and hiding with VAs is presented for asymptotic trajectory recovery by fault hiding based on a model-reference control approach. In that paper, a set-membership fault estimation is used to provide confidence intervals for the fault parameters, and the effects of fault estimation errors are analyzed, although they are not compensated or attenuated. Some other research also integrates the fault estimation and hiding without dealing with the fault estimation error effects in the reconfiguration [192, 193]. Otherwise, in [194] , an interval estimation for the fault parameters (including additive faults) is also performed and an interval VA with model reference control is designed to guarantee the trajectory recovery by fault hiding. Interval VAs have been also proposed in [195] to deal with the interval of actuator faults. For nonlinear systems represented by quasi-LPV models, including the T-S fuzzy ones, it is worthy to notice that not only the fault estimation errors but also the sensor faults affect the fault hiding performance since the measured scheduling parameters are subject to deviations due to sensor faults. In this sense, the robust RBs proposed in [105] are able to deal with both problems, since the fault parameters are embedded as scheduling parameters and the fault hiding conditions take into account the unmeasured parameters, including that affected by faulty sensors.

When integrating FDI and fault hiding systems, it is also important to consider the time delays due to the late fault diagnosis. This problem is considered in [123, 157], which provides a design methodology for VAs which guarantee the stability recovery by fault hiding considering input saturation and FDI delays.

Some fault hiding approaches based on sensor reconciliation blocks [44, 45, 158, 159, 46] or adaptive VAs [47, 48, 49, 53, 52, 50, 54, 51] inherently merge the fault estimation and FTC tasks. In particular, the sensor reconciliation approaches integrate Unknown Input Observers (UIOs) with LSM: the UIO is used to decouple disturbances and estimate the system states and additive faults; and Least Squares

Methods (LSMs) are used to estimate the multiplicative fault parameters which are fed back to the UIO. Otherwise, adaptive fault hiding approaches are based on adaptive rules for the VA parameters which guarantees their convergence to the parameters of the faulty system. Notice that UIOs are also employed in other fault hiding approaches for fault estimation [147, 196].

2.4 Structures of Reconfiguration Block

Most of the fault hiding approaches are based on the canonical RBs, which are the VSs and VAs. VSs and VAs present the following basic characteristics:

a) VSs and VAs structures are based on the internal model principle, i.e., their parameters are directly related to the plant parameters;

b) they can be used only for strictly proper systems with sensor or actuator faults, i.e., considering that Σ_{P} and $\Sigma_{\mathrm{P_f}}$ represent, respectively, the nominal and faulty plant model, then $\boldsymbol{f}\left(\boldsymbol{x}(t)\right) = \boldsymbol{f}_{\mathrm{f}}\left(\boldsymbol{x}(t)\right)$ and $\boldsymbol{j}\left(\boldsymbol{x}(t), \boldsymbol{u}_{\mathrm{p}}(t)\right) = \boldsymbol{j}_{\mathrm{f}}\left(\boldsymbol{x}(t), \boldsymbol{u}_{\mathrm{p}}(t)\right) = \boldsymbol{0}$.

However, a few RBs independent from the internal model principle have been proposed, for instance the PBs [129] and generic SRBs [127, 106]. The advantages of RBs free from internal model principle are their flexibility and less sensitivity with respect to FDI errors and delays.

In this section, the main structures of RBs found in the literature for fault hiding are presented.

2.4.1 Static Reconfiguration Blocks

The VSs are the RB structures used for correcting the sensor measurements when sensor faults occur. The simplest VS structure is the SVS proposed by [17] and inspired by the so-called pseudo-inverse method for control reconfiguration [197]. The linear SVS structure Σ_{SVS} for an LTI system is described as follows

$$\Sigma_{SVS} : \boldsymbol{y}_{\mathrm{r}} = \boldsymbol{C}\boldsymbol{C}_{\mathrm{f}}^{\dagger}\boldsymbol{y}. \tag{2.13}$$

Otherwise, the VAs structures can be used to recover the system from actuator faults by reallocating the control effort required by the controller between the healthy

actuators. Just like SVS, the SVA proposed by [17] is the simplest VA structure and is also based on the pseudo-inverse method. The SVA structure Σ_{SVA} is described as follows

$$\Sigma_{SVA} : \boldsymbol{u}_{\mathrm{r}} = \boldsymbol{B}_{\mathrm{f}}^{\dagger}\boldsymbol{B}\boldsymbol{u}_{\mathrm{c}}. \tag{2.14}$$

For quasi-LPV systems, the following LPV or T-S fuzzy versions of the SRBs are proposed [162, 120]

$$\Sigma_{SVS} : \boldsymbol{y}_{\mathrm{r}} = \boldsymbol{C}\left(\hat{\boldsymbol{z}}(\boldsymbol{x}(t))\right)\boldsymbol{C}_{\mathrm{f}}\left(\hat{\boldsymbol{z}}(\boldsymbol{x}(t))\right)^{\dagger}\boldsymbol{y}, \tag{2.15}$$

$$\Sigma_{SVA} : \boldsymbol{u}_{\mathrm{r}} = \boldsymbol{B}_{\mathrm{f}}\left(\hat{\boldsymbol{z}}(\boldsymbol{x}(t))\right)^{\dagger}\boldsymbol{B}\left(\hat{\boldsymbol{z}}(\boldsymbol{x}(t))\right)\boldsymbol{u}_{\mathrm{c}}, \tag{2.16}$$

where $\hat{\boldsymbol{z}}(\boldsymbol{x}(t))$ is the estimate of the vector of scheduling parameters (membership functions). Most of the fault hiding approaches consider $\hat{\boldsymbol{z}}(\boldsymbol{x}(t)) = \boldsymbol{z}(\boldsymbol{x}(t))$, which may be unrealistic particularly in systems subject to sensor faults or disturbances as in [120, 145, 156, 119, 114, 153, 163].

According to the inactivity principle, it would be desirable that the RBs for fault hiding do not change the system dynamics in the absence of faults. The static blocks described in (2.13)–(2.15) naturally meet the inactivity principle. For example, if $\boldsymbol{B}_{\mathrm{f}} = \boldsymbol{B}$ ($\boldsymbol{C}_{\mathrm{f}} = \boldsymbol{C}$), the product $\boldsymbol{B}\boldsymbol{B}_{\mathrm{f}}^{\dagger}$ ($\boldsymbol{C}_{\mathrm{f}}^{\dagger}\boldsymbol{C}$) is equivalent to the identity matrix.

However, the SRBs, i.e., SVS and SVA, are not enough to ensure the recovery of faulty system, for instance, when the faulty part of the system is required for stabilization of the remaining part [17]. For this reason, in [109, 17, 18], it is proposed the use of Dynamic Reconfiguration Blocks (DRBs) for fault hiding.

2.4.2 Dynamic Reconfiguration Blocks

The general structure of DRBs is presented in (2.4). In particular, the DVS function is analogue to state estimators, and the structure proposed in [17] is similar to the Luenberguer observer. The structure of the DVS Σ_{DVS} is described as follows

$$\Sigma_{DVS} : \begin{cases} \dot{\boldsymbol{x}}_{\mathrm{r}}(t) = (\boldsymbol{A} - \boldsymbol{L}\boldsymbol{C}_{\mathrm{f}})\boldsymbol{x}_{\mathrm{r}}(t) + \boldsymbol{L}\boldsymbol{y}(t) + \boldsymbol{B}_{\mathrm{f}}\boldsymbol{u}_{\mathrm{c}}(t), \\ \boldsymbol{y}_{\mathrm{r}}(t) = (\boldsymbol{C} - \boldsymbol{J}\boldsymbol{C}_{\mathrm{f}})\boldsymbol{x}_{\mathrm{r}}(t) + \boldsymbol{J}\boldsymbol{y}(t), \\ \boldsymbol{u}_{\mathrm{r}}(t) = \boldsymbol{u}_{\mathrm{c}}(t), \end{cases} \tag{2.17}$$

where the matrix gains $\boldsymbol{L} \in \mathbb{R}^{n\times p}$ and $\boldsymbol{J} \in \mathbb{R}^{p\times p}$ are designed to achieve the fault hiding goals after sensor faults.

Note that the DVS is based on the internal model principle and requires the nominal plant model as well as the appropriate fault estimation expressed by the matrix $\boldsymbol{B}_{\mathrm{f}}$. Due to the similarity between the DVS described in (2.17) and the state observers, the design methodologies are also similar, for instance, the stability of the closed-loop system can be ensured by simply choosing a $\boldsymbol{L}$ gain such that $(\boldsymbol{A}-\boldsymbol{L}\boldsymbol{C}_{\mathrm{f}})$ is Hurwitz.

The structure of Dynamic Virtual Actuators (DVAs) is also based on the internal model principle. The structure of the DVA Σ_{DVA} is described as follows

$$\Sigma_{DVA}: \begin{cases} \dot{\boldsymbol{x}}_{\mathrm{r}}(t) = (\boldsymbol{A}-\boldsymbol{B}_{\mathrm{f}}\boldsymbol{M})\boldsymbol{x}_{\mathrm{r}}(t) + (\boldsymbol{B}-\boldsymbol{B}_{\mathrm{f}}\boldsymbol{N})\boldsymbol{u}_{\mathrm{c}}(t), \\ \boldsymbol{y}_{\mathrm{r}}(t) = \boldsymbol{C}\boldsymbol{x}_{\mathrm{r}}(t) + \boldsymbol{y}(t), \\ \boldsymbol{u}_{\mathrm{r}}(t) = \boldsymbol{M}\boldsymbol{x}_{\mathrm{r}}(t) + \boldsymbol{N}\boldsymbol{u}_{\mathrm{c}}(t), \end{cases} \tag{2.18}$$

where the matrix gains $\boldsymbol{M} \in \mathbb{R}^{m\times n}$ and $\boldsymbol{N} \in \mathbb{R}^{m\times m}$ are designed to achieve the fault hiding goals after actuator faults.

In [55], it is shown that the design of DVA is analogous to the dual observer problem described in [56]. Thus, the choice of $\boldsymbol{M}$ such that $(\boldsymbol{A}-\boldsymbol{B}_{\mathrm{f}}\boldsymbol{M})$ is Hurwitz is also sufficient to ensure the stability of the reconfigured system.

As discussed in Subsection 2.4.1 for Static Virtual Sensors (SVSs) and Static Virtual Actuators (SVAs), the Dynamic Virtual Sensors (DVSs) and DVAs can be slightly modified for obtaining the LPV or T-S fuzzy versions to deal with quasi-LPV systems. The LPV (or the T-S fuzzy) DVSs and DVAs are described as follows:

$$\Sigma_{DVS}: \begin{cases} \dot{\boldsymbol{x}}_{\mathrm{r}}(t) = \boldsymbol{A}_{\Delta,\mathrm{S}}\left(\hat{\boldsymbol{z}}(\boldsymbol{x}(t))\right)\boldsymbol{x}_{\mathrm{r}}(t) + \boldsymbol{L}\left(\hat{\boldsymbol{z}}(\boldsymbol{x}(t))\right)\boldsymbol{y}(t) + \boldsymbol{B}_{\mathrm{f}}\left(\hat{\boldsymbol{z}}(\boldsymbol{x}(t))\right)\boldsymbol{u}_{\mathrm{c}}(t), \\ \boldsymbol{y}_{\mathrm{r}}(t) = \boldsymbol{C}_{\Delta}\left(\hat{\boldsymbol{z}}(\boldsymbol{x}(t))\right)\boldsymbol{x}_{\mathrm{r}}(t) + \boldsymbol{J}\left(\hat{\boldsymbol{z}}(\boldsymbol{x}(t))\right)\boldsymbol{y}(t), \\ \boldsymbol{u}_{\mathrm{r}}(t) = \boldsymbol{u}_{\mathrm{c}}(t), \end{cases} \tag{2.19}$$

$$\Sigma_{DVA}: \begin{cases} \dot{\boldsymbol{x}}_{\mathrm{r}}(t) = \boldsymbol{A}_{\Delta,\mathrm{A}}\left(\hat{\boldsymbol{z}}(\boldsymbol{x}(t))\right)\boldsymbol{x}_{\mathrm{r}}(t) + \boldsymbol{B}_{\Delta}\left(\hat{\boldsymbol{z}}(\boldsymbol{x}(t))\right)\boldsymbol{u}_{\mathrm{c}}(t), \\ \boldsymbol{y}_{\mathrm{r}}(t) = \boldsymbol{C}\left(\hat{\boldsymbol{z}}(\boldsymbol{x}(t))\right)\boldsymbol{x}_{\mathrm{r}}(t) + \boldsymbol{y}(t), \\ \boldsymbol{u}_{\mathrm{r}}(t) = \boldsymbol{M}\left(\hat{\boldsymbol{z}}(\boldsymbol{x}(t))\right)\boldsymbol{x}_{\mathrm{r}}(t) + \boldsymbol{N}\left(\hat{\boldsymbol{z}}(\boldsymbol{x}(t))\right)\boldsymbol{u}_{\mathrm{c}}(t), \end{cases} \tag{2.20}$$

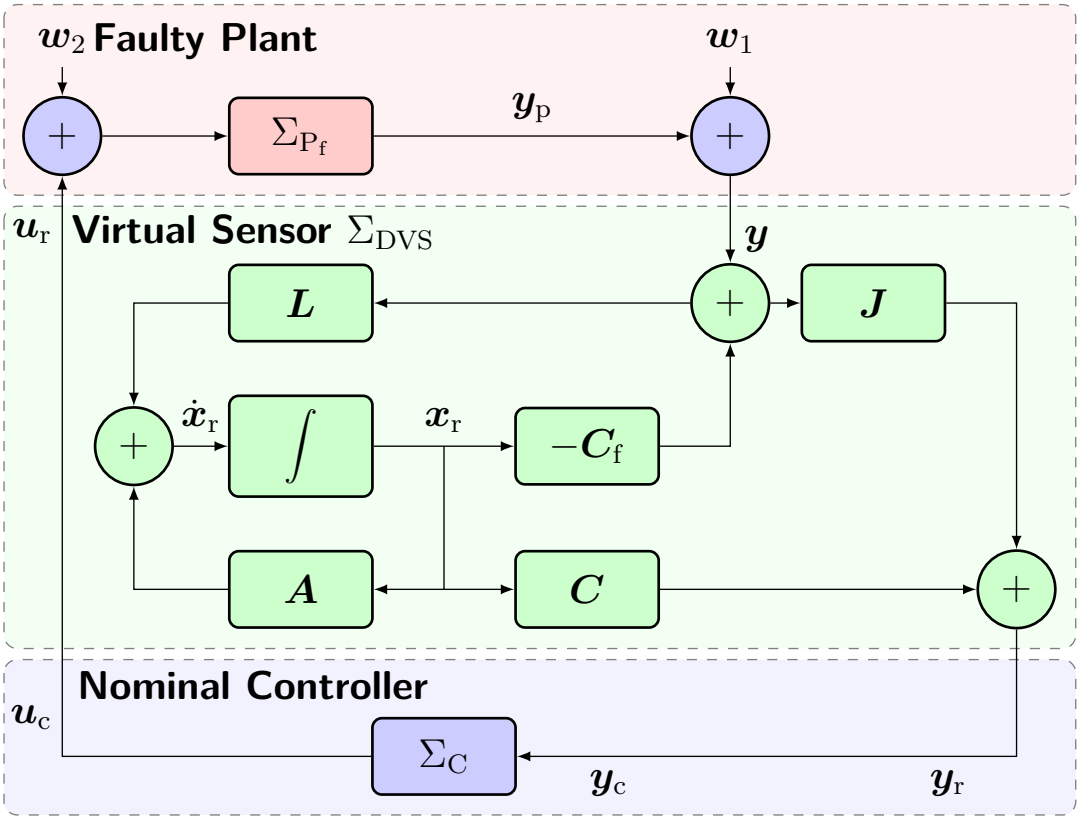

Figure 2.5 – Fault hiding by using a VS Σ_{DVS}.

where

$$
\begin{aligned}
&\boldsymbol{A}_{\Delta,\mathrm{S}}\left(\hat{\boldsymbol{z}}(\boldsymbol{x}(t))\right) = \boldsymbol{A}\left(\hat{\boldsymbol{z}}(\boldsymbol{x}(t))\right) - \boldsymbol{L}\left(\hat{\boldsymbol{z}}(\boldsymbol{x}(t))\right)\boldsymbol{C}_{\mathrm{f}}\left(\hat{\boldsymbol{z}}(\boldsymbol{x}(t))\right),\\
&\boldsymbol{C}_{\Delta}\left(\hat{\boldsymbol{z}}(\boldsymbol{x}(t))\right) = \boldsymbol{C}\left(\hat{\boldsymbol{z}}(\boldsymbol{x}(t))\right) - \boldsymbol{J}\left(\hat{\boldsymbol{z}}(\boldsymbol{x}(t))\right)\boldsymbol{C}_{\mathrm{f}}\left(\hat{\boldsymbol{z}}(\boldsymbol{x}(t))\right),\\
&\boldsymbol{A}_{\Delta,\mathrm{A}}\left(\hat{\boldsymbol{z}}(\boldsymbol{x}(t))\right) = \boldsymbol{A}\left(\hat{\boldsymbol{z}}(\boldsymbol{x}(t))\right) - \boldsymbol{B}_{\mathrm{f}}\left(\hat{\boldsymbol{z}}(\boldsymbol{x}(t))\right)\boldsymbol{M}\left(\hat{\boldsymbol{z}}(\boldsymbol{x}(t))\right),\\
&\boldsymbol{B}_{\Delta}\left(\hat{\boldsymbol{z}}(\boldsymbol{x}(t))\right) = \boldsymbol{B}\left(\hat{\boldsymbol{z}}(\boldsymbol{x}(t))\right) - \boldsymbol{B}_{\mathrm{f}}\left(\hat{\boldsymbol{z}}(\boldsymbol{x}(t))\right)\boldsymbol{N}\left(\hat{\boldsymbol{z}}(\boldsymbol{x}(t))\right),\\
&\begin{bmatrix}\boldsymbol{L}\left(\hat{\boldsymbol{z}}(\boldsymbol{x}(t))\right)\\ \boldsymbol{J}\left(\hat{\boldsymbol{z}}(\boldsymbol{x}(t))\right)\end{bmatrix} \in \mathrm{Co}\left\{\begin{bmatrix}\boldsymbol{L}_i\\ \boldsymbol{J}_i\end{bmatrix}\right\}, \quad i \in \mathbb{N}_{\leq r},\\
&\begin{bmatrix}\boldsymbol{M}\left(\hat{\boldsymbol{z}}(\boldsymbol{x}(t))\right) & \boldsymbol{N}\left(\hat{\boldsymbol{z}}(\boldsymbol{x}(t))\right)\end{bmatrix} \in \mathrm{Co}\left\{\begin{bmatrix}\boldsymbol{M}_i & \boldsymbol{N}_i\end{bmatrix}\right\}, \quad i \in \mathbb{N}_{\leq r}.
\end{aligned}
$$

Notice that the gains of LPV or T-S fuzzy RBs in (2.19) and (2.20) also depend on the time-varying scheduling parameters (or premise variables in T-S fuzzy models) $\boldsymbol{z}(\boldsymbol{x}(t))$ and belongs to a polytopic domain. Therefore, the matrix gains $\boldsymbol{L}\left(\hat{\boldsymbol{z}}(\boldsymbol{x}(t))\right)$,

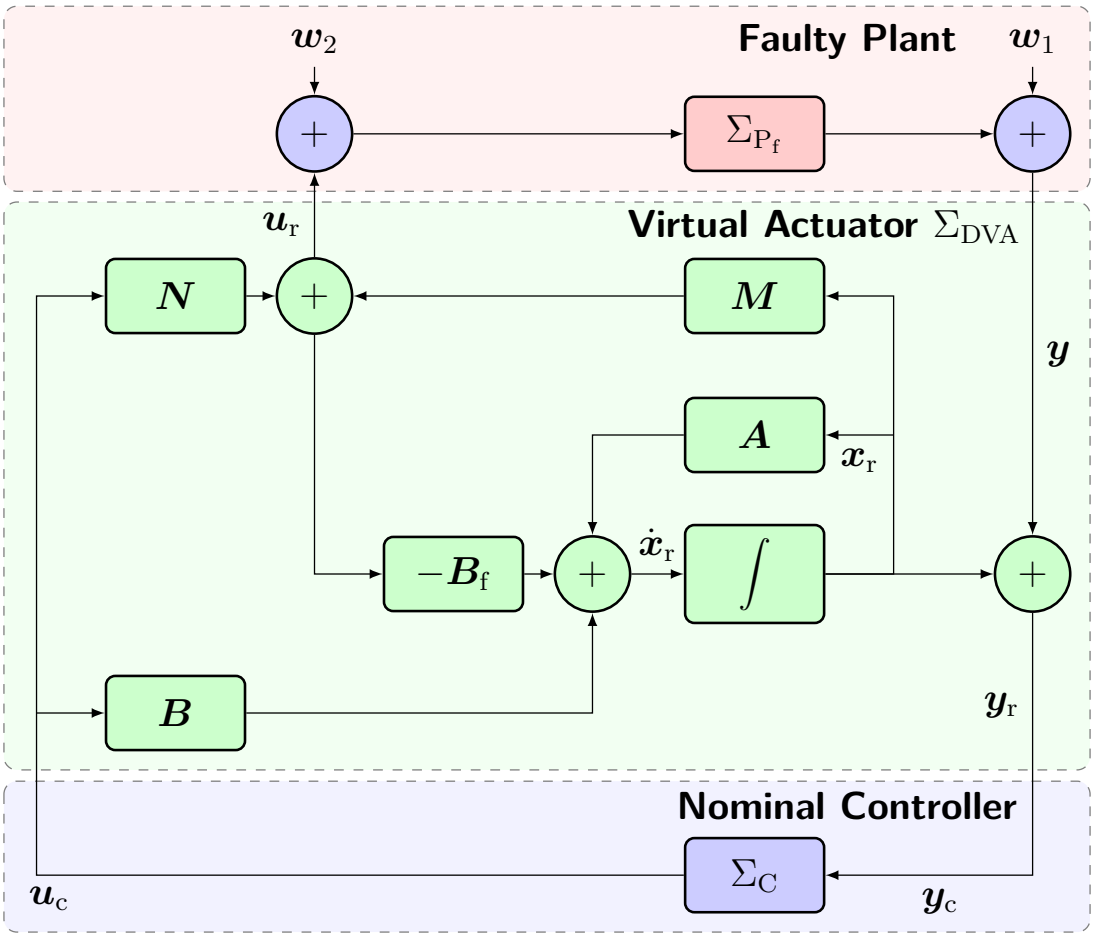

Figure 2.6 – Fault hiding by using a VA Σ_{DVA}.

$\boldsymbol{J}\left(\hat{\boldsymbol{z}}(\boldsymbol{x}(t))\right)$, $\boldsymbol{M}\left(\hat{\boldsymbol{z}}(\boldsymbol{x}(t))\right)$, and $\boldsymbol{N}\left(\hat{\boldsymbol{z}}(\boldsymbol{x}(t))\right)$ are vertex-wise designed to guarantee the fault hiding goal.

2.4.3 Internal Model-based Nonlinear Reconfiguration Blocks

In the literature, several nonlinear RBs have been proposed, for example: L'ure [118], Hammerstein-Wiener [18], and input-affine [121] VSs and VAs. The rule of thumb for building those RBs is the internal model principle. In this regard, the general RB representation in (2.4) is written as a function of the state-space maps of the nominal and faulty plant models, respectively, Σ_{P} (cf. (2.1)) and $\Sigma_{\mathrm{P_f}}$ (cf. (2.2)).

In particular, the DVSs for a faulty system $\Sigma_{\mathrm{P_f}}$ described as (2.2) are:

$$\Sigma_{DVS}: \begin{cases} \dot{\boldsymbol{x}}_{\mathrm{r}}(t) = \boldsymbol{f}\left(\boldsymbol{x}_{\mathrm{r}}(t)\right) + \boldsymbol{g}_{\mathrm{f}}\left(\boldsymbol{x}_{\mathrm{r}}(t), \boldsymbol{u}_{\mathrm{c}}(t)\right) + \boldsymbol{l}\left(\boldsymbol{y}(t)\right) - \boldsymbol{l}\left(\boldsymbol{y}_{\mathrm{r}}(t)\right), \\ \boldsymbol{y}_{\mathrm{r}}(t) = \boldsymbol{h}_{\mathrm{f}}\left(\boldsymbol{x}_{\mathrm{r}}(t)\right) + \boldsymbol{j}\left(\boldsymbol{y}(t)\right) - \boldsymbol{j}\left(\boldsymbol{y}_{\mathrm{r}}(t)\right), \\ \boldsymbol{u}_{\mathrm{r}}(t) = \boldsymbol{u}_{\mathrm{c}}(t), \end{cases} \tag{2.21}$$

where the vector-valued maps $\boldsymbol{l}$ and $\boldsymbol{j}$ with appropriate dimensions are designed to achieve the fault hiding objectives after sensor faults. Moreover, the general nonlinear form of DVAs based on the internal model principle is described as follows

$$\Sigma_{DVA}: \begin{cases} \dot{\boldsymbol{x}}_{\mathrm{r}}(t) = \boldsymbol{f}\left(\boldsymbol{x}_{\mathrm{r}}(t)\right) + \boldsymbol{g}\left(\boldsymbol{x}_{\mathrm{r}}(t), \boldsymbol{u}_{\mathrm{c}}(t)\right) - \boldsymbol{g}_{\mathrm{f}}\left(\boldsymbol{x}_{\mathrm{r}}(t), \boldsymbol{u}_{\mathrm{r}}(t)\right), \\ \boldsymbol{y}_{\mathrm{r}}(t) = \boldsymbol{h}\left(\boldsymbol{x}_{\mathrm{r}}(t)\right) + \boldsymbol{y}(t), \\ \boldsymbol{u}_{\mathrm{r}}(t) = \boldsymbol{m}\left(\boldsymbol{x}_{\mathrm{r}}(t)\right) + \boldsymbol{n}\left(\boldsymbol{u}_{\mathrm{c}}(t)\right), \end{cases} \tag{2.22}$$

where the vector-valued maps $\boldsymbol{m}$ and $\boldsymbol{n}$ with appropriate dimensions are designed to achieve the fault hiding objectives after actuator faults.

Indeed one can notice that the linear, LPV, and T-S fuzzy DVSs and DVAs described in (2.17)–(2.20) are particular cases of the nonlinear DVSs and DVSs based on the internal model principle described in (2.21) and (2.22). Moreover, other nonlinear fault hiding strategies in the literature are also based on those structures (2.21)–(2.22), namely: the L'ure VAs used in [118, 142, 143]; the Hammerstein-Wiener VSs and VAs used in [18, 111, 102, 198], PWA VSs and VAs used in [18, 112, 136], input-affine VAs used in [121], and Lipschitz VAs used in [140, 141].

2.4.4 Reconfiguration Blocks Independent of Internal Model

All the RBs discussed in Subsections 2.4.1–2.3.3 reuse the parameters from nominal and faulty models Σ_{P} and $\Sigma_{\mathrm{P_f}}$. It means that any model inaccuracy and fault estimation error result in bad-tuned RBs. It is clear that for static VAs and VSs in (2.13)–(2.16) the direct use of $\boldsymbol{C}, \boldsymbol{C}_{\mathrm{f}}, \boldsymbol{B}$, and $\boldsymbol{B}_{\mathrm{f}}$ is a straightforward application of the pseudo-inverse method which is already a well-known alternative for control reconfiguration. However, the pseudo-inverse of faulty matrices $\boldsymbol{C}_{\mathrm{f}}$ and $\boldsymbol{B}_{\mathrm{f}}$ is particularly sensitive to FDI errors. Therefore, generic SRBs structures that do not use pseudo-inverse of faulty matrices are welcome [106]. In particular, the following generic SRB

structure can be used

$$\Sigma_{\mathrm{R}} : \begin{cases} \boldsymbol{y}_{\mathrm{r}}(t) = \boldsymbol{R}_1 \boldsymbol{y}(t) + \boldsymbol{R}_2 \boldsymbol{u}_{\mathrm{c}}(t), \\ \boldsymbol{u}_{\mathrm{r}}(t) = \boldsymbol{R}_3 \boldsymbol{y}(t) + \boldsymbol{R}_4 \boldsymbol{u}_{\mathrm{c}}(t), \end{cases} \tag{2.23}$$

where $\boldsymbol{R}_1$, $\boldsymbol{R}_2$, $\boldsymbol{R}_3$, and $\boldsymbol{R}_4$ are the matrix gains of Σ_{R} which are designed to achieve the fault hiding goals.

This SRB can also be represented as linear transformation of controller input-output signals:

$$\Sigma_R : \begin{bmatrix} \boldsymbol{y}_{\mathrm{r}} \\ \boldsymbol{u}_{\mathrm{r}} \end{bmatrix} = \boldsymbol{R} \begin{bmatrix} \boldsymbol{y} \\ \boldsymbol{u}_c \end{bmatrix}, \tag{2.24}$$

$$\boldsymbol{R} \triangleq \begin{bmatrix} \boldsymbol{R}_1 & \boldsymbol{R}_2 \\ \boldsymbol{R}_3 & \boldsymbol{R}_4 \end{bmatrix}. \tag{2.25}$$

Moreover, a dynamic version of the RB presented in (2.23) can also be used for fault hiding. In this case, the generic DRB structure exhibits parameters independent of the internal model principle. Although, the use of the internal model principle for VSs and VAs is natural due to their relation with the Luenberger observer design. Indeed, the use of an internal model eases the mathematical manipulation of the error dynamics between the blocks and plant states and allows to obtain design separability conditions. However, the internal model also makes the VSs and VAs more sensitive to faults and makes the conditions more conservative. Although the fault model must be considered in the design of DRBs that does not depend on internal models, their absence in the block structure provides degrees of freedom and reduces the impact of eventual FDI errors. The generic DRB is described as follows:

$$\Sigma_R : \begin{cases} \dot{\boldsymbol{x}}_{\mathrm{r}}(t) = \boldsymbol{A}_{\mathrm{r}} \boldsymbol{x}_{\mathrm{r}}(t) + \boldsymbol{B}_{\mathrm{r,y}} \boldsymbol{y}(t) + \boldsymbol{B}_{\mathrm{r,u}} \boldsymbol{u}_{\mathrm{c}}(t), \\ \boldsymbol{y}_{\mathrm{r}}(t) = \boldsymbol{C}_{\mathrm{r,y}} \boldsymbol{x}_{\mathrm{r}}(t) + \boldsymbol{R}_1 \boldsymbol{y}(t) + \boldsymbol{R}_2 \boldsymbol{u}_{\mathrm{c}}(t), \\ \boldsymbol{u}_{\mathrm{r}}(t) = \boldsymbol{C}_{\mathrm{r,u}} \boldsymbol{x}_{\mathrm{r}}(t) + \boldsymbol{R}_3 \boldsymbol{y}(t) + \boldsymbol{R}_4 \boldsymbol{u}_{\mathrm{c}}(t), \end{cases} \tag{2.26}$$

with $\boldsymbol{x}_{\mathrm{r}}(t) \in \mathbb{R}^{n_{\mathrm{r}}}$ and gain matrices $\boldsymbol{A}_{\mathrm{r}}$, $\boldsymbol{B}_{\mathrm{r,y}}$, $\boldsymbol{B}_{\mathrm{r,u}}$, $\boldsymbol{C}_{\mathrm{r,y}}$, $\boldsymbol{C}_{\mathrm{r,u}}$ with proper dimensions.

When the static and dynamic RBs, described in (2.23) and (2.26), respectively, are designed for passivation of the faulty system, they are also referred as passivation [129] or dissipation [199] blocks. Indeed the concept of passivation blocks is

borrowed from [200] that proposes the static passivation blocks which perform simultaneously feedback, feed-forward, and cascade passivation to guarantee that the plant will present the desirable dissipative properties. Moreover, this concept is also employed for data-driven FTC in [201].

LPV (T-S fuzzy) versions of (2.23) and (2.26) are also possible [127]:

$$\Sigma_{\mathrm{R}}: \begin{cases} \boldsymbol{y}_{\mathrm{r}}(t) = \boldsymbol{R}_1\left(\hat{\boldsymbol{z}}(\boldsymbol{x}(t))\right)\boldsymbol{y}(t) + \boldsymbol{R}_2\left(\hat{\boldsymbol{z}}(\boldsymbol{x}(t))\right)\boldsymbol{u}_{\mathrm{c}}(t), \\ \boldsymbol{u}_{\mathrm{r}}(t) = \boldsymbol{R}_3\left(\hat{\boldsymbol{z}}(\boldsymbol{x}(t))\right)\boldsymbol{y}(t) + \boldsymbol{R}_4\left(\hat{\boldsymbol{z}}(\boldsymbol{x}(t))\right)\boldsymbol{u}_{\mathrm{c}}(t), \end{cases} \tag{2.27}$$

$$\Sigma_R: \begin{cases} \dot{\boldsymbol{x}}_{\mathrm{r}}(t) = \boldsymbol{A}_{\mathrm{r}}\left(\hat{\boldsymbol{z}}(\boldsymbol{x}(t))\right)\boldsymbol{x}_{\mathrm{r}}(t) + \boldsymbol{B}_{\mathrm{r,y}}\left(\hat{\boldsymbol{z}}(\boldsymbol{x}(t))\right)y(t) + \boldsymbol{B}_{\mathrm{r,u}}\left(\hat{\boldsymbol{z}}(\boldsymbol{x}(t))\right)\boldsymbol{u}_{\mathrm{c}}(t), \\ \boldsymbol{y}_{\mathrm{r}}(t) = \boldsymbol{C}_{\mathrm{r,y}}\left(\hat{\boldsymbol{z}}(\boldsymbol{x}(t))\right)\boldsymbol{x}_{\mathrm{r}}(t) + \boldsymbol{R}_1\left(\hat{\boldsymbol{z}}(\boldsymbol{x}(t))\right)y(t) + \boldsymbol{R}_2\left(\hat{\boldsymbol{z}}(\boldsymbol{x}(t))\right)\boldsymbol{u}_{\mathrm{c}}(t), \\ \boldsymbol{u}_{\mathrm{r}}(t) = \boldsymbol{C}_{\mathrm{r,u}}\left(\hat{\boldsymbol{z}}(\boldsymbol{x}(t))\right)\boldsymbol{x}_{\mathrm{r}}(t) + \boldsymbol{R}_3\left(\hat{\boldsymbol{z}}(\boldsymbol{x}(t))\right)\boldsymbol{y}(t) + \boldsymbol{R}_4\left(\hat{\boldsymbol{z}}(\boldsymbol{x}(t))\right)\boldsymbol{u}_{\mathrm{c}}(t), \end{cases} \tag{2.28}$$

where,

$$\begin{bmatrix} \boldsymbol{A}_{\mathrm{r}}\left(\hat{\boldsymbol{z}}(\boldsymbol{x}(t))\right) & \boldsymbol{B}_{\mathrm{r,y}}\left(\hat{\boldsymbol{z}}(\boldsymbol{x}(t))\right) & \boldsymbol{B}_{\mathrm{r,u}}\left(\hat{\boldsymbol{z}}(\boldsymbol{x}(t))\right), \\ \boldsymbol{C}_{\mathrm{r,y}}\left(\hat{\boldsymbol{z}}(\boldsymbol{x}(t))\right) & \boldsymbol{R}_1\left(\hat{\boldsymbol{z}}(\boldsymbol{x}(t))\right) & \boldsymbol{R}_2\left(\hat{\boldsymbol{z}}(\boldsymbol{x}(t))\right), \\ \boldsymbol{C}_{\mathrm{r,u}}\left(\hat{\boldsymbol{z}}(\boldsymbol{x}(t))\right) & \boldsymbol{R}_3\left(\hat{\boldsymbol{z}}(\boldsymbol{x}(t))\right) & \boldsymbol{R}_4\left(\hat{\boldsymbol{z}}(\boldsymbol{x}(t))\right) \end{bmatrix} \in \mathrm{Co}\left\{ \begin{bmatrix} \boldsymbol{A}_{r,i} & \boldsymbol{B}_{\mathrm{r,y},i} & \boldsymbol{B}_{\mathrm{r,u},i} \\ \boldsymbol{C}_{\mathrm{r,y},i} & \boldsymbol{R}_{1,i} & \boldsymbol{R}_{2,i} \\ \boldsymbol{C}_{\mathrm{r,u},i} & \boldsymbol{R}_{3,i} & \boldsymbol{R}_{4,i} \end{bmatrix} \right\}.$$

for $i \in \mathbb{N}_{\leq r}$. However, in those cases, (2.27) and (2.28) become dependent on the nonlinear map $\hat{\boldsymbol{z}}(\boldsymbol{x}(t))$ which is related to the nonlinearities of the plant nominal and faulty models Σ_{P} and $\Sigma_{\mathrm{P_f}}$.

2.4.5 Other Reconfiguration Blocks

In addition to the RBs presented in the previous sections, some other structures for RBs have been proposed to address specific problems or deal with a particular class of system. Those alternative structures are listed as follows:

a) **Prediction-based VA [135]** uses the prediction of the VA states in the reconfigured input to compensate for actuator faults in NCSs subject to networked-induced delays.

b) **Reconfiguration Blocks for discrete-event systems [202]**, where the nominal control strategy is frequently implemented by human operators, which accommodates the fault in the plant while mimicking its nominal behavior for the nominal controller.

c) **Decentralized VAs [181, 180]** for fault hiding in LSSs which allow the local reconfiguration to guarantee the recovery of whole LSS.

d) **Switching VAs [146]** for fault-hiding of plants represented by switching models.

e) **PI VAs [168, 163]** that are DVAs with an integral term to compensate for the error and improve the fault hiding performance.

f) **Varying sampling rate VAs [188]** for fault hiding of NCSs which allows its integration to aperiodic control approaches, e.g., event-triggered control.

g) **Sensor reconciliation blocks [44, 45, 46]** are particular structures for fault hiding of sensor faults inspired by the sensor data reconciliation approaches [40]. Sensor reconciliation blocks integrate the fault estimation, disturbance decoupling, and fault hiding by providing the rectified sensor measurements.

h) **Reduced-order VAs [203]** are designed to address the fault hiding of subsystems in which the VA design is admissible;

i) **Adaptive VAs [47, 48, 49]** integrate the fault estimation and fault hiding mechanisms for systems with actuator faults. Their parameters are updated online based on update rules, which are designed offline to ensure the fault hiding objectives.

j) **Descriptor VAs[126, 204]** are used for fault hiding of descriptor systems with actuator faults.

k) **Adaptive Nonlinear VAs [54]** are the nonlinear version of the adaptive VAs [47, 48, 49].

l) **Moving horizon VAs [130, 131]** are DVAs whose computed reconfigured inputs are obtained by solving a Model Predictive Controls (MPCs) problem considering input constraints.

m) **Anti-windup RBs [205]** are blocks that act as virtual thrusters with the anti-windup structure to handle thruster faults and input saturation.

n) **Geometric RBs [206]** use geometric control theory for trajectory recovery after actuator faults.

2.5 Design Methodologies and Applications

In this section, an overview of the design methodologies for RBs to guarantee the fault hiding objectives.

2.5.1 Model Matching

First, the model matching approaches to design VSs and VAs for stability recovery by fault hiding. Here the concepts will be illustrated for quasi-LPV systems and blocks, but they can be adapted to other classes of systems without loss of generality.

For VSs, the design techniques are based on the analysis of the dynamics of the error $\boldsymbol{e}_{\mathrm{VS}}(t) = \boldsymbol{x}_{\mathrm{r}} - \boldsymbol{x}$ between the VS and plant states considering (2.11) and (2.19):

$$\begin{aligned}\dot{e}_{\mathrm{VS}}(t) =& \dot{\boldsymbol{x}}_{\mathrm{r}} - \dot{\boldsymbol{x}} \\ =& \boldsymbol{A}_{\Delta,\mathrm{S}}\left(\hat{\boldsymbol{z}}(\boldsymbol{x}(t))\right)\boldsymbol{x}_{\mathrm{r}}(t) + \boldsymbol{L}\left(\hat{\boldsymbol{z}}(\boldsymbol{x}(t))\right)\boldsymbol{y}(t) + \boldsymbol{B}_{\mathrm{f}}\left(\hat{\boldsymbol{z}}(\boldsymbol{x}(t))\right)\boldsymbol{u}_{\mathrm{c}}(t) \\ & - \left(\boldsymbol{A}_{\mathrm{f}}\left(\boldsymbol{z}(\boldsymbol{x}(t))\right)\boldsymbol{x}(t) + \boldsymbol{B}_{\mathrm{f}}\left(\boldsymbol{z}(\boldsymbol{x}(t))\right)\boldsymbol{u}_{\mathrm{c}}(t)\right) + \boldsymbol{A}_{\Delta,\mathrm{S}}\left(\hat{\boldsymbol{z}}(\boldsymbol{x}(t))\right)\boldsymbol{x}(t) \\ & - \boldsymbol{A}_{\Delta,\mathrm{S}}\left(\hat{\boldsymbol{z}}(\boldsymbol{x}(t))\right)\boldsymbol{x}(t) \\ =& \boldsymbol{A}_{\Delta,\mathrm{S}}\left(\hat{\boldsymbol{z}}(\boldsymbol{x}(t))\right)\boldsymbol{e}_{\mathrm{VS}}(t) + \left(\boldsymbol{A}_{\Delta,\mathrm{S}}\left(\hat{\boldsymbol{z}}(\boldsymbol{x}(t))\right) - \boldsymbol{A}_{\Delta,\mathrm{S}}\left(\boldsymbol{z}(\boldsymbol{x}(t))\right)\right)\boldsymbol{x}(t).\end{aligned} \tag{2.29}$$

For LTI systems or by assuming $\hat{\boldsymbol{z}}(\boldsymbol{x}(t)) = \boldsymbol{z}(\boldsymbol{x}(t))$ (which is the usual assumption in literature), it is reduced to

$$\dot{e}_{\mathrm{VS}}(t) = \boldsymbol{A}_{\Delta,\mathrm{S}}\left(\hat{\boldsymbol{z}}(\boldsymbol{x}(t))\right)\boldsymbol{e}_{\mathrm{VS}}(t), \tag{2.30}$$

and the asymptotic trajectory recovery is guaranteed by choosing $\boldsymbol{L}\left(\hat{\boldsymbol{z}}(\boldsymbol{x}(t))\right)$ such that $\boldsymbol{A}\left(\hat{\boldsymbol{z}}(\boldsymbol{x}(t))\right) - \boldsymbol{L}\left(\hat{\boldsymbol{z}}(\boldsymbol{x}(t))\right)\boldsymbol{C}_{\mathrm{f}}\left(\hat{\boldsymbol{z}}(\boldsymbol{x}(t))\right)$ is Hurwitz, which can be performed by vertex-wise or based on Pólya-like relaxations. Moreover, to guarantee the model matching with $\boldsymbol{y}(t) = \boldsymbol{y}_{\mathrm{r}}(t)$, the matrix $\boldsymbol{J}\left(\hat{\boldsymbol{z}}(\boldsymbol{x}(t))\right)$ is chosen as follows

$$\boldsymbol{J}\left(\hat{\boldsymbol{z}}(\boldsymbol{x}(t))\right) = \boldsymbol{C}\left(\hat{\boldsymbol{z}}(\boldsymbol{x}(t))\right)\boldsymbol{C}_{\mathrm{f}}\left(\hat{\boldsymbol{z}}(\boldsymbol{x}(t))\right)^{\dagger}. \tag{2.31}$$

If the assumption $\hat{\boldsymbol{z}}(\boldsymbol{x}(t)) = \boldsymbol{z}(\boldsymbol{x}(t))$ is not possible, then the term due to the scheduling parameter (membership degree) estimation ($\boldsymbol{A}_{\Delta,\mathrm{S}}\left(\hat{\boldsymbol{z}}(\boldsymbol{x}(t))\right) -$

$\boldsymbol{A}_{\Delta,\mathrm{S}}\left(\boldsymbol{z}(\boldsymbol{x}(t))\right)$) must be handled [105]. Similarly, in the presence of disturbance, $\boldsymbol{J}\left(\hat{\boldsymbol{z}}(\boldsymbol{x}(t))\right)$ should be modified to guarantee the disturbance decoupling [17, 18].

Likewise for VAs, under the assumption $\hat{\boldsymbol{z}}(\boldsymbol{x}(t)) = \boldsymbol{z}(\boldsymbol{x}(t))$, the stability recovery by fault hiding is guaranteed if the $\boldsymbol{A}\left(\hat{\boldsymbol{z}}(\boldsymbol{x}(t))\right) - \boldsymbol{B}_{\mathrm{f}}\left(\hat{\boldsymbol{z}}(\boldsymbol{x}(t))\right)\boldsymbol{M}\left(\hat{\boldsymbol{z}}(\boldsymbol{x}(t))\right)$ is Hurwitz. Moreover, to guarantee the model matching with $\boldsymbol{u}(t) = \boldsymbol{u}_{\mathrm{r}}(t)$, the matrix $\boldsymbol{M}\left(\hat{\boldsymbol{z}}(\boldsymbol{x}(t))\right)$ is chosen as follows

$$\boldsymbol{N}\left(\hat{\boldsymbol{z}}(\boldsymbol{x}(t))\right) = \boldsymbol{B}_{\mathrm{f}}\left(\hat{\boldsymbol{z}}(\boldsymbol{x}(t))\right)^{\dagger}\boldsymbol{B}\left(\hat{\boldsymbol{z}}(\boldsymbol{x}(t))\right). \tag{2.32}$$

2.5.2 LMI-based Stability Recovery

As discussed in the previous section, the stability recovery of plants with sensor faults by means of VSs is guaranteed by a Hurwitz $\boldsymbol{A}\left(\hat{\boldsymbol{z}}(\boldsymbol{x}(t))\right) - \boldsymbol{L}\left(\hat{\boldsymbol{z}}(\boldsymbol{x}(t))\right)\boldsymbol{C}_{\mathrm{f}}\left(\hat{\boldsymbol{z}}(\boldsymbol{x}(t))\right)$. In this sense, if the following LMI conditions are satisfied

$$\boldsymbol{Y}_{\mathrm{VS}}(i,j) = \mathrm{He}\left\{\boldsymbol{P}\boldsymbol{A}_i - \bar{\boldsymbol{L}}_j\boldsymbol{C}_{\mathrm{f},i}\right\}, \tag{2.33}$$

$$\boldsymbol{Y}_{\mathrm{VS}}(i,j) \prec \boldsymbol{0}, \quad \text{for } i = j,\ i,j \in \mathbb{N}_{\leq r}, \tag{2.34}$$

$$\boldsymbol{Y}_{\mathrm{VS}}(i,j) + \boldsymbol{Y}_{\mathrm{VS}}(j,i) \prec \boldsymbol{0}, \quad \text{for } i < j,\ i,j \in \mathbb{N}_{\leq r}, \tag{2.35}$$

for some symmetric positive definite $\boldsymbol{P}$ and matrices $\bar{\boldsymbol{L}}_j$, for $j \in \mathbb{N}_{\leq r}$, then the VS with gains given by $\boldsymbol{L}_j = \boldsymbol{P}^{-1}\bar{\boldsymbol{L}}_j$ guarantees the stability recovery by fault hiding.

Similarly, for fault hiding of plants with actuator faults by means of VAs, if the following LMI conditions

$$\boldsymbol{Y}_{\mathrm{VA}}(i,j) = \mathrm{He}\left\{\boldsymbol{A}_i\boldsymbol{X} - \boldsymbol{B}_{\mathrm{f},i}\bar{\boldsymbol{M}}_j\right\}, \tag{2.36}$$

$$\boldsymbol{Y}_{\mathrm{VA}}(i,j) \prec \boldsymbol{0}, \quad \text{for } i = j,\ i,j \in \mathbb{N}_{\leq r}, \tag{2.37}$$

$$\boldsymbol{Y}_{\mathrm{VA}}(i,j) + \boldsymbol{Y}_{\mathrm{VA}}(j,i) \prec \boldsymbol{0}, \quad \text{for } i < j,\ i,j \in \mathbb{N}_{\leq r}, \tag{2.38}$$

are satisfied for some symmetric positive definite $\boldsymbol{X}$ and matrices $\bar{\boldsymbol{M}}_j$, for $j \in \mathbb{N}_{\leq r}$, then the VA with gains given by $\boldsymbol{M}_j = \bar{\boldsymbol{M}}_j\boldsymbol{X}^{-1}$ guarantees the stability recovery by fault hiding.

The aforementioned conditions (2.33)–(2.38) are sufficient for solving the stability recovery by fault hiding problem when there are no disturbances and under assumption $\hat{\boldsymbol{z}}(\boldsymbol{x}(t)) = \boldsymbol{z}(\boldsymbol{x}(t))$. However, they can be adapted to deal with estimation

errors in scheduling parameter $\hat{\boldsymbol{z}}(\boldsymbol{x}(t)) \neq \boldsymbol{z}(\boldsymbol{x}(t))$ [105], minimizing the effect of disturbances [18], or obtaining $\mathcal{D}$-stabilization [162, 120, 119, 154, 146, 114, 115, 147] and ISS conditions [145, 128].

2.5.3 Other methods

Although most of the design approaches in the literature are variations of those discussed in Subsections 2.5.1 and 2.5.2, some other methods can be mentioned. The main alternative design methods reported in the literature are listed as follows:

a) **Sensor masking [38, 39, 207, 208]** - it is the origin of the fault hiding for sensor faults in which the sensor masking blocks act as nonlinear VSs, i.e., they act as observers which are able to recover the correct measurements before injecting it into the nominal controller.

b) **KYP Lemma [111]** - it is used to guarantee the stability recovery as a consequence of the passivity property for Hammerstein systems;

c) **Control re-allocation [209, 210]** - as in the control re-allocation, the VAs can also be designed solving a constrained optimization problem to approximate the faulty actuator effectiveness with VA to the nominal effectiveness.

d) **Backstepping [121]** - is used for designing VAs for input-affine systems.

e) **Feedback Linearization [122]** - re-linearizing terms are designed to allow the use nonlinear static VA for guaranteeing the fault hiding based on the linearized dynamics.

f) **Adaptive control [47, 48, 49, 53, 52, 54, 50, 51]** - the update laws are designed to guarantee the convergence of the adaptive VAs parameters and the fault hiding goal.

g) **Sensor reconciliation [44, 45, 158, 159, 46]** - it is also an adaptive approach which integrates the estimation of the fault parameters by LSM with the disturbance decoupling based on UIO, and fault hiding for plants with sensor faults.

h) **MPC [131, 130, 211]** - optimal receding horizon control is used to design moving horizon VAs considering input and state constraints.

i) **Stability recovery independent of internal model [127, 129]** - for RBs independent of internal model principle, it is not simple to write the error dynamics, and it is also not necessary to guarantee the convergence between the RBs and faulty systems' states. This thesis presents a solution to this problem in chapter 3 and chapter 4 based on a two-step method, where in the first step a Lyapunov function is obtained from an LMI stability analysis for the nominal system, and then the same function is used to synthesize the RBs for the faulty systems.

j) **Expert knowledge [176, 177, 175]** - In this case, fuzzy RBs are expert systems designed based on a rule base extracted from an expert's experience.

k) **Passivation-based [129, 199]** - the RBs are designed by means of LMI-based conditions to ensure that the block dissipativity properties is able to compensate for the lack of passivity due to the fault occurrence. Passivation can be used either to design the canonical RBs (VSs and VAs), or RBs independent of internal model, the latter are also known as PBs or dissipation blocks [199]. This is another contribution of this thesis presented in chapter 6.

2.6 Applications

Clearly, fault hiding is the main motivation for the existence of RBs. In particular, the practical applications of RBs for fault hiding include power systems, wind turbines, aerospace systems, vessels, robots, industrial processes, etc. Table 2.1 summarizes most of the literature on fault hiding and classifies them by applications, class of mathematical model used to represent the faulty plant, and the design methods.

Table 2.1 indicates the dominance of LMI-based design methods, in particular for plants represented by fuzzy and LPV systems. However, most of the approaches for those systems, as well as for other differential polytopic inclusions (e.g., Lipschitzian, L'ure, and PWA), are based on the internal model principle. It is still lacking applications to generic nonlinear systems, in particular without the dependence on the internal model principle.

In addition to the fault hiding applications of RBs, the recent literature exhibits alternative applications such as performance improvement of power grids and cyber-

secure control [212, 213, 214].

Table 2.1 – Literature on fault hiding, design methods and applications.

Classes of systems	Design methods: Model-matching	LMI-based	Adaptive and Nonlinear Methods	Stability recovery w/o internal model and Passivation	Other methods
LTI	Thermofluid processes [108, 132, 16, 134, 203], Hydraulic systems [17, 110, 7, 133, 215], Aerospace systems [109, 17, 16, 116, 193, 216, 191, 183], Power systems [210, 217], Boiler-turbine [218], Numerical examples [113, 219, 220]	Vessels [18], Aircrafts [189], Thermofluid processes [103], Power systems [221, 204, 185], Flexible manipulators [222], Wind turbines [223], Hydraulic systems [103, 224, 189], Numerical examples [126, 168, 225, 104, 195, 206]	a) Adaptive: Vessels [53, 49] b) Sensor reconciliation: Numerical example [45]	a) Stability recovery: Vessel [226] b) Passivation: Aircraft [106], Heat exchange system [106], and Hydraulic system [199]	a) Control re-allocation: Hydraulic systems [209], Vessels [76, 77], Aerospace vehicles [192] b) Sensor masking: Winding machine [207] c) KYP Lemma: Aircraft [106] d) MPC: Hydraulic systems [211], and Chemical processes [130, 131, 227]
Hammerstein-Wiener	-	Thermofluid processes [18], Vessels [18], Hydraulic systems [102], Aerospace systems [196]	-	a) Stability recovery: Vessel [226]	a) KYP Lemma: Hydraulic systems [111], Electric motors [198]
PWA	-	Thermofluid processes [18], Vessels [18], Hydraulic systems [18, 112, 136]	-	-	-
LPV	Wind turbines [160], and Numerical examples [228]	Aerospace vehicles [114, 115, 147, 149, 148], Hydraulic systems [120, 128], Wind turbines [119], Ground mobile robots [146], Fuel cells [154], Induction motors [145], Turbofan engines [229, 161], and Numerical examples [144, 150, 152, 123, 155, 153, 157, 156, 194]	a) Sensor reconciliation: Hydraulic systems [46], and Numerical examples [44, 159, 158]	-	a) Sensor masking: Hot rolling mill [208]
Fuzzy	-	Aerospace vehicles [167], Fuel cells [162], Hydraulic systems [164, 165, 163], Hydraulic systems [105], Microgrids [166], and Numerical examples [117]	-	a) Stability recovery: Power system [127]	a) Expert knowledge: Greenhouses [175], Ground mobile robots [176, 177]
L'ure and Lipschitzian	-	Drilling gear [118], Power systems [142, 143], Robot manipulators [140, 141, 230]	a) Adaptive: Aircrafts [47], Numerical examples [51]	-	-
Distributed, MASs, LSSs and NCSs	Hydraulic systems [187, 188], Aerospace vehicles [183, 101], and Numerical examples [135, 182]	Power systems [179], Industrial processes [100], Hydraulic systems [180], and Numerical examples [186, 184]	a) Adaptive: Aircrafts [48, 54, 52], Vessels [50], Flexible manipulators [54]	a) Stability recovery: Network of pendulums [129]	-
Other nonlinear systems	-	-	a) Backstepping: Vessels [121] b) Feedback linearization: Thermofluid processes [122]	a) Passivation: Numerical examples [106, 106]	a) Sensor masking : Vessels [38, 39] b) Control re-allocation: Vessels [205]

3 STABILITY RECOVERY OF LINEAR SYSTEMS WITH INPUT SATURATION

This chapter addresses the problem of stability recovery by fault hiding of linear systems by means of SRBs whose parameters do not depend on internal model principle or pseudo-inverse method. In particular, novel conditions for stability recovery by fault hiding are presented based on the a novel SRB structure and on the Lyapunov stability theory. In section 3.1, the stability recovery by fault hiding problem is presented. In section 3.2, the general idea for obtaining RBs structures that are able to ensure the recovery is provided. In section 3.4, conditions for stability recovery for linear systems and systems with input saturation are given. The results presented in this chapter are based on those ones previously published in [226].

3.1 Problem statement

Consider the plant whose nominal (fault-free) dynamics is described by the following linear model Σ_{P} with input saturation

$$\Sigma_{\mathrm{P}}: \begin{cases} \dot{\boldsymbol{x}}(t) = \boldsymbol{A}\boldsymbol{x}(t) + \boldsymbol{B}\mathrm{sat}\left(\boldsymbol{u}_{\mathrm{p}}(t)\right), \\ \boldsymbol{y}_{\mathrm{p}}(t) = \boldsymbol{C}\boldsymbol{x}(t), \end{cases} \tag{3.1}$$

where $\boldsymbol{x}(t) \in \mathbb{R}^n$ is the state vector, $\boldsymbol{u}_{\mathrm{p}}(t) \in \mathbb{R}^m$ is the plant input vector, $\boldsymbol{y}_{\mathrm{p}}(t) \in \mathbb{R}^p$ is the plant output vector, $\boldsymbol{A}$, $\boldsymbol{B}$, and $\boldsymbol{C}$ are state-space matrices with appropriate dimensions, and the input $\boldsymbol{u}_{\mathrm{p}}(t)$ is subject to the component-wise saturation map $\mathrm{sat}\left(\cdot\right) : \mathbb{R}^m \to \mathbb{R}^m$ defined as

$$\mathrm{sat}\left(u_{\mathrm{p},(l)}\right) = \max\left\{\min\left\{u_{\mathrm{p},(l)}, \bar{u}_{\mathrm{p},(l)}\right\}, -\bar{u}_{\mathrm{p},(l)}\right\}, \quad \forall l \in \mathbb{N}_{\leq m}, \tag{3.2}$$

where $\bar{u}_{\mathrm{p},(l)} \in \mathbb{R}_{>0}$ is the bound of the l-th entry $u_{\mathrm{p},(l)}$ of the control input $\boldsymbol{u}_{\mathrm{p}}(t)$ due to the actuator saturation.

As depicted in Figure 3.1, the plant is connected to the output-feedback controller Σ_{C} described as follows

$$\Sigma_{\mathrm{C}}: \begin{cases} \dot{\boldsymbol{x}}_{\mathrm{c}}(t) = \boldsymbol{A}_{\mathrm{c}}\boldsymbol{x}_{\mathrm{c}}(t) + \boldsymbol{B}_{\mathrm{c}}\boldsymbol{y}_{\mathrm{c}}(t), \\ \boldsymbol{u}_{\mathrm{c}}(t) = \boldsymbol{C}_{\mathrm{c}}\boldsymbol{x}_{\mathrm{c}}(t), \end{cases} \tag{3.3}$$

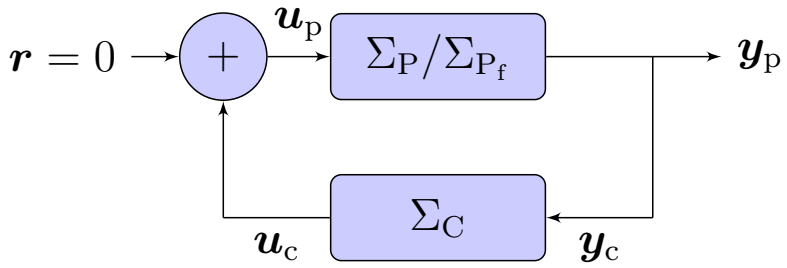

Figure 3.1 – Feedback interconnection between Σ_P (or $\Sigma_{\mathrm{P_f}}$) and Σ_C.

where $\boldsymbol{x}_\mathrm{c}(t) \in \mathbb{R}^{n_\mathrm{c}}$, and $\boldsymbol{A}_\mathrm{c}$, $\boldsymbol{B}_\mathrm{c}$, and $\boldsymbol{C}_\mathrm{c}$ are matrices with appropriate dimensions. For the same plant whose nominal model is given by (3.1) , the faulty dynamics is described by the following model $\Sigma_{\mathrm{P_f}}$:

$$\Sigma_{\mathrm{P_f}} : \begin{cases} \dot{\boldsymbol{x}}(t) = \boldsymbol{A}\boldsymbol{x}(t) + \boldsymbol{B}_\mathrm{f}\mathrm{sat}\left(\boldsymbol{u}_\mathrm{p}(t)\right), \\ \boldsymbol{y}_\mathrm{p}(t) = \boldsymbol{C}_\mathrm{f}\boldsymbol{x}(t), \end{cases} \tag{3.4}$$

where $\boldsymbol{B}_\mathrm{f}$ and $\boldsymbol{C}_\mathrm{f}$ are state-space matrices which represent the effects of, respectively, actuator and sensor multiplicative faults. In particular, let the nominal model matrices $\boldsymbol{B}$ and $\boldsymbol{C}$ be

$$\boldsymbol{B} = \left[\boldsymbol{B}_1\ \boldsymbol{B}_2\ \ldots\ \boldsymbol{B}_m\right],$$
$$\boldsymbol{C} = \left[\boldsymbol{C}_1^\top\ \boldsymbol{C}_2^\top\ \boldsymbol{C}_p^\top\right]^\top.$$

if the i-th actuator fails, the i-th column of B ($\boldsymbol{B}_i$) is modified. A total loss in the i-th actuator is represented by replacing $\boldsymbol{B}_i$ with 0, and efficiency loss is represented by replacing $\boldsymbol{B}_i$ with $f_{\mathrm{s},i} \cdot B_i$, for $0 \leq f_{\mathrm{a},i} \leq 1$, where $f_{a,i}$ is the i-th element of $\boldsymbol{f}_a$. In other words, the actuator fault matrix $\boldsymbol{B}_\mathrm{f}$ is

$$\boldsymbol{B}_\mathrm{f} = \boldsymbol{B}\mathrm{diag}\left\{\boldsymbol{f}_\mathrm{a}\right\}.$$

Similarly, for sensor faults in the i-th sensor, the fault model is obtained by substituting $\boldsymbol{C}_i$ with $f_{\mathrm{a},i} \cdot C_i$, for $0 \leq f_{\mathrm{s},i} \leq 1$, where $f_{\mathrm{s},i}$ is the i-th element of $\boldsymbol{f}_s$, i.e.,

$$\boldsymbol{C}_\mathrm{f} = \mathrm{diag}\left\{\boldsymbol{f}_s\right\}\boldsymbol{C}.$$

In this chapter, the faulty model's parameters $\boldsymbol{f}_\mathrm{a}$ and $\boldsymbol{f}_\mathrm{s}$ are assumed to be precisely and timely known, as stated in the next assumption.

Assumption 3.1. *The estimation of fault parameters $\boldsymbol{f}_{\mathrm{a}}$ and $\boldsymbol{f}_{\mathrm{s}}$ is assumed to be always available and accurate.*

Remark 3.1. *This assumption is considered because this thesis is focused only on the FTC problem. Although the approaches proposed in this thesis are based on RBs whose parameters are not explicitly dependent on the fault model's parameters, it is still necessary to use them for tuning the RB gains. In practice, those parameters are provided by a FDI system that classifies and estimates the fault parameters. Naturally, the FDI is subject to estimation errors, delays, and fault misclassification which may lead to the loss of reconfiguration guarantees. Only a few works address the fault hiding under those FDI imperfections, for example, the FDI delays are considered in [123], and the design of RBs robust to several classes of faults is addressed in [128, 105]. The novel RBs proposed in this thesis can ease the development of fault hiding approaches aware of FDI imperfections, however, it is out of the scope of this thesis.*

To recover the stability after fault occurrence, the following SRBs Σ_{R} is inserted between $\Sigma_{\mathrm{P_f}}$ and Σ_{C}:

$$\Sigma_{\mathrm{R}}: \begin{cases} \boldsymbol{y}_{\mathrm{r}}(t) = \boldsymbol{R}_1 \boldsymbol{y}_{\mathrm{p}}(t) + \boldsymbol{R}_2 \boldsymbol{u}_{\mathrm{c}}(t), \\ \boldsymbol{u}_{\mathrm{r}}(t) = \boldsymbol{R}_3 \boldsymbol{y}_{\mathrm{p}}(t) + \boldsymbol{R}_4 \boldsymbol{u}_{\mathrm{c}}(t), \end{cases} \tag{3.5}$$

where $\boldsymbol{R}_1$, $\boldsymbol{R}_2$, $\boldsymbol{R}_3$, and $\boldsymbol{R}_4$ are the matrix gains of Σ_{R} which are designed to solve the following problem. The RB in (3.5) can be used for both sensor and actuator faults, what does not occur in the classic static VSs and VAs presented in [17].

Problem 3.1. ***Asymptotic Stability Recovery by Fault Hiding for Linear Systems with Input Saturation***

Let Σ_{P} and $\Sigma_{\mathrm{P_f}}$ be the nominal and the faulty models, respectively, with dynamics described by (3.1) *and* (3.4) *for a plant interconnected by feedback to controller Σ_{C}. Assume that the origin of $(\Sigma_{\mathrm{P}}, \Sigma_{\mathrm{C}})$ is asymptotically stable. Find the gains $\boldsymbol{R}_1$, $\boldsymbol{R}_2$, $\boldsymbol{R}_3$, and $\boldsymbol{R}_4$ of the RB Σ_{R} (cf.* (3.5)*), such that the origin of the reconfigured system $(\Sigma_{\mathrm{P_f}}, \Sigma_{\mathrm{R}}, \Sigma_{\mathrm{C}})$ is also asymptotically stable.*

In the remainder of this chapter, for the sake of simplicity, the time dependence is omitted in some variables, e.g., $x(t)$ is simply denoted x.

3.2 Overview of stability recovery

This section presents the concept of stability recovery by fault hiding in Definition 3.1. In addition, it is presented a general procedure for obtaining sufficient conditions for the existence of Σ_{R} that is able to recover the stability of faulty system by fault hiding when the origin of interconnected autonomous nominal system $(\Sigma_{\mathrm{P}}, \Sigma_{\mathrm{C}})$ is stable before the fault occurrence.

Definition 3.1. ***Stability recovery by fault hiding***
Let Σ_{P} and $\Sigma_{\mathrm{P_f}}$ be nominal and faulty models with dynamics described respectively as (3.1) *and* (3.4) *for the same system interconnected by feedback to a controller Σ_{C} as depicted in Figure 3.1. Assuming that the origin of $(\Sigma_{\mathrm{P}}, \Sigma_{\mathrm{C}})$ is asymptotically stable, then $\Sigma_{\mathrm{P_f}}$ is stable by fault hiding if there exists a reconfiguration block Σ_{R} described by* (3.5) *such that the origin of $(\Sigma_{\mathrm{P_f}}, \Sigma_{\mathrm{R}}, \Sigma_{\mathrm{C}})$ is also asymptotically stable. In this case, Σ_{R} is a solution of Problem 3.1.*

The stability recovery by fault hiding problem is usually solved in the literature [18] through the stability analysis of the error dynamics between the nominal system response and reconfigured system response. According to this analysis, $\Sigma_{\mathrm{P_f}}$ is stable if there exists some Σ_{R} such that the origin of the error dynamics is asymptotically stable [18]. In this thesis proposal, a different procedure is used for obtaining a Σ_{R} that solves the stability recovery by fault hiding problem. In the proposed solution, a Lyapunov function that it is used to show the asymptotic stability of the origin of $(\Sigma_{\mathrm{P}}, \Sigma_{\mathrm{C}})$ is found, i.e., the derivative of Lyapunov function is negative definite. Then, the origin of the reconfigured system $(\Sigma_{\mathrm{P_f}}, \Sigma_{\mathrm{R}}, \Sigma_{\mathrm{C}})$ is also stable if there is a Σ_{R} such that the derivative of the same Lyapunov function is also negative-definite for $(\Sigma_{\mathrm{P_f}}, \Sigma_{\mathrm{R}}, \Sigma_{\mathrm{C}})$. This procedure is formalized by means of Lemma 3.1.

Lemma 3.1. *Let Σ_{P} and $\Sigma_{\mathrm{P_f}}$ be nominal and faulty models, respectively, with dynamics described in* (3.1) *and* (3.4) *considering the same plant. Let Σ_{C} be an output feedback controller interconnected as depicted in Figure 3.1, such that the origin of $(\Sigma_{\mathrm{P}}, \Sigma_{\mathrm{C}})$ is asymptotically stable. If there exist a Σ_{R} and a positive definite continuously differentiable $V(\cdot)$ such that $\frac{\partial V}{\partial \boldsymbol{x}} \boldsymbol{f}(\boldsymbol{x}, \boldsymbol{u}_c) \leq 0$ and $\frac{\partial V}{\partial \boldsymbol{x}} \boldsymbol{f}_{\mathrm{f}}(\boldsymbol{x}, \boldsymbol{u}_r) < 0$, then $\Sigma_{\mathrm{P_f}}$ is stable by fault hiding with the proposed Σ_{R}.*

Proof. Figure 3.1 depicts the interconnection between Σ_{P} ($\Sigma_{\mathrm{P_f}}$) and Σ_{C} with zero input. According to [139, Theorem 4.14], if the unforced origin of $(\Sigma_{\mathrm{P}}, \Sigma_{\mathrm{C}})$ is stable, then there exists a positive definite continuously differentiable $V(\cdot)$ such that $\frac{\partial V}{\partial \boldsymbol{x}} \boldsymbol{f}(\boldsymbol{x}, \boldsymbol{u}_c) \leq 0$. Assume that the same $V(\boldsymbol{x})$ is a Lyapunov candidate for $(\Sigma_{\mathrm{P_f}}, \Sigma_{\mathrm{R}}, \Sigma_{\mathrm{C}})$. If there exists Σ_{R} such that $\frac{\partial V}{\partial \boldsymbol{x}} f_{\mathrm{f}}(\boldsymbol{x}, \boldsymbol{u}_r) \leq 0$, then the unforced origin of $(\Sigma_{\mathrm{P_f}}, \Sigma_{\mathrm{R}}, \Sigma_{\mathrm{C}})$ is asymptotically stable. Therefore $\Sigma_{\mathrm{P_f}}$ is stable by fault hiding according to Definition 3.1. □

Lemma 3.1 provides the general procedure for obtaining sufficient conditions for stability by fault hiding from a Lyapunov function inherited from the nominal system which is assumed stable. It proposes a two-steps procedures, where the Lyapunov function that indicates the stability of the nominal synthesis is obtained in the first analysis step, that is followed by a synthesis step wherein the RB is designed to guarantee the stability recovery according to the same Lyapunov function. This procedure is employed in the next sections to obtain conditions for stability by fault hiding with the SRBs in (3.5) as depicted in Fig. 3.1.

Remark 3.2. *In this chapter, it is exploited the idea of re-using the same Lyapunov function to induce the asymptotic stability recovery by inserting an RB in the loop which also guarantees the negativity of* $\frac{\partial V}{\partial \boldsymbol{x}} f_{\mathrm{f}}(\boldsymbol{x}, \boldsymbol{u}_r)$. *This approach is convenient to guarantee the linearity of the matrix inequalities, presented in the next results of this chapter, used to obtain sufficient stabilization by fault hiding conditions. However, it is clear that several solutions could be employed to achieve similar guarantees with a different Lyapunov function for the RB design. One can notice the similarity between this synthesis problem with the LMI-based design of SOF controllers. The design of SOF controllers is challenging per si due to the non-convex characterization [231]. Several studies have been carried out attempting to provide numerically tractable solutions for SOF control design, such as two-step and iterative methods [232], and the use of slack variables with a lower-triangular structure [233]. SOF* $\mathcal{H}_\infty$ *gain-scheduling control design conditions are presented for LPV systems in [234, 231]. In particular, those conditions are not based on iterative methods and do not require constraints over the system's structure or the gain-scheduled control law. Those approaches could be adapted to deal with the problem of LMI-based design of RBs proposed in this thesis for fault hiding of polytopic differential inclusions. Indeed, the re-use of the Lyapunov*

function obtained at the analysis poses some pros and cons. On the one hand, it guarantees some local properties. The level sets of this Lyapunov function are also positively invariant after the reconfiguration, which guarantees the same estimation of the domain of attraction. On the other hand, it increases the conservativeness of the design conditions that may become unfeasible for the same Lyapunov function.

3.3 Static Reconfiguration Blocks for Stability Recovery of Linear Systems

The following Theorem 3.1 is an original contribution of this thesis. It provides condition to design the SRB Σ_{R} in (3.5) for solving the Problem 3.1 for LTI systems (cf. (3.1), (3.2) and (3.4)) without input saturation, i.e., $u_{\mathrm{p},(l)} = \infty,\ \forall l \in \mathbb{N}_{\leq m}$ and interconnected to the controller Σ_{C} (cf. (3.3)).

Theorem 3.1. *Let Σ_{P} and $\Sigma_{\mathrm{P_f}}$ be the nominal and faulty models for a plant interconnected to an output feedback controller Σ_{C} such that there exists a symmetric positive definite matrices $\boldsymbol{P}_{11}$ and $\boldsymbol{P}_{22}$, and a matrix $\boldsymbol{P}_{12}$ satisfying*

$$\boldsymbol{P}\tilde{\boldsymbol{A}} + \tilde{\boldsymbol{A}}^{\top}\boldsymbol{P} \prec 0, \tag{3.6}$$

where

$$\boldsymbol{P} = \begin{bmatrix} \boldsymbol{P}_{11} & \boldsymbol{P}_{12} \\ \star & \boldsymbol{P}_{22} \end{bmatrix}, \tag{3.7}$$

$$\tilde{\boldsymbol{A}} \triangleq \begin{bmatrix} \boldsymbol{A} & \boldsymbol{B}\boldsymbol{C}_{\mathrm{c}} \\ \boldsymbol{B}_{\mathrm{c}}\boldsymbol{C} & \boldsymbol{A}_{\mathrm{c}} \end{bmatrix}. \tag{3.8}$$

$\Sigma_{\mathrm{P_f}}$ is stable by fault hiding, with Σ_{R} described in (3.5)*, if there exist $\boldsymbol{R}_1$, $\boldsymbol{R}_2$, $\boldsymbol{R}_3$, and $\boldsymbol{R}_4$ satisfying the following inequality:*

$$\begin{bmatrix} \boldsymbol{L}_{11} & \boldsymbol{L}_{12} \\ \star & \boldsymbol{L}_{22} \end{bmatrix} \prec 0, \tag{3.9}$$

$$\begin{aligned}
\boldsymbol{L}_{11} &= \mathrm{He}\left\{\boldsymbol{P}_{11}(\boldsymbol{A} + \boldsymbol{B}_{\mathrm{f}}\boldsymbol{R}_3\boldsymbol{C}_{\mathrm{f}}) + \boldsymbol{P}_{12}\boldsymbol{B}_{\mathrm{c}}\boldsymbol{R}_1\boldsymbol{C}_{\mathrm{f}}\right\}, \\
\boldsymbol{L}_{12} &= \mathrm{He}\left\{\boldsymbol{P}_{11}\boldsymbol{B}_{\mathrm{f}}\boldsymbol{R}_4\boldsymbol{C}_{\mathrm{c}} + \boldsymbol{P}_{12}(\boldsymbol{A}_{\mathrm{c}} + \boldsymbol{B}_{\mathrm{c}}\boldsymbol{R}_2\boldsymbol{C}_{\mathrm{c}})\right\} \\
\boldsymbol{L}_{22} &= \mathrm{He}\left\{\boldsymbol{P}_{12}\boldsymbol{B}_{\mathrm{f}}\boldsymbol{R}_4\boldsymbol{C}_{\mathrm{c}} + \boldsymbol{P}_{22}(\boldsymbol{A}_{\mathrm{c}} + \boldsymbol{B}_{\mathrm{c}}\boldsymbol{R}_2\boldsymbol{C}_{\mathrm{c}})\right\}
\end{aligned}$$

Proof. The interconnection between (3.1) and (3.3) is equivalent to consider $\boldsymbol{u} = \boldsymbol{u}_c$ and $\boldsymbol{y}_c = \boldsymbol{y}$, thus the following autonomous system is obtained

$$(\Sigma_{\mathrm{P}}, \Sigma_{\mathrm{C}}) : \begin{cases} \dot{\boldsymbol{x}} = \boldsymbol{A}\boldsymbol{x} + \boldsymbol{B}\boldsymbol{C}_{\mathrm{c}}\boldsymbol{x}_{\mathrm{c}}, \\ \dot{\boldsymbol{x}}_{\mathrm{c}} = \boldsymbol{B}_{\mathrm{c}}\boldsymbol{C}\boldsymbol{x} + \boldsymbol{A}_{\mathrm{c}}\boldsymbol{x}_{\mathrm{c}}. \end{cases} \tag{3.10}$$

By defining $\tilde{\boldsymbol{x}} \triangleq [\boldsymbol{x}^\top \ \boldsymbol{x}_{\mathrm{c}}^\top]^\top$, (3.10) is equivalent to $\dot{\tilde{\boldsymbol{x}}} = \tilde{\boldsymbol{A}}\tilde{\boldsymbol{x}}$. If the origin of $(\Sigma_{\mathrm{P}}, \Sigma_{\mathrm{C}})$ is asymptotically stable, then there exists a Lyapunov function $V(\tilde{\boldsymbol{x}}) = \tilde{\boldsymbol{x}}^\top \boldsymbol{P}\tilde{\boldsymbol{x}}$ (cf. [139, Theorem 4.14]), such that

$$\boldsymbol{P} = \boldsymbol{P}^\top = \begin{bmatrix} \boldsymbol{P}_{11} & \star \\ \boldsymbol{P}_{12} & \boldsymbol{P}_{22} \end{bmatrix} \succ 0,$$

$$\boldsymbol{P}\tilde{\boldsymbol{A}} + \tilde{\boldsymbol{A}}^\top \boldsymbol{P} \prec 0,$$

The reconfigured interconnection of faulty system $(\Sigma_{\mathrm{P_f}}, \Sigma_{\mathrm{R}}, \Sigma_{\mathrm{C}})$ is the following autonomous system obtained by applying $\boldsymbol{y}_{\mathrm{c}} = \boldsymbol{y}_{\mathrm{r}}$ and $\boldsymbol{u} = \boldsymbol{u}_{\mathrm{r}}$ to (3.4) and (3.3)

$$(\Sigma_{\mathrm{P_f}}, \Sigma_{\mathrm{R}}, \Sigma_{\mathrm{C}}) : \begin{cases} \dot{\boldsymbol{x}} = (\boldsymbol{A} + \boldsymbol{B}_{\mathrm{f}}\boldsymbol{R}_3\boldsymbol{C}_{\mathrm{f}})\boldsymbol{x} + \boldsymbol{B}_{\mathrm{f}}\boldsymbol{R}_4\boldsymbol{C}_c\boldsymbol{x}_c, \\ \dot{\boldsymbol{x}}_c = \boldsymbol{B}_c\boldsymbol{R}_1\boldsymbol{C}_{\mathrm{f}}\boldsymbol{x} + (\boldsymbol{A}_c + \boldsymbol{B}_c\boldsymbol{R}_2\boldsymbol{C}_c)\boldsymbol{x}_{\mathrm{c}}, \end{cases} \tag{3.11}$$

that is equivalent to $\dot{\tilde{\boldsymbol{x}}} = \tilde{\boldsymbol{A}}_{\mathrm{r}}\tilde{\boldsymbol{x}}$ where

$$\tilde{\boldsymbol{A}}_{\mathrm{r}} \triangleq \begin{bmatrix} \boldsymbol{A} + \boldsymbol{B}_{\mathrm{f}}\boldsymbol{R}_3\boldsymbol{C}_{\mathrm{f}} & \boldsymbol{B}_{\mathrm{f}}\boldsymbol{R}_4\boldsymbol{C}_{\mathrm{c}} \\ \boldsymbol{B}_{\mathrm{c}}\boldsymbol{R}_1\boldsymbol{C}_{\mathrm{f}} & \boldsymbol{A}_{\mathrm{c}} + \boldsymbol{B}_{\mathrm{c}}\boldsymbol{R}_2\boldsymbol{C}_{\mathrm{c}} \end{bmatrix}, \tag{3.12}$$

According to Lemma 3.1, the same Lyapunov function $V(\tilde{\boldsymbol{x}}) = \tilde{\boldsymbol{x}}^\top \boldsymbol{P}\tilde{\boldsymbol{x}}$ (with the same positive definite matrix $\boldsymbol{P}$) may be used for the reconfigured system. Then, the origin of $(\Sigma_{\mathrm{P}}, \Sigma_{\mathrm{R}}, \Sigma_{\mathrm{C}})$ is asymptotically stable if

$$\boldsymbol{P}\tilde{\boldsymbol{A}}_{\mathrm{r}} + \tilde{\boldsymbol{A}}_{\mathrm{r}}^\top \boldsymbol{P} \prec 0. \tag{3.13}$$

Notice that (3.13) is equivalent to (3.9). Therefore, if there exist $\boldsymbol{R}_1$, $\boldsymbol{R}_2$, $\boldsymbol{R}_3$, and $\boldsymbol{R}_4$ satisfying (3.9), then $\Sigma_{\mathrm{P_f}}$ is stable by fault hiding. □

The next Corollary 3.1 extends the result of Theorem 3.1 for the case wherein the output feedback controller is static.

Corollary 3.1. *Let Σ_{P} and $\Sigma_{\mathrm{P_f}}$ be the nominal and faulty models for a plant interconnected to a static output feedback controller Σ_{C} described as follows*

$$\Sigma_{\mathrm{C}} : \boldsymbol{u}_{\mathrm{c}} = \boldsymbol{K}\boldsymbol{y}_{\mathrm{c}}, \tag{3.14}$$

such that the following inequality is satisfied for some symmetric positive definite matrix $\boldsymbol{P}$:

$$\boldsymbol{P}\left(\boldsymbol{A}+\boldsymbol{B}\boldsymbol{K}\boldsymbol{C}\right)+\left(\boldsymbol{A}+\boldsymbol{B}\boldsymbol{K}\boldsymbol{C}\right)^{\top}\boldsymbol{P} \prec 0. \tag{3.15}$$

$\Sigma_{\mathrm{P_f}}$ is stable by fault hiding, with Σ_{R} described in (3.5) *with $\boldsymbol{R}_1 = \boldsymbol{I}$ and $\boldsymbol{R}_2 = \boldsymbol{0}$, if there exist matrices $\boldsymbol{R}_3$ and $\boldsymbol{R}_4$ satisfying the following inequality:*

$$\boldsymbol{P}\tilde{\boldsymbol{A}}_{\mathrm{r}} + \tilde{\boldsymbol{A}}_{\mathrm{r}}^{\top}\boldsymbol{P} \prec 0, \tag{3.16}$$

where $\tilde{\boldsymbol{A}}_{\mathrm{r}} = \boldsymbol{A} + \boldsymbol{B}_{\mathrm{f}}\boldsymbol{R}_3\boldsymbol{C}_{\mathrm{f}} + \boldsymbol{B}_{\mathrm{f}}\boldsymbol{R}_4\boldsymbol{K}\boldsymbol{C}_{\mathrm{f}}$.

Proof. The same reasoning of the proof of Theorem 3.1 can be used here. However, if Σ_{C} is a static output feedback controller as (3.14), it is redundant to compensate $\boldsymbol{u}_{\mathrm{c}}$ and $\boldsymbol{y}$, since these signals are proportional due to the controller structure, then it is chosen $\boldsymbol{y}_{\mathrm{r}} = \boldsymbol{y}$, therefore $\boldsymbol{R}_1 = \boldsymbol{I}$ and $\boldsymbol{R}_2 = \boldsymbol{0}$. In addition, $(\Sigma_{\mathrm{P}}, \Sigma_{\mathrm{C}})$ and $(\Sigma_{\mathrm{P_f}}, \Sigma_{\mathrm{R}}, \Sigma_{\mathrm{C}})$ are changed to

$$(\Sigma_{\mathrm{P}}, \Sigma_{\mathrm{C}}) : \dot{\boldsymbol{x}} = \left(\boldsymbol{A}+\boldsymbol{B}\boldsymbol{K}\boldsymbol{C}\right)\boldsymbol{x},$$

$$(\Sigma_{\mathrm{P_f}}, \Sigma_{\mathrm{R}}, \Sigma_{\mathrm{C}}) : \dot{\boldsymbol{x}} = (\boldsymbol{A} + \boldsymbol{B}_{\mathrm{f}}\boldsymbol{R}_3\boldsymbol{C}_{\mathrm{f}} + \boldsymbol{B}_{\mathrm{f}}\boldsymbol{R}_4\boldsymbol{K}\boldsymbol{C}_{\mathrm{f}})\boldsymbol{x},$$

i.e., (3.16) is equivalent to (3.13) for $\tilde{\boldsymbol{A}}_{\mathrm{r}} = \boldsymbol{A} + \boldsymbol{B}_{\mathrm{f}}\boldsymbol{R}_3\boldsymbol{C}_{\mathrm{f}} + \boldsymbol{B}_{\mathrm{f}}\boldsymbol{R}_4\boldsymbol{K}\boldsymbol{C}_{\mathrm{f}}$. □

Example 3.1. *Consider the closed-loop system $(\Sigma_{\mathrm{P}}, \Sigma_{\mathrm{C}})$ connected as Fig. 3.1, where Σ_{P} is described by* (3.1) *and*

$$\Sigma_{\mathrm{C}} : \begin{cases} \dot{\boldsymbol{x}}_{\mathrm{c}} = (\boldsymbol{A}+\boldsymbol{L}\boldsymbol{C})\boldsymbol{x}_{\mathrm{c}} - \boldsymbol{L}\boldsymbol{y}_{\mathrm{c}}, \\ \boldsymbol{u}_{\mathrm{c}} = \boldsymbol{K}\boldsymbol{x}_{\mathrm{c}}, \end{cases}$$

$$\boldsymbol{A} = \begin{bmatrix} 1 & 2 \\ 2 & -1.5 \end{bmatrix}, \quad \boldsymbol{B} = \begin{bmatrix} 4 & 1 \\ 0.5 & 1 \end{bmatrix}, \quad \boldsymbol{C} = \begin{bmatrix} 1 & 0 \end{bmatrix},$$

$$\boldsymbol{K} = \begin{bmatrix} -0.2357 & -0.8071 \\ -0.8071 & 1.1536 \end{bmatrix}, \quad \boldsymbol{L} = \begin{bmatrix} -0.9000 \\ -3.5333 \end{bmatrix}.$$

In this simulation, it is considered the complete loss of the first actuator due to an actuator fault that changes matrix $\boldsymbol{B}$ *to* $\boldsymbol{B}_{\mathrm{f}}$ *occurs at* $t = 0.75$ *s, such that:*

$$\boldsymbol{B}_{\mathrm{f}} = \begin{bmatrix} 0 & 1 \\ 0 & 1 \end{bmatrix}.$$

By using $V(\tilde{\boldsymbol{x}}) = \tilde{\boldsymbol{x}}^{\top}\boldsymbol{P}\tilde{\boldsymbol{x}}$*, it is possible to show that the origin of* $(\Sigma_{\mathrm{P}}, \Sigma_{\mathrm{C}})$ *is stable since there is a* $\boldsymbol{P} = \boldsymbol{P}^{\top} \succ 0$ *that satisfies* $\boldsymbol{P}\tilde{\boldsymbol{A}} + \tilde{\boldsymbol{A}}^{\top}\boldsymbol{P} \prec 0$ *for* $\tilde{\boldsymbol{A}}$ *given by* (3.8)*, where* $\boldsymbol{A}_{\mathrm{c}} = \boldsymbol{A} + \boldsymbol{L}\boldsymbol{C}$*,* $\boldsymbol{B}_{\mathrm{c}} = -\boldsymbol{L}$*, and* $\boldsymbol{C}_{\mathrm{c}} = \boldsymbol{K}$*. Solving that LMI in MATLAB environment using the YALMIP parser [235] with the MOSEK solver [236], the following* $\boldsymbol{P}$ *matrix is obtained:*

$$\boldsymbol{P} = \begin{bmatrix} 2.0065 & 0.6773 & -0.6369 & -0.7026 \\ 0.6773 & 1.2657 & -0.6606 & -1.1612 \\ -0.6369 & -0.6606 & 0.8784 & 0.7570 \\ -0.7026 & -1.1612 & 0.7570 & 1.5028 \end{bmatrix}. \tag{3.17}$$

According to Theorem 3.1, the same $\boldsymbol{P}$ *matrix in* (3.17) *can be used to solve* (3.9) *and find* $\boldsymbol{R}_1$*,* $\boldsymbol{R}_2$*,* $\boldsymbol{R}_3$*, and* $\boldsymbol{R}_4$ *to reconfigure* $\Sigma_{\mathrm{P_f}}$*. Then, solving* (3.9) *in MATLAB environment using the YALMIP parser [235] with the MOSEK solver [236], the following reconfiguration block gains are obtained:*

$$\boldsymbol{R}_1 = 0.9947 \quad \boldsymbol{R}_2 = \begin{bmatrix} 0.6938 & -0.0742 \end{bmatrix},$$

$$\boldsymbol{R}_3 = \begin{bmatrix} 0 \\ -0.0475 \end{bmatrix} \quad \boldsymbol{R}_4 = \begin{bmatrix} 0 & 0 \\ 3.8429 & 0.8129 \end{bmatrix}.$$

Figures 3.2-3.7 present the simulation results with the proposed RB for $\Sigma_{\mathrm{P_f}}$ *for initial conditions* $\tilde{\boldsymbol{x}}(0) = [1.5 \quad -0.25 \quad 0 \quad 0]^{\top}$*. In particular, Figure 3.2 compares the output of* $\Sigma_{\mathrm{P_f}}$ *with and without the proposed RB. Note that, the system response without RB becomes unstable after the fault occurrence (*$t = 0.75$ *s) while the response with the proposed RB converges to the equilibrium point.*

The proposed SRB provides to corrective faults during the reconfiguration. The first action is the reconfiguration of the measurement signal $\boldsymbol{y}_{\mathrm{p}}$ *by injecting a signal* $\boldsymbol{y}_{\mathrm{r}}$ *into the controller by hiding the fault effects from this controller. Figures 3.3*

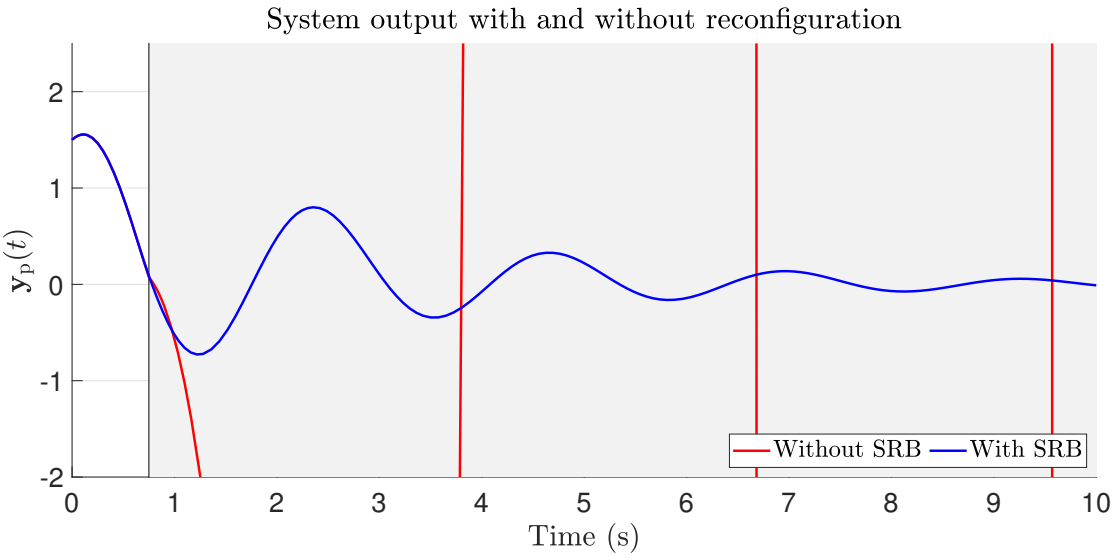

Figure 3.2 – Comparison between the output of faulty plant with and without RB.

and 3.4 depict the controller signals with and without SRB, and Figure 3.5 depicts the measurement signal injected into the controller with and without reconfiguration. Notice that the signal $\boldsymbol{y}_r$ is slightly modifies the plant output to reduce the impact of the fault in the controller signals.

The second action of the proposed SRB is the control re-allocation which redistributes the controller signals into the remaining healthy actuators. Figures 3.6 and 3.7 depict the signals injected into, respectively, the first and the second plant actuator. Although Figures 3.3 and 3.4 indicate that the controller require some control effort from both actuators, the RB re-allocate the whole control effort to the second actuator, since the first has failed.

The results presented in this example indicates the efficacy of the proposed fault hiding approach and reveal the idea behind the use of RBs. However, it is worthy to notice that the reconfiguration requires more effort from the remaining actuators, which may be a problem in real world applications, since there are constraints related to the actuators operation, e.g., saturation. The next section provides a way to deal with saturating inputs.

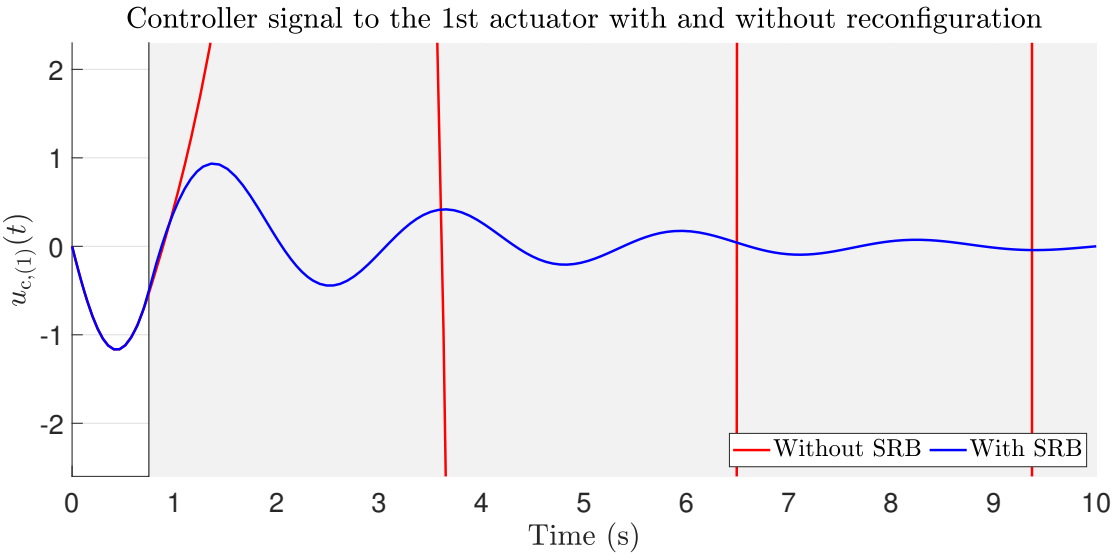

Figure 3.3 – Comparison between the controller signal $u_{c,(1)}$ with and without RB.

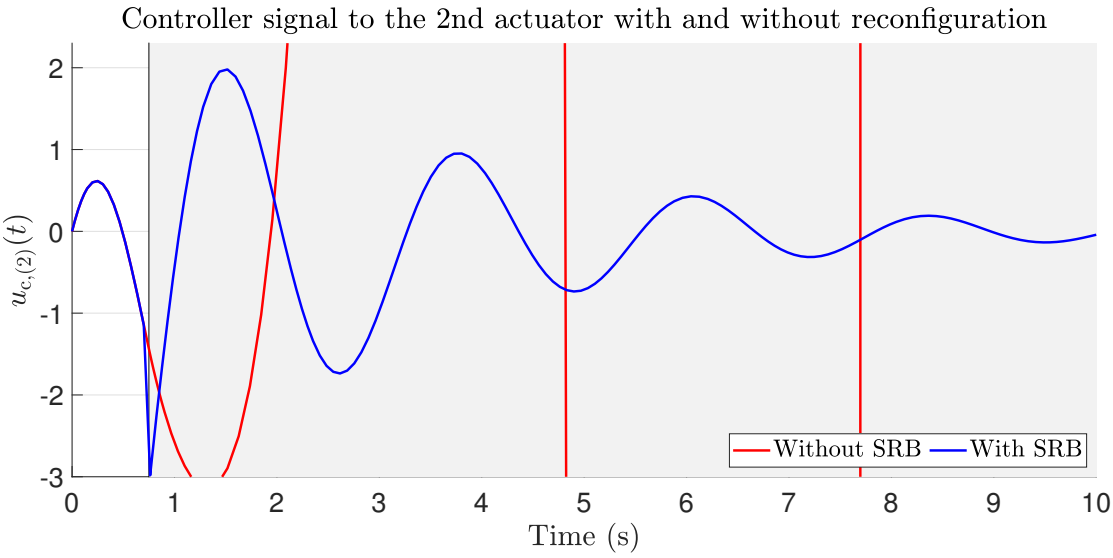

Figure 3.4 – Comparison between the controller signal $u_{c,(2)}$ with and without RB.

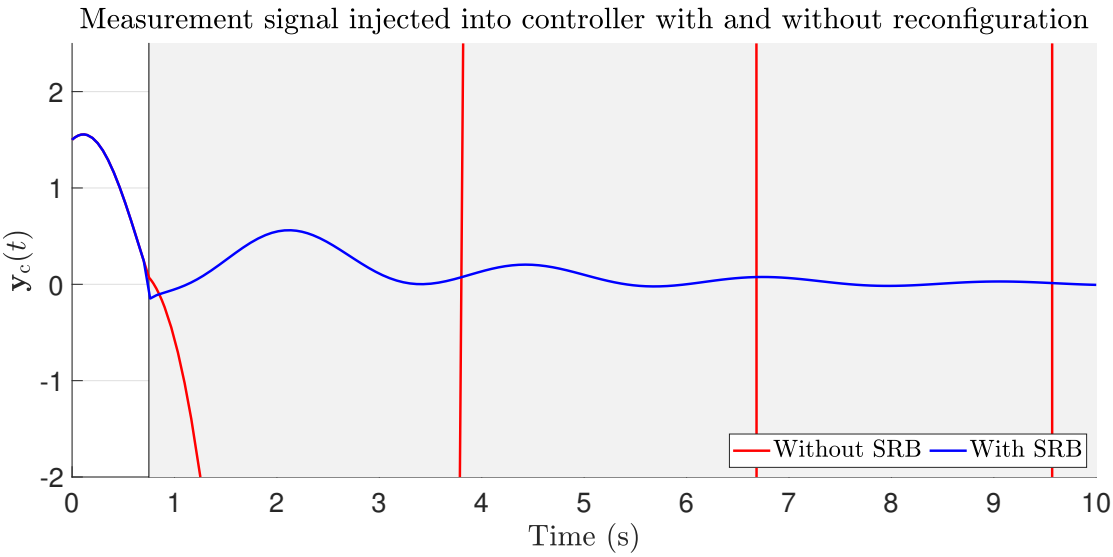

Figure 3.5 – Measurement signal $\boldsymbol{y}_c$ injected into the controller with and without RB.

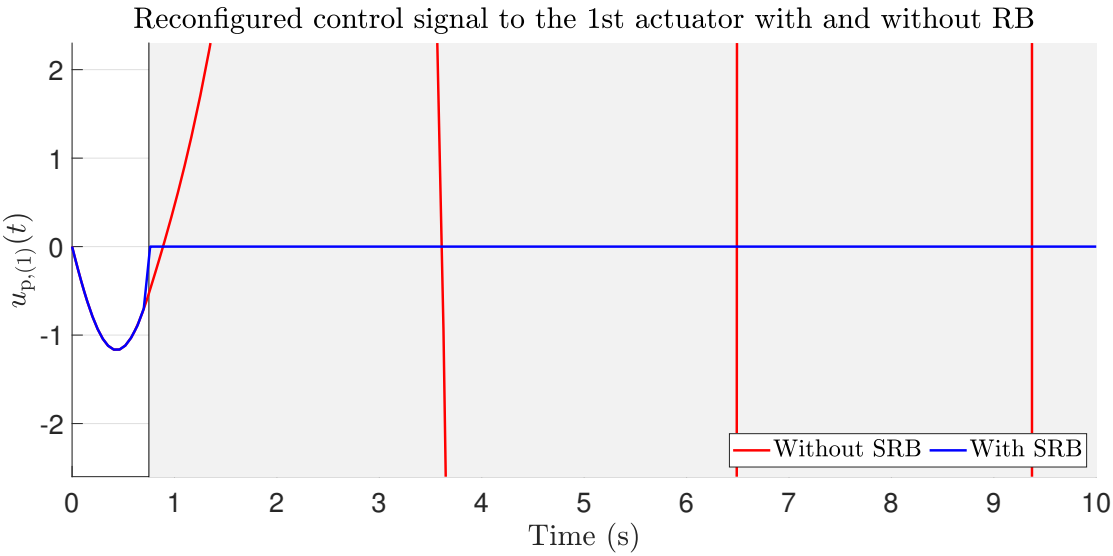

Figure 3.6 – Control signal $u_{p,1}$ injected into the plant with and without RB.

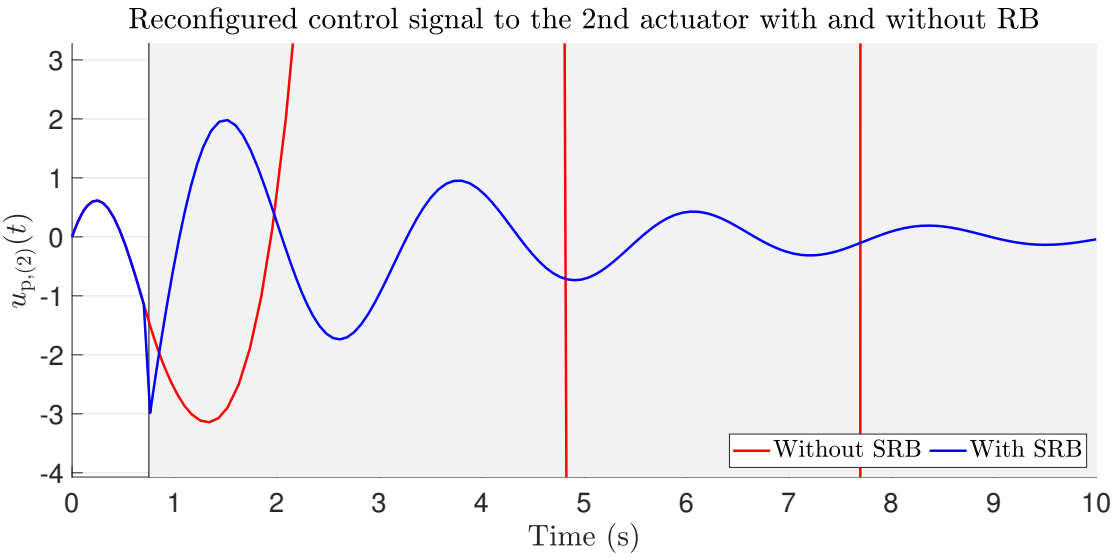

Figure 3.7 – Control signal $u_{\mathrm{p},2}$ injected into the plant with and without RB.

3.4 Fault Hiding of Linear Systems with Input Saturation

It is shown in 3.1 that control reconfiguration with VA tends to reallocate the control effort to the remaining actuators. Eventually, this reallocation may overburden the healthy actuator or result in saturation. Thus, it is important to deal with the input saturation issue when fault hiding FTC approaches are employed. Indeed, the design of virtual actuators by considering input saturation is already considered in the literature [18, 123, 237, 55].

To deal with the input saturation, it is usual to write it as a function of a dead-zone nonlinearity $\psi : \mathbb{R}^m \to \mathbb{R}^m$:

$$\psi(\boldsymbol{u}) = \mathrm{sat}(\boldsymbol{u}) - \boldsymbol{u}, \tag{3.18}$$

for which the following condition holds.

Lemma 3.2 (Adapted from [238]). *Let the control input be defined as $\boldsymbol{u} = \boldsymbol{M}\boldsymbol{x}$ for all $\boldsymbol{x} \in \mathbb{R}^n$ and a given $\boldsymbol{M} \in \mathbb{R}^{m\times n}$, and the set $\mathscr{D}_u$ be defined as*

$$\mathscr{D}_u = \left\{ \boldsymbol{x} \in \mathbb{R}^n : \left| \left(\boldsymbol{M}_{(l)} - \boldsymbol{W}_{(l)} \right) \boldsymbol{x} \right| \leq \bar{u}_{\mathrm{p},(l)},\ l \in \mathbb{N}_{\leq m} \right\}, \tag{3.19}$$

for a given matrix $\boldsymbol{W} \in \mathbb{R}^{m\times n}$.

If $\boldsymbol{x} \in \mathscr{D}_u$*, then*

$$\psi\left(\boldsymbol{u}\right)^{\top} \boldsymbol{T}^{-1} \left(\psi(\,\boldsymbol{u}\,)+\boldsymbol{W}\tilde{\boldsymbol{x}}\right) \leq 0, \tag{3.20}$$

holds for any diagonal $\boldsymbol{T} \succ 0$*.*

Thus, the next theorem provides sufficient conditions for stability recovery by fault hiding of linear systems with input saturation. In this result, the Problem 3.1 is solved considering the nominal model Σ_{P} (cf. (3.1) and faulty model $\Sigma_{\mathrm{P_f}}$ (cf. (3.4)) for a plant interconnected with the dynamic output feedback controller Σ_{C} (cf. (3.3)).

Theorem 3.2. *Let* Σ_{P} *and* $\Sigma_{\mathrm{P_f}}$ *be respectively the nominal and fault models for the same plant connected by feedback to an output feedback controller* Σ_{C}*, such that there exist some symmetric positive definite matrices* $\boldsymbol{P}_{11}$ *and* $\boldsymbol{P}_{22}$*, and matrices* $\boldsymbol{P}_{12}$*,* $\boldsymbol{W}_1$*, and* $\boldsymbol{W}_2$ *satisfying*

$$\begin{bmatrix} \mathrm{He}\left\{\tilde{\boldsymbol{A}}^{\top}\boldsymbol{P}\right\} & \boldsymbol{P}\tilde{\boldsymbol{B}} - \boldsymbol{W} \\ * & -2\boldsymbol{I}_m \end{bmatrix} \preceq 0, \tag{3.21}$$

$$\begin{bmatrix} \boldsymbol{P} & \tilde{\boldsymbol{C}}_{\mathrm{c},(l)}^{\top} - \boldsymbol{W}_{(l)}^{\top} \\ \star & \bar{u}_{\mathrm{p},(l)}^{2} \end{bmatrix} \succ 0, \quad \forall l \in \mathbb{N}_{\leq m}, \tag{3.22}$$

where

$$\boldsymbol{P} = \begin{bmatrix} \boldsymbol{P}_{11} & \boldsymbol{P}_{12} \\ \star & \boldsymbol{P}_{22} \end{bmatrix}, \quad \tilde{\boldsymbol{A}} = \begin{bmatrix} \boldsymbol{A} & \boldsymbol{B}\boldsymbol{C}_{\mathrm{c}} \\ \boldsymbol{B}_{\mathrm{c}}\boldsymbol{C} & \boldsymbol{A}_c \end{bmatrix}, \quad \tilde{\boldsymbol{B}} = \begin{bmatrix} \boldsymbol{B} \\ \boldsymbol{0} \end{bmatrix},$$
$$\tilde{\boldsymbol{C}}_{\mathrm{c}} = \begin{bmatrix} \boldsymbol{0} & \boldsymbol{C}_{\mathrm{c}} \end{bmatrix}, \quad \boldsymbol{W} = \begin{bmatrix} \boldsymbol{W}_1 & \boldsymbol{W}_2 \end{bmatrix},$$

If there exist some matrices $\bar{\boldsymbol{W}}_1$*,* $\bar{\boldsymbol{W}}_2$*,* $\boldsymbol{R}_1$*,* $\boldsymbol{R}_2$*,* $\boldsymbol{R}_3$ *and* $\boldsymbol{R}_4$*, and diagonal matrix* $\boldsymbol{T}$ *that satisfy*

$$\begin{bmatrix} \boldsymbol{L}_{11} & \boldsymbol{L}_{12} & \boldsymbol{P}_{11}\boldsymbol{B}_{\mathrm{f}}\boldsymbol{T}, -\bar{\boldsymbol{W}}_1^{\top} \\ \star & \boldsymbol{L}_{22} & \boldsymbol{P}_{12}\boldsymbol{B}_{\mathrm{f}}\boldsymbol{T} - \bar{\boldsymbol{W}}_2^{\top} \\ \star & \star & -2\boldsymbol{T} \end{bmatrix} \prec 0, \tag{3.23}$$

$$\begin{bmatrix} \boldsymbol{P} & \tilde{\boldsymbol{R}}_{(l)}^{\top} - \bar{\boldsymbol{W}}_{(l)}^{\top} \\ \star & \bar{u}_{\mathrm{p},(l)}^{2} \end{bmatrix} \succ 0, \quad \forall l \in \mathbb{N}_{\leq m} \tag{3.24}$$

where

$$
\begin{aligned}
\boldsymbol{L}_{11} &= \mathrm{He}\left\{\boldsymbol{P}_{11}(\boldsymbol{A}+\boldsymbol{B}_{\mathrm{f}}\boldsymbol{R}_3\boldsymbol{C}_{\mathrm{f}}) + \boldsymbol{P}_{12}\boldsymbol{B}_{\mathrm{c}}\boldsymbol{R}_1\boldsymbol{C}_{\mathrm{f}} + \boldsymbol{C}_{\mathrm{f}}^{\top}\boldsymbol{R}_1^{\top}\boldsymbol{B}_{\mathrm{c}}^{\top}\boldsymbol{P}_{12}\right\},\\
\boldsymbol{L}_{12} &= \boldsymbol{P}_{11}\boldsymbol{B}_{\mathrm{f}}\boldsymbol{R}_4\boldsymbol{C}_{\mathrm{c}} + \mathrm{He}\left\{\boldsymbol{P}_{12}(\boldsymbol{A}_{\mathrm{c}}+\boldsymbol{B}_{\mathrm{c}}\boldsymbol{R}_2\boldsymbol{C}_{\mathrm{c}})\right\} + \boldsymbol{C}^{\top}\boldsymbol{R}_1^{\top}\boldsymbol{B}_{\mathrm{c}}^{\top}\boldsymbol{P}_{22},\\
\boldsymbol{L}_{22} &= \mathrm{He}\left\{\boldsymbol{P}_{12}\boldsymbol{B}_{\mathrm{f}}\boldsymbol{R}_4\boldsymbol{C}_{\mathrm{c}} + \boldsymbol{P}_{22}(\boldsymbol{A}_{\mathrm{c}}+\boldsymbol{B}_{\mathrm{c}}\boldsymbol{R}_2\boldsymbol{C}_{\mathrm{c}})\right\},\\
\tilde{\boldsymbol{R}} &= \begin{bmatrix}\boldsymbol{R}_3\boldsymbol{C} & \boldsymbol{R}_4\boldsymbol{C}_{\mathrm{c}}\end{bmatrix},\ \ \bar{\boldsymbol{W}} = \begin{bmatrix}\bar{\boldsymbol{W}}_1 & \bar{\boldsymbol{W}}_2,\end{bmatrix}
\end{aligned}
$$

then $\Sigma_{\mathrm{P_f}}$ *is stable by fault hiding with* Σ_{R} *described by* (3.5)*. Moreover, the following set* $\mathscr{D}_x$ *is an estimate of the domain of attraction of the reconfigured system* $(\Sigma_{\mathrm{P}}, \Sigma_{\mathrm{R}}, \Sigma_{\mathrm{C}})$*:*

$$\mathscr{D}_x = \{\tilde{x} \in \mathbb{R}^{n+n_{\mathrm{c}}} : V(\tilde{\boldsymbol{x}}) \leq 1\}. \tag{3.25}$$

Proof. Considering (3.18) to deal with the saturating actuators, and substituting it in (3.1), the following closed-loop model for $(\Sigma_{\mathrm{P}}, \Sigma_{\mathrm{C}})$ is obtained

$$\dot{\tilde{\boldsymbol{x}}} = \tilde{\boldsymbol{A}}\tilde{\boldsymbol{x}} + \tilde{\boldsymbol{B}}\psi(\boldsymbol{u}_{\mathrm{c}}). \tag{3.26}$$

Choose the Lyapunov candidate function $V(\tilde{\boldsymbol{x}}) = \tilde{\boldsymbol{x}}^{\top}\boldsymbol{P}\tilde{\boldsymbol{x}}$ whose derivative is

$$\dot{V}(\tilde{\boldsymbol{x}}) = \tilde{\boldsymbol{x}}^{\top}(\tilde{\boldsymbol{A}}^{\top}\boldsymbol{P} + \boldsymbol{P}\tilde{\boldsymbol{A}})\tilde{\boldsymbol{x}} + \psi^{\top}(\boldsymbol{u}_{\mathrm{c}})\tilde{\boldsymbol{B}}^{\top}\boldsymbol{P}\tilde{\boldsymbol{x}} + \tilde{\boldsymbol{x}}^{\top}\boldsymbol{P}\tilde{\boldsymbol{B}}\psi(\boldsymbol{u}_{\mathrm{c}}). \tag{3.27}$$

Based on the Schur's complement Lemma, the inequalities (3.22) imply

$$\boldsymbol{P} - \bar{u}_{\mathrm{p},(l)}^{-2}\left(\tilde{\boldsymbol{C}}_{\mathrm{c},(l)} - \boldsymbol{W}_{(l)}\right)^{\top}\left(\tilde{\boldsymbol{C}}_{\mathrm{c},(l)} - \boldsymbol{W}_{(l)}\right) \succ 0,,\ \forall l \in \mathbb{N}_{\leq m}. \tag{3.28}$$

It follows that

$$
\begin{aligned}
\tilde{\boldsymbol{x}}^{\top}\boldsymbol{P}\tilde{\boldsymbol{x}} &> \frac{\|\left(\tilde{\boldsymbol{C}}_{\mathrm{c},(l)} - \boldsymbol{W}_{(l)}\right)\tilde{\boldsymbol{x}}\|^2}{\bar{u}_{\mathrm{p},(l)}^2},\\
V(\tilde{\boldsymbol{x}}) &> \frac{\|\left(\tilde{\boldsymbol{C}}_{\mathrm{c},(l)} - \boldsymbol{W}_{(l)}\right)\tilde{\boldsymbol{x}}\|^2}{\bar{u}_{\mathrm{p},(l)}^2}.
\end{aligned} \tag{3.29}
$$

Notice that the set $\mathscr{D}_x$, given by (3.25), is a level set of $V(\tilde{\boldsymbol{x}})$. The inequality (3.29) implies $\mathscr{D}_x \subset \mathscr{D}_u$, such that $\mathscr{D}_u$ is defined as follows

$$\mathscr{D}_u = \left\{\tilde{\boldsymbol{x}} \in \mathbb{R}^{n+n_{\mathrm{c}}} : \left|\left(\tilde{\boldsymbol{C}}_{\mathrm{c},(l)} - \boldsymbol{W}_{(l)}\right)\tilde{\boldsymbol{x}}\right| \leq \bar{u}_{\mathrm{p},(l)},\ l \in \mathbb{N}_{\leq m}\right\}.. \tag{3.30}$$

Thus, according to Lemma 3.2 and for $\tilde{\boldsymbol{x}} \in \mathscr{D}_x$, if the inequalities (3.22) are satisfied, then

$$\psi^\top(\boldsymbol{u}_\mathrm{c})(\psi(\boldsymbol{u}_\mathrm{c}) + \boldsymbol{W}\tilde{\boldsymbol{x}}) \leq 0. \tag{3.31}$$

Considering (3.27), the inequality (3.21) is equivalent to

$$\dot{V}(\tilde{\boldsymbol{x}}) < 2\psi^\top(\boldsymbol{u}_\mathrm{c})(\psi(\boldsymbol{u}_\mathrm{c}) + \boldsymbol{W}\tilde{\boldsymbol{x}}), \tag{3.32}$$

Thus, assuming that (3.22) and $\tilde{\boldsymbol{x}}(0) \in \mathscr{D}_x$, (3.32) and (3.31) imply $\dot{V}(\tilde{\boldsymbol{x}}) < 0$, which ensures that $\mathscr{D}_x$ is positively invariant. Therefore, the origin of $(\Sigma_\mathrm{P}, \Sigma_\mathrm{C})$ is asymptotically stable and $\mathscr{D}_x$ is an estimate of its domain of attraction.

Furthermore, the same $\boldsymbol{P}$ matrix that satisfies (3.21) can be used to find a sufficient condition for stability recovery of the reconfigured system $(\Sigma_\mathrm{P}, \Sigma_\mathrm{R}, \Sigma_\mathrm{C})$:

$$\dot{\boldsymbol{x}} = \tilde{\boldsymbol{A}}_r\tilde{\boldsymbol{x}} + \tilde{\boldsymbol{B}}_r\psi\left(\boldsymbol{u}_\mathrm{r}\right), \tag{3.33}$$

$$\tilde{\boldsymbol{A}}_r \triangleq \begin{bmatrix} \boldsymbol{A} + \boldsymbol{B}_\mathrm{f}\boldsymbol{R}_3 C_\mathrm{f} & \boldsymbol{B}_\mathrm{f}\boldsymbol{R}_4\boldsymbol{C}_c, \\ \boldsymbol{B}_c\boldsymbol{R}_1\boldsymbol{C}_\mathrm{f} & \boldsymbol{A}_c + \boldsymbol{B}_c\boldsymbol{R}_2\boldsymbol{C}_c \end{bmatrix} \quad \tilde{\boldsymbol{B}}_r \triangleq \begin{bmatrix} \boldsymbol{B}_\mathrm{f} \\ 0 \end{bmatrix},$$

Using the same arguments used for nominal closed-loop system, assuming $\tilde{\boldsymbol{x}} \in \mathscr{D}_x$, and considering Lemma 3.2, if (3.30) is satisfied, then the following sector inequality holds

$$\psi^\top\left(\boldsymbol{u}_\mathrm{r}\right)\boldsymbol{T}^{-1}(\psi\left(\boldsymbol{u}_\mathrm{r}\right) + \boldsymbol{W}\tilde{\boldsymbol{x}}) \leq 0. \tag{3.34}$$

Thus, the origin of (3.33) is asymptotically stable if there exist $\boldsymbol{R}_1$, $\boldsymbol{R}_2$, $\boldsymbol{R}_3$, $\boldsymbol{R}_4$, $\bar{\boldsymbol{W}}_1$, $\bar{\boldsymbol{W}}_2$, and diagonal matrix $\boldsymbol{T}$ that satisfy the following inequality

$$\dot{V}(\tilde{\boldsymbol{x}}) = \mathrm{He}\left\{\tilde{\boldsymbol{x}}^\top\tilde{\boldsymbol{A}}^\top\boldsymbol{P}\tilde{\boldsymbol{x}} + \psi^\top\left(\boldsymbol{u}_\mathrm{r}\right)\tilde{\boldsymbol{B}}_\mathrm{f}^\top\boldsymbol{P}\tilde{\boldsymbol{x}}\right\} < 2\psi^\top\left(\boldsymbol{u}_\mathrm{r}\right)\boldsymbol{T}^{-1}(\psi\left(\boldsymbol{u}_\mathrm{r}\right) + \bar{\boldsymbol{W}}\tilde{\boldsymbol{x}}), \tag{3.35}$$

that is equivalent to

$$\begin{bmatrix} \mathrm{He}\left\{\tilde{\boldsymbol{A}}_\mathrm{r}^\top\boldsymbol{P}\right\} & \boldsymbol{P}\tilde{\boldsymbol{B}}_\mathrm{r} - \bar{\boldsymbol{W}}^\top\boldsymbol{T}^{-1} \\ \star & -2\boldsymbol{T}^{-1} \end{bmatrix} \preceq 0, \tag{3.36}$$

Pre- and post-multiplying (3.36) by $\mathrm{diag}\left\{\boldsymbol{I}_{n+n_\mathrm{c}}, \boldsymbol{T}\right\}$, it follows that

$$\begin{bmatrix} \mathrm{He}\left\{\tilde{\boldsymbol{A}}_\mathrm{r}^\top\boldsymbol{P}\right\} & \boldsymbol{P}\tilde{\boldsymbol{B}}_\mathrm{f}\boldsymbol{T} - \bar{\boldsymbol{W}}^\top \\ \star & -2\boldsymbol{T} \end{bmatrix} \preceq 0, \tag{3.37}$$

Note that $\tilde{\boldsymbol{A}}_{\mathrm{r}}^{\top}\boldsymbol{P}+\boldsymbol{P}\tilde{\boldsymbol{A}}_{\mathrm{r}}$ is presented in the proof of Theorem 3.1

$$\tilde{\boldsymbol{A}}_{\mathrm{r}}^{\top}\boldsymbol{P}+\boldsymbol{P}\tilde{\boldsymbol{A}}_{\mathrm{r}}=\begin{bmatrix}\boldsymbol{L}_{11} & \boldsymbol{L}_{12}\\ * & \boldsymbol{L}_{22}\end{bmatrix}, \tag{3.38}$$

The block $\boldsymbol{P}\tilde{\boldsymbol{B}}_{\mathrm{r}}\boldsymbol{T}-\boldsymbol{W}^{\top}$ is equivalent to

$$\begin{bmatrix}\boldsymbol{P}_{11}\boldsymbol{B}_{\mathrm{f}}\boldsymbol{T}-\bar{\boldsymbol{W}}_{1}^{\top}\\ \boldsymbol{P}_{12}\boldsymbol{B}_{\mathrm{f}}\boldsymbol{T}-\bar{\boldsymbol{W}}_{2}^{\top}\end{bmatrix} \tag{3.39}$$

finally, (3.23) is obtained by substituting (3.38) and (3.39) in (3.36). Consequently, if there exist $\boldsymbol{R}_1$, $\boldsymbol{R}_2$, $\boldsymbol{R}_3$ and $\boldsymbol{R}_4$ that satisfy (3.23), then the origin of $(\Sigma_{\mathrm{P}},\Sigma_{\mathrm{R}},\Sigma_{\mathrm{C}})$ is asymptotically stable, therefore, $\Sigma_{\mathrm{P_f}}$ is stable by fault hiding with Σ_{R} described by (3.5) (cf. Definition 3.1), and $\mathscr{D}_x$ is also an estimate of its domain of attraction. □

Example 3.2. *Consider the same plant and controller models in 3.1 with saturating input. Again, it is simulated the total lost of the first actuator, such that $f_1=0$, which occurs at $t=0.75$ s. Note that the origin of $(\Sigma_{\mathrm{P}},\Sigma_{\mathrm{C}})$ is asymptotically stable and* (3.21) *is satisfied with*

$$\boldsymbol{P}=\begin{bmatrix}1.5414 & 0.4459 & -0.6546 & -0.4316\\ 0.4459 & 1.0937 & -0.6367 & -0.9712\\ -0.6546 & -0.6367 & 0.7946 & 0.7417\\ -0.4316 & -0.9712 & 0.7417 & 1.2551\end{bmatrix}, \tag{3.40}$$

computed in MATLAB environment using the YALMIP parser [235] with the MOSEK solver [236]. The same $\boldsymbol{P}$ matrix in (3.40) *is used to find $\boldsymbol{R}_1$, $\boldsymbol{R}_2$, $\boldsymbol{R}_3$, and $\boldsymbol{R}_4$ by means of Theorem 3.2 for actuator saturation bounds $\bar{u}_{\mathrm{p},(1)}=\bar{u}_{\mathrm{p},(2)}=1.5$. Then, the following gains are obtained*

$$\boldsymbol{R}_1=0.9218 \quad \boldsymbol{R}_2=\begin{bmatrix}1.0493 & 0.0182\end{bmatrix},$$

$$\boldsymbol{R}_3=\begin{bmatrix}0\\ -1.1363\end{bmatrix} \quad \boldsymbol{R}_4=\begin{bmatrix}0 & 0\\ 3.5814 & 0.9202\end{bmatrix}.$$

To illustrate the advantage of the approach proposed for systems with input saturation, another RB is designed using the Theorem 3.1 and provided in 3.1. In this simulation example, the initial conditions are also $\tilde{\boldsymbol{x}}(0)=[1.5 \quad -0.25 \quad 0 \quad 0]^{\top}$.

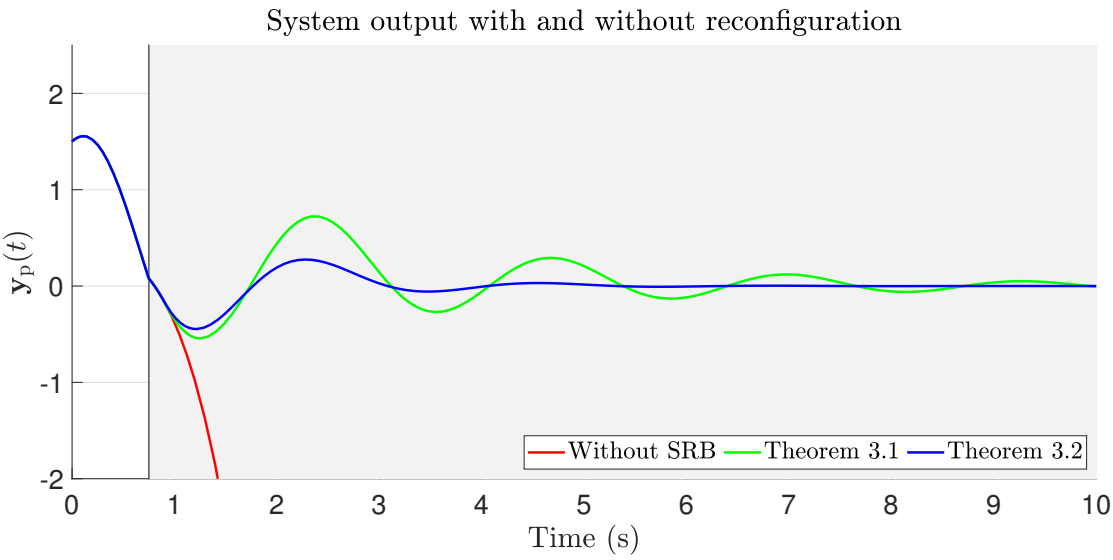

Figure 3.8 – Comparison of output responses for 3.2 with RBs obtained by Theorem 3.1, Theorem 3.2, and without RB.

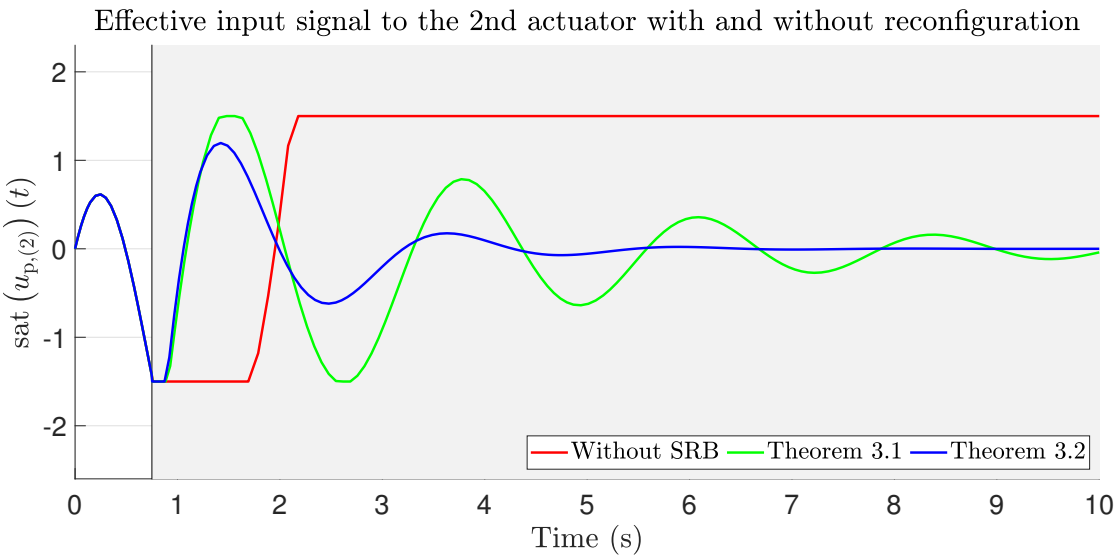

Figure 3.9 – Comparison of effective input signals $u_{p,(2)}$ injected into the plant considering input saturation for 3.2 with RBs obtained by Theorem 3.1, Theorem 3.2, and without RB.

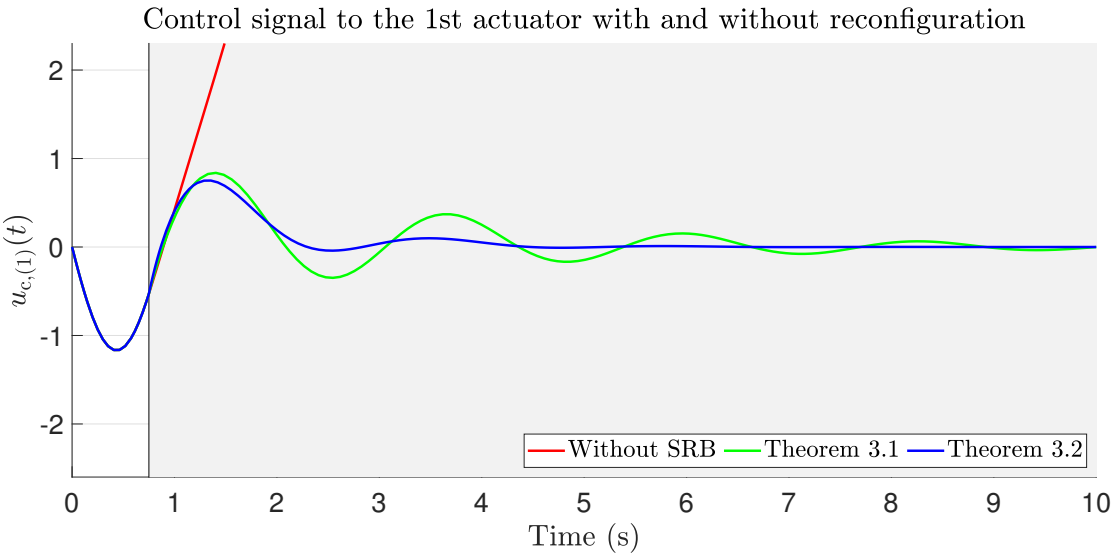

Figure 3.10 – Comparison of controller signals for the first actuator $u_{c,(1)}$ for 3.2 with RBs obtained by Theorem 3.1, Theorem 3.2, and without RB.

The results for this example including comparisons between the block designed by Theorem 3.1, Theorem 3.2, and the faulty system without SRB are depicted in Figures 3.8–3.12. In particular, Figure 3.8 depicts the plant output response. Notice that both blocks, designed by Theorem 3.1 and Theorem 3.2, are able to guarantee the stabilization of the system after the fault occurrence. However, the block whose design is achieved based on Theorem 3.1 which ignores the input saturation presents some oscillation and takes more time to converge. It occurs, because the reconfigured control signal produces more saturation as depicted in Figure 3.9 which compares the control signal of the healthy actuator considering the input saturation. Notice, that Theorem 3.2 is not proposed to avoid saturation, but its design improve the response since it is aware of the saturating actuators and guarantees the stability recovery. Therefore, as depicted Figure 3.9, the reconfigured control signal provided by the SRB designed by means of Theorem 3.2 is subject to fast saturation just after the fault occurrence and the reconfiguration, but it does not affect the recovery ability of that block.

The controller signals are depicted in Figure 3.10 and Figure 3.11. They indicate that both SRBs are able to effectively hide the fault effects from the controllers, whose signals are smooth even after the fault occurrence. It occurs because of the

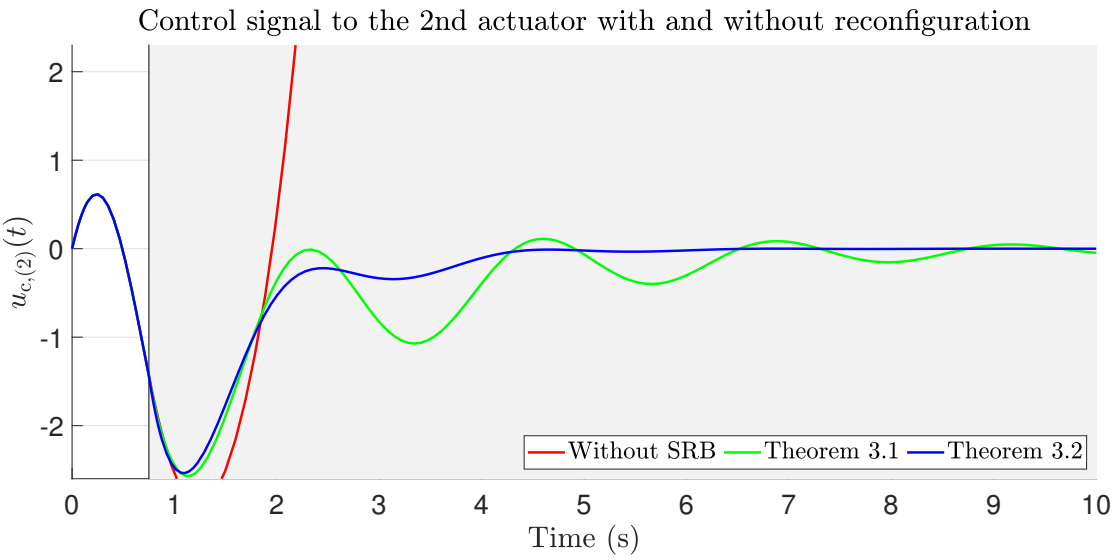

Figure 3.11 – Comparison of controller signals for the first actuator $u_{c,(2)}$ for 3.2 with RBs obtained by Theorem 3.1, Theorem 3.2, and without RB.

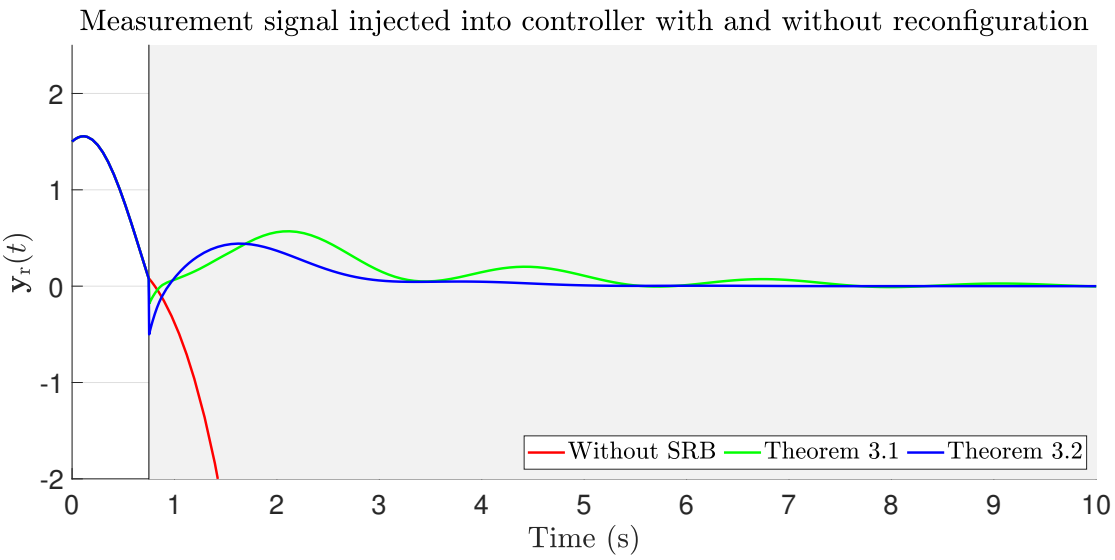

Figure 3.12 – Comparison of measurement signals injected into the controller for 3.2 with RBs obtained by Theorem 3.1, Theorem 3.2, and without RB.

compensation in the output measurements by injecting $\boldsymbol{y}_{\mathrm{r}}$ *into the controller. The reconfigured measurement signals injected into the controller are depicted in Figure 3.12 that shows the modifications on the measurements to hide the fault effects from the controller.*

4 STABILITY RECOVERY OF TAKAGI-SUGENO FUZZY SYSTEMS

This chapter presents novel centralized and decentralized T-S fuzzy SRB for control reconfiguration of plants represented by NT-S fuzzy models. In particular, novel conditions for stability recovery by fault hiding are presented based on a novel SRB structure and on the Lyapunov stability theory. section 4.1 presents the problem of centralized and distributed fault hiding for NT-S fuzzy model. section 4.2 presents Lyapunov-based conditions to design T-S fuzzy SRBs for stability recovery of NT-S fuzzy models. section 4.3 presents Lyapunov-based conditions to design distributed T-S fuzzy SRBs, and a centralized alternative to address the same problem. Finally, section 4.4 provides application examples to evaluate the proposed approach and compare with other approaches in the literature. The results presented in this chapter are based on those ones previously published in [127].

The following notation is also used in addition to that defined in section 1.5. The operator $\bigoplus_{i=1}^{N} M_i$ denotes the horizontal concatenation of the matrices $M_1, \ldots, M_N$, i.e., $\bigoplus_{i=1}^{N} M_i \triangleq [M_1 | \ldots | M_N]$; and $I[\rho]$ denotes the indicator function, which is equal to 1 if the logical proposition ρ is true and is equal to 0 otherwise. For a nonlinear map $\varphi : \mathbb{R}^n \to \mathbb{R}^{\varphi}$, the notation $\varphi(\boldsymbol{x}) \in [\boldsymbol{V}_1, \boldsymbol{V}_2]$ indicates that $\varphi(\boldsymbol{x}) \in \mathrm{Co}\{\boldsymbol{V}_1, \boldsymbol{V}_2\}$.

4.1 Problem statement

4.1.1 Fault hiding of Takagi-Sugeno Fuzzy Systems with Nonlinear Consequent

Let Σ_{P} be the nominal NT-S fuzzy model for a plant described as follows

$$\Sigma_{\mathrm{P}} : \begin{cases} \dot{\boldsymbol{x}} = \sum_{k_p=1}^{r} \mu^{k_p}(\boldsymbol{z}) \left(\boldsymbol{A}^{k_p}\boldsymbol{x} + \boldsymbol{B}^{k_p}\boldsymbol{u}_{\mathrm{p}} + \boldsymbol{G}^{k_p}\Phi(\boldsymbol{x}) \right), \\ \boldsymbol{y}_{\mathrm{p}} = \sum_{k_p=1}^{r} \mu^{k_p}(\boldsymbol{z}) \boldsymbol{C}^{k_p}\boldsymbol{x}, \end{cases} \tag{4.1}$$

where r is the number of fuzzy rules, $z \in \mathbb{R}^{n_z}$ is the measured premises vector, $\mu^{k_p} : \mathbb{R}^{n_z} \to [0, 1]$ is the normalized membership function of the k_p-th fuzzy set that

holds the convex sum property, i.e., $\sum_{k_p}^{r} \mu^{k_p}(\boldsymbol{z}) = 1$, $\boldsymbol{A}^{k_p}$, $\boldsymbol{B}^{k_p}$, and $\boldsymbol{C}^{k_p}$ are real state-space matrices of the k_p-th rule with adequate dimensions, $\boldsymbol{x} \in \mathbb{R}^n$ is state vector, $u \in \mathbb{R}^m$ is the input vector, $y \in \mathbb{R}^p$ is the measured output vector, $\boldsymbol{G}^{k_p}$ is a constant matrix related to the nonlinearity Φ of the k_p-th rule with appropriate dimensions, and the nonlinear map $\Phi : \mathbb{R}^n \to \mathbb{R}^n$ satisfies the following sector bound condition.

Definition 4.1. ***Sector nonlinearity [139]*** *– The nonlinear mapping $\Phi(\cdot) : \mathbb{R}^n \to \mathbb{R}^{n_g}$ is said to satisfy the inclusion $\Phi(\boldsymbol{x}) \in [\boldsymbol{0}, \boldsymbol{E}]$ if and only if it satisfies the following inequality for any diagonal positive definite matrix $\boldsymbol{W} \in \mathbb{R}^{n_g \times n_g}$*

$$\Phi^{\top}(\boldsymbol{x})\,\boldsymbol{W}\,(\Phi(\boldsymbol{x}) - \boldsymbol{E}\boldsymbol{x}) \leq 0, \quad \forall \boldsymbol{x} \in \mathbb{R}^n. \tag{4.2}$$

Remark 4.1. *The matrix $\boldsymbol{E}$ is chosen to ensure that the nonlinearity $\Phi(\boldsymbol{x})$ is bounded by $\boldsymbol{0}$ and $\boldsymbol{E}\boldsymbol{x}$, i.e., $\Phi(\boldsymbol{x}) \in [\boldsymbol{0}, \boldsymbol{E}]$. The procedure for computing the $\boldsymbol{E}$ matrix for a wide class of continuously differentiable nonlinear mappings is presented in [239].*

Σ_{P} is connected to an OF-PDC Σ_{C} described as follows

$$\Sigma_{\mathrm{C}} : \boldsymbol{u}_{\mathrm{c}} = \sum_{k_c=1}^{r} \mu^{k_c}(\boldsymbol{z}) \boldsymbol{K}^{k_c} \boldsymbol{y}_{\mathrm{c}}, \tag{4.3}$$

where $\boldsymbol{y}_{\mathrm{c}}$ is the controller input from the plant sensors measurements, u_c is the control signal to the plant actuators, $\mu^{k_c} : \mathbb{R}^{n_z} \to [0, 1]$ is the normalized membership function of the k_c-th fuzzy set that holds the convex sum property, for $k_c \in \mathbb{N}_{\leq r}$, $\boldsymbol{K}^{k_c} \in \mathbb{R}^{m \times p}$ is the controller gain of the k_c-th rule. Nominally, the resulting fault-free closed-loop system $(\Sigma_{\mathrm{P}}, \Sigma_{\mathrm{C}})$ is obtained by the following connections: $\boldsymbol{y}_{\mathrm{c}} \leftarrow \boldsymbol{y}$ and $\boldsymbol{u} \leftarrow \boldsymbol{u}_{\mathrm{c}}$.

In addition, let $\Sigma_{\mathrm{P_f}}$ be the following fault model for the same plant described by Σ_{P}

$$\Sigma_{\mathrm{P_f}} : \begin{cases} \dot{\boldsymbol{x}} = \sum_{k_p=1}^{r} \mu^{k_p}(\boldsymbol{z}) \left(\boldsymbol{A}^{k_p} \boldsymbol{x} + \boldsymbol{B}_{\mathrm{f}}^{k_p} \boldsymbol{u}_{\mathrm{p}} + \boldsymbol{G}^{k_p} \Phi(\boldsymbol{x}) \right), \\ \boldsymbol{y}_{\mathrm{p}} = \sum_{k_p=1}^{r} \mu^{k_p}(\boldsymbol{z}) \boldsymbol{C}_{\mathrm{f}}^{k_p} \boldsymbol{x}, \end{cases} \tag{4.4}$$

where $\boldsymbol{B}_{\mathrm{f}}^{k_p}$ and $\boldsymbol{C}_{\mathrm{f}}^{k_p}$ are k_p-th rule matrices which represent the effects of, respectively, actuator and sensor multiplicative faults. In particular, let the nominal model matrices

$\boldsymbol{B}^{k_p}$ and $\boldsymbol{C}^{k_p}$ for all $k_p \in \mathbb{N}_{\leq r}$ be

$$\boldsymbol{B}^{k_p} = \left[\boldsymbol{B}_1^{k_p}\ \boldsymbol{B}_2^{k_p}\ \ldots\ \boldsymbol{B}_m^{k_p}\right],$$

$$\boldsymbol{C}^{k_p} = \left[\boldsymbol{C}_1^{k_p\top}\ \boldsymbol{C}_2^{k_p\top}\ \boldsymbol{C}_p^{k_p\top}\right]^\top.$$

if the i-th actuator fails, the i-th column of each $\boldsymbol{B}^{k_p}$ ($\boldsymbol{B}_i^{k_p}$) is modified. A total loss in the i-th actuator is represented by replacing $\boldsymbol{B}_i^{k_p}$ with 0, and effectiveness loss is represented by replacing $\boldsymbol{B}_i^{k_p}$ with $f_{\mathrm{s},i} \cdot B_i^{k_p}$, for $0 \leq f_{\mathrm{a},i} \leq 1$, where $f_{a,i}$ is the i-th element of $\boldsymbol{f}_a$. In other words, the actuator fault matrix $\boldsymbol{B}_\mathrm{f}$ is

$$\boldsymbol{B}_\mathrm{f}^{k_p} = \boldsymbol{B}^{k_p}\mathrm{diag}\left\{\boldsymbol{f}_\mathrm{a}\right\}.$$

Similarly, for sensor faults in the i-th sensor, the fault model is obtained by substituting $\boldsymbol{C}_i^{k_p}$ with $f_{\mathrm{a},i} \cdot C_i$, for $0 \leq f_{\mathrm{s},i} \leq 1$, where $f_{\mathrm{s},i}$ is the i-th element of $\boldsymbol{f}_s$, i.e.,

$$\boldsymbol{C}_\mathrm{f}^{k_p} = \mathrm{diag}\left\{\boldsymbol{f}_s\right\}\boldsymbol{C}^{k_p}.$$

In this chapter, the following static TSRB is proposed to be inserted between the faulty plant and the nominal controller aiming at mitigating the fault effects:

$$\Sigma_\mathrm{R}: \begin{cases} \boldsymbol{y}_\mathrm{r} = \displaystyle\sum_{k_r=1}^{r} \mu^{k_r}(\boldsymbol{z})(\boldsymbol{R}_1^{k_r}\boldsymbol{y}_\mathrm{p} + \boldsymbol{R}_2^{k_r}\boldsymbol{u}_\mathrm{c}), \\ \boldsymbol{u}_\mathrm{r} = \displaystyle\sum_{k_r=1}^{r} \mu^{k_p}(\boldsymbol{z})(\boldsymbol{R}_3^{k_r}\boldsymbol{y}_\mathrm{p} + \boldsymbol{R}_4^{k_r}\boldsymbol{u}_\mathrm{c}), \end{cases} \tag{4.5}$$

or equivalently

$$\begin{bmatrix} \boldsymbol{y}_\mathrm{r} \\ \boldsymbol{u}_\mathrm{r} \end{bmatrix} \triangleq \sum_{k_r=1}^{r} \mu^{k_r}(\boldsymbol{z}) \begin{bmatrix} \boldsymbol{R}_1^{k_r} & \boldsymbol{R}_2^{k_r} \\ \boldsymbol{R}_3^{k_r} & \boldsymbol{R}_4^{k_r} \end{bmatrix} \begin{bmatrix} \boldsymbol{y}_\mathrm{p} \\ \boldsymbol{u}_\mathrm{c} \end{bmatrix}. \tag{4.6}$$

where $\boldsymbol{y}_\mathrm{r} \in \mathbb{R}^p$ is the vector of reconfigured measurements, $\boldsymbol{u}_\mathrm{r} \in \mathbb{R}^p$ is the vector of reconfigured control inputs, $\mu^{k_r} : \mathbb{R}^{n_z} \to [0, 1]$ is the normalized membership function of the k_r-th fuzzy set that holds the convex sum property, for $k_r \in \mathbb{N}_{\leq r}$, and the real matrices $\boldsymbol{R}_1^{k_r}$, $\boldsymbol{R}_2^{k_r}$, $\boldsymbol{R}_3^{k_r}$, and $\boldsymbol{R}_4^{k_r}$ are the TSRB gains of the k_r-th rule.

The TSRB described by (4.5) and (4.6) can be generically employed as VAs and VSs for reconfiguration of system with both sensor and actuator faults. Figure 4.1

depicts the equivalent reconfigured loop when the proposed TSRB in (4.5) is inserted. Furthermore, the conditions provided in the next section eases the achievement of feasible solutions for the proposed static RB disregarding the use of pseudoinverse calculations.

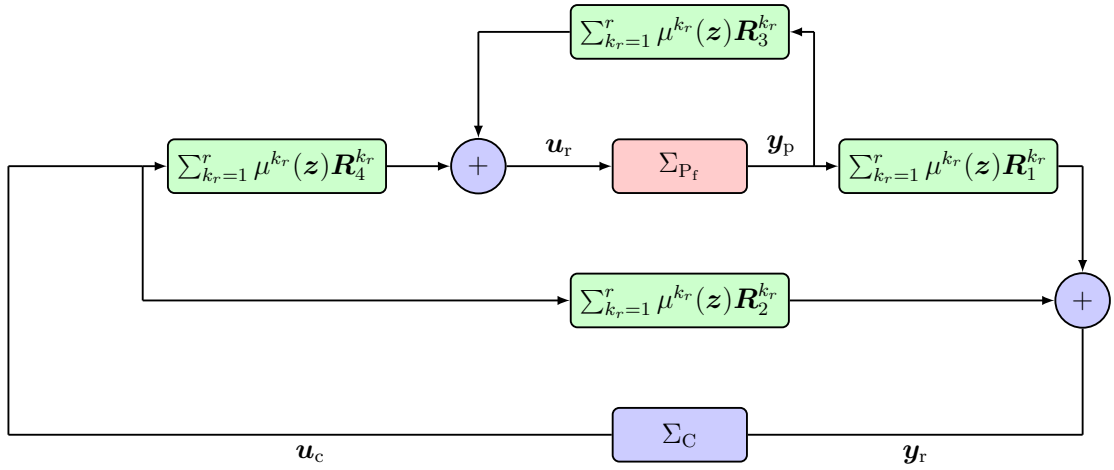

Figure 4.1 – Equivalent block diagram for $(\Sigma_{\mathrm{P_f}}, \Sigma_\mathrm{R}, \Sigma_\mathrm{C})$.

To support the results presented in this chapter, the following underlying assumptions are considered.

Assumption 4.1. *The measurement of the vector of premise variables $\mu^{k_r}(\boldsymbol{z})$ is always available even during fault occurrences.*

Assumption 4.2. *The estimation of fault parameters $\boldsymbol{f}_\mathrm{a}$ and $\boldsymbol{f}_\mathrm{s}$ is assumed to be always available and accurate.*

Thus, for plants represented by NT-S fuzzy model, the following fault hiding problem is addressed here.

Problem 4.1. ***Asymptotic Stability Recovery by Fault Hiding for NT-S fuzzy model***

Let Σ_P and $\Sigma_{\mathrm{P_f}}$ be the nominal and the faulty NT-S fuzzy models, respectively, with dynamics described by (4.1) *and* (4.4) *for a plant interconnected by feedback to an OF-PDC Σ_C (cf.* (4.3)*). Assume that the origin of $(\Sigma_\mathrm{P}, \Sigma_\mathrm{C})$ is asymptotically stable. Find the gains $\boldsymbol{R}_1^{k_r}$, $\boldsymbol{R}_2^{k_r}$, $\boldsymbol{R}_3^{k_r}$, and $\boldsymbol{R}_4^{k_r}$ for $k_r \in \mathbb{N}_{\leq r}$ of the RB Σ_R (cf.* (4.5)*),*

such that the origin of the reconfigured system $(\Sigma_{\mathrm{P_f}}, \Sigma_{\mathrm{R}}, \Sigma_{\mathrm{C}})$ *is also asymptotically stable.*

A solution for Problem 4.1 is proposed in section 4.2 based on the procedure provided by Lemma 3.1.

4.1.2 Fault hiding of Distributed Takagi-Sugeno Fuzzy Systems with Nonlinear Consequent

In this section, the stability recovery by fault hiding problem (Problem 4.1) presented in subsection 4.1.1 is extended for LSSs represented by distributed NT-S fuzzy models. For this purpose, consider the distributed system composed of N interconnected NT-S fuzzy models, such that the nominal model $\Sigma_{\mathrm{P}} = \{\Sigma_{\mathrm{P}_1}, \ldots, \Sigma_{\mathrm{P}_N}\}$ and the faulty model $\Sigma_{\mathrm{P_f}} = \left\{\Sigma_{\mathrm{P_{f,1}}}, \ldots, \Sigma_{\mathrm{P_{f},}_N}\right\}$ have their i-th subsystem dynamics described as follows

$$\Sigma_{\mathrm{P}_i} : \begin{cases} \dot{\boldsymbol{x}}_i = & \sum\limits_{k_p=1}^{r} \mu_i^{k_p}(\boldsymbol{z}) \left(\boldsymbol{A}_i^{k_p}\boldsymbol{x}_i + \boldsymbol{B}_i^{k_p}\boldsymbol{u}_{\mathrm{p},i}\right) + \\ & \sum\limits_{k_p=1}^{r} \mu_i^{k_p}(\boldsymbol{z}) \sum\limits_{\substack{j=1,\\ j\neq i}}^{N} \alpha_{ij}\left(\boldsymbol{H}_i\boldsymbol{x}_j + \boldsymbol{G}_i^{k_p}\Phi_j(\boldsymbol{x}_j)\right) + \boldsymbol{G}_i^{k_p}\Phi_i(\boldsymbol{x}_i), \\ \boldsymbol{y}_{\mathrm{p},i} = & \sum\limits_{k_p=1}^{r} \mu_i^{k_p}(\boldsymbol{z})\boldsymbol{C}_i^{k_p}\boldsymbol{x}_i, \end{cases} \tag{4.7}$$

$$\Sigma_{\mathrm{P_{f},}i} : \begin{cases} \dot{\boldsymbol{x}}_i = & \sum\limits_{k_p=1}^{r} \mu_i^{k_p}(\boldsymbol{z})(\boldsymbol{A}_i^{k_p}\boldsymbol{x}_i + \boldsymbol{B}_{\mathrm{f},i}^{k_p}\boldsymbol{u}_{\mathrm{p},i}) + \\ & \sum\limits_{\substack{j=1,\\ j\neq i}}^{N} \alpha_{ij}(\boldsymbol{H}_i\boldsymbol{x}_j + \boldsymbol{G}_i^{k_p}\Phi_i(\boldsymbol{x}_j)) + \boldsymbol{G}_i^{k_p}\Phi_i(\boldsymbol{x}_i)), \\ \boldsymbol{y}_{\mathrm{p},i} = & \sum\limits_{k_p=1}^{r} \mu_i^{k_p}(\boldsymbol{z})\boldsymbol{C}_{\mathrm{f},i}^{k_p}\boldsymbol{x}_i, \end{cases} \tag{4.8}$$

where, for the i-th subsystem, $\mu_i^{k_p} : \mathbb{R}^{n_z} \to [0,1]$ is the normalized membership function of the k_p-th fuzzy set that holds the convex sum property, $\boldsymbol{A}_i^{k_p}$, $\boldsymbol{B}_i^{k_p}$ ($\boldsymbol{B}_{\mathrm{f},i}^{k_p}$), and $\boldsymbol{C}_i^{k_p}$

($\boldsymbol{C}_{\mathrm{f},i}^{k_p}$) are real state-space matrices of the k_p-th rule with adequate dimensions, $\boldsymbol{x}_i \in \mathbb{R}^n$ is the state vector, $\boldsymbol{u}_{\mathrm{p},i} \in \mathbb{R}^m$ is the input vector, $\boldsymbol{y}_{\mathrm{p},i} \in \mathbb{R}^p$ is the measured output vector, the nonlinear map $\Phi_i : \mathbb{R}^n \to \mathbb{R}^n$ satisfies the sector bound condition described in Definition 4.1, $\boldsymbol{G}_i^{k_p}$ is a constant matrix with appropriate dimensions of the k_p-th rule related to the nonlinearities of the local subsystem and the other subsystems connected to it, and $\boldsymbol{H}_i$ is a constant matrix with appropriate dimensions of the k_p-th rule related to the linear interconnection with other subsystems. Moreover, the existing interconnections are described by the network adjacency matrix $\mathcal{A} = [\alpha_{ij}]_{N\times N}$, such as $\alpha_{ij} = 1$ if there is a connection between the i-th and j-th subsystem, and $\alpha_{ij} = 0$, otherwise.

Furthermore, this plant is controlled by a distributed OF-PDC $\Sigma_{\mathrm{C}} = \{\Sigma_{\mathrm{C}_1}, \ldots, \Sigma_{\mathrm{C}_N}\}$ that has its i-th subsystem dynamics described as follows

$$\Sigma_{\mathrm{C}_i} : \boldsymbol{u}_{c_i} = \sum_{k_c=1}^{r} \mu_i^{k_c} \boldsymbol{K}_i^{k_c} \boldsymbol{y}_{\mathrm{p},i} + \sum_{\substack{j=1,\\ j\neq i}}^{N} \alpha_{ij} \boldsymbol{F}_{ij} \boldsymbol{y}_{\mathrm{p},j}, \tag{4.9}$$

where $\boldsymbol{K}_i^{k_c} \in \mathbb{R}^{m\times p}$, for all the rules $k_c \in \mathbb{N}_{\leq r}$, is the i-th local controller gain with respect to the local measurements for the k_c-th rule, and $\boldsymbol{F}_{ij} \in \mathbb{R}^{m\times p}$ is the i-th controller gain with respect to the measurements from the j-th subsystem interconnected to it.

Differently, the second approach uses a centralized reconfiguration block, i.e., an unique Σ_{R} as described in (4.5) for all the interconnected system. The first approach is based on the Theorem 4.3.

Two approaches are presented in this chapter to recover the stability of the distributed system described in (4.7) and (4.8). The first approach uses distributed reconfiguration blocks, and the second approach uses a centralized reconfiguration block, i.e., a unique Σ_{R} as described in (4.5) for the whole interconnected system by solving the Problem 4.1. For the first approach, a different $\Sigma_{\mathrm{R},i}$ is used for each i-th subsystem for $i = \mathbb{N}_{\leq N}$, i.e., a decentralized TSRB $\Sigma_{\mathrm{R}} = \{\Sigma_{\mathrm{R}_1}, \ldots, \Sigma_{\mathrm{R}_N}\}$ is used in the reconfigured distributed system $(\Sigma_{\mathrm{P_f}}, \Sigma_{\mathrm{R}}, \Sigma_{\mathrm{C}})$. In this case, the TSRB for the i-th

subsystem is described as follows

$$\Sigma_{\mathrm{R}_i}: \begin{cases} \boldsymbol{y}_{\mathrm{r},i} = \sum_{k_r=1}^{r} \mu_i^{k_r}(\boldsymbol{z})(\boldsymbol{R}_{1,i}^{k_r}\boldsymbol{y}_{\mathrm{p},i} + \boldsymbol{R}_{2,i}^{k_r}\boldsymbol{u}_{\mathrm{c},i}), \\ \boldsymbol{u}_{\mathrm{r},i} = \sum_{k_r=1}^{r} \mu_i^{k_r}(\boldsymbol{z})(\boldsymbol{R}_{3,i}^{k_r}\boldsymbol{y}_{\mathrm{p},i} + \boldsymbol{R}_{4,i}^{k_r}\boldsymbol{u}_{\mathrm{c},i}), \end{cases} \tag{4.10}$$

where, for the i-th block, $\mu_i^{k_r}: \mathbb{R}^{n_z} \to [0,1]$ is the normalized membership function of the k_r-th fuzzy set that holds the convex sum property, for $k_r \in \mathbb{N}_{\leq r}$, and the real matrices $\boldsymbol{R}_{1,i}^{k_r}$, $\boldsymbol{R}_{2,i}^{k_r}$, $\boldsymbol{R}_{3,i}^{k_r}$, and $\boldsymbol{R}_{4,i}^{k_r}$ are the gains of the i-th TSRB.

For the first approach based on the decentralized static TSRB (4.10), the following distributed fault hiding problem is also addressed in this chapter.

Problem 4.2. ***Asymptotic Stability Recovery by Decentralized Fault Hiding for Distributed NT-S fuzzy model***

Let $\Sigma_{\mathrm{P}} = \{\Sigma_{\mathrm{P}_1}, \ldots, \Sigma_{\mathrm{P}_N}\}$ and $\Sigma_{\mathrm{P_f}} = \left\{\Sigma_{\mathrm{P}_{\mathrm{f},1}}, \ldots, \Sigma_{\mathrm{P}_{\mathrm{f},N}}\right\}$ be the nominal and the faultyNT-S fuzzy models, respectively, for a distributed plant whose dynamics for the i-th subsystem are described by (4.7) *and* (4.8)*. This distributed plant is interconnected by feedback to a decentralized OF-PDC $\Sigma_{\mathrm{C}} = \{\Sigma_{\mathrm{C}_1}, \ldots, \Sigma_{\mathrm{C}_N}\}$ described by* (4.9)*. Assume that the origin of $(\Sigma_{\mathrm{P}}, \Sigma_{\mathrm{C}})$ is asymptotically stable. Find the gains $\boldsymbol{R}_{1,i}^{k_r}$, $\boldsymbol{R}_{2,i}^{k_r}$, $\boldsymbol{R}_{3,i}^{k_r}$, and $\boldsymbol{R}_{4,i}^{k_r}$ for $k_r \in \mathbb{N}_{\leq r}$ and $i \in \mathbb{N}_{\leq N}$ of the distributed TSRB $\Sigma_{\mathrm{R}} = \{\Sigma_{\mathrm{R}_1}, \ldots, \Sigma_{\mathrm{R}_N}\}$ (cf.* (4.10)*), such that the origin of the reconfigured system $(\Sigma_{\mathrm{P_f}}, \Sigma_{\mathrm{R}}, \Sigma_{\mathrm{C}})$ is also asymptotically stable.*

4.2 Fault hiding of Takagi-Sugeno Fuzzy Systems

In this section, a solution for the Problem 4.1 is presented. For this purpose, novel conditions for stability recovery of nonlinear systems represented by means of T-S fuzzy by using the T-S fuzzy SRBspresented in (4.5). In particular, NT-S fuzzy model is described by (4.1) and allows to obtain a T-S fuzzy for exact representation of nonlinear systems that reduces the number of rules maintaining the affordability of designing tools of T-S fuzzys with linear consequent.

In the sequel, Theorem 4.1 provides sufficient conditions for the existence of Σ_{R} described by (4.5) for stability recovery by fault hiding of NT-S fuzzy model described by (4.1) and (4.4) with $\boldsymbol{G}^{k_p} = 0$ for $k_p \in \mathbb{N}_{\leq r}$.

Theorem 4.1. *Let Σ_{P} and $\Sigma_{\mathrm{P_f}}$ be the nominal and faulty T-S fuzzy with dynamics described, respectively, in* (4.1) *and* (4.4) *for the same plant, with $\boldsymbol{G}^{k_p} = 0$, interconnected by feedback to an OF-PDC Σ_{C} described in* (4.3)*. Assume that there exists $\boldsymbol{P} = \boldsymbol{P}^\top \succ 0$ such that*

$$\boldsymbol{P}\boldsymbol{A}^{k_p,k_c} + \boldsymbol{A}^{k_p,k_c}{}^\top \boldsymbol{P} \prec 0, \quad k_p, k_c \in \mathbb{N}_{\leq r}, \tag{4.11}$$

where

$$\boldsymbol{A}^{k_p,k_c} \triangleq \boldsymbol{A}^{k_p} + \boldsymbol{B}^{k_p}\boldsymbol{K}^{k_c}\boldsymbol{C}^{k_p}, \tag{4.12}$$

For given $\boldsymbol{K}^{k_c}$ and $\boldsymbol{P}$ satisfying (4.11)*, if there exist $\boldsymbol{R}_3^{k_r}$ and $\boldsymbol{R}_4^{k_r}$ such that the following inequalities hold*

$$\boldsymbol{P}\boldsymbol{A}_r^{k_p,k_c,k_r} + \boldsymbol{A}^{k_p,k_c,k_r}{}^\top \boldsymbol{P} \prec 0\ , \quad k_p, k_c, k_r \in \mathbb{N}_{\leq r}, \tag{4.13}$$

with

$$\boldsymbol{A}^{k_p,k_c,k_r} \triangleq \boldsymbol{A}^{k_p}+\boldsymbol{B}_{\mathrm{f}}^{k_p}\boldsymbol{R}_3^{k_r}\boldsymbol{C}_{\mathrm{f}}^{k_p}+\boldsymbol{B}_{\mathrm{f}}^{k_p}\boldsymbol{R}_4^{k_r}\boldsymbol{K}^{k_c}\boldsymbol{C}_{\mathrm{f}}^{k_p}, \quad \boldsymbol{R}_1^{k_r} = \boldsymbol{I}_p, \text{ and } \boldsymbol{R}_2^{k_r} = \boldsymbol{0}_{p\times m}, \forall k_r \in \mathbb{N}_{\leq r},$$

then $\Sigma_{\mathrm{P_f}}$ is stable by fault hiding with Σ_{R} described by (4.5)*.*

Proof. The closed-loop system $(\Sigma_{\mathrm{P}}, \Sigma_{\mathrm{C}})$ is equivalent to

$$\begin{cases} \dot{\boldsymbol{x}} = \displaystyle\sum_{k_p=1}^{r}\sum_{k_c=1}^{r} \mu^{k_p}(\boldsymbol{z})\mu^{k_c}(\boldsymbol{z})(\boldsymbol{A}^{k_p} + \boldsymbol{B}^{k_p}\boldsymbol{K}^{k_c}\boldsymbol{C}^{k_p})\boldsymbol{x}, \\ \boldsymbol{y} = \displaystyle\sum_{k_p=1}^{r} \mu^{k_p}(\boldsymbol{z})\boldsymbol{C}^{k_p}\boldsymbol{x}, \end{cases}$$

If there exists $\boldsymbol{P} = \boldsymbol{P}^\top \succ 0$ that satisfies (4.11), then the origin of $(\Sigma_{\mathrm{P}}, \Sigma_{\mathrm{C}})$ (described above) is asymptotically stable. Following Lemma 3.1, the same Lyapunov function $V(\boldsymbol{x}) = \boldsymbol{x}^\top\boldsymbol{P}\boldsymbol{x}$ will be used to investigate the stability of the reconfigured system $(\Sigma_{\mathrm{P_f}}, \Sigma_{\mathrm{R}}, \Sigma_{\mathrm{C}})$, that is described by follows

$$\begin{cases} \dot{\boldsymbol{x}} = \displaystyle\sum_{k_p=1}^{r}\sum_{k_c=1}^{r}\sum_{k_r=1}^{r} \mu^{k_p}(\boldsymbol{z})\mu^{k_c}(\boldsymbol{z})\mu^{k_r}(\boldsymbol{z}) \Big[\boldsymbol{A}^{k_p} + \boldsymbol{B}_{\mathrm{f}}^{k_p}\boldsymbol{R}_3^{k_r}\boldsymbol{C}_{\mathrm{f}}^{k_p} \\ \qquad +\boldsymbol{B}_{\mathrm{f}}^{k_p}\boldsymbol{R}_4^{k_r}(\boldsymbol{I}_m - \boldsymbol{K}^{k_c}\boldsymbol{R}_2^{k_r})^{-1}\boldsymbol{K}^{k_c}\boldsymbol{R}_1^{k_r}\boldsymbol{C}_{\mathrm{f}}^{k_p}\Big]\boldsymbol{x}, \\ \boldsymbol{y} = \displaystyle\sum_{k_p=1}^{r} \mu_i^{k_p}(\boldsymbol{z})\boldsymbol{C}_{\mathrm{f}}^{k_p}\boldsymbol{x}, \end{cases}$$

According to [Theorem 1][20], the origin of $(\Sigma_{\mathrm{P_f}}, \Sigma_{\mathrm{R}}, \Sigma_{\mathrm{C}})$ is asymptotically stable if the following set of inequalities is satisfied for $k_p, k_c, k_r \in \mathbb{N}_{\leq r}$:

$$\boldsymbol{P}\tilde{\boldsymbol{A}} + \tilde{\boldsymbol{A}}^{\top}\boldsymbol{P} \prec 0, \tag{4.14}$$

where

$$\tilde{\boldsymbol{A}} = \boldsymbol{A}^{k_p} + \boldsymbol{B}_{\mathrm{f}}^{k_p}\boldsymbol{R}_3^{k_r}\boldsymbol{C}_{\mathrm{f}}^{k_p} + \boldsymbol{B}_{\mathrm{f}}^{k_p}\boldsymbol{R}_4^{k_r}(\boldsymbol{I}_m - \boldsymbol{K}^{k_c}\boldsymbol{R}_2^{k_r})^{-1}\boldsymbol{K}^{k_c}\boldsymbol{R}_1^{k_r}\boldsymbol{C}_{\mathrm{f}}^{k_p}, \tag{4.15}$$

Considering that Σ_{C} is a static output feedback controller, it is redundant to compensate $\boldsymbol{u}_c$ and $\boldsymbol{y}$, since these signals are proportional due to the controller structure. Then, Σ_{R} is chosen such that $\boldsymbol{y}_r = \boldsymbol{y}$, therefore $\boldsymbol{R}_1^{k_r} = \boldsymbol{I}_p$ and $\boldsymbol{R}_2^{k_r} = \boldsymbol{0}_{p\times m}$ for all $k_r \in \mathbb{N}_{\leq r}$. Thus, (4.15) is equivalent to

$$\tilde{\boldsymbol{A}} = \boldsymbol{A}^{k_p} + \boldsymbol{B}_{\mathrm{f}}^{k_p}\boldsymbol{R}_3^{k_r}\boldsymbol{C}_{\mathrm{f}}^{k_p} + \boldsymbol{B}_{\mathrm{f}}^{k_p}\boldsymbol{R}_4^{k_r}\boldsymbol{K}^{k_c}\boldsymbol{C}_{\mathrm{f}}^{k_p} = \boldsymbol{A}^{k_p,k_c,k_r},$$

Finally, (4.14) is equivalent to (4.13), i.e., the origin of the reconfigured system $(\Sigma_{\mathrm{P_f}}, \Sigma_{\mathrm{R}}, \Sigma_{\mathrm{C}})$ is asymptotically stable if there exist $\boldsymbol{R}_3^{k_r}$ and $\boldsymbol{R}_4^{k_r}$, $k_r \in \mathbb{N}_{\leq r}$, satisfying (4.13), therefore $\Sigma_{\mathrm{P_f}}$ is stable by fault hiding according to Definition 3.1. □

The next theorem provides conditions for the existence of Σ_{R} described by (4.5) to recover the stability of the closed-loop system $(\Sigma_{\mathrm{P_f}}, \Sigma_{\mathrm{R}}, \Sigma_{\mathrm{C}})$, given that $(\Sigma_{\mathrm{P}}, \Sigma_{\mathrm{C}})$ is stable, for Σ_{P} and $\Sigma_{\mathrm{P_f}}$ described by (4.1) and (4.4), respectively. Unlike Theorem 4.1, the next theorem considers that the consequent of T-S fuzzy Σ_{P} and $\Sigma_{\mathrm{P_f}}$ are nonlinear, i.e., $\boldsymbol{G}^{k_p} \neq 0$.

Theorem 4.2. *Let Σ_{P} and $\Sigma_{\mathrm{P_f}}$ be the nominal and faulty NT-S fuzzy models with dynamics described in* (4.1) *and* (4.4)*, respectively, and considering the same plant interconnected by feedback to a static OF-PDC Σ_{C} described in* (4.3)*, such that the origin of $(\Sigma_{\mathrm{P}}, \Sigma_{\mathrm{C}})$ is asymptotically stable. Assume that there exist $\boldsymbol{P} = \boldsymbol{P}^{\top} \succ 0$, a diagonal matrix $\boldsymbol{W} \succ 0$, and a matrix $\boldsymbol{Y}$ satisfying the following inequalities:*

$$\begin{bmatrix} \boldsymbol{A}^{k_p,k_c\top}\boldsymbol{P} + \boldsymbol{P}\boldsymbol{A}^{k_p,k_c} & \star \\ \boldsymbol{G}^{k_p\top}\boldsymbol{P} + \boldsymbol{Y} & -2\boldsymbol{W} \end{bmatrix} \prec 0 \ , \quad k_p, k_c \in \mathbb{N}_{\leq r}, \tag{4.16}$$

with

$$\boldsymbol{A}^{k_p,k_c} \triangleq \boldsymbol{A}^{k_p} + \boldsymbol{B}^{k_p}\boldsymbol{K}^{k_c}\boldsymbol{C}^{k_p}.$$

For given $\boldsymbol{K}^{k_c}$, $\boldsymbol{P}$, $\boldsymbol{W}$ *and* $\boldsymbol{Y}$ *satisfying* (4.16), *if there exist* $\boldsymbol{R}_3^{k_r}$ *and* $\boldsymbol{R}_4^{k_r}$, *such that the following inequalities hold*

$$\left[\begin{array}{cc} \boldsymbol{A}^{k_p,k_c,k_r\top}\boldsymbol{P}+\boldsymbol{P}\boldsymbol{A}^{k_p,k_c,k_r} & \star \\ \boldsymbol{G}^{k_p\top}\boldsymbol{P}+\boldsymbol{Y} & -2\boldsymbol{W} \end{array}\right] \prec 0\ , \quad k_p,k_c,k_r \in \mathbb{N}_{\leq r}, \tag{4.17}$$

with

$$\boldsymbol{A}^{k_p,k_c,k_r} \triangleq \boldsymbol{A}^{k_p}+\boldsymbol{B}_{\mathrm{f}}^{k_p}\boldsymbol{R}_3^{k_r}\boldsymbol{C}_{\mathrm{f}}^{k_p}+\boldsymbol{B}_{\mathrm{f}}^{k_p}\boldsymbol{R}_4^{k_r}\boldsymbol{K}^{k_c}\boldsymbol{C}_{\mathrm{f}}^{k_p}$$

then $\Sigma_{\mathrm{P_f}}$ *is stable by fault hiding with* Σ_{R} *described in* (4.5).

Proof. The following closed-loop model for $(\Sigma_{\mathrm{P}},\Sigma_{\mathrm{C}})$ is obtained using (4.3) and (4.1):

$$\left\{\begin{array}{l} \dot{\boldsymbol{x}} = \displaystyle\sum_{k_p=1}^{r}\sum_{k_c=1}^{r}\mu^{k_c}(\boldsymbol{z})\left(\boldsymbol{A}^{k_p}(\boldsymbol{z})\mu^{k_c}(\boldsymbol{z})\boldsymbol{A}^{k_p,k_c}\boldsymbol{x}+\boldsymbol{G}^{k_p}\Phi(\boldsymbol{x})\right), \\ \boldsymbol{y} = \displaystyle\sum_{k_p=1}^{r}\mu^{k_c}(\boldsymbol{z})\boldsymbol{C}^{k_p}\boldsymbol{x}, \end{array}\right. \tag{4.18}$$

for $\boldsymbol{A}^{k_p,k_c} \triangleq \boldsymbol{A}^{k_p}+\boldsymbol{B}^{k_p}\boldsymbol{K}^{k_c}\boldsymbol{C}^{k_p}$.

Consider now the quadratic Lyapunov candidate $V(\boldsymbol{x})=\boldsymbol{x}^\top\boldsymbol{P}\boldsymbol{x}$ and $-\rho \leq \boldsymbol{x}-\boldsymbol{E}\boldsymbol{x} \leq \rho$ for some $\boldsymbol{E}$ and ρ. Then, according to Definition 4.1, for some diagonal matrix $\boldsymbol{W} \succ 0$

$$\Phi^\top(\boldsymbol{x})\boldsymbol{W}(\Phi(\boldsymbol{x})-\boldsymbol{E}\boldsymbol{x}) \leq 0, \tag{4.19}$$

The derivative of $V(\boldsymbol{x})$ is

$$\dot{V}(\boldsymbol{x}) = \boldsymbol{x}^\top(\boldsymbol{A}^{k_p,k_c}\boldsymbol{P}+\boldsymbol{P}\boldsymbol{A}^{k_p,k_c})\boldsymbol{x}+\Phi^\top(\boldsymbol{x})\boldsymbol{G}^{k_p\top}\boldsymbol{P}\boldsymbol{x}+\boldsymbol{x}^\top\boldsymbol{P}\boldsymbol{G}^{k_p}\Phi(\boldsymbol{x}), \tag{4.20}$$

From (4.20) and (4.19), the origin of $(\Sigma_{\mathrm{P}},\Sigma_{\mathrm{C}})$ is asymptotically stable if there exist any $\boldsymbol{P}=\boldsymbol{P}^\top \succ 0$ such that

$$\dot{V}(\boldsymbol{x}) < 2\Phi^\top(\boldsymbol{x})\boldsymbol{W}(\Phi(\boldsymbol{x})-\boldsymbol{E}\boldsymbol{x}), \tag{4.21}$$

considering

$$\Phi^\top(\boldsymbol{x})\boldsymbol{W}\boldsymbol{E}\boldsymbol{x} = \frac{\Phi^\top(\boldsymbol{x})\boldsymbol{W}\boldsymbol{E}\boldsymbol{x}+\boldsymbol{x}^\top\boldsymbol{E}^\top\boldsymbol{W}\Phi}{2},$$

the inequality (4.21) is equivalent to

$$\begin{bmatrix} \boldsymbol{x} \\ \Phi(\boldsymbol{x}) \end{bmatrix}^\top \begin{bmatrix} \boldsymbol{A}^{k_p,k_c}\boldsymbol{P} + \boldsymbol{P}\boldsymbol{A}^{k_p,k_c} & \star \\ {\boldsymbol{G}^{k_p}}^\top \boldsymbol{P} + \boldsymbol{W}\boldsymbol{E} & -2\boldsymbol{W} \end{bmatrix} \begin{bmatrix} \boldsymbol{x} \\ \Phi(\boldsymbol{x}) \end{bmatrix} \prec 0,$$

Defining $\boldsymbol{Y} \triangleq \boldsymbol{W}\boldsymbol{E}$, the above inequality implies (4.16).

The same Lyapunov function with the same $\boldsymbol{P}$ can be used, according to Lemma 3.1, to investigate the stability of the reconfigured system $(\Sigma_{\mathrm{P_f}}, \Sigma_{\mathrm{R}}, \Sigma_{\mathrm{C}})$. Considering $\boldsymbol{R}_1^{k_r} = \boldsymbol{I}_p$ and $\boldsymbol{R}_2^{k_r} = \boldsymbol{0}_{p\times m}$ for all $k_r \in \mathbb{N}_{\leq r}$, the reconfigured system is described as follows

$$\begin{cases} \dot{\boldsymbol{x}} = \displaystyle\sum_{k_p=1}^{r}\sum_{k_c=1}^{r}\sum_{k_r=1}^{r} \mu^{k_c}(\boldsymbol{z})\left(\boldsymbol{A}^{k_p}(\boldsymbol{z})\mu^{k_c}(\boldsymbol{z})\mu^{k_r}(\boldsymbol{z})\boldsymbol{A}^{k_p,k_c,k_r}x + \boldsymbol{G}^{k_p}\Phi(\boldsymbol{x})\right), \\ \boldsymbol{y} = \displaystyle\sum_{k_p=1}^{r} \mu^{k_c}(\boldsymbol{z})\boldsymbol{A}^{k_p}(\boldsymbol{z})\boldsymbol{C}^{k_p}\boldsymbol{x}, \end{cases} \tag{4.22}$$

where $\boldsymbol{A}^{k_p,k_c,k_r} \triangleq \boldsymbol{A}^{k_p} + \boldsymbol{B}_{\mathrm{f}}^{k_p}\boldsymbol{R}_3^{k_r}\boldsymbol{C}_f^{k_c} + \boldsymbol{B}_{\mathrm{f}}^{k_p}\boldsymbol{R}_4^{k_r}\boldsymbol{K}^{k_c}\boldsymbol{C}_{\mathrm{f}}^{k_p}$, $\boldsymbol{R}_1^{k_r} = I$, $\boldsymbol{R}_4^{k_r} = 0$, for all $k_p, k_c, k_r \in \mathbb{N}_{\leq r}$. In this case, the derivative of $V(\boldsymbol{x})$ is

$$\dot{V}(\boldsymbol{x}) = \boldsymbol{x}^\top(\boldsymbol{A}^{k_p,k_c,k_r}\boldsymbol{P} + \boldsymbol{P}{\boldsymbol{A}^{k_p,k_c,k_r}}^\top)\boldsymbol{x} + \Phi^\top(\boldsymbol{x}){\boldsymbol{G}^{k_p}}^\top\boldsymbol{P}\boldsymbol{x} + \boldsymbol{x}^\top\boldsymbol{P}\boldsymbol{G}^{k_p}\Phi(\boldsymbol{x}). \tag{4.23}$$

The reconfigured system $(\Sigma_{\mathrm{P_f}}, \Sigma_{\mathrm{R}}, \Sigma_{\mathrm{C}})$ is asymptotically stable if

$$\dot{V}(\boldsymbol{x}) < 2\Phi^\top(\boldsymbol{x})\boldsymbol{W}(\Phi(\boldsymbol{x}) - \boldsymbol{E}\boldsymbol{x})$$

for the same $\boldsymbol{W}$ and $\boldsymbol{Y}$ that satisfy (4.16) and considering $\boldsymbol{E} = \boldsymbol{W}^{-1}\boldsymbol{Y}$. Therefore, if there exist some $\boldsymbol{R}_3^{k_r}$ and $\boldsymbol{R}_4^{k_r}$ satisfying the inequalities

$$\begin{bmatrix} {\boldsymbol{A}^{k_p,k_c,k_r}}^\top\boldsymbol{P} + \boldsymbol{P}\boldsymbol{A}^{k_p,k_c,k_r} & \star \\ {\boldsymbol{G}^{k_p}}^\top\boldsymbol{P} + \boldsymbol{W}\boldsymbol{E} & -2\boldsymbol{W} \end{bmatrix} \prec 0. \tag{4.24}$$

Since that $\boldsymbol{Y} = \boldsymbol{W}\boldsymbol{E}$, inequalities (4.24) are equivalent to (4.17). If (4.17) hold, then $\Sigma_{\mathrm{P_f}}$ is stable by fault hiding according to Definition 3.1. □

4.3 Stability Recovery of Distributed Takagi-Sugeno Fuzzy Systems

4.3.1 Distributed Fault Hiding

In this Section, Problem 4.2 is addressed. For this purpose, this Section provides sufficient conditions for stability recovery, by means of a distributed TSRB $\Sigma_{\mathrm{R}} = \{\Sigma_{\mathrm{R}_1}, \ldots, \Sigma_{\mathrm{R}_N}\}$ (cf. (4.10)), of a distributed system composed of N interconnected T-S fuzzy, such that the nominal and fault dynamics, $\Sigma_{\mathrm{P}} = \{\Sigma_{\mathrm{P}_1}, \ldots, \Sigma_{\mathrm{P}_N}\}$ and $\Sigma_{\mathrm{P_f}} = \left\{\Sigma_{\mathrm{P}_{\mathrm{f},1}}, \ldots, \Sigma_{\mathrm{P}_{\mathrm{f},N}}\right\}$, respectively, of the i-th subsystem are given by (4.7) and (4.8).

Theorem 4.3. *Let $\Sigma_{\mathrm{P}} = \{\Sigma_{\mathrm{P}_1}, \ldots, \Sigma_{\mathrm{P}_N}\}$ and $\Sigma_{\mathrm{P_f}} = \left\{\Sigma_{\mathrm{P}_{\mathrm{f},1}}, \ldots, \Sigma_{\mathrm{P}_{\mathrm{f},N}}\right\}$ be, respectively, the nominal and faulty model for a distributed plant, whose subsystems' dynamics are described in (4.7) and (4.8), interconnected by feedback to distributed static OF-PDC $\Sigma_{\mathrm{C}} = \{\Sigma_{\mathrm{C}_1}, \ldots, \Sigma_{\mathrm{C}_N}\}$ described in (4.9). Assume that the origin of $(\Sigma_{\mathrm{P}}, \Sigma_{\mathrm{C}})$ is asymptotically stable and there exist $\boldsymbol{P} = \boldsymbol{P}^\top \succ 0$, diagonal matrices $\boldsymbol{W}_i \succ 0$, and matrices $\boldsymbol{Y}_i$, for $i \in \mathbb{N}_{\leq N}$, satisfying the following inequalities:*

$$\begin{bmatrix} \tilde{\boldsymbol{A}}^{k_p,k_c\top}\boldsymbol{P} + \boldsymbol{P}\tilde{\boldsymbol{A}}^{k_p,k_c} & \star & \ldots & \star & \star \\ \tilde{\boldsymbol{G}}_1^{k_p\top}\boldsymbol{P} + \boldsymbol{Y}_1 & 2\boldsymbol{W}_1^{-1} & \star & \ldots & \star \\ \tilde{\boldsymbol{G}}_2^{k_p\top}\boldsymbol{P} + \boldsymbol{Y}_2 & 0 & 2\boldsymbol{W}_2^{-1} & \ldots & \star \\ \vdots & \vdots & \vdots & \ddots & \vdots \\ \tilde{\boldsymbol{G}}_N^{k_p\top}P + \boldsymbol{Y}_N & 0 & 0 & \ldots & 2\boldsymbol{W}_N^{-1} \end{bmatrix} \prec 0, \tag{4.25}$$

where $k_p, k_c \in \mathbb{N}_{\leq r}$, $\tilde{\boldsymbol{G}}_i^{k_p} \triangleq \bigoplus_{j=1}^{N}(\alpha_{ij} + I[j=i])\boldsymbol{G}_i^{k_p}$, and

$$\tilde{\boldsymbol{A}}^{k_p,k_c} \triangleq \begin{bmatrix} \boldsymbol{A}_{11}^{k_p,k_c} & \boldsymbol{A}_{12}^{k_p,k_c} & \ldots & \boldsymbol{A}_{1N}^{k_p,k_c} \\ \boldsymbol{A}_{21}^{k_p,k_c} & \boldsymbol{A}_{22}^{k_p,k_c} & \ldots & \boldsymbol{A}_{2N}^{k_p,k_c} \\ \vdots & \vdots & \ddots & \vdots \\ \boldsymbol{A}_{N1}^{k_p,k_c} & \boldsymbol{A}_{N2}^{k_p,k_c} & \ldots & \boldsymbol{A}_{NN}^{k_p,k_c} \end{bmatrix} \tag{4.26}$$

$$\boldsymbol{A}_{ij}^{k_p,k_c} \triangleq \begin{cases} \boldsymbol{A}_i^{k_p} + \boldsymbol{B}_i^{k_p}\boldsymbol{K}^{k_c}\boldsymbol{C}_i^{k_p}, & \text{if } \ i = j, \\ \boldsymbol{B}_i^{k_p}\alpha_{ij}\boldsymbol{F}_{ij}\boldsymbol{C}_j^{k_p} + \alpha_{ij}\boldsymbol{H}_i, & \text{otherwise.} \end{cases} \tag{4.27}$$

For given $\boldsymbol{K}_i^{k_c}$ and $\boldsymbol{P}$, $\boldsymbol{W}_i$ and $\boldsymbol{Y}_i$ satisfying (4.25), if there exist $\boldsymbol{R}_{3,i}^{k_r}$ and $\boldsymbol{R}_{4,i}^{k_r}$ such that the following inequalities hold for $k_p, k_c, k_r \in \mathbb{N}_{\leq r}$

$$\begin{bmatrix} \tilde{\boldsymbol{A}}^{k_p,k_c,k_r\top}\boldsymbol{P}+\boldsymbol{P}\tilde{\boldsymbol{A}}^{k_p,k_c,k_r} & \star & \dots & \star & \star \\ \tilde{\boldsymbol{G}}_1^{k_p\top}\boldsymbol{P}+\boldsymbol{Y}_1 & 2\boldsymbol{W}_1^{-1} & \star & \dots & \star \\ \tilde{\boldsymbol{G}}_2^{k_p\top}\boldsymbol{P}+\boldsymbol{Y}_2 & 0 & 2\boldsymbol{W}_2^{-1} & \dots & \star \\ \vdots & \vdots & \vdots & \ddots & \vdots \\ \tilde{\boldsymbol{G}}_N^{k_p\top}\boldsymbol{P}+\boldsymbol{Y}_N & 0 & 0 & \dots & 2\boldsymbol{W}_N^{-1} \end{bmatrix} \prec 0, \tag{4.28}$$

with

$$\tilde{\boldsymbol{A}}^{k_p,k_c,k_r} \triangleq \begin{bmatrix} \boldsymbol{A}_{11}^{k_p,k_c,k_r} & \boldsymbol{A}_{12}^{k_p,k_c,k_r} & \dots & \boldsymbol{A}_{1N}^{k_p,k_c,k_r}, \\ \boldsymbol{A}_{21}^{k_p,k_c,k_r} & \boldsymbol{A}_{22}^{k_p,k_c,k_r} & \dots & \boldsymbol{A}_{2N}^{k_p,k_c,k_r}, \\ \vdots & \vdots & \ddots & \vdots \\ \boldsymbol{A}_{N1}^{k_p,k_c,k_r} & \boldsymbol{A}_{N2}^{k_p,k_c,k_r} & \dots & \boldsymbol{A}_{NN}^{k_p,k_c,k_r}, \end{bmatrix} \tag{4.29}$$

$$\boldsymbol{A}_{ij}^{k_p,k_c,k_r} \triangleq \begin{cases} \boldsymbol{A}_i^{k_p}+\boldsymbol{B}_{\mathrm{f},i}^{k_p}\boldsymbol{R}_{3,i}^{k_r}\boldsymbol{C}_{\mathrm{f},i}^{k_p}+\boldsymbol{B}_{\mathrm{f},i}^{k_p}\boldsymbol{R}_{4,i}^{k_r}\boldsymbol{K}_i^{k_c}\boldsymbol{C}_{\mathrm{f},i}^{k_p}, & \text{if } \ i=j, \\ \boldsymbol{B}_{\mathrm{f},i}^{k_p}\boldsymbol{R}_{4,i}^{k_r}\alpha_{ij}\boldsymbol{F}_{ij}\boldsymbol{C}_{\mathrm{f},i}^{k_p}+\alpha_{ij}\boldsymbol{H}_i, & \text{otherwise}, \end{cases} \tag{4.30}$$

$$\boldsymbol{R}_{1,i}^{k_r}=\boldsymbol{I}_p \qquad \boldsymbol{R}_{2,i}^{k_r}=\boldsymbol{0}_{p\times m},$$

then $\Sigma_{\mathrm{P_f}}$ *is stable by fault hiding with* $\Sigma_{\mathrm{R}}=\{\Sigma_{\mathrm{R}_1},\dots,\Sigma_{\mathrm{R}_N}\}$ *given by* (4.10).

Proof. The following closed-loop model for each subsystem $(\Sigma_{P_i},\Sigma_{\mathrm{C}_i})$ is obtained using (4.7) and (4.9):

$$\begin{cases} \dot{\boldsymbol{x}}_i = \displaystyle\sum_{k_p=1}^{r}\sum_{k_c=1}^{r}\mu^{k_p}(\boldsymbol{z})\mu^{k_c}(\boldsymbol{z})\left[(\boldsymbol{A}_i^{k_p}+\boldsymbol{B}_i^{k_p}\boldsymbol{K}^{k_c}\boldsymbol{C}_i^{k_p})\boldsymbol{x}_i+\sum_{\substack{j=1,\\ j\neq i,}}^{N}(\boldsymbol{B}_i^{k_p}\alpha_{ij}\boldsymbol{F}_{ij}\boldsymbol{C}_j^{k_p}+\alpha_{ij}\boldsymbol{H}_i)\boldsymbol{x}_j\right] \\ \qquad +\displaystyle\sum_{j=1}^{N}\boldsymbol{G}_i^{k_p}\Phi_i(\boldsymbol{x}_j) \\ \boldsymbol{y}_i = \displaystyle\sum_{k_p=1}^{r}\mu^{k_c}(\boldsymbol{z})\boldsymbol{C}_i^{k_p}\boldsymbol{x}_i, \end{cases} \tag{4.31}$$

the overall interconnected system dynamics is described as follows

$$\dot{\boldsymbol{x}} = \sum_{k_p=1}^{r}\sum_{k_c=1}^{r}\mu^{k_p}(\boldsymbol{z})\mu^{k_c}(\boldsymbol{z})\tilde{\boldsymbol{A}}^{k_p,k_c}\boldsymbol{x}+\sum_{j=1}^{N}\tilde{\boldsymbol{G}}_j^{k_p}\bar{\Phi}_j(\boldsymbol{x}), \tag{4.32}$$

for $\boldsymbol{A}^{k_p,k_c}$ defined in (4.26) and (4.27),

$$\boldsymbol{x} \triangleq \begin{bmatrix} \boldsymbol{x}_1 \\ \vdots \\ \boldsymbol{x}_N \end{bmatrix}, \ \bar{\Phi}_i(\boldsymbol{x}) \triangleq \begin{bmatrix} \Phi_i(\boldsymbol{x}_1) \\ \vdots \\ \Phi_i(\boldsymbol{x}_N) \end{bmatrix}, \ \tilde{\boldsymbol{G}}_i^{k_p} \triangleq \bigoplus_{j=1}^{N} (\alpha_{ij} + I[j=i]) \boldsymbol{G}_i^{k_p}.$$

Consider that all nonlinearities are sector bounded and can be expressed as indicated by Definition 4.1 for appropriate $\boldsymbol{E}_i$ and diagonal $\boldsymbol{W}_i$

$$\bar{\Phi}_i^{\top}(\boldsymbol{x}) \boldsymbol{W}_i (\bar{\Phi}_i(\boldsymbol{x}) - \boldsymbol{E}_i \boldsymbol{x}) \leq 0, \tag{4.33}$$

for $i \in \mathbb{N}_{\leq N}$. Choosing the quadratic Lyapunov candidate $V(\boldsymbol{x}) = \boldsymbol{x}^{\top} \boldsymbol{P} \boldsymbol{x}$, the derivative of $V(\boldsymbol{x})$ is

$$\dot{V}(\boldsymbol{x}) = \boldsymbol{x}^{\top} \left(\tilde{\boldsymbol{A}}^{k_p,k_c \top} \boldsymbol{P} + \boldsymbol{P} \tilde{\boldsymbol{A}}^{k_p,k_c} \right) x + \sum_{j=1}^{N} \left(\bar{\Phi}_j^{\top}(\boldsymbol{x}) \tilde{\boldsymbol{G}}_j^{k_p \top} \boldsymbol{P} \boldsymbol{x} + \boldsymbol{x}^{\top} P \tilde{\boldsymbol{G}}_j^{k_p} \bar{\Phi}_j(\boldsymbol{x}) \right), \tag{4.34}$$

From (4.34) and (4.33), the origin of the overall interconnected system $(\Sigma_{\mathrm{P}}, \Sigma_{\mathrm{C}})$ is asymptotically stable if there exists any $\boldsymbol{P} = \boldsymbol{P}^{\top} \succ 0$ such that

$$\dot{V}(\boldsymbol{x}) < \sum_{j=1}^{N} 2\Phi_j^{\top}(\boldsymbol{x}) \boldsymbol{W}_j (\Phi_j(\boldsymbol{x}) - \boldsymbol{E}_j \boldsymbol{x}). \tag{4.35}$$

Given that $2\Phi_j^{\top}(\boldsymbol{x}) \boldsymbol{W}_j \boldsymbol{E}_j x$ is scalar, the following fact holds

$$2\Phi_j^{\top}(\boldsymbol{x}) \boldsymbol{W}_j \boldsymbol{E}_j \boldsymbol{x} = \frac{\Phi_j^{\top}(\boldsymbol{x}) \boldsymbol{W}_j \boldsymbol{E}_j \boldsymbol{x} + \boldsymbol{x}^{\top} \boldsymbol{E}_j^{\top} \boldsymbol{W}_j \Phi_j(\boldsymbol{x})}{2}, \tag{4.36}$$

then, (4.35) implies

$$\begin{bmatrix} \boldsymbol{x} \\ \bar{\Phi}_1(\boldsymbol{x}) \\ \vdots \\ \bar{\Phi}_N(\boldsymbol{x}) \end{bmatrix}^{\top} \begin{bmatrix} \tilde{\boldsymbol{A}}^{k_p,k_c T} \boldsymbol{P} + \boldsymbol{P} \tilde{\boldsymbol{A}}^{k_p,k_c} & \star & \dots & \star & \star \\ \tilde{\boldsymbol{G}}_1^{k_p \top} P + \boldsymbol{W}_1 \boldsymbol{E}_1 & 2\boldsymbol{W}_1^{-1} & \star & \dots & \star \\ \tilde{\boldsymbol{G}}_2^{k_p \top} P + \boldsymbol{W}_2 \boldsymbol{E}_2 & 0 & 2\boldsymbol{W}_2^{-1} & \dots & \star \\ \vdots & \vdots & \vdots & \ddots & \vdots \\ \tilde{\boldsymbol{G}}_{N\,N}^{k_p \top} P + \boldsymbol{W}_N \boldsymbol{E}_N & 0 & 0 & \dots & 2\boldsymbol{W}_N^{-1} \end{bmatrix} \begin{bmatrix} \boldsymbol{x} \\ \bar{\Phi}_1(\boldsymbol{x}) \\ \vdots \\ \bar{\Phi}_N(\boldsymbol{x}) \end{bmatrix} \prec 0,$$

Defining $\boldsymbol{Y}_i \triangleq \boldsymbol{W}_i \boldsymbol{E}_i$, the above inequality is equivalent to (4.25).

The dynamics of each reconfigured subsystem $(\Sigma_{\mathrm{P}_{\mathrm{f},i}}, \Sigma_{\mathrm{R}_i}, \Sigma_{\mathrm{C}_i})$ is obtained by combining (4.9), (4.10), and (4.8)

$$\begin{cases} \dot{\boldsymbol{x}}_i = \displaystyle\sum_{k_p=1}^{r}\sum_{k_c=1}^{r}\sum_{k_r=1}^{r} \mu^{k_p}(\boldsymbol{z})\mu^{k_c}(\boldsymbol{z})\mu^{k_r}(\boldsymbol{z}) \Big[(\boldsymbol{A}_i^{k_p} + \boldsymbol{B}_{\mathrm{f},i}^{k_p}\boldsymbol{R}_{3,i}^{k_r}\boldsymbol{C}_{\mathrm{f},i}^{k_p} + \boldsymbol{B}_{\mathrm{f},i}^{k_p}\boldsymbol{R}_{4,i}^{k_r}\boldsymbol{K}^{k_c}\boldsymbol{C}_{\mathrm{f},i}^{k_p})\boldsymbol{x}_i \\ \qquad\qquad + \displaystyle\sum_{\substack{j=1,\\ j\neq i}}^{N} \alpha_{ij}(\boldsymbol{B}_{\mathrm{f},i}^{k_p}\boldsymbol{R}_{4,i}^{k_r}\boldsymbol{F}_{ij}\boldsymbol{C}_{f,j}^{k_p} + \boldsymbol{H}_i)\boldsymbol{x}_j \Big] \\ \qquad\qquad + \displaystyle\sum_{\substack{j=1,\\ j\neq i}}^{N} \boldsymbol{G}_i^{k_p}\Phi_i(\boldsymbol{x}_j) \\ \boldsymbol{y}_i = \displaystyle\sum_{k_p=1}^{r} \mu^{k_c}(\boldsymbol{z})\boldsymbol{C}_{\mathrm{f},i}^{k_p}\boldsymbol{x}_i \end{cases}, \tag{4.37}$$

for $\boldsymbol{R}_{1,i}^{k_r} = I$, $\boldsymbol{R}_{2,i}^{k_r} = 0$, and $i \in \mathbb{N}_{\leq N}$.

Based on (4.37), the dynamics of the overall interconnected faulty system $(\Sigma_{\mathrm{P_f}}, \Sigma_{\mathrm{R}}, \Sigma_{\mathrm{C}})$ is described as follows

$$\dot{\boldsymbol{x}} = \sum_{k_p=1}^{r}\sum_{k_c=1}^{r}\sum_{k_r=1}^{r} \mu^{k_p}(\boldsymbol{z})\mu^{k_c}(\boldsymbol{z})\mu^{k_r}(\boldsymbol{z})\tilde{\boldsymbol{A}}^{k_p,k_c,k_r}x + \sum_{j=1}^{N}\tilde{\boldsymbol{G}}_j^{k_p}\bar{\Phi}_j(\boldsymbol{x}), \tag{4.38}$$

where $\tilde{\boldsymbol{A}}^{k_p,k_c,k_r}$ is defined as (4.29) and (4.30).

The same Lyapunov function $V(\boldsymbol{x}) = \boldsymbol{x}^\top \boldsymbol{P}\boldsymbol{x}$ with the same $\boldsymbol{P}$ of the nominal system can be used, following Lemma 3.1, to find reconfiguration blocks that ensure the stability of the reconfigured system $(\Sigma_{\mathrm{P_f}}, \Sigma_{\mathrm{R}}, \Sigma_{\mathrm{C}})$. In this case, the derivative of $V(\boldsymbol{x})$ is

$$\dot{V}(\boldsymbol{x}) = \boldsymbol{x}^\top \left(\tilde{\boldsymbol{A}}^{k_p,k_c,k_r\top}\boldsymbol{P} + \boldsymbol{P}\tilde{\boldsymbol{A}}^{k_p,k_c,k_r} \right) x + \sum_{j=1}^{N} \left(\bar{\Phi}_j^\top(\boldsymbol{x})\tilde{\boldsymbol{G}}_j^{k_p\top}\boldsymbol{P}\boldsymbol{x} + \boldsymbol{x}^\top P\tilde{\boldsymbol{G}}_j^{k_p}\bar{\Phi}_j(\boldsymbol{x}) \right). \tag{4.39}$$

The reconfigured system $(\Sigma_{\mathrm{P_f}}, \Sigma_{\mathrm{R}}, \Sigma_{\mathrm{C}})$ is asymptotically stable if

$$\dot{V}(\boldsymbol{x}) < \sum_{j=1}^{N} 2\bar{\Phi}_j^{\top}(\boldsymbol{x})\boldsymbol{W}_j(\bar{\Phi}_j(\boldsymbol{x}) + \boldsymbol{E}_j\boldsymbol{x})$$

for the same $\boldsymbol{W}_j$ and $\boldsymbol{Y}_j$ that satisfy (4.25) and considering $\boldsymbol{E}_j = \boldsymbol{W}_j^{-1}\boldsymbol{Y}_j$. Therefore, if there exist some $\boldsymbol{R}_3^{k_r}$ and $\boldsymbol{R}_4^{k_r}$ satisfying the inequalities (4.28), then $\Sigma_{\mathrm{P_f}}$ is stable by fault hiding according to Definition 3.1. □

4.3.2 Centralized Fault Hiding

The second approach for fault hiding of distributed systems is based on Theorem 4.2 and uses a single centralized TSRB described in (4.5). An overall T-S fuzzy is obtained for the distributed system by gathering the models of every subsystem. Then, the overall interconnected nominal and fault model can be described by (4.1) and (4.8) from (4.7). In this sense, the following nominal and faulty model is obtained

$$\Sigma_{\mathrm{P}} : \begin{cases} \dot{\boldsymbol{x}} = & \sum_{k_p=1}^{r} \mu_i^{k_p}(\boldsymbol{z})(\boldsymbol{A}^{k_p}\boldsymbol{x} + \boldsymbol{B}^{k_p}\boldsymbol{u}_{\mathrm{p}}) + \boldsymbol{G}^{k_p}\Phi_i(\boldsymbol{x}), \\ \boldsymbol{y}_{\mathrm{p}} = & \sum_{k_p=1}^{r} \mu_i^{k_p}(\boldsymbol{z})\boldsymbol{C}^{k_p}\boldsymbol{x}, \end{cases} \tag{4.40}$$

$$\Sigma_{\mathrm{P_f}} : \begin{cases} \dot{\boldsymbol{x}} = & \sum_{k_p=1}^{r} \mu_i^{k_p}(\boldsymbol{z})(\boldsymbol{A}^{k_p}x + \boldsymbol{B}_{\mathrm{f}}^{k_p}\boldsymbol{u}_{\mathrm{p}}) + \boldsymbol{G}^{k_p}\Phi_i(\boldsymbol{x}), \\ \boldsymbol{y}_{\mathrm{p}} = & \sum_{k_p=1}^{r} \mu_i^{k_p}(\boldsymbol{z})\boldsymbol{C}_{\mathrm{f}}^{k_p}\boldsymbol{x}, \end{cases} \tag{4.41}$$

where

$$\boldsymbol{A}^{k_p} = \begin{bmatrix} \boldsymbol{A}_1^{k_p} & \alpha_{12}\boldsymbol{H}_1 & \alpha_{13}\boldsymbol{H}_1 & \dots & \alpha_{1N}\boldsymbol{H}_1 \\ \alpha_{21}\boldsymbol{H}_2 & \boldsymbol{A}_2^{k_p} & \alpha_{23}\boldsymbol{H}_1 & \dots & \alpha_{2N}\boldsymbol{H}_2 \\ \alpha_{31}\boldsymbol{H}_3 & \alpha_{32}\boldsymbol{H}_3 & \boldsymbol{A}_3^{k_p} & \dots & \alpha_{3N}\boldsymbol{H}_3 \\ \vdots & \vdots & \vdots & \ddots & \vdots \\ \alpha_{N1}\boldsymbol{H}_N & \alpha_{N2}\boldsymbol{H}_N & \alpha_{N3}\boldsymbol{H}_N & \dots & \boldsymbol{A}_N^{k_p} \end{bmatrix}, \quad \boldsymbol{x} \triangleq \begin{bmatrix} \boldsymbol{x}_1 \\ \vdots \\ \boldsymbol{x}_N \end{bmatrix},$$

$$\boldsymbol{B}^{k_p} = \begin{bmatrix} \boldsymbol{B}_1^{k_p} & 0 & \dots & 0 \\ 0 & \boldsymbol{B}_2^{k_p} & \dots & 0 \\ \vdots & \vdots & \ddots & \vdots \\ 0 & 0 & \dots & \boldsymbol{B}_N^{k_p} \end{bmatrix}, \quad \boldsymbol{B}_{\mathrm{f}}^{k_p} = \begin{bmatrix} \boldsymbol{B}_{f,1}^{k_p} & 0 & \dots & 0 \\ 0 & \boldsymbol{B}_{f,2}^{k_p} & \dots & 0 \\ \vdots & \vdots & \ddots & \vdots \\ 0 & 0 & \dots & \boldsymbol{B}_{f,N}^{k_p} \end{bmatrix},$$

$$\boldsymbol{C}^{k_p} = \begin{bmatrix} \boldsymbol{C}_1^{k_p} & 0 & \dots & 0 \\ 0 & \boldsymbol{C}_2^{k_p} & \dots & 0 \\ \vdots & \vdots & \ddots & \vdots \\ 0 & 0 & \dots & \boldsymbol{C}_N^{k_p} \end{bmatrix}, \quad \boldsymbol{C}_{\mathrm{f}}^{k_p} = \begin{bmatrix} \boldsymbol{C}_{f,1}^{k_p} & 0 & \dots & 0 \\ 0 & \boldsymbol{C}_{f,2}^{k_p} & \dots & 0 \\ \vdots & \vdots & \ddots & \vdots \\ 0 & 0 & \dots & \boldsymbol{C}_{f,N}^{k_p} \end{bmatrix},$$

$$\boldsymbol{G}^{k_p} = \bigoplus_{i=1}^{N} \bigoplus_{j=1}^{N} (\alpha_{ij} + I[j=i]) \boldsymbol{G}_i^{k_p}, \quad \boldsymbol{u}_{\mathrm{p}} = \begin{bmatrix} \boldsymbol{u}_{\mathrm{p},1} \\ \vdots \\ \boldsymbol{u}_{\mathrm{p},N} \end{bmatrix}, \quad \boldsymbol{y}_{\mathrm{p}} = \begin{bmatrix} \boldsymbol{y}_{\mathrm{p},1} \\ \vdots \\ \boldsymbol{y}_{\mathrm{p},N} \end{bmatrix}.$$

Therefore, Theorem 4.2 can be directly used to design the centralized block Σ_{R} given by (4.5) that guarantees the stability recovery by fault hiding of (4.40).

4.4 Application examples

4.4.1 Interconnected generators

Consider a nonlinear model of a power system with two interconnected generators as described in [240]. The model described in [240] is adapted here in order to simulate sensor and actuator faults. The nonlinear model is described as follows:

$$\begin{cases} \dot{x}_1 = x_2, \\ \dot{x}_2 = -\frac{1}{H} P_s \sin x_1 - \frac{D}{H} x_2 + u + d, \end{cases} \tag{4.42}$$

where x_1 is the relative voltage angle between the electrical machines, x_2 is the relative electrical angular speed between them, d is a disturbance, H is the inertia constant of the generators, D is the damping coefficient of machines, and P_m is the mechanical power of the generator.

An equivalent T-S fuzzy model, as given in (4.1), with two rules can be obtained

$$\boldsymbol{A}^1 = \begin{bmatrix} 0 & 1 \\ -\frac{a_1}{H} P_s & -\frac{D}{H} \end{bmatrix}, \quad \boldsymbol{A}^2 = \begin{bmatrix} 0 & 1 \\ -\frac{a_2}{H} P_s & -\frac{D}{H} \end{bmatrix},$$

$$\boldsymbol{G}^1 = \boldsymbol{G}^2 = 0,$$

$$\boldsymbol{B}^1 = \boldsymbol{B}^2 = \begin{bmatrix} 0 \\ 1 \end{bmatrix},$$

$$\boldsymbol{C}^1 = \boldsymbol{C}^2 = \boldsymbol{I}_2,$$
$$\mu^1(z) = \frac{z - a_2}{a_1 - a_2} \ , \ \mu^2(z) = \frac{a_1 - z}{a_1 - a_2},$$

where $z = \frac{\sin x_1}{x_1}$ $H = 0.06$, $D = 0.1$, $P_s = 3$, $a_1 = 1$, $a_2 = -0.22$.

A fault T-S fuzzy described in (4.4) is obtained for $k_p = 1, 2$:

$$\boldsymbol{C}_f^{k_p} = \begin{bmatrix} 1 - f_1 & 0 \\ 0 & 1 - f_2 \end{bmatrix} \boldsymbol{C}^{k_p},$$
$$B_f^{k_p} = (1 - f_3)\boldsymbol{B}^{k_p},$$

where f_1 and f_2 are multiplicative fault indicators in the sensors that represent attenuation of measurements of x_1 and x_2, respectively, and f_3 represents a loss in the actuator effectiveness, such that $f_1, f_2, f_3 \in [0, 1]$.

4.4.1.1 Fault hiding based on TSRBs for interconnected generators

Three fault scenarios are investigated. In all those scenarios the fault occurs at $t = 5$ s. Moreover, it is inserted impulsive disturbances d (cf. (4.42)) at $t = 2.5$ s, $t = 5.25$ s, and $t = 15$ s. In the first scenario, an actuator fault occurs at $t = 0.3$ s such that $f_3 = 0.9$, i.e. there is an effectiveness loss of 90% in the plant actuator. In the second and third scenarios, sensor faults occur at $t = 5$ s with $f_2 = 0.75$ and $f_3 = 0.8$, respectively. In all scenarios, the initial condition is $\boldsymbol{x}(0) = [\ 0.25 \quad -0.5\ ]^\top$ and an impulsive disturbance d is added at $t = 4$ s.

In both scenarios, the OF-PDC described in (4.3) is employed with the following gains

$$\boldsymbol{K}^1 = \begin{bmatrix} -73.7723 & -2.9152 \end{bmatrix} \ , \ \boldsymbol{K}^2 = \begin{bmatrix} 17.5804 & -3.4554 \end{bmatrix}.$$

In those experiments, the proposed TSRB is compared to the static TSRB proposed in [162] for multiplicative faults. In [162], it is presented the following Takagi-Sugeno static virtual actuator structure based on pseudoinverse

$$\Sigma_{\mathrm{R}}: \ \boldsymbol{u}_{\mathrm{r}} = \left(\sum_{k_r=1}^{r} \mu^{k_r}(z)\boldsymbol{B}^{k_r} \right)^{\dagger} \sum_{k_r=1}^{r} \mu^{k_r}(z)\boldsymbol{B}_f^{k_r}\boldsymbol{u}_{\mathrm{c}} \ . \tag{4.43}$$

The VA in (4.43) is used to handle the multiplicative actuator faults as the fault that occurs in the fist simulation scenario ($f_3 = 0.9$). In [162], it is not presented a similar static TSRB for sensor faults, however, the same fault compensation idea can be easily used to derive the following static VS for multiplicative faults:

$$\Sigma_{\mathrm{R}}: \ \boldsymbol{y}_{\mathrm{r}} = \sum_{k_r=1}^{r} \mu^{k_r}(z)\boldsymbol{C}^{k_r} \left(\sum_{k_r=1}^{r} \mu^{k_r}(z)\boldsymbol{C}_{\mathrm{f}}^{k_r} \right)^{\dagger} \boldsymbol{y}_{\mathrm{p}} \ . \tag{4.44}$$

Figures 4.2–4.4 depict the power system time response comparing its behavior with the proposed TSRB (4.5), with the static VA proposed in [162] and described in (4.43), and without any FTC strategy.

Particularly the results for the first scenario (fault instant $t = 0.3$ s and $f_3 = 0.9$) is obtained using the proposed TSRB described in (4.5), with the following gains

$$\begin{gathered}
\boldsymbol{R}_1^{k_r} = \boldsymbol{I}_2 \ , \ \boldsymbol{R}_2^{k_r} = \boldsymbol{0}_{2\times 1}, \ \forall k_r, \\
\boldsymbol{R}_3^1 = \boldsymbol{R}_3^2 = \begin{bmatrix} -0.9225 & -3.7616 \end{bmatrix} \times 10^4, \\
\boldsymbol{R}_4^1 = \boldsymbol{R}_4^2 = -2.7183 \times 10^{-12}.
\end{gathered}$$

obtained using Theorem 4.1. The results of Figure 4.2 indicate that the fault occurrence is compensated for in both approaches, even without RB. However, the recovery and the disturbance rejection ability of the reconfigured system with the proposed TSRB, and the performance of the VA proposed in [162] is only slightly better than the faulty system without RB.

In the second scenario, it occurs a sensor fault with magnitude $f_2 = 0.75$. The proposed TSRB obtained for this scenario using Theorem 4.1 presents the following gains

$$\begin{gathered}
\boldsymbol{R}_1^{k_r} = \boldsymbol{I}_2 \ , \ \boldsymbol{R}_2^{k_r} = \boldsymbol{0}_{2\times 1}, \ \forall k_r, \\
\boldsymbol{R}_3^1 = \boldsymbol{R}_3^2 = \begin{bmatrix} -0.0923 & -1.5047 \end{bmatrix} \times 10^4, \\
\boldsymbol{R}_4^1 = \boldsymbol{R}_4^2 = -2.645 \times 10^{-14}.
\end{gathered}$$

The results depicted in Figure 4.3 also indicate that both, reconfigured systems and faulty system without the reconfiguration block, maintain the stability of the origin. The reconfigured system with the proposed TSRB is not affected by the disturbance at

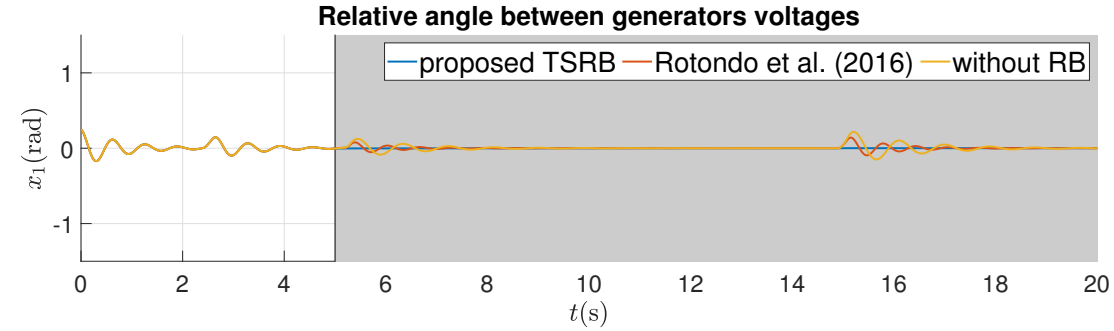

(a)

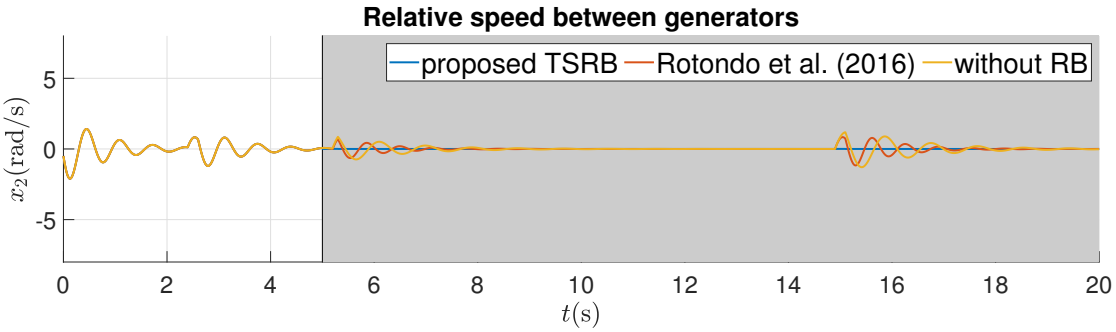

(b)

Figure 4.2 – Comparison of the interconnected generators' behavior with the proposed TSRB, with the TSRB in [162] and without reconfiguration block for $f_3 = 0.9$.

$t = 4s$, but the speed of the faulty system without reconfiguration blocks and that of the reconfigured system with the VS described in (4.44) is affected and oscillates for a few seconds. It is worth noting that the reconfigured system with the proposed TSRB presents better oscillations damping performance after the fault occurrence.

The last scenario also considers a sensor fault that affects the angle sensor with magnitude $f_1 = 0.75$. Theorem 4.1 is used to obtain a T-S fuzzy simplified reconfiguration block with the following gains

$$\boldsymbol{R}_1^{k_r} = \boldsymbol{I}_2 \ , \ \boldsymbol{R}_2^{k_r} = \boldsymbol{0}_{2\times 1}, \ \forall k_r,$$

$$\boldsymbol{R}_3^1 = \boldsymbol{R}_3^2 = \begin{bmatrix} -4.6125 & -3.7616 \end{bmatrix} \times 10^3,$$

$$\boldsymbol{R}_4^1 = \boldsymbol{R}_4^2 = -2.166 \times 10^{-13}.$$

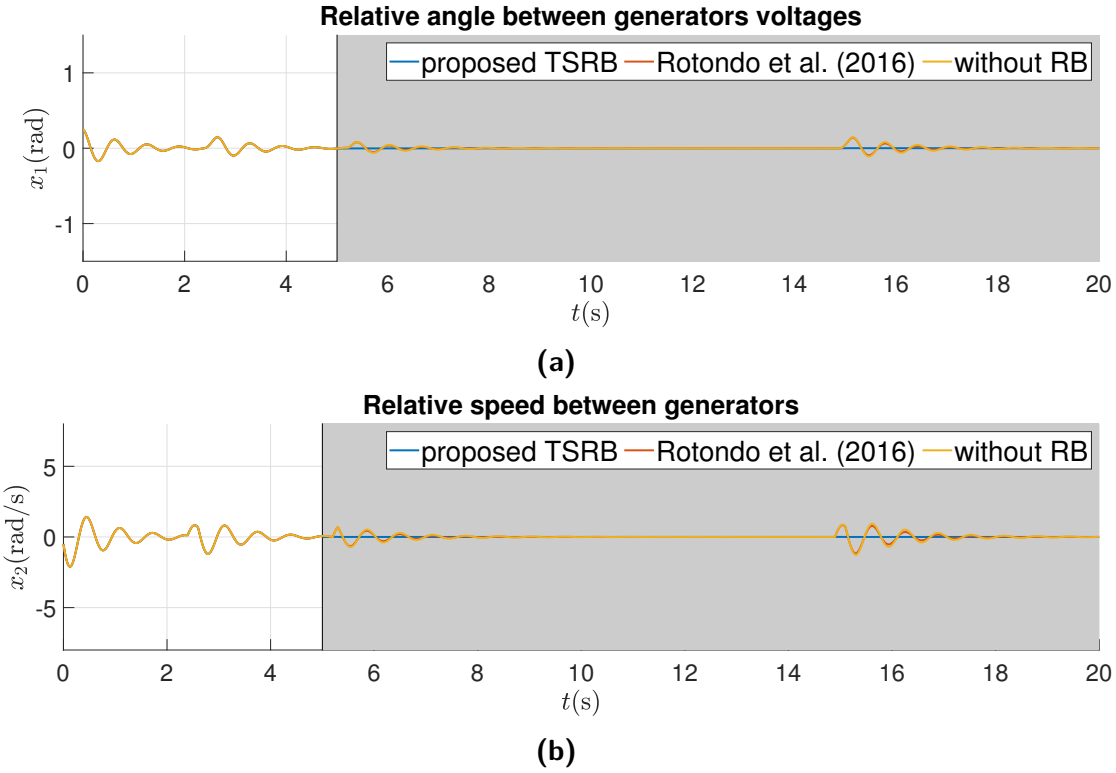

Figure 4.3 – Comparison of the interconnected generators' behavior with the proposed TSRB, with the TSRB in [162] and without reconfiguration block for $f_2 = 0.75$.

Figure 4.4 depicts the results for this scenario comparing the faulty system without RB with the reconfigured systems using the proposed TSRB and the VS described in (4.44). Similarly to the previous scenarios, the faulty system without reconfiguration block and the reconfigured system with the VS described in (4.44) present more intense oscillations after the fault occurrence. Furthermore, the reconfigured system with the proposed TSRB is able to avoid the disturbance in $t = 4$ s but the faulty system without RB and the reconfigured system with the VS described in (4.44) exhibit some oscillations after the disturbance occurrence.

4.4.1.2 Effect of FDI delays and fault estimation errors

In this subsection, the same simulations of Subsection 4.4.1.1 are repeated and it is considered the existence of some imperfections on the FDI system which provides

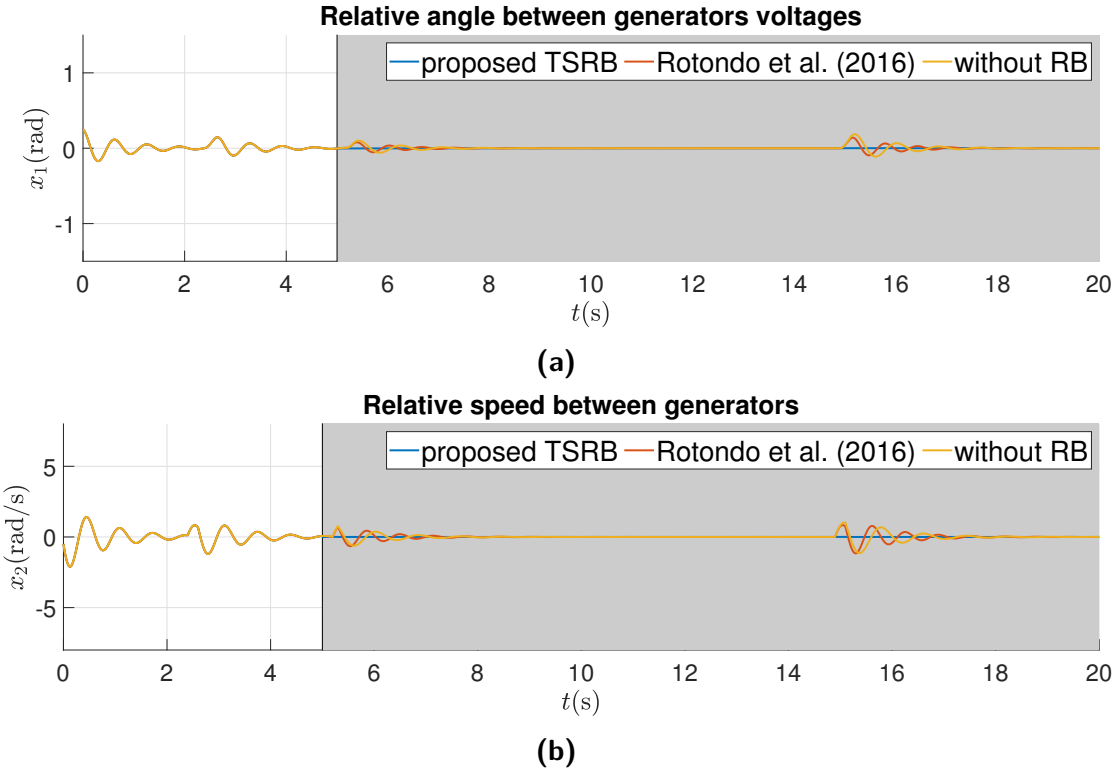

Figure 4.4 – Comparison of the interconnected generators' behavior with the proposed TSRB, with the TSRB in [162] and without reconfiguration block for $f_1 = 0.8$.

the information on the fault occurrence and its magnitude. In particular, it is considered that the fault information is available for the fault hiding mechanisms only 2 s after the fault occurrence, i.e., the faults occurs at $t = 5$ s but the reconfiguration will not occur before of $t = 7$ s. Moreover, although the fault magnitudes in the three scenarios previously investigated are, respectively, $f_3 = 0.9$, $f_2 = 0.75$, and $f_1 = 0.8$, the RBs will be designed and implemented based on wrong estimates: $\hat{f}_3 = 0.72$, $\hat{f}_2 = 0.9$, and $f_1 = 0.96$.

Figures 4.5, 4.6, and 4.7 depict the simulation results for the first, second, and third scenarios respectively. Those figures also provides the trajectories of the nominal (fault-free) system which may be compared to the response of the faulty system, and the reconfigured systems (with the proposed RB and with the RB proposed in [162]).

In addition to the observations Subsection 4.4.1.1, those figures show the

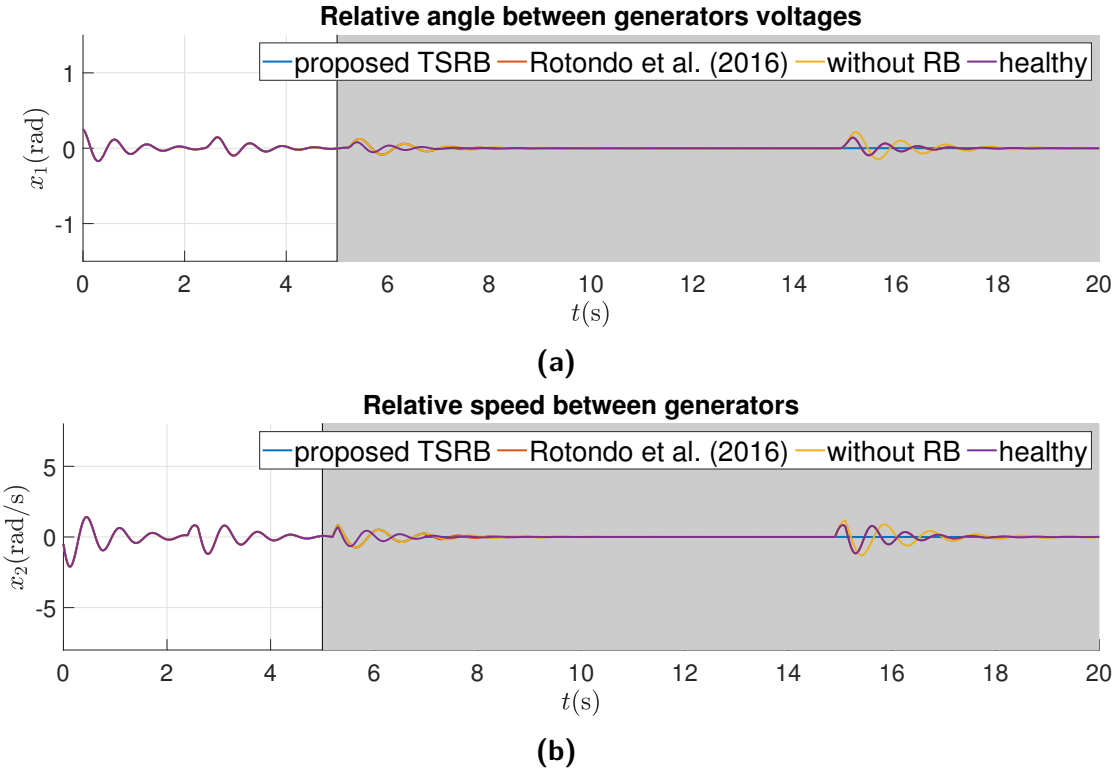

Figure 4.5 – Comparison of the interconnected generators' behavior with the proposed TSRB, with the TSRB in [162] and without reconfiguration block for $f_3 = 0.9$ considering FDI delays and fault estimation error.

conceptual differences between the proposed RB and the RB proposed in [162], as well as to assess their sensitivity with respect to the FDI delays and fault estimation errors.

The classic SRBs, which includes these proposed in [162], are based on the pseudoinverse method, thus they are able to guarantee exact trajectory recovery since the fault estimation is perfect. For this reason, when the FDI is assumed to be perfect as in Subsection 4.4.1.1, the response with the TSRB proposed in [162] is identical to the fault-free response. Otherwise, the RBs proposed in this thesis are not concerned with the exact trajectory recovery, but with the recovery of properties, in particular, the asymptotic stability recovery. Indeed, it was able to recover the stability and provided better disturbance rejection than the fault-free system and the faulty system reconfigured by means of the RBs proposed by [162].

However, when the reconfiguration is subject to FDI delays and fault estimation

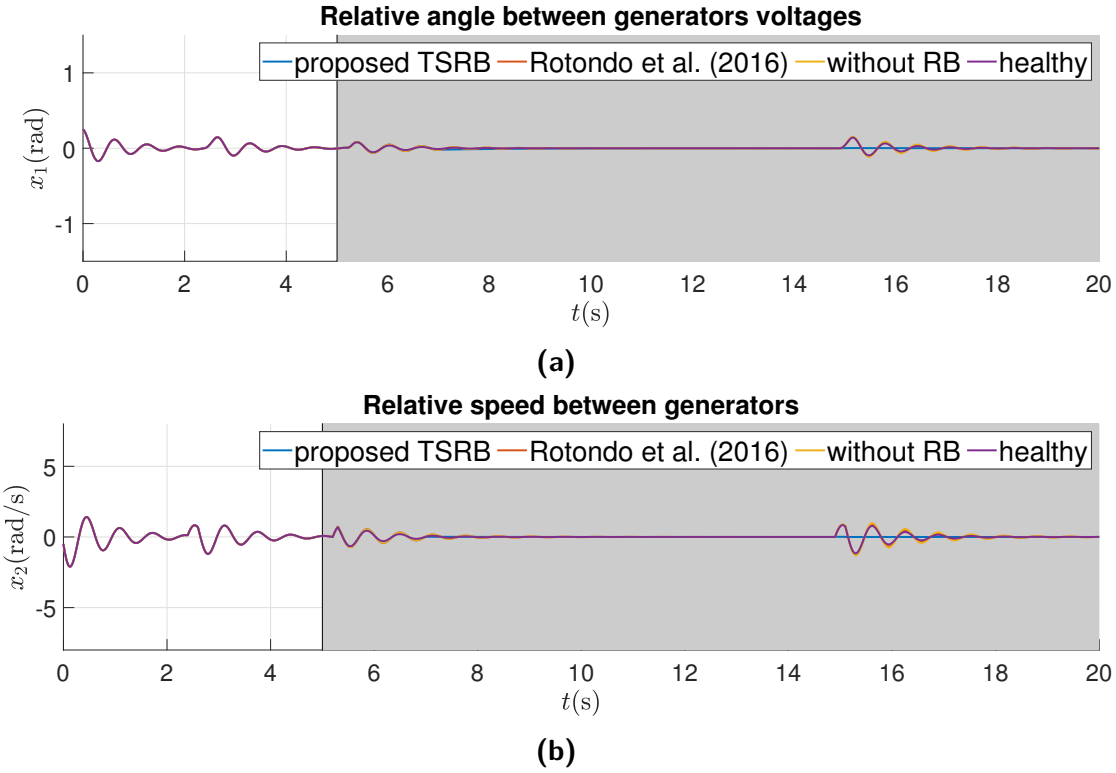

Figure 4.6 – Comparison of the interconnected generators' behavior with the proposed TSRB, with the TSRB in [162] and without reconfiguration block for $f_2 = 0.75$ considering FDI delays and fault estimation error.

errors one can see that the trajectories of the faulty system reconfigured by means of the RBs proposed by [162] are strongly affected by those effects. Although that RBs are still able to guarantee the stability, its performance appears to be very sensitive to the fault parameters, since they are explicitly used in their structures. Indeed, one can notice in Figures 4.5, 4.6, and 4.7 that the responses provided by the RBs proposed by [162] are closer to the responses of the faulty system without FTC than to the responses of the healthy system. It does not occur in the trajectories provided by the Takagi-Sugeno Fuzzy Reconfiguration Blocks (TSRBs) proposed in this thesis, since they were insensitive to the FDI delays and fault estimation errors. It suggests that the proposed is naturally more robust to the integration with imperfect FDI systems.

It is worth to mention that the interconnected generators are open-loop stable which reduces the impacts of the abovementioned sensitivity. It is expected that it can

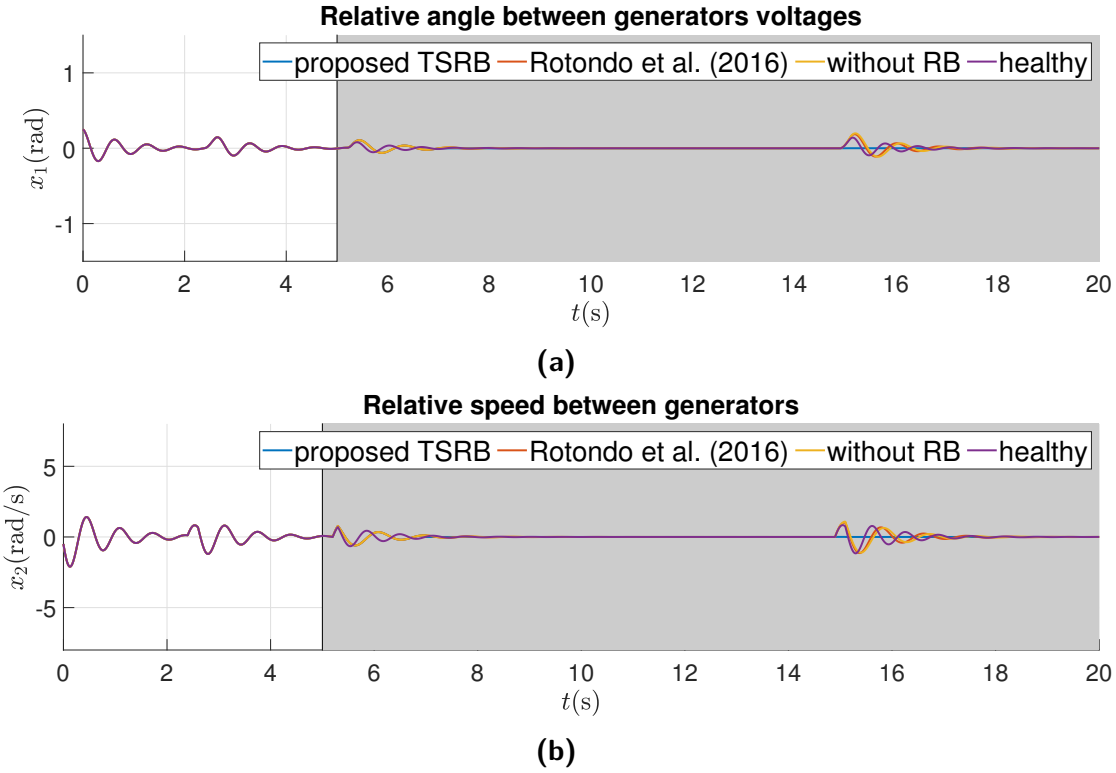

Figure 4.7 – Comparison of the interconnected generators' behavior with the proposed TSRB, with the TSRB in [162] and without reconfiguration block for $f_1 = 0.8$.

be fatal for the reconfiguration of unstable systems.

4.4.2 Inverted pendulum network

In order to evaluate the proposed T-S fuzzy simplified reconfiguration block structure as well as the proposed stability recovery results presented in Theorems 4.1, 4.2, and 4.3, consider a distributed pendulum system with nonlinear interconnections whose model for the i-th pendulum is described as follows:

$$\begin{cases} \dot{x}_{i1} = & x_{i2}, \\ \dot{x}_{i2} = & \frac{g}{l}\sin x_{i1} - \frac{1}{m_i l_i^2}\sum_{j=1}^{N}\left(k_l\alpha_{ij}(x_{i1}-x_{j1}) - k_n\alpha_{ij}(x_{i1}-x_{j1})^3\right) + \dfrac{1}{m_i l_i^2}u_{\mathrm{p},i}, \end{cases} \tag{4.45}$$

where $i, j = 1, \ldots, N$, x_{i1} is the rod angle with respect to the upright position, x_{i2} is the angular velocity, $\boldsymbol{u}_i$ is the torque applied to the base of the i-th pendulum, g is the gravitational acceleration, m_i and l_i are the mass and rod length of i-th pendulum, and k_l and k_n are the linear and nonlinear elastic coefficients of springs between two pendulums respectively.

The dynamics of each pendulum subsystem in this network can be described by the following T-S fuzzy with nonlinear consequent:

$$\Sigma_{P_i}: \begin{cases} \dot{\boldsymbol{x}}_i = \displaystyle\sum_{k_p=1}^{r} \mu_i^{k_p}(z)(\boldsymbol{A}_i^{k_p} x_i + \boldsymbol{B}_i^{k_p} u_{\mathrm{p},i}) + \sum_{\substack{j=1,\\ j\neq i}}^{N} \alpha_{ij}\left[\boldsymbol{H}_i(\boldsymbol{x}_i - \boldsymbol{x}_j) + \boldsymbol{G}_i \Phi_i(\boldsymbol{x}_j)\right], \\ \boldsymbol{y}_i = \displaystyle\sum_{k_p=1}^{r} \mu_i^{k_p}(z)\boldsymbol{C}_i^{k_p}\boldsymbol{x}_i, \end{cases} \tag{4.46}$$

with

$$\Phi_i(\boldsymbol{x}_j) = \begin{bmatrix} 0 \\ \frac{k_n^2}{m_i l_i^2}(x_{2i} - x_{2j})^3 \end{bmatrix},$$

$$\boldsymbol{A}_i^1 = \begin{bmatrix} 0 & 1 \\ \frac{g}{l_i} b_1 & 0 \end{bmatrix}, \ \boldsymbol{A}_i^2 = \begin{bmatrix} 0 & 1 \\ \frac{g}{l_i} b_2 & 0 \end{bmatrix},$$

$$\boldsymbol{B}_i^1 = \boldsymbol{B}_i^2 = \begin{bmatrix} 0 \\ \frac{1}{m_i l_i^2} \end{bmatrix}, \ \boldsymbol{C}_i^1 = \boldsymbol{C}_i^2 = \begin{bmatrix} 1 & 0 \\ 0 & 1 \end{bmatrix},$$

$$\boldsymbol{H}_i = \begin{bmatrix} 0 & 0 \\ -\frac{k_l}{m_i l_i^2} & 0 \end{bmatrix},$$

$$\boldsymbol{G}_i^1 = \boldsymbol{G}_i^3 = \begin{bmatrix} 0 & -\frac{k_n}{m_i l_i^2} \\ -\alpha_{ij}\frac{k_{ij}}{m_i l_i^2} & 0 \end{bmatrix},$$

$\boldsymbol{x}_i = [x_{i1}\ x_{i2}]^\top$, $z_i \in \left[\frac{2}{\pi}, 1\right]$ is a sector bounded nonlinearity, such that $z_i = \sin x_{i1}$ for $i = 1, \ldots, N$.

The system parameters are listed as follows: $N = 3$, $g = 9.81$ m/s^2, $m_1 = m_2 = 0.35$ kg, $m_3 = 0.30$ kg, $l_1 = l_2 = 1.2$ m, $l_3 = 1.3$ m, $b_1 = 1$, $b_2 = 0.9329$, and

the adjacency matrix is:

$$\mathcal{A} = \begin{bmatrix} 0 & 1 & 0 \\ 1 & 0 & 1 \\ 0 & 1 & 0 \end{bmatrix}.$$

The network is stabilized by a distributed OF-PDC described by (4.9). It is considered the occurrence of faults related to the loss of effectiveness of some subsystem actuator. The fault is modeled such that the fault f_i represents a fault on the i-th subsystem with $\boldsymbol{B}_{\mathrm{f},i} = (1 - f_i)\boldsymbol{B}_i$. It is worth mentioning that the results of this simulation are not compared to the other RBs in the literature because to the best of the authors' knowledge, there is no other fault hiding solutions that supports NT-S fuzzy models.

4.4.2.1 Inverted pendulum network with linear interconnections

In this first example, the nonlinearities of the interconnections between the pendulums as described in (4.46) are disregarded, i.e., it is assumed that $\boldsymbol{G}_i = 0$ for $i \in \mathbb{N}_{\leq N}$ and only linear interconnections are considered. The decentralized reconfiguration block described by (4.10) is evaluated and its matrices are obtained using Theorem 4.1.

In this simulation scenario, the linear elastic coefficient is $k_l = 120$ N/m and the OF-PDC described by (4.9) presents the following gains

$$\boldsymbol{F}_{1,2} = \begin{bmatrix} -119.1167 & 2.2736 \end{bmatrix}, \ \boldsymbol{F}_{2,1} = \begin{bmatrix} -119.1901 & -2.0729 \end{bmatrix},$$

$$\boldsymbol{F}_{2,3} = \begin{bmatrix} -119.3863 & -4.9073 \end{bmatrix}, \ \boldsymbol{F}_{3,3} = \begin{bmatrix} -119.1106 & 5.1507 \end{bmatrix},$$

$$\boldsymbol{F}_{1,1} = \boldsymbol{F}_{1,3} = \boldsymbol{F}_{2,2} = \boldsymbol{F}_{3,1} = \boldsymbol{F}_{3,3} = \begin{bmatrix} 0 & 0 \end{bmatrix},$$

$$\boldsymbol{K}_1^1 = \begin{bmatrix} 108.3942 & -1.4159 \end{bmatrix}, \ \boldsymbol{K}_1^2 = \begin{bmatrix} 109.8914 & -1.4159 \end{bmatrix},$$

$$\boldsymbol{K}_2^1 = \begin{bmatrix} 228.7719 & -5.1547 \end{bmatrix}, \ \boldsymbol{K}_2^2 = \begin{bmatrix} 230.2691 & -5.1547 \end{bmatrix},$$

$$\boldsymbol{K}_3^1 = \begin{bmatrix} 108.2058 & -0.5758 \end{bmatrix}, \ \boldsymbol{K}_3^2 = \begin{bmatrix} 109.5960 & -0.5758 \end{bmatrix},$$

It is simulated a loss in the actuator effectiveness of the second actuator such that $f_2 = 0.8$ after $t = 6$ s. Using Theorem 4.1, the following reconfiguration blocks are obtained

$$\boldsymbol{R}_{1,i}^{k_r} = \boldsymbol{I}_2 \ \ \boldsymbol{R}_{2,i}^{k_r} = \boldsymbol{0}_{2\times 1} \ \forall i, k_r,$$
$$\boldsymbol{R}_{3,1}^1 = \boldsymbol{R}_{3,1}^2 = \begin{bmatrix} 2.5678 & -5.4589 \end{bmatrix},$$
$$\boldsymbol{R}_{3,2}^1 = \boldsymbol{R}_{3,2}^2 = \begin{bmatrix} -67.6674 & 1.6714 \end{bmatrix},$$
$$\boldsymbol{R}_{3,3}^1 = \boldsymbol{R}_{3,3}^2 = \begin{bmatrix} 6.5446 & -6.6242 \end{bmatrix},$$
$$\boldsymbol{R}_{4,1}^1 = \boldsymbol{R}_{4,1}^2 = 1.0016, \quad \boldsymbol{R}_{4,2}^1 = \boldsymbol{R}_{4,2}^2 = 5.0837, \quad \boldsymbol{R}_{4,3}^1 = \boldsymbol{R}_{4,3}^2 = 0.9945.$$

Figures 4.8a–4.9b depict the simulation results with T-S fuzzy distributed reconfiguration block (Figures 4.8b and 4.9b) and without it (Figures 4.8a and 4.9a). Impulsive perturbations are applied over the angular position dynamics (x_{i1}) at the instant $t = 3$ s (before the fault occurrence) and $t = 12$ s (after the fault occurrence), and the initial condition is $x(0) = [0.1 \ 0 \ -0.05 \ 0 \ 0.05 \ 0]^\top$. The closed-loop system without reconfiguration block tends to reject the first perturbation but became unstable after the fault occurrence. Differently, the closed-loop system with reconfiguration block oscillates after the fault occurrence, but it is able to recover the stability, and the second perturbation is rejected even without an actuator for the third pendulum.

4.4.2.2 Inverted pendulums network with nonlinear interconnections

Now the decentralized reconfiguration block described in (4.10) is obtained using Theorem 4.2 for the pendulum network described by (4.46).

In this simulation scenario, the interconnection is nonlinear, i.e., $\boldsymbol{G}_i \neq 0$, and the elastic coefficients are $k_l = 60$ N/m and $k_n = 2.4$ N/m^3. The controller used is described in (4.9), with:

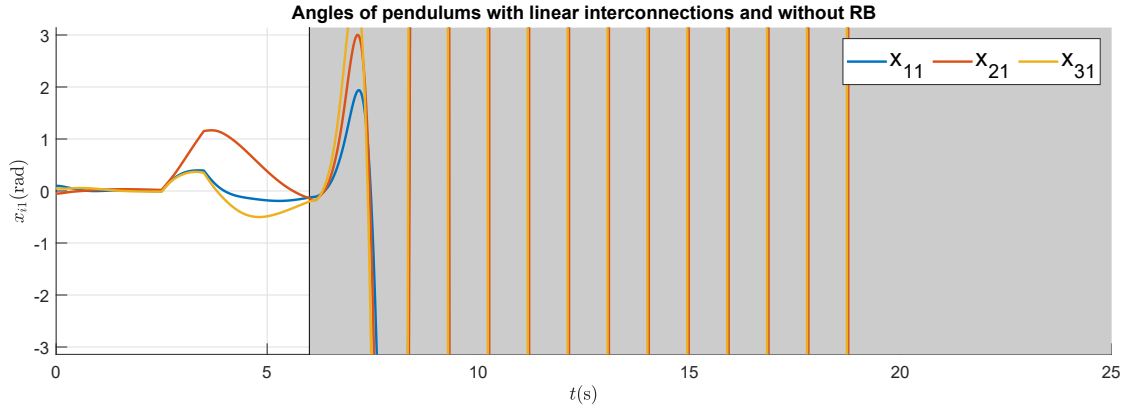

(a)

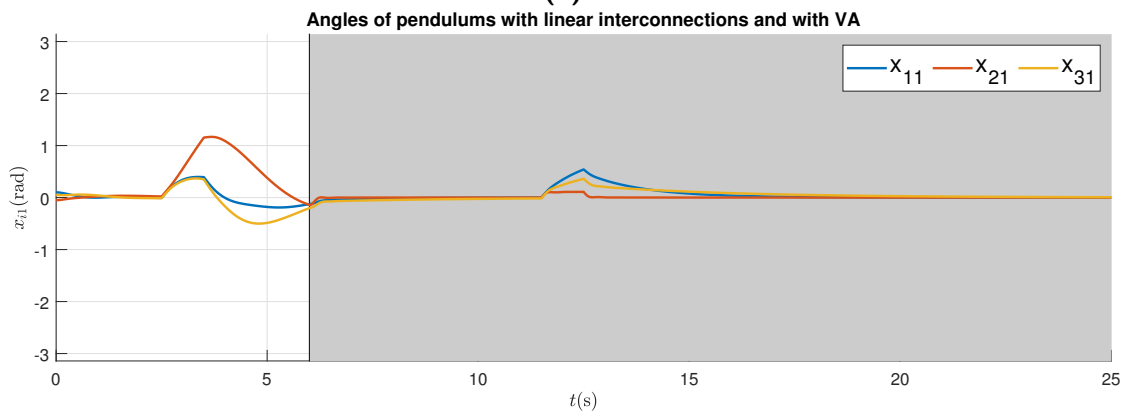

(b)

Figure 4.8 – Comparison of angles trajectories of the network of pendulums with and without reconfiguration block when a fault occurs in the second actuator such that $f_2 = 0.8$.

$$\boldsymbol{F}_{1,2} = \begin{bmatrix} -65.1830 & 2.6251 \end{bmatrix}, \ \boldsymbol{F}_{2,1} = \begin{bmatrix} -84.3104 & -2.7612 \end{bmatrix},$$

$$\boldsymbol{F}_{2,3} = \begin{bmatrix} -69.7608 & 1.6384 \end{bmatrix}, \ \boldsymbol{F}_{3,2} = \begin{bmatrix} -84.7336 & -1.7220 \end{bmatrix},$$

$$\boldsymbol{F}_{1,1} = \boldsymbol{F}_{1,3} = \boldsymbol{F}_{2,2} = \boldsymbol{F}_{3,1} = \boldsymbol{F}_{3,3} = \begin{bmatrix} 0 & 0 \end{bmatrix},$$

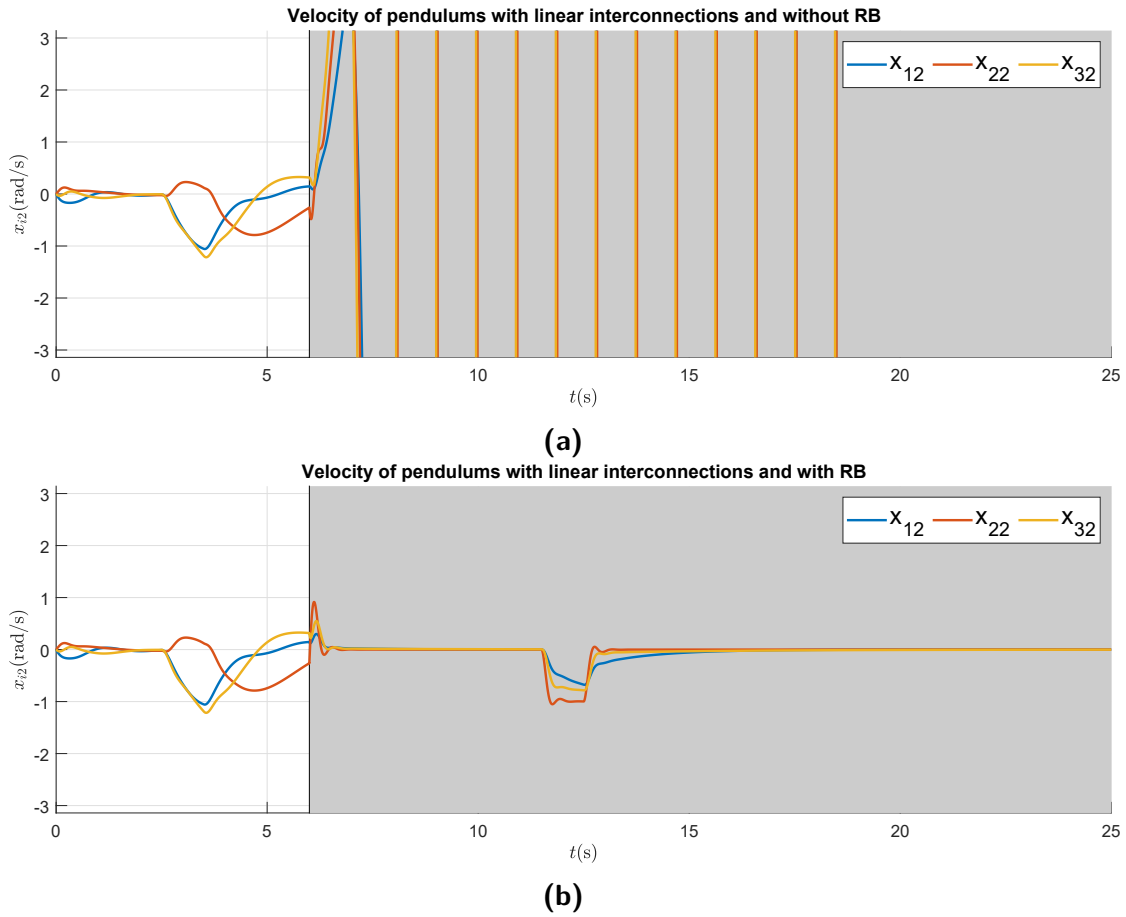

Figure 4.9 – Comparison of the velocities trajectories of the network of pendulums with and without reconfiguration block when a fault occurs in the second actuator such that $f_2 = 0.8$.

$$\boldsymbol{K}_1^1 = \begin{bmatrix} 15.6604 & -2.6304 \end{bmatrix}, \quad \boldsymbol{K}_1^2 = \begin{bmatrix} 17.1576 & -2.6304 \end{bmatrix},$$

$$\boldsymbol{K}_2^1 = \begin{bmatrix} 12.0243 & -4.0508 \end{bmatrix}, \quad \boldsymbol{K}_2^2 = \begin{bmatrix} 13.5215 & -4.0508 \end{bmatrix},$$

$$\boldsymbol{K}_3^1 = \begin{bmatrix} 15.8759 & -2.6403 \end{bmatrix}, \quad \boldsymbol{K}_3^2 = \begin{bmatrix} 17.2662 & -2.6403 \end{bmatrix}.$$

A fault occurs in the first actuator at $t = 6$ s such that $f_3 = 0.9$. Using Theorem 4.2, the following reconfiguration blocks are obtained

$$\boldsymbol{R}_{1,i}^{k_r} = \boldsymbol{I}_2 \ , \ \boldsymbol{R}_{2,i}^{k_r} = \boldsymbol{0}_{2\times 1}, \ \forall i, k_r$$

$$\boldsymbol{R}_{3,1}^{1} = \boldsymbol{R}_{3,1}^{2} = \begin{bmatrix} 18.1709 & -16.4871 \end{bmatrix}$$

$$\boldsymbol{R}_{3,2}^{1} = \boldsymbol{R}_{3,2}^{2} = \begin{bmatrix} 62.5708 & -19.1694 \end{bmatrix}$$

$$\boldsymbol{R}_{3,3}^{1} = \boldsymbol{R}_{3,3}^{2} = \begin{bmatrix} -58.3747 & -157.3098 \end{bmatrix}$$

$$\boldsymbol{R}_{4,1}^{1} = \boldsymbol{R}_{4,1}^{2} = 0.9032, \quad \boldsymbol{R}_{4,2}^{1} = \boldsymbol{R}_{4,2}^{2} = 0.8434, \quad \boldsymbol{R}_{4,3}^{1} = \boldsymbol{R}_{4,3}^{2} = 7.0303,$$

Figures 4.10a–4.11b depict the simulation results with the T-S fuzzy distributed reconfiguration block (Figures 4.10b and 4.11b) and without it (Figures 4.10a and 4.11a). Impulsive perturbations at angle position (x_{i1}) are considered at $t = 3$ s and $t = 12$ s, and the initial condition is $x(0) = [0.1 \ 0 \ -0.05 \ 0 \ 0.05 \ 0]$. The closed-loop system without reconfiguration block is able to reject the first perturbation again but it became unstable after the second perturbation due to the effects of the fault occurrence in a single pendulum. The closed-loop system with reconfiguration block is able to reject both perturbations and mitigate the fault effects.

4.4.2.3 Reconfiguration with centralized reconfiguration blocks

In this subsection, the centralized approach for decentralized T-S fuzzy is applied to the pendulum network.

In the first set of experiments, the interconnections are linear, i.e., $\boldsymbol{G}_i = 0$, for $i \in \mathbb{N}_{\leq N}$. The linear elastic coefficients are $k_l = 70$ N/m. An OF-PDC is used as described in (4.9) with

$$\boldsymbol{F}_{1,2} = \begin{bmatrix} -45.6545 & 9.8429 \end{bmatrix}, \quad \boldsymbol{F}_{2,1} = \begin{bmatrix} -89.4600 & -10.0421 \end{bmatrix},$$

$$\boldsymbol{F}_{2,3} = \begin{bmatrix} -60.2578 & 6.1591 \end{bmatrix}, \quad \boldsymbol{F}_{3,2} = \begin{bmatrix} -88.4860 & -6.3235 \end{bmatrix},$$

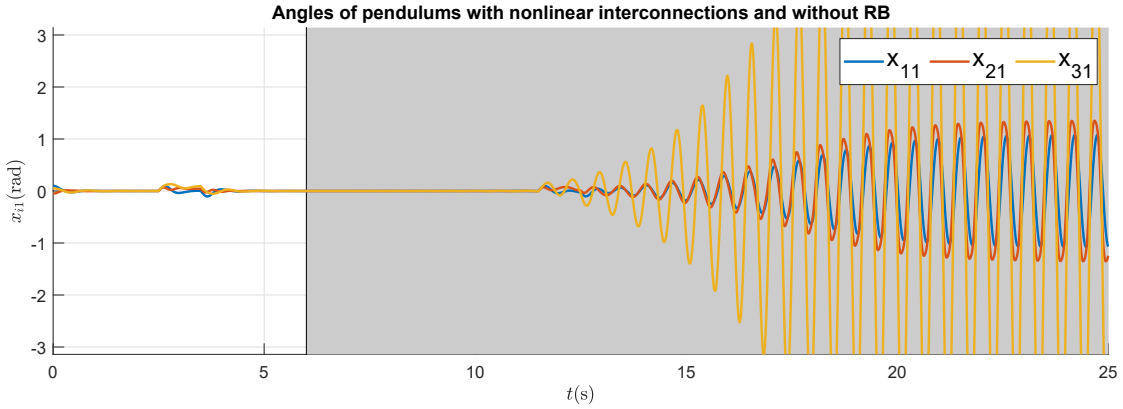

(a)

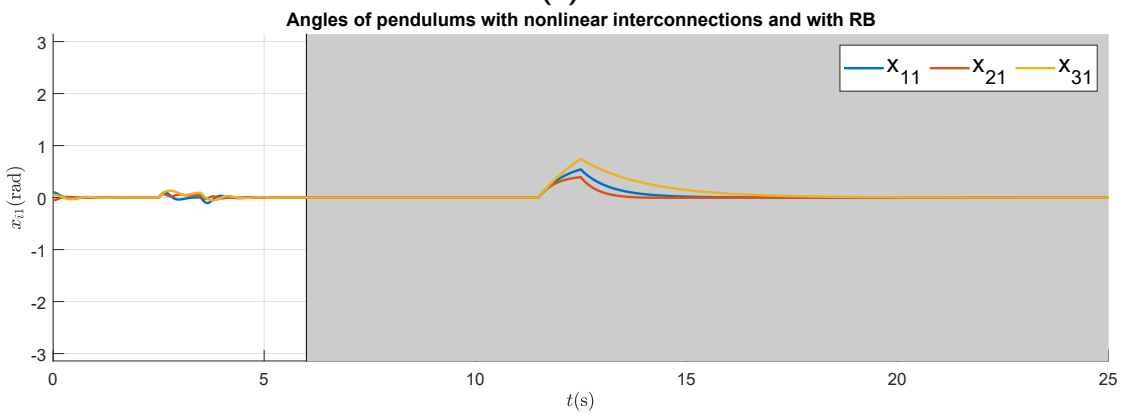

(b)

Figure 4.10 – Comparison of angles trajectories of the network of pendulums with nonlinear interconnections with and without reconfiguration block when occurs an effectiveness loss fault in the third actuator ($f_3 = 0.9$).

$$\boldsymbol{F}_{1,1} = \boldsymbol{F}_{1,3} = \boldsymbol{F}_{2,2} = \boldsymbol{F}_{3,1} = \boldsymbol{F}_{3,3} = \begin{bmatrix} 0 & 0 \end{bmatrix},$$

$$\boldsymbol{K}_1^1 = \begin{bmatrix} 57.8405 & -1.1288 \end{bmatrix}, \quad \boldsymbol{K}_1^2 = \begin{bmatrix} 59.3377 & -1.1288 \end{bmatrix},$$

$$\boldsymbol{K}_2^1 = \begin{bmatrix} 116.4197 & -1.6873 \end{bmatrix}, \quad \boldsymbol{K}_2^2 = \begin{bmatrix} 117.9169 & -1.6873 \end{bmatrix},$$

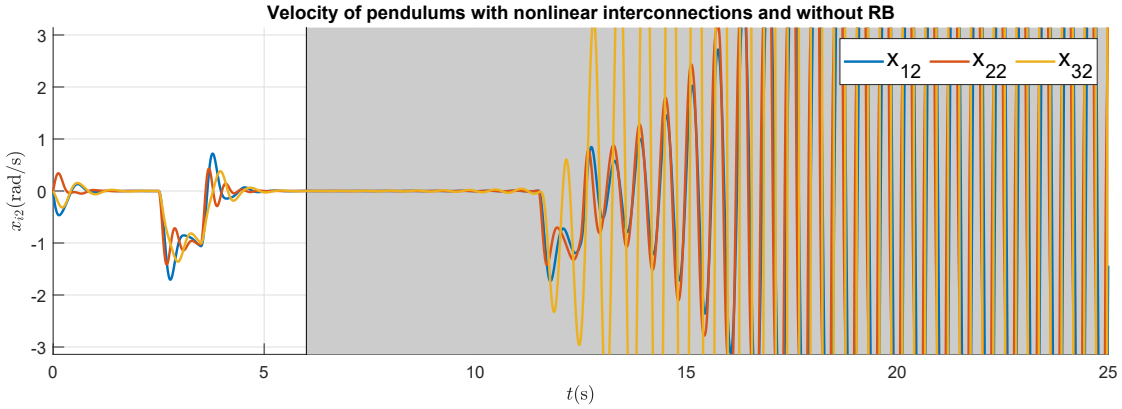

(a)

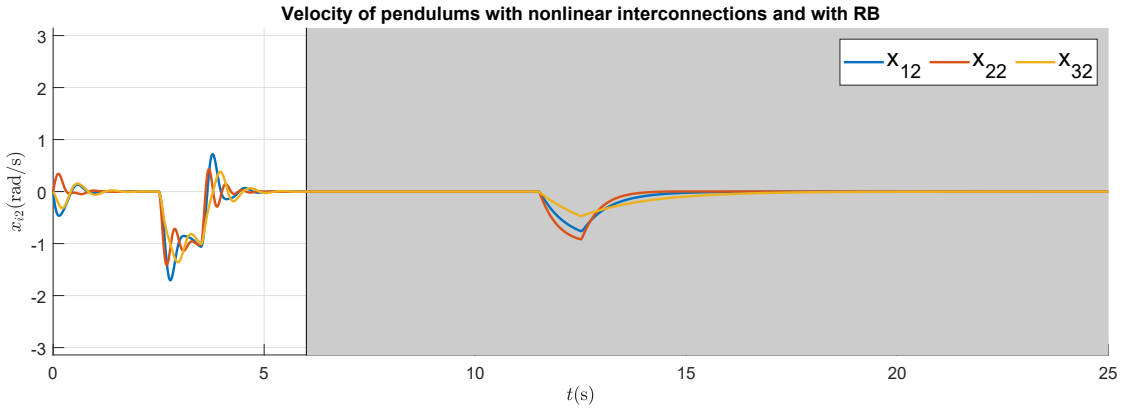

(b)

Figure 4.11 – Comparison of velocities trajectories of the network of pendulums with nonlinear interconnections with and without reconfiguration block when occurs an effectiveness loss fault in the third actuator ($f_3 = 0.9$).

$$\boldsymbol{K}_3^1 = \begin{bmatrix} 58.0869 & -1.1355 \end{bmatrix}, \quad \boldsymbol{K}_3^2 = \begin{bmatrix} 59.4772 & -1.1355 \end{bmatrix}.$$

In this scenario, a fault occurs in the first actuator at $t = 6$ s, such that $f_1 = 0.25$, i.e., an effectiveness loss of 25%. Using the Theorem 4.1, the reconfiguration block described in (4.5) is obtained such that

$$\boldsymbol{R}_1^i = \boldsymbol{I}_6, \ \boldsymbol{R}_2^i = \boldsymbol{0}_{6\times 3},$$

$$\boldsymbol{R}_3^i = \begin{bmatrix} 0.0000 & -0.5979 & 1.3612 & 0.3608 & -0.2947 & -1.1314 \\ -0.4688 & -0.1171 & -0.3496 & -0.0142 & 0.4018 & 0.4207 \\ 0.3563 & 0.4985 & -0.7044 & -0.2409 & -0.1041 & 0.4538 \end{bmatrix} \times 10^3,$$

$$\boldsymbol{R}_4^i = \begin{bmatrix} 0.4238 & -0.3829 & -0.5531 \\ 0.1259 & 0.4249 & -0.0190 \\ -0.2475 & 0.2905 & 0.2998 \end{bmatrix} \times 10^{-11},$$

for $i = 1, \ldots, 8$

Figures 4.12a–4.13b depict the simulation results with reconfiguration block (Figures 4.12b and 4.13b) and without it (Figures 4.12a and 4.13a). Impulsive perturbations are added at $t = 3$ s and $t = 12$ s and the initial condition is $x(0) = [-0.05\ 0\ 0.2\ 0\ \ -0.2\ 0]^\top$. The closed-loop system without reconfiguration block compensates the first perturbation, but presents a small oscillation after the fault occurrence, and became clearly unstable after the second perturbation that occurs during the fault occurrence. However, the closed-loop system with the proposed reconfiguration block is able to reject both perturbations and mitigate the fault effects.

In the second set of experiments, the interconnections are nonlinear. The linear and nonlinear elastic coefficients are $k_l = 90$ N/m and $k_n = 8.1$ N/m^3. An OF-PDC is used as described in (4.9) with

$$\boldsymbol{F}_{1,2} = \begin{bmatrix} -138.0934 & 1.6586 \end{bmatrix}, \quad \boldsymbol{F}_{2,1} = \begin{bmatrix} -156.2654 & -1.8629 \end{bmatrix},$$

$$\boldsymbol{F}_{2,3} = \begin{bmatrix} -138.0111 & 0.9168 \end{bmatrix}, \quad \boldsymbol{F}_{3,2} = \begin{bmatrix} -162.4693 & -1.1184 \end{bmatrix},$$

$$\boldsymbol{F}_{1,1} = \boldsymbol{F}_{1,3} = \boldsymbol{F}_{2,2} = \boldsymbol{F}_{3,1} = \boldsymbol{F}_{3,3} = \begin{bmatrix} 0 & 0 \end{bmatrix},$$

$$\boldsymbol{K}_1^1 = \begin{bmatrix} -151.8591 & -4.3598 \end{bmatrix}, \quad \boldsymbol{K}_1^2 = \begin{bmatrix} -150.3619 & -4.3598 \end{bmatrix},$$

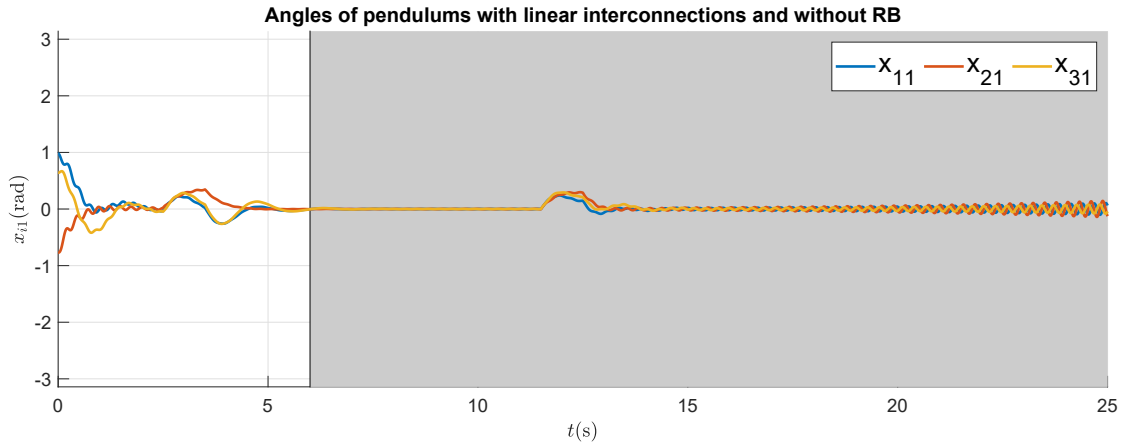

(a)

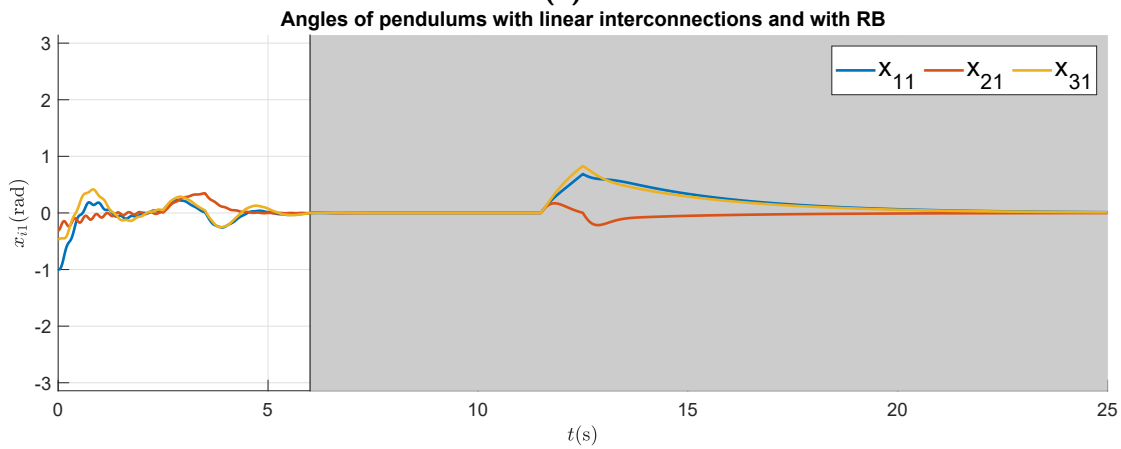

(b)

Figure 4.12 – Comparison of angles trajectories of the network of pendulums with nonlinear interconnections with and without reconfiguration block when occurs an effectiveness loss fault in the first actuator ($f_1 = 0.25$).

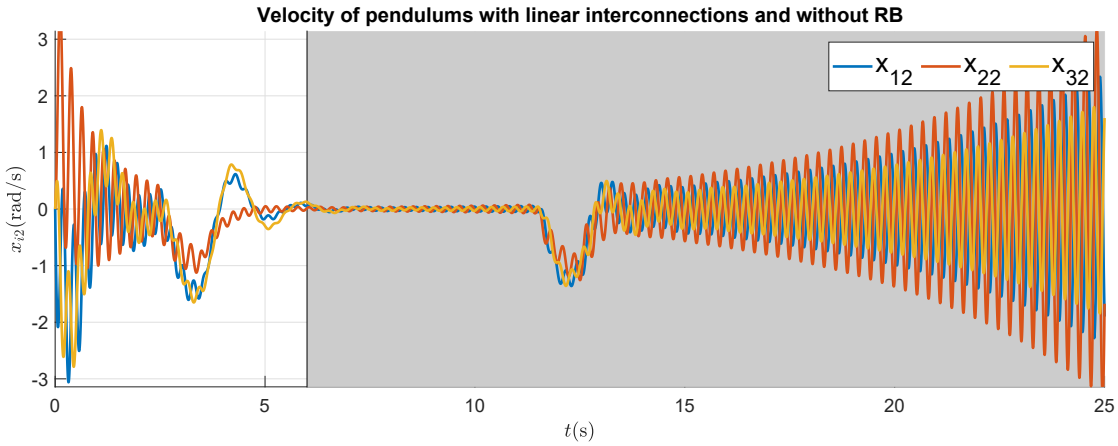

(a)

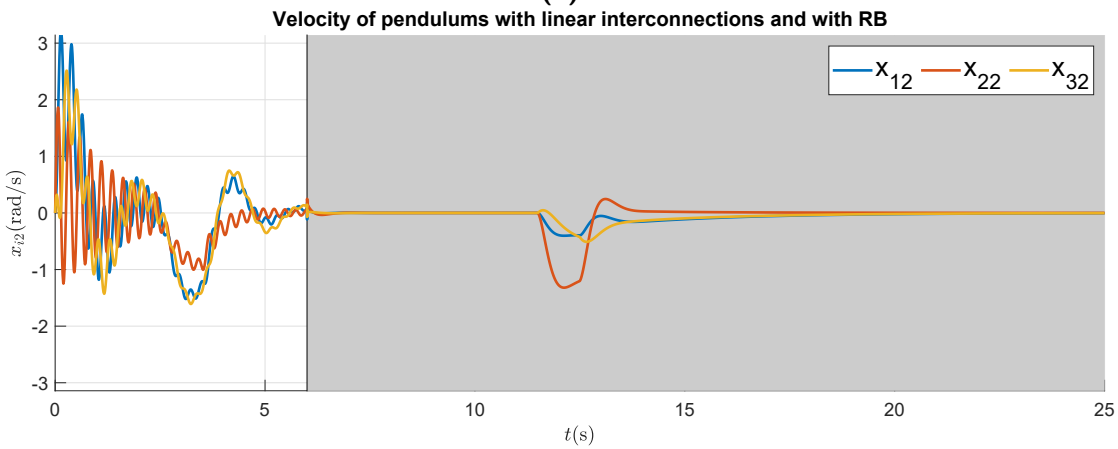

(b)

Figure 4.13 – Comparison of velocities trajectories of the network of pendulums with nonlinear interconnections with and without reconfiguration block when occurs an effectiveness loss fault in the first actuator ($f_1 = 0.25$).

$$\boldsymbol{K}_2^1 = \begin{bmatrix} -395.0900 & -6.3589 \end{bmatrix}, \quad \boldsymbol{K}_2^2 = \begin{bmatrix} -393.5928 & -6.3589 \end{bmatrix},$$

$$\boldsymbol{K}_3^1 = \begin{bmatrix} -151.7622 & -4.3821 \end{bmatrix}, \quad \boldsymbol{K}_3^2 = \begin{bmatrix} -150.3720 & -4.3821 \end{bmatrix},$$

In this simulation, an effectiveness loss of the second pendulum actuator happens such that $f_2 = 0.9$. This fault occurs at $t = 6$ s. Using Theorem 4.2, the reconfiguration block described in (4.5) is obtained with the following gains

$$\boldsymbol{R}_1^i = \boldsymbol{I}_6, \ \boldsymbol{R}_2^i = \boldsymbol{0}_{6\times 3}, \quad i = 1, \ldots, 8,$$

$$\boldsymbol{R}_3^i = \boldsymbol{R}_3^2 = \boldsymbol{R}_3^4 = \boldsymbol{R}_3^5 = \boldsymbol{R}_3^6 = \boldsymbol{R}_3^7 = \boldsymbol{R}_3^8 = \begin{bmatrix} 381.7312 & -102.3317 & 82.7076 \\ 23.3249 & -221.5593 & 128.8239 \\ -645.3332 & 98.7467 & 135.5241 \\ -99.4251 & -736.6991 & -42.8216 \\ 554.1545 & -101.2848 & -135.1592 \\ -37.0876 & 1.5529 & -33.6795 \end{bmatrix}^\top,$$

$$\boldsymbol{R}_3^3 = \begin{bmatrix} 311.2 & 34.7 & -146.7 & -253.6 & 195.8 & 1055.4 \\ -1885.9 & 2565.6 & -2738.7 & 978.7 & -2.462 & -2.9353 \\ -484 & -1056.3 & -1221.8 & -195 & 90.4 & -142 \end{bmatrix},$$

$$\boldsymbol{R}_4^1 = \boldsymbol{R}_4^2 = \boldsymbol{R}_4^4 = \boldsymbol{R}_4^5 = \boldsymbol{R}_4^6 = \boldsymbol{R}_4^7 = \boldsymbol{R}_4^8 = \begin{bmatrix} 20.7938 & -16.2770 & 18.5871 \\ -7.7736 & 16.4341 & -7.9980 \\ -0.4179 & 0.5062 & 0.0349 \end{bmatrix},$$

$$\boldsymbol{R}_4^3 \approx 0$$

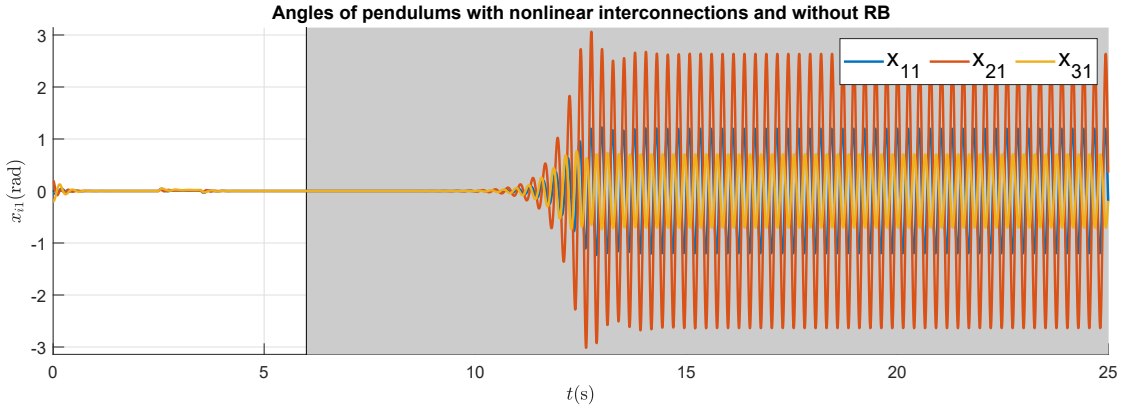

(a)

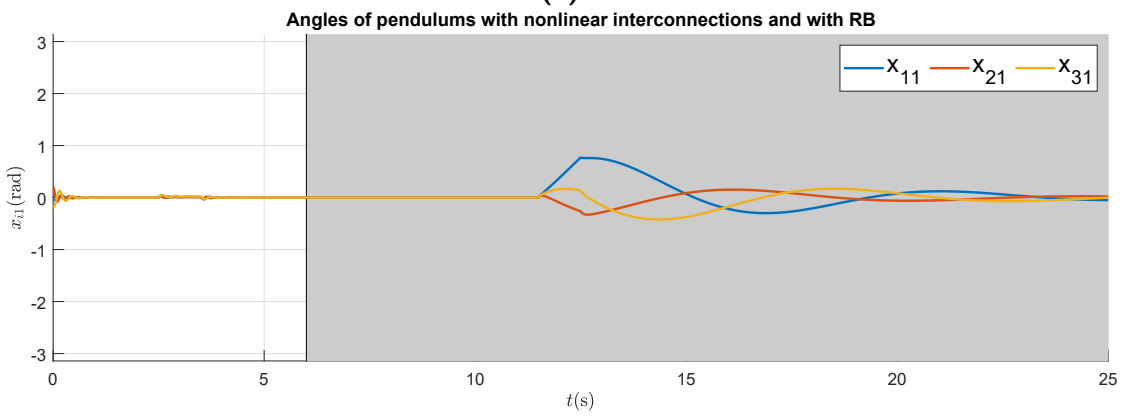

(b)

Figure 4.14 – Comparison of angles trajectories of the network of pendulums with nonlinear interconnections with and without reconfiguration block when occurs an effectiveness loss fault in the second actuator ($f_2 = 0.9$).

Figures 4.14a–4.15b depict the simulation results with reconfiguration block (Figures 4.14b and 4.15b) and without it (Figures 4.14a and 4.15a). Impulsive perturbations are added at $t = 3$ s and $t = 12$ s, and the initial condition is $x(0) = [-0.05\ 0\ 0.2\ 0\ \ -0.2\ 0]^\top$. The closed-loop system without reconfiguration block is unable to reject the second perturbation when there is an actuator fault. Differently, the closed-loop system with reconfiguration block is able to reject both perturbations and mitigate the fault effects.

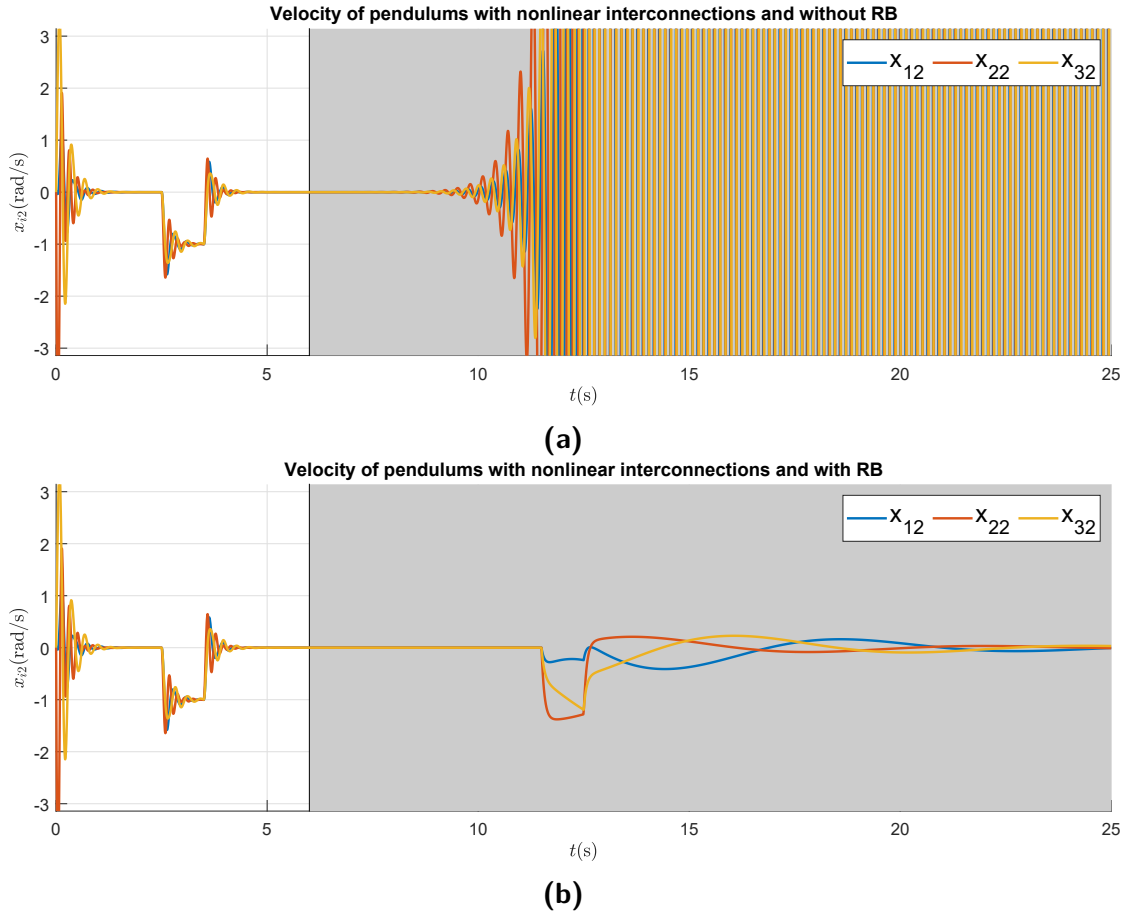

Figure 4.15 – Comparison of velocities trajectories of the network of pendulums with nonlinear interconnections with and without reconfiguration block when occurs an effectiveness loss fault in the second actuator ($f_2 = 0.9$).

5 DISSIPATIVITY RECOVERY BY FAULT HIDING

Dissipativity and passivity theory [241] is an important paradigm in nonlinear system analysis due to its relation with input-output stability [178, 139] and also because these properties are preserved under compositions such as parallel and feedback interconnections. In particular, the passivity indices [242] and passivation techniques [243, 244] are studied to obtain closed-loop systems with desired passivity properties.

The dissipativity/passivity framework is already used to design controllers for various classes of systems, e.g., switched [245], multi-agent systems [246], stochastic systems [247] and networked systems [248], but there are few results for process monitoring and FTC. The general idea of dissipativity-based control synthesis is to find control laws that ensure the closed-loop system dissipativity with respect to a given supply rate. Particular cases of dissipativity may be related to specific supply rate families and could imply in special conclusions, *e.g.*, supply rates whose structure depends on passivity indices allow to analyze the input/output passivity of a system, and the values of passivity indices provide a notion about the excess or shortage of passivity. Then, the desired passivity condition can be obtained for a closed-loop system by synthesizing a controller that ensures the dissipativity with respect to a supply rate with related passivity indices. This kind of result is derived from dissipativity analysis of interconnected systems assuming the dissipativity of each subsystem [249, 178, 250, 242] and can be used to ensure asymptotic stability, input-output stability, and even robust performance [200].

Despite the potential of the dissipativity- and passivation-based control, there are only few applications in the context of FTC. In [251], the concepts of global dissipativity and passivity are proposed to quantify the fault tolerance of dynamical systems and decide if it is necessary to design an FTC law for each fault mode. In [252] is presented a fault diagnosis methodology based on the analysis of the system dissipativity. Dissipativity and passivity theory is also used to obtain PFTC systems in some recent works [253, 254, 255, 256]. However, to the best of the of our knowledge, there is no application of dissipativity theory and passivation for fault hiding before of [106], whose content is the basis of this chapter.

In this chapter, a SRB is used to mitigate the fault effects and ensure the stability of the reconfigured system by means of passivity and dissipativity recovery for faulty (linear or nonlinear) systems. Compared with the previously published fault hiding approaches in the literature, the proposed dissipativity-based approach and SRB are able to mitigate both sensor and actuator faults simultaneously by means of the same RB and to ensure the recovering of exactly the same dissipativity properties as the healthy scenario, implying the recovering of stability and robustness properties. Furthermore, it is able to handle even nonlinear systems without employing differential polytopic inclusions, unlike the results of the previous chapters. In summary, the main contributions in this chapter are:

a) to define the passivity and $(\boldsymbol{Q}, \boldsymbol{S}, \boldsymbol{R})$-dissipativity recovery by fault hiding;

b) to establish the relation between passivity and $(\boldsymbol{Q}, \boldsymbol{S}, \boldsymbol{R})$-dissipativity recovery by fault hiding and the asymptotic stability recovery for nonlinear systems;

c) to provide conditions for stability recovery after sensor, actuator, and plant faults.

The results presented in this chapter are based on those ones previously published in [106]. This chapter is organized as follows. section 5.1 provides some basic concepts on dissipativity and passivity, and it describes the problem solved in this chapter, and concepts the dissipativity recovery by fault hiding procedure. section 5.2 uses that concept for passivity and stability recovery by fault hiding of nonlinear systems. Moreover, section 5.2 presents new LMI-based conditions for designing SRBs which guarantee the stability recovery by recovering the passivity of the faulty system. Similarly, section 5.3 uses the same concept for $(\boldsymbol{Q}, \boldsymbol{S}, \boldsymbol{R})$-dissipativity and stability recovery for nonlinear systems and provides LMI-based design conditions for SRBs which guarantee the stability recovery by recovering the $(\boldsymbol{Q}, \boldsymbol{S}, \boldsymbol{R})$-dissipativity of the faulty system.

5.1 Preliminaries

5.1.1 Dissipativity and passivity

Consider the nonlinear system Σ described as follows

$$\Sigma : \begin{cases} \dot{\boldsymbol{x}}(t) = \boldsymbol{f}\left(\boldsymbol{x}(t)\right) + \boldsymbol{g}\left(\boldsymbol{x}(t), \boldsymbol{u}(t)\right), \\ \boldsymbol{y}(t) = \boldsymbol{h}\left(\boldsymbol{x}(t)\right) + \boldsymbol{j}\left(\boldsymbol{x}(t), \boldsymbol{u}(t)\right), \end{cases} \tag{5.1}$$

where $\boldsymbol{x}(t) \in \mathbb{R}^n$, $\boldsymbol{u}(t) \in \mathbb{R}^m$, and $\boldsymbol{y}(t) \in \mathbb{R}^m$ are, respectively, the state, input and output vectors, and the maps $\boldsymbol{f}$, $\boldsymbol{g}$, $\boldsymbol{h}$, and $\boldsymbol{j}$, such that $\boldsymbol{f}(0) = 0$ and $\boldsymbol{h}(0) = 0$, are sufficiently smooth to ensure that (5.1) is well defined, i.e., for any $x\left(t_0\right)$ and admissible $\boldsymbol{u}(t)$, there exists a unique solution for $t \geq t_0$ such that $\boldsymbol{y}(t)$ is locally integrable. Furthermore, assume also Σ is ZSD [19].

Dissipativity is a useful concept for dynamic system analysis that allows to investigate their stability by means of the energy balance, i.e., the difference between the stored and supplied energy.

Definition 5.1. ***Dissipative systems [241]***
The system Σ described in (5.1) *is dissipative with respect to a supply rate function (t) if there exists a positive semidefinite continuously differentiable function $V(\boldsymbol{x})$, called storage function, such that the following dissipation inequality is satisfied*

$$\frac{\partial V}{\partial \boldsymbol{x}} \boldsymbol{f}\left(\boldsymbol{x}(t)\right) + \frac{\partial V}{\partial \boldsymbol{x}} \boldsymbol{g}\left(\boldsymbol{x}(t), \boldsymbol{u}(t)\right) \leq (\boldsymbol{u}, \boldsymbol{y}). \tag{5.2}$$

Different supply functions can be used for dissipativity analysis. An important case is the $(\boldsymbol{Q}, \boldsymbol{S}, \boldsymbol{R})$-dissipativity that is defined as follows.

Definition 5.2. $(\boldsymbol{Q}, \boldsymbol{S}, \boldsymbol{R})$***-dissipative systems [241]***
The system Σ is $(\boldsymbol{Q}, \boldsymbol{S}, \boldsymbol{R})$-dissipative if it is dissipative with respect to the following supply rate:

$$(\boldsymbol{u}, \boldsymbol{y}) = \boldsymbol{y}^\top \boldsymbol{Q} \boldsymbol{y} + 2\boldsymbol{u}^\top \boldsymbol{S} \boldsymbol{y} + \boldsymbol{u}^\top \boldsymbol{R} \boldsymbol{u}. \tag{5.3}$$

An important property of $(\boldsymbol{Q}, \boldsymbol{S}, \boldsymbol{R})$-dissipativity is its relation to asymptotic stability as stated in Lemma 5.1. In particular, if the system Σ described by (5.1) is ZSD and $(\boldsymbol{Q}, \boldsymbol{S}, \boldsymbol{R})$-dissipative, the all the storage functions $V(\boldsymbol{x})$ that satisfy the

dissipation inequality (5.2) are positive definite [19, Lemma 1]. It enables the relation between the storage and Lyapunov functions when $\boldsymbol{u} = 0$. Based on this relation, the following theorem establishes the relation between $(\boldsymbol{Q}, \boldsymbol{S}, \boldsymbol{R})$-dissipativity and asymptotic stability.

Lemma 5.1. ***Stability of*** $(\boldsymbol{Q}, \boldsymbol{S}, \boldsymbol{R})$***-dissipative systems [19, Theorem 2]*** *Let the system* Σ *be* $(\boldsymbol{Q}, \boldsymbol{S}, \boldsymbol{R})$*-dissipative and ZSD. Then the unforced origin of* Σ *is stable if* $\boldsymbol{Q} \preceq 0$ *and asymptotically stable if* $\boldsymbol{Q} \prec 0$.

Passivity is a special case of dissipativity for which the storage function is positive semidefinite storage functions $V(\boldsymbol{x})$. In particular, a system is said to be passive if it is dissipative with respect to the supply rate $(\boldsymbol{u}, \boldsymbol{y}) = \boldsymbol{u}^\top \boldsymbol{y}$ for some positive semidefinite $V(\boldsymbol{x})$. Moreover, it is said strictly passive if it is dissipative with respect to the supply rate $(\boldsymbol{u}, \boldsymbol{y}) = \boldsymbol{u}^\top \boldsymbol{y} - \psi(\boldsymbol{x})$ for some positive definite function ψ and for some positive semidefinite $V(\boldsymbol{x})$. Additionally, it is said output strictly passive if it is dissipative with respect to the supply rate $(\boldsymbol{u}, \boldsymbol{y}) = \boldsymbol{u}^\top \boldsymbol{y} - \boldsymbol{y}^\top \rho(\boldsymbol{y})$ and $\boldsymbol{y}^\top \rho(\boldsymbol{y}) > 0$ for all $\boldsymbol{y} \neq 0$ for some positive semidefinite $V(\boldsymbol{x})$. The stability of the origin of a system can be also related to the passivity. In this case, if a system is passive then its unforced origin is stable [139, Lemma 6.6]. Finally, if a system is strictly passive or if it is output strictly passive and ZSD, its unforced origin is asymptotically stable [139, Lemma 6.7].

Dissipativity theory provides an effective tool for analysis of interconnected systems. Lemma 5.2 summarizes some results on dissipativity and stability of a feedback interconnection between two systems.

Lemma 5.2. ***[178, 257, 258]*** *Consider two systems, interconnected by feedback as*

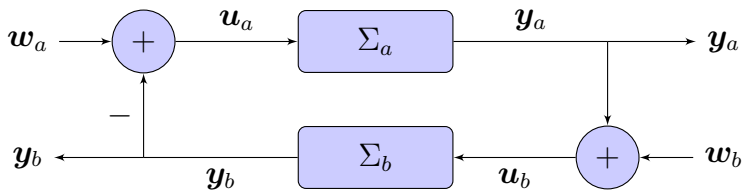

Figure 5.1 – Feedback interconnection between Σ_a and Σ_b.

depicted in Figure 5.1, $\Sigma_a : (\boldsymbol{y}_a(t), \boldsymbol{x}_a(t)) = \Omega_a(\boldsymbol{x}_a(0), \boldsymbol{u}_a(t))$ *and* $\Sigma_b : (\boldsymbol{y}_b(t), \boldsymbol{x}_b(t)) = \Omega_b(\boldsymbol{x}_b(0), \boldsymbol{u}_b(t))$ *such that* $(\Sigma_a, \Sigma_b) : (\bar{\boldsymbol{y}}(t), \bar{\boldsymbol{x}}(t)) = \bar{\Omega}(\bar{\boldsymbol{x}}(0), w(t))$, *where* $\bar{\boldsymbol{x}} =$

$\left[\begin{array}{cc} \boldsymbol{x}_a(t)^\top & \boldsymbol{x}_b(t)^\top \end{array}\right]^\top$, $\bar{\boldsymbol{w}} = \left[\begin{array}{cc} \boldsymbol{w}_a(t)^\top & \boldsymbol{w}_b(t)^\top \end{array}\right]^\top$, $\bar{\boldsymbol{y}} = \left[\begin{array}{cc} \boldsymbol{y}_a(t)^\top & \boldsymbol{y}_b(t)^\top \end{array}\right]^\top$, $\boldsymbol{u}_a(t) = \boldsymbol{w}_a(t) - \boldsymbol{y}_b(t)$, *and* $\boldsymbol{u}_b(t) = \boldsymbol{w}_b(t) + \boldsymbol{y}_a(t)$.

a) If Σ_a is strictly passive and Ω_b is a passive memoryless function, then the origin of (Σ_a, Σ_b) is asymptotically stable with $\boldsymbol{w}_a(t) = \boldsymbol{w}_b(t) = 0$.

b) If Σ_a and Σ_b are strictly passive, then the origin of (Σ_a, Σ_b) is asymptotically stable with $\boldsymbol{w}_a(t) = \boldsymbol{w}_b(t) = 0$.

c) If Σ_a and Σ_b are, respectively, $(\boldsymbol{Q}_a,\boldsymbol{S}_a,\boldsymbol{R}_a)$-dissipative and $(\boldsymbol{Q}_b,\boldsymbol{S}_b,\boldsymbol{R}_b)$-dissipative, then (Σ_a, Σ_b) is $(\bar{\boldsymbol{Q}},\bar{\boldsymbol{S}},\bar{\boldsymbol{R}})$-dissipative with

$$\bar{\boldsymbol{Q}} = \left[\begin{array}{cc} \boldsymbol{Q}_a + \boldsymbol{R}_b & \boldsymbol{S}_b - \boldsymbol{S}_a^\top \\ \boldsymbol{S}_b^\top - \boldsymbol{S}_a & \boldsymbol{Q}_b + \boldsymbol{R}_a \end{array}\right], \bar{\boldsymbol{S}} = \left[\begin{array}{cc} \boldsymbol{S}_a & \frac{1}{2}\mathrm{He}\left\{\boldsymbol{R}_b\right\} \\ -\frac{1}{2}\mathrm{He}\left\{\boldsymbol{R}_a\right\} & \boldsymbol{S}_b \end{array}\right],$$

$$\bar{\boldsymbol{R}} = \left[\begin{array}{cc} \boldsymbol{R}_a & 0 \\ 0 & \boldsymbol{R}_b \end{array}\right].$$

Furthermore, for $\boldsymbol{w}_a(t) = \boldsymbol{w}_b(t) = 0$, if Σ_a and Σ_b are ZSD and $\bar{\boldsymbol{Q}} \prec 0$, then (Σ_a, Σ_b) is asymptotically stable.

5.1.2 Problem Statement

Let a fault-free plant be represented by the following nominal model Σ_{P}:

$$\Sigma_{\mathrm{P}} : \left\{\begin{array}{l} \dot{\boldsymbol{x}}(t) = \boldsymbol{f}\left(\boldsymbol{x}(t)\right) + \boldsymbol{g}\left(\boldsymbol{x}(t), \boldsymbol{u}_{\mathrm{p}}(t)\right), \\ \boldsymbol{y}_{\mathrm{p}}(t) = \boldsymbol{h}\left(\boldsymbol{x}(t)\right) + \boldsymbol{j}\left(\boldsymbol{x}(t), \boldsymbol{u}_{\mathrm{p}}(t)\right), \end{array}\right. \tag{5.4}$$

associated to the operator $\Sigma_{\mathrm{P}} : \left(\boldsymbol{y}_{\mathrm{p}}(t), \boldsymbol{x}(t)\right) = \Omega\left(\boldsymbol{u}_{\mathrm{p}}(t), \boldsymbol{x}_0\right)$, where $\boldsymbol{x}(t) \in \mathbb{R}^n$, $\boldsymbol{u}(t) \in \mathbb{R}^m$, and $\boldsymbol{y}(t) \in \mathbb{R}^m$ are, respectively, the vectors of state, input, and output variables; $\boldsymbol{x}_0 = \boldsymbol{x}\left(0\right)$; and the matrix-valued maps $\boldsymbol{f}$, $\boldsymbol{g}$, $\boldsymbol{h}$, and $\boldsymbol{j}$ are sufficiently smooth with appropriate dimensions. The same plant under faulty operation is represented by the following faulty model $\Sigma_{\mathrm{P_f}}$:

$$\Sigma_{\mathrm{P_f}} : \left\{\begin{array}{l} \dot{\boldsymbol{x}}(t) = \boldsymbol{f}_{\mathrm{f}}\left(\boldsymbol{x}(t)\right) + \boldsymbol{g}_{\mathrm{f}}\left(\boldsymbol{x}(t), \boldsymbol{u}_{\mathrm{p}}(t)\right), \\ \boldsymbol{y}_{\mathrm{p}}(t) = \boldsymbol{h}_{\mathrm{f}}\left(\boldsymbol{x}(t)\right) + \boldsymbol{j}_{\mathrm{f}}\left(\boldsymbol{x}(t), \boldsymbol{u}_{\mathrm{p}}(t)\right), \end{array}\right. \tag{5.5}$$

associated to the operator $\Sigma_{\mathrm{P_f}} : \left(\boldsymbol{y}_{\mathrm{p}}(t), \boldsymbol{x}(t)\right) = \Omega_{\mathrm{f}}\left(\boldsymbol{u}_{\mathrm{p}}(t), \boldsymbol{x}_{\mathrm{f},0}\right)$, where $\boldsymbol{x}_{\mathrm{f},0} = \boldsymbol{x}\left(t_{\mathrm{f}}\right)$, t_{f} is the time when the fault begins, $\boldsymbol{x}(t) \in \mathbb{R}^n$, $\boldsymbol{u}_{\mathrm{p}}(t) \in \mathbb{R}^m$, and $\boldsymbol{y}(t) \in \mathbb{R}^m$ are,

respectively, the vectors of state, input, and output variables; the matrix-valued maps $\boldsymbol{f}_{\mathrm{f}}$, $\boldsymbol{g}_{\mathrm{f}}$, $\boldsymbol{h}_{\mathrm{f}}$, and $\boldsymbol{j}_{\mathrm{f}}$ are sufficiently smooth with appropriate dimensions.

The plant is interconnected by feedback to a dynamic output feedback controller Σ_{C} described as follows:

$$\Sigma_{\mathrm{C}}: \begin{cases} \dot{\boldsymbol{x}}_{\mathrm{c}}(t) = \boldsymbol{f}_{\mathrm{c}}\left(\boldsymbol{x}_{\mathrm{c}}(t)\right) + \boldsymbol{g}_{\mathrm{c}}\left(\boldsymbol{x}(t)\right)\boldsymbol{y}_{\mathrm{c}}(t), \\ \boldsymbol{u}_{\mathrm{c}}(t) = \boldsymbol{h}_{\mathrm{c}}\left(\boldsymbol{x}(t)\right) + \boldsymbol{j}_{\mathrm{c}}\left(\boldsymbol{x}_{\mathrm{c}}(t)\right)\boldsymbol{y}_{\mathrm{c}}(t). \end{cases} \tag{5.6}$$

where $\boldsymbol{x}_{\mathrm{c},0} = \boldsymbol{x}_{\mathrm{c}}(0)$; the matrix-valued maps $\boldsymbol{f}_{\mathrm{c}}$, $\boldsymbol{g}_{\mathrm{c}}$, $\boldsymbol{h}_{\mathrm{c}}$, and $\boldsymbol{j}_{\mathrm{c}}$ are sufficiently smooth with appropriate dimensions.

To recover the system properties after fault occurrence, the following SRBs Σ_{R} is inserted between $\Sigma_{\mathrm{P_f}}$ and Σ_{C}:

$$\Sigma_{\mathrm{R}}: \begin{cases} \boldsymbol{y}_{\mathrm{r}}(t) = \boldsymbol{R}_1\boldsymbol{y}_{\mathrm{p}}(t) + \boldsymbol{R}_2\boldsymbol{u}_{\mathrm{c}}(t), \\ \boldsymbol{u}_{\mathrm{r}}(t) = \boldsymbol{R}_3\boldsymbol{y}_{\mathrm{p}}(t) + \boldsymbol{R}_4\boldsymbol{u}_{\mathrm{c}}(t), \end{cases} \tag{5.7}$$

where $\boldsymbol{y}_{\mathrm{r}}(t) \in \mathbb{R}^m$ and $\boldsymbol{u}_{\mathrm{r}}(t) \in \mathbb{R}^m$ are, respectively, the vectors of reconfigured measurements injected into controller and reconfigured control signals injected into the plant; and the real matrices $\boldsymbol{R}_1$, $\boldsymbol{R}_2$, $\boldsymbol{R}_3$, and $\boldsymbol{R}_4$ are gains of the SRB Σ_{R} which are designed to solve the fault hiding problem.

5.1.3 Overview of Dissipativity Recovery

The idea behind of dissipativity recovery is to find RB that ensures that the reconfigured plant $(\Sigma_{\mathrm{P_f}}, \Sigma_{\mathrm{R}})$ exhibits the same dissipativity properties of the nominal (fault-free) system Σ_{P}. To illustrate it, suppose that Σ_{P} described in (5.4) is dissipative with respect to the supply rate function $S : \mathbb{R}^m \times \mathbb{R}^m \to \mathbb{R}$, i.e., there exist a non-negative continuously differentiable storage function $V : \mathbb{R}^n \to \mathbb{R}_{\geq 0}$ such that the following dissipation inequality holds

$$\dot{V}(\boldsymbol{x}) \leq (\boldsymbol{u}_{\mathrm{p}}, \boldsymbol{y}_{\mathrm{p}}). \tag{5.8}$$

The dissipativity of Σ_{P} may be related to several other properties, such as asymptotic stability, $\mathcal{L}_2$-stability, and passivity. Moreover, the combination of dissipativity properties of the controller Σ_{C} and the plant Σ_{P}, interconnected as depicted in

Figure 5.2, is related to the closed-loop guarantees which motivate the controller design. Indeed, the closed-loop guarantees can be usually expressed as dissipation inequalities and some control strategies are based on the manipulation of those dissipation properties, e.g., interconnection and damping assignment passivity based control [259] and energy shaping [260].

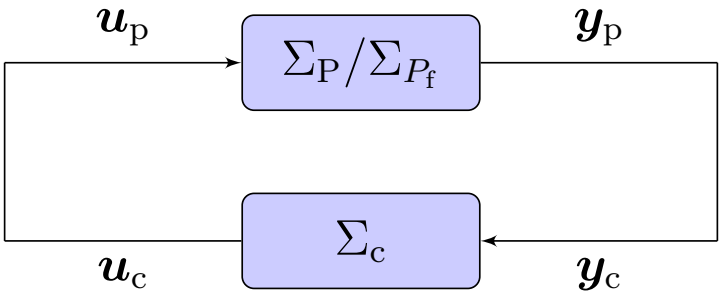

Figure 5.2 – Control loop with $\Sigma_\mathrm{P}/\Sigma_{\mathrm{P_f}}$ and Σ_C and without reconfiguration.

In addition to the evident effects in the parameters of $\Sigma_{\mathrm{P_f}}$ described in (5.5), the fault effects may also lead to the loss of the dissipativity, i.e., $\Sigma_{\mathrm{P_f}}$ may no longer meet dissipation inequality (5.8) anymore. The dissipativity recovery by fault hiding using an RB consists of inserting the RB in the control loop as depicted in Figure 5.3 to guarantee that the reconfigured plant $(\Sigma_{\mathrm{P_f}}, \Sigma_\mathrm{R})$ meets the dissipation inequality (5.8).

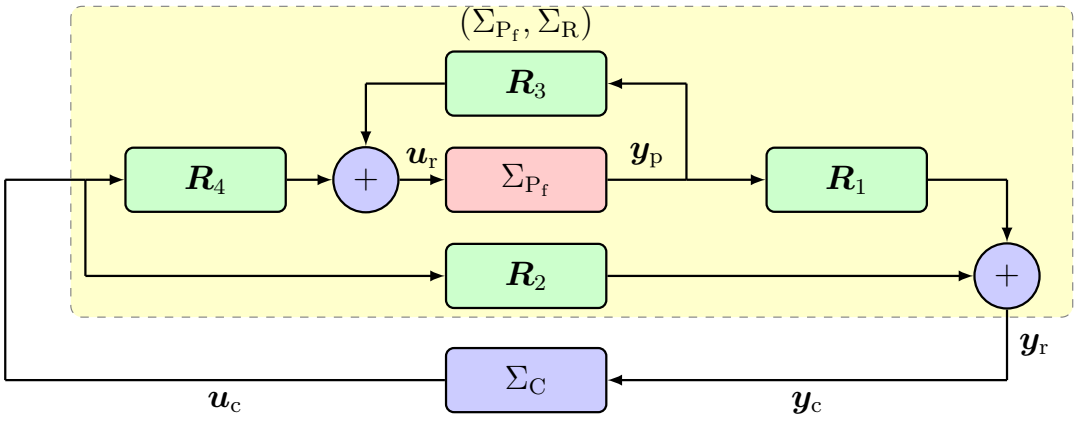

Figure 5.3 – Equivalent reconfigured loop of $(\Sigma_{\mathrm{P_f}}, \Sigma_\mathrm{R}, \Sigma_\mathrm{C})$.

Therefore, the following fault hiding problem is addressed in this chapter related to the dissipativity recovery.

Problem 5.1. – ***Dissipativity Recovery by Fault Hiding***

Let Σ_{P} and $\Sigma_{\mathrm{P_f}}$ be the nominal and the faulty models, respectively, with dynamics described by (5.4) *and* (5.5) *both interconnected by feedback to controller Σ_{C}. Assume Σ_{P} is dissipative with respect to a supply rate function $(\boldsymbol{u}_{\mathrm{p}}, \boldsymbol{y}_{\mathrm{p}})$. Find an SRB Σ_{R}, described by* (5.7)*, such that the origin of $(\Sigma_{\mathrm{P_f}}, \Sigma_{\mathrm{R}})$ is also dissipative with respect to $(\boldsymbol{u}_{\mathrm{c}}(t), \boldsymbol{y}_{\mathrm{r}}(t))$.*

This chapter provides solutions to Problem 5.1 by considering two particular cases of dissipativity: the passivity and the $(\boldsymbol{Q}, \boldsymbol{S}, \boldsymbol{R})$-dissipativity. Moreover, the dissipativity recovery is used for recovering also the asymptotic stability. For solving Problem 5.1, the following definitions are used to characterize the faulty system $\Sigma_{\mathrm{P_f}}$ whose dissipativity and stability were recovered by fault hiding.

Definition 5.3. ***Dissipativity recovery by fault hiding***

Let Σ_{P} and $\Sigma_{\mathrm{P_f}}$ be the nominal and the faulty models with dynamics described, respectively, by (5.4) *and* (5.5)*. Assume that Σ_{P} is dissipative with respect to a supply rate function $(\boldsymbol{u}_{\mathrm{p}}, \boldsymbol{y}_{\mathrm{p}})$ with a non-negative continuously differentiable storage function $V(\boldsymbol{x})$, i.e., Σ_{P} satisfies the dissipation inequality* (5.8)*. $\Sigma_{\mathrm{P_f}}$ is dissipative by fault hiding if there exists an RB Σ_{R} such that $(\Sigma_{\mathrm{P_f}}, \Sigma_{\mathrm{R}})$ is also dissipative with respect to $(\boldsymbol{u}_{\mathrm{c}}(t), \boldsymbol{y}_{\mathrm{r}}(t))$. Therefore, Σ_{R} is a solution of Problem 5.1.*

Definition 5.4. ***Stability recovery by fault hiding***

Let Σ_{P} and $\Sigma_{\mathrm{P_f}}$ be nominal and faulty models with dynamics described respectively as (5.4) *and* (5.5) *for the same system interconnected by feedback to a controller Σ_{C} as depicted in Figure 5.2. Assuming that the origin of $(\Sigma_{\mathrm{P}}, \Sigma_{\mathrm{C}})$ is asymptotically stable, then $\Sigma_{\mathrm{P_f}}$ is stable by fault hiding if there exists a reconfiguration block Σ_{R} described by* (5.7) *such that the origin of $(\Sigma_{\mathrm{P_f}}, \Sigma_{\mathrm{R}}, \Sigma_{\mathrm{C}})$ is also asymptotically stable.*

5.2 Passivity Recovery by Fault Hiding

The following lemma provides sufficient conditions for asymptotic stability of faulty systems by means of passivity recovery by fault hiding.

Lemma 5.3. *Let Σ_{P} and $\Sigma_{\mathrm{P_f}}$ be the nominal and the faulty models, respectively, with dynamics described by* (5.4) *and* (5.5) *for a plant that is interconnected, as*

depicted in Figure 5.2, to an strictly passive output feedback controller Σ_{C}. *Assume that* Σ_{P} *is strictly passive and there exists a positive definite continuously differentiable* $V(\cdot)$ *such that* $\dot{V}(\boldsymbol{x}) < \boldsymbol{u}_{\mathrm{p}}^{\top}(t)\boldsymbol{y}_{\mathrm{p}}(t)$. *If there exist* $\boldsymbol{R}_1$,$\boldsymbol{R}_2$,$\boldsymbol{R}_3$, $\boldsymbol{R}_4$, *such that the reconfigured plant* $(\Sigma_{\mathrm{P_f}}, \Sigma_{\mathrm{R}})$, *as depicted in Figure 5.3, is also strictly passive and* $\dot{V}(\boldsymbol{x}) < \boldsymbol{u}_{\mathrm{c}}^{\top}(t)\boldsymbol{y}_{\mathrm{r}}(t)$ *for the same* $V(\cdot)$, *then* $\Sigma_{\mathrm{P_f}}$ *is stable by fault hiding with* Σ_{R} *described in* (5.7).

Proof. Since Σ_{P} and Σ_{C} are strictly passive, Lemma 5.2 ensures that the origin of feedback interconnection $(\Sigma_{\mathrm{P}}, \Sigma_{\mathrm{C}})$ is asymptoticaly stable. Given that $V(\boldsymbol{x})$ is positive definite, assume that it is taken as storage function for $(\Sigma_{\mathrm{P_f}}, \Sigma_{\mathrm{R}})$. If there exists any Σ_{R}, such that

$$\dot{V}(\boldsymbol{x}) \leq W_2(\boldsymbol{x}),$$

then $\Sigma_{\mathrm{P_f}}$ is dissipative by fault hiding with respect to $(\boldsymbol{u}_{\mathrm{c}}(t), \boldsymbol{y}_{\mathrm{r}}(t)) = W_2(\boldsymbol{x}) = \boldsymbol{u}_{\mathrm{c}}^{\top}(t)\boldsymbol{y}_{\mathrm{r}}(t) - \psi_2(\boldsymbol{x})$, according to Definition 5.3, and $(\Sigma_{\mathrm{P_f}}, \Sigma_{\mathrm{R}})$ is strictly passive. Finally, given that $(\Sigma_{\mathrm{P_f}}, \Sigma_{\mathrm{R}})$ and Σ_{C} are strictly passive systems with positive definite storage functions interconnected as depicted in Figure 5.3, it follows that $(\Sigma_{\mathrm{P_f}}, \Sigma_{\mathrm{R}}, \Sigma_{\mathrm{C}})$ is strictly passive and its unforced origin is asymptotically stable, therefore $\Sigma_{\mathrm{P_f}}$ is stable by fault hiding according to Definition 3.1. □

Example 5.1. *Let* Σ_{P} *and* $\Sigma_{\mathrm{P_f}}$ *be, respectively, the nominal and faulty model for the same system described as follows*

$$\Sigma_{\mathrm{P}} : \begin{cases} a\dot{x}(t) = -x(t) + u_{\mathrm{p}}(t), \\ y_{\mathrm{p}}(t) = h(x(t)), \end{cases}, \quad \Sigma_{\mathrm{P_f}} : \begin{cases} a\dot{x}(t) = -x(t) + f \cdot u_{\mathrm{p}}(t), \\ y_{\mathrm{p}}(t) = h(x(t)), \end{cases}$$

such that $h(\cdot) \in (0, \infty]$ *and* $0 < f < 1$. *Consider that the origin of* $(\Sigma_{\mathrm{P}}, \Sigma_{\mathrm{C}})$ *is asymptotically stable with the strictly passive output feedback controller* Σ_{C} *connected as depicted in Figure 2.2.*

Considering $V(x) = \int_0^x h(\sigma)d\sigma$, *it is possible to show that* $\dot{V}(x) < u_{\mathrm{c}}(t)y_{\mathrm{p}}(t)$, *thus,* Σ_{P} *is passive.*

Using the same storage function $V(x) = \int_0^x h(\sigma)d\sigma$ *for the configuration* $(\Sigma_{\mathrm{P_f}}, \Sigma_{\mathrm{R}})$, *it follows that:*

$$\dot{V}(x) - u_{\mathrm{c}}y_{\mathrm{r}} = h(x)[-x + f(R_3h(x) + R_4u_{\mathrm{c}})] - (R_1h(x) + R_2u_{\mathrm{c}})u_{\mathrm{c}} < 0,$$

Thus, if $R_1 = f \cdot R_4$, $R_2 > 0$, *and* $R_3 < 0$, *then* $\dot{V}(x) < u_{\mathrm{c}}(t)y_{\mathrm{r}}(t)$ *implies that* $(\Sigma_{\mathrm{P_f}}, \Sigma_{\mathrm{R}})$ *is passive. Given that* Σ_{C} *is strictly passive, the origin of* $(\Sigma_{\mathrm{P_f}}, \Sigma_{\mathrm{R}}, \Sigma_{\mathrm{C}})$ *is asymptotically stable, i.e.,* $\Sigma_{\mathrm{P_f}}$ *is stable by fault hiding with* Σ_{R} *such that* $R_1 = f \cdot R_4$, $R_2 > 0$, *and* $R_3 < 0$.

The next theorem tackles the particular case of passivity recovery for linear systems.

Theorem 5.1. *Let* Σ_{P} *and* $\Sigma_{\mathrm{P_f}}$ *be the nominal and faulty models, respectively, with dynamics described as follows*

$$\Sigma_{\mathrm{P}} : \begin{cases} \dot{\boldsymbol{x}}(t) = \boldsymbol{A}\boldsymbol{x}(t) + \boldsymbol{B}\boldsymbol{u}_{\mathrm{p}}(t), \\ \boldsymbol{y}_{\mathrm{p}}(t) = \boldsymbol{C}\boldsymbol{x}(t), \end{cases} \tag{5.9}$$

$$\Sigma_{\mathrm{P_f}} : \begin{cases} \dot{\boldsymbol{x}}(t) = \boldsymbol{A}_{\mathrm{f}}\boldsymbol{x}(t) + \boldsymbol{B}_{\mathrm{f}}\boldsymbol{u}_{\mathrm{r}}(t), \\ \boldsymbol{y}_{\mathrm{p}}(t) = \boldsymbol{C}_{\mathrm{f}}\boldsymbol{x}(t), \end{cases} \tag{5.10}$$

for the same plant interconnected, as depicted in Figure 2.2, to a strictly passive output feedback controller Σ_{C}. *Assume that there exists* $\boldsymbol{P} = \boldsymbol{P}^\top \succ 0$, *such that* $\boldsymbol{A}^\top\boldsymbol{P} + \boldsymbol{P}\boldsymbol{A} \prec 0$ *and* $\boldsymbol{B}^\top\boldsymbol{P} = \boldsymbol{C}$. *The faulty system* $\Sigma_{\mathrm{P_f}}$ *is stable by fault hiding with* Σ_{R} *described by* (5.7) *if there exist* $\boldsymbol{R}_1$, $\boldsymbol{R}_2$, $\boldsymbol{R}_3$, *and* $\boldsymbol{R}_4$ *that satisfy, with the same* $\boldsymbol{P}$, *the following inequality:*

$$\begin{bmatrix} \mathrm{He}\left\{\boldsymbol{P}\left(\boldsymbol{A}_{\mathrm{f}} + \boldsymbol{B}_{\mathrm{f}}\boldsymbol{R}_3\boldsymbol{C}\right)\right\} & \boldsymbol{P}\boldsymbol{B}_{\mathrm{f}}\boldsymbol{R}_4 - \boldsymbol{C}_{\mathrm{f}}^\top\boldsymbol{R}_1^\top \\ \star & -\mathrm{He}\left\{\boldsymbol{R}_2\right\} \end{bmatrix} \prec 0. \tag{5.11}$$

Proof. According to KYP lemma [241, Lemma 2.16], if there exists $\boldsymbol{P} = \boldsymbol{P}^\top \succ 0$, such that $\boldsymbol{A}^\top\boldsymbol{P} + \boldsymbol{P}\boldsymbol{A} \prec 0$ and $\boldsymbol{B}^\top\boldsymbol{P} = \boldsymbol{C}$, then Σ_{P} is strictly passive. Given that Σ_{C} is also strictly passive, then Lemma 5.2 ensures that $(\Sigma_{\mathrm{P}}, \Sigma_{\mathrm{C}})$ is asymptotically stable, since it is an interconnection of strictly passive systems.

Lemma 5.3 indicates that the same storage function, with the same matrix $\boldsymbol{P}$, can be used to ensure the passivity of the reconfigured plant $(\Sigma_{\mathrm{P}}, \Sigma_{\mathrm{R}})$. The reconfigured system $(\Sigma_{\mathrm{P_f}}, \Sigma_{\mathrm{R}})$ is described as follows, with $\boldsymbol{A}_{\mathrm{R}} = \boldsymbol{A}_{\mathrm{f}} + \boldsymbol{B}_{\mathrm{f}}\boldsymbol{R}_3\boldsymbol{C}_{\mathrm{f}}$, $\boldsymbol{B}_{\mathrm{R}} = \boldsymbol{B}_{\mathrm{f}}\boldsymbol{R}_4$, $\boldsymbol{C}_{\mathrm{R}} = \boldsymbol{R}_1\boldsymbol{C}_{\mathrm{f}}$, and $\boldsymbol{D}_{\mathrm{R}} = \boldsymbol{R}_2$:

$$(\Sigma_{\mathrm{P_f}}, \Sigma_{\mathrm{R}}) : \begin{cases} \dot{\boldsymbol{x}}(t) = \boldsymbol{A}_{\mathrm{R}}\boldsymbol{x}(t) + \boldsymbol{B}_{\mathrm{R}}\boldsymbol{u}_{\mathrm{c}}(t) \\ \boldsymbol{y}_{\mathrm{r}}(t) = \boldsymbol{C}_{\mathrm{R}}\boldsymbol{x}(t) + \boldsymbol{D}_{\mathrm{R}}\boldsymbol{u}_{\mathrm{c}}(t) \end{cases}. \tag{5.12}$$

Thus, according to KYP Lemma [241, Lemma 2.16], $(\Sigma_{\mathrm{P_f}}, \Sigma_{\mathrm{R}})$ is strictly passive if (5.11) is satisfied for some $\boldsymbol{R}_1$, $\boldsymbol{R}_2$, $\boldsymbol{R}_3$, and $\boldsymbol{R}_4$. In this case, the closed-loop reconfigured system $(\Sigma_{\mathrm{P_f}}, \Sigma_{\mathrm{R}}, \Sigma_{\mathrm{C}})$ is asymptotically stable according to Lemma 5.2, since Σ_{C} is also a strictly passive system. Therefore, according to Lemma 5.3, $\Sigma_{\mathrm{P_f}}$ is stable by fault hiding with Σ_{R} defined as (5.7). □

Remark 5.1. *If Σ_{P} is an SISO strictly passive system, Σ_{C} is a static output feedback controller such that $u_{\mathrm{c}}(t) = k y_{\mathrm{c}}(t)$ and $k > 0$, then the result of Theorem 5.1 is also valid, since it is a passive memoryless function.*

Example 5.2. *Let Σ_{P} be a heat exchange system model [241], controlled by a static output feedback controller $\Sigma_{\mathrm{C}} : \boldsymbol{u}_{\mathrm{c}} = \boldsymbol{y}_{\mathrm{r}}$, and described by* (5.9) *with*

$$\boldsymbol{A} = \begin{bmatrix} -690.87 & 279.17 \\ 69.254 & -375.29 \end{bmatrix}, \quad \boldsymbol{B} = \begin{bmatrix} 411.7 & 0 \\ 0 & 306.03 \end{bmatrix}, \quad \boldsymbol{C} = \begin{bmatrix} 1 & 0 \\ 0 & 1 \end{bmatrix}.$$

According to KYP lemma, Σ_{P} is strictly passive for the storage function $V(\boldsymbol{x}) = \boldsymbol{x}^T \boldsymbol{P} \boldsymbol{x}$ with

$$\boldsymbol{P} = \begin{bmatrix} 0.0008 & 0.0003 \\ 0.0003 & 0.0017 \end{bmatrix}. \tag{5.13}$$

Consider that an actuator fault occurs such that $\Sigma^2_{\mathrm{P_f}}$ is described by (5.10) *with*

$$\boldsymbol{A}^1_{\mathrm{f}} = \boldsymbol{A}, \quad \boldsymbol{B}^1_{\mathrm{f}} = \begin{bmatrix} 0 & 0 \\ 0 & 275.427 \end{bmatrix}, \quad \boldsymbol{C}^1_{\mathrm{f}} = \boldsymbol{C}.$$

The following RB Σ^1_{R} is obtained based on Theorem 5.1 by solving the LMI (5.11) *using* (5.13) *and the LMILAB*

$$\boldsymbol{R}^1_1 = \begin{bmatrix} 0.7179 & 0.3951 \\ 0.1019 & 1.3910 \end{bmatrix}, \quad \boldsymbol{R}^1_2 = \begin{bmatrix} 0.9715 & 0 \\ 0 & 0.9715 \end{bmatrix},$$

$$\boldsymbol{R}^1_3 = \begin{bmatrix} 0 & 0 \\ -0.1327 & -0.8374 \end{bmatrix}, \quad \boldsymbol{R}^1_4 = \begin{bmatrix} 1.9431 & -1.0235 \\ 1.0235 & 2.1976 \end{bmatrix}.$$

Consider now that a plant fault occurs such that $\Sigma^2_{\mathrm{P_f}}$ is described by (5.10) *with*

$$\boldsymbol{A}^2_{\mathrm{f}} = \begin{bmatrix} -461.7000 & 50.0000 \\ 69.2540 & -375.2900 \end{bmatrix}, \quad \boldsymbol{B}^2_{\mathrm{f}} = \boldsymbol{B}, \quad \boldsymbol{C}^2_{\mathrm{f}} = \boldsymbol{C}.$$

In this case, an RB Σ_{R}^2 *is obtained based on Theorem 5.1 by means of LMILAB. The computed gains of* Σ_{R}^2 *are described as follows:*

$$\boldsymbol{R}_1^2 = \begin{bmatrix} 41.8884 & -7.0504 \\ 17.3065 & 57.8189 \end{bmatrix}, \quad \boldsymbol{R}_2^2 = \begin{bmatrix} 38.3822 & 0 \\ 0 & 38.3822 \end{bmatrix},$$

$$\boldsymbol{R}_3^2 = \begin{bmatrix} -127.0821 & 45.0768 \\ 24.1794 & -86.7559 \end{bmatrix}, \quad \boldsymbol{R}_4^2 = \begin{bmatrix} 87.1790 & 34.6017 \\ -32.6280 & 85.8490 \end{bmatrix}.$$

Consider a third scenario with sensor fault occurrence such that $\Sigma_{\mathrm{P_f}}^3$ *is described by* (5.10) *with*

$$\boldsymbol{A}_{\mathrm{f}}^3 = \boldsymbol{A}, \quad \boldsymbol{B}_{\mathrm{f}}^3 = \boldsymbol{B}, \quad \boldsymbol{C}_{\mathrm{f}}^3 = \begin{bmatrix} 1 & 0 \\ 0 & 0 \end{bmatrix}.$$

In this case, according to Theorem 5.1, an RB Σ_{R}^3 *is obtained with the following gains*

$$\boldsymbol{R}_1^3 = \begin{bmatrix} 1.0669 & -0.0476 \\ 0.0476 & 1.8886 \end{bmatrix}, \quad \boldsymbol{R}_2^3 = \begin{bmatrix} 0.9443 & 0 \\ 0 & 0.9443 \end{bmatrix},$$

$$\boldsymbol{R}_3^3 = \begin{bmatrix} -1.5051 & 0 \\ 0.4646 & 0 \end{bmatrix}, \quad \boldsymbol{R}_4^3 = \begin{bmatrix} 2.0816 & -0.2607 \\ -0.0764 & 1.2709 \end{bmatrix}.$$

Finally, supposes that the three faults above described occurs simultaneously, i.e., $\Sigma_{\mathrm{P_f}}^4$ *is described by* (5.10) *with*

$$\boldsymbol{A}_{\mathrm{f}}^4 = \boldsymbol{A}_{\mathrm{f}}^2, \quad \boldsymbol{B}_{\mathrm{f}}^4 = \boldsymbol{B}_{\mathrm{f}}^1, \quad \boldsymbol{C}_{\mathrm{f}}^4 = \boldsymbol{C}_{\mathrm{f}}^3.$$

In this case, according to Theorem 5.1, an RB Σ_{R}^4 *is obtained by means of LMILAB with the following gains*

$$\boldsymbol{R}_1^4 = \begin{bmatrix} 0.4968 & -0.0986 \\ 0.0986 & 1.4511 \end{bmatrix}, \quad \boldsymbol{R}_2^4 = \begin{bmatrix} 0.7255 & 0 \\ 0 & 0.7255 \end{bmatrix},$$

$$\boldsymbol{R}_3^3 = \begin{bmatrix} 0 & 0 \\ -0.0560 & 0 \end{bmatrix}, \quad \boldsymbol{R}_4^3 = \begin{bmatrix} 1.4511 & -0.1907 \\ 0.1907 & 0.9579 \end{bmatrix}.$$

5.3 (Q,S,R)-dissipativity Recovery by Fault Hiding

The next lemma provides conditions for asymptotically stabilization with RBs after a fault occurrence by means of dissipativity recovery by fault hiding.

Lemma 5.4. *Let Σ_{P} and $\Sigma_{\mathrm{P_f}}$ be nominal and faulty models, respectively, with dynamics described by* (2.1) *and* (2.2) *for the same plant interconnected, as depicted in Figure 2.2, to an output feedback controller Σ_{C}. Assume that Σ_{P}, $\Sigma_{\mathrm{P_f}}$, and Σ_{C} are ZSD; Σ_{P} is $(\boldsymbol{Q}, \boldsymbol{S}, \boldsymbol{R})$-dissipative; Σ_{C} is $(\boldsymbol{Q_c}, \boldsymbol{S_c}, \boldsymbol{R_c})$-dissipative; and the following inequality holds*

$$\begin{bmatrix} \boldsymbol{Q} + \boldsymbol{R}_{\mathrm{c}} & \boldsymbol{S}_{\mathrm{c}} - \boldsymbol{S}^{\top} \\ \boldsymbol{S}_{\mathrm{c}}^{\top} - \boldsymbol{S} & \boldsymbol{Q}_{\mathrm{c}} + \boldsymbol{R} \end{bmatrix} \prec 0. \tag{5.14}$$

If there exist $\boldsymbol{R}_1$, $\boldsymbol{R}_2$, $\boldsymbol{R}_3$, $\boldsymbol{R}_4$, such that $(\Sigma_{\mathrm{P_f}}, \Sigma_{\mathrm{R}})$ is also $(\boldsymbol{Q}, \boldsymbol{S}, \boldsymbol{R})$-dissipative, then $\Sigma_{\mathrm{P_f}}$ is stable by fault hiding with Σ_{R} described in (5.7).

Proof. Assuming that Σ_{P} is $(\boldsymbol{Q}, \boldsymbol{S}, \boldsymbol{R})$-dissipative, Σ_{C} is $(\boldsymbol{Q}_{\mathrm{c}},\boldsymbol{S}_{\mathrm{c}},\boldsymbol{R}_{\mathrm{c}})$-dissipative, Σ_{P} and Σ_{C} are ZSD, and (5.14) is satisfied, then the unforced origin of $(\Sigma_{\mathrm{P}}, \Sigma_{\mathrm{C}})$ is asymptotically stable according to Lemma 5.2. Similarly, if there exists any Σ_{R}, such that $(\Sigma_{\mathrm{P_f}}, \Sigma_{\mathrm{R}})$ is also $(\boldsymbol{Q}, \boldsymbol{S}, \boldsymbol{R})$-dissipative, then (5.14) is still satisfied. Given that $(\Sigma_{\mathrm{P_f}}$ is ZSD, $(\Sigma_{\mathrm{P_f}}, \Sigma_{\mathrm{R}})$ is also ZSD, and the unforced origin of $(\Sigma_{\mathrm{P_f}}, \Sigma_{\mathrm{R}}, \Sigma_{\mathrm{C}})$ is also asymptotically stable according to Lemma 5.2. Therefore $\Sigma_{\mathrm{P_f}}$ is stable by fault hiding according to Definition 3.1. □

Example 5.3. *Consider the nonlinear system with nominal and fault models, respectively Σ_{P} and $\Sigma_{\mathrm{P_f}}$, described as follows:*

$$\Sigma_{\mathrm{P}} : \begin{cases} \dot{x}(t) = -4x^3(t) - 4u_{\mathrm{p}}x(t), \\ y_{\mathrm{p}}(t) = x^2(t), \end{cases} \quad \Sigma_{\mathrm{P_f}} : \begin{cases} \dot{x}(t) = 2x^3(t) - 4u_{\mathrm{p}}x(t), \\ y_{\mathrm{p}}(t) = x^2(t), \end{cases}$$

interconnected as depicted in Figure 2.2 to an output feedback controller described as follows

$$\Sigma_{\mathrm{C}} : \begin{cases} \dot{x}_{\mathrm{c}}(t) = -x_{\mathrm{c}}(t) + y_{\mathrm{c}}(t), \\ u_{\mathrm{c}}(t) = \frac{1}{2}x_{\mathrm{c}}(t). \end{cases} \tag{5.15}$$

Adopting $V(x(t)) = \frac{1}{2}x^2(t)$ as the storage function, Σ_{P} is (Q,S,R)-dissipative, i.e., $\dot{V}(x) \leq (y_{\mathrm{p}}, u_{\mathrm{p}})$ for the supply function $(y_{\mathrm{p}}, u_{\mathrm{p}})$ defined in (5.3)*, if the following*

inequality is satisfied for some Q, S, *and* R

$$x(-4x^3 - 4u_{\mathrm{p}}x) \leq Qx^4 + 2Sx^2u_{\mathrm{p}} + Ru_{\mathrm{p}}^2,$$

or equivalently

$$\dot{V}(x) - (x, u_{\mathrm{p}}) = -(Q+4)x^4 - (2S+4)u_{\mathrm{p}}x^2 - Ru_{\mathrm{p}}^2 \leq 0. \tag{5.16}$$

Therefore (5.16) *is satisfied with* $Q = -4$, $S = -2$, *and* $R = 0$. *Similarly, adopting* $V_{\mathrm{c}}(x_{\mathrm{c}}) = \frac{1}{2}x_{\mathrm{c}}^2$, Σ_{C} *is* (Q_{c},S_{c},R_{c})*-dissipative if*

$$\dot{V}_{\mathrm{c}}(x_{\mathrm{c}}) - (x_{\mathrm{c}}, y_{\mathrm{r}}) = -\left(\frac{Q_{\mathrm{c}}}{4} + 1\right)x_{\mathrm{c}}^2 - (S_{\mathrm{c}} - 1)\, y_{\mathrm{r}}x_{\mathrm{c}} - R_{\mathrm{c}}y_{\mathrm{r}}^2 \leq 0,$$

is satisfied for some Q_{c}, S_{c}, *and* R_{c}, *implying that* $Q_{\mathrm{c}} = -4$, $S_{\mathrm{c}} = 1$, *and* $R_{\mathrm{c}} = 0$. *Note that* Q, S, R, Q_{c}, S_{c}, *and* R_{c} *satisfy* (5.14), *then the nominal system is asymptotically stable. According to Lemma 5.4,* $\Sigma_{\mathrm{P_f}}$ *is stable by fault hiding if* $(\Sigma_{\mathrm{P_f}}, \Sigma_{\mathrm{R}})$, *as depicted in Figure 5.3, is also* (Q,S,R)*-dissipative. The model of* $(\Sigma_{\mathrm{P_f}}, \Sigma_{\mathrm{R}})$ *is described as follows*

$$(\Sigma_{\mathrm{P_f}}, \Sigma_{\mathrm{R}}) : \begin{cases} \dot{x} = (2 - 4R_3)\, x^3 - 4R_4u_{\mathrm{p}}x \\ y_{\mathrm{r}} = R_1x^2 + R_2u_{\mathrm{p}} \end{cases} \tag{5.17}$$

$(\Sigma_{\mathrm{P_f}}, \Sigma_{\mathrm{R}})$ *is* (Q,S,R)*-dissipative with the same storage and supply functions used for* Σ_{P} *if there exist* R_1, R_2, R_3, *and* R_4 *that satisfy* $\dot{V}(x) - (x, u_{\mathrm{c}}) \leq 0$, *or equivalently*

$$-\left(4R_3 - 4R_1^2 - 2\right)x^4 - (4R_4 - 8R_1R_2 - 4)\, u_{\mathrm{p}}x^2 + \left(4R_2 + 4R_2^2\right)u_{\mathrm{p}}^2 \leq 0. \tag{5.18}$$

Therefore, any Σ_{R} *satisfying* (5.18) *recovers the asymptotic stability of* $\Sigma_{\mathrm{P_f}}$, *e.g.,* $R_1 = \frac{1}{4}$, $R_2 = -\frac{1}{2}$, $R_3 = \frac{3}{2}$, *and* $R_4 = \frac{3}{4}$.

The next Theorem provides LMI-based conditions to design an SRBs Σ_{R} (cf. (5.7)) that guarantees the stability recovery by fault hiding of LTI systems.

Theorem 5.2. *Let* Σ_{P} *and* $\Sigma_{\mathrm{P_f}}$ *be the nominal and faulty models, respectively, with dynamics described in* (5.9) *and* (5.10) *interconnected (as depicted in Figure 2.2) to an output feedback* $(\boldsymbol{Q_{\mathrm{c}}}, \boldsymbol{S_{\mathrm{c}}}, \boldsymbol{R_{\mathrm{c}}})$*-dissipative controller* Σ_{C}. *Assume that there exist* $\boldsymbol{P} = \boldsymbol{P}^\top \succ 0$, $\boldsymbol{Q} = \boldsymbol{Q}^\top \prec 0$, $\boldsymbol{S}$, *and* $\boldsymbol{R} = \boldsymbol{R}^\top$ *that satisfy the inequalities* (5.14) *and*

$$\begin{bmatrix} \mathrm{He}\{\boldsymbol{PA}\} - \boldsymbol{C}^\top\boldsymbol{QC} & \boldsymbol{PB} - \boldsymbol{C}^\top\boldsymbol{S}^\top \\ \star & -\boldsymbol{R} \end{bmatrix} \preceq 0. \tag{5.19}$$

For given $\boldsymbol{P}$, $\boldsymbol{Q}$, $\boldsymbol{S}$ *and* $\boldsymbol{R}$ *satisfying* (5.19), *if there exist* $\boldsymbol{R}_1$, $\boldsymbol{R}_2$, $\boldsymbol{R}_3$, *and* $\boldsymbol{R}_4$ *that satisfy the following inequality with* $\boldsymbol{A}_{\mathrm{R}} = \boldsymbol{A}_{\mathrm{f}} + \boldsymbol{B}_{\mathrm{f}}\boldsymbol{R}_3\boldsymbol{C}_{\mathrm{f}}$

$$\begin{bmatrix} \boldsymbol{Q}^{-1} & \boldsymbol{R}_1\boldsymbol{C}_{\mathrm{f}} & \boldsymbol{R}_2 \\ \star & \mathrm{He}\left\{\boldsymbol{P}\boldsymbol{A}_{\mathrm{R}}\right\} & \boldsymbol{P}\boldsymbol{B}_{\mathrm{f}}\boldsymbol{R}_4 - \boldsymbol{C}_{\mathrm{f}}^{\top}\boldsymbol{R}_1^{\top}\boldsymbol{S}^{\top} \\ \star & \star & -\boldsymbol{R} \end{bmatrix} \prec 0, \tag{5.20}$$

then $\Sigma_{\mathrm{P_f}}$ *is stable by fault hiding with* Σ_{R} *described by* (5.7).

Proof. According to [178], Σ_{P} is $(\boldsymbol{Q}, \boldsymbol{S}, \boldsymbol{R})$-dissipative with the storage function $V(\boldsymbol{x}) = \boldsymbol{x}^{\top}\boldsymbol{P}\boldsymbol{x}$ if and only if there exist $\boldsymbol{P} = \boldsymbol{P}^{\top} \succ 0$, $\boldsymbol{Q} = \boldsymbol{Q}^{\top} \prec 0$, $\boldsymbol{S}$, and $\boldsymbol{R} = \boldsymbol{R}^{\top}$ that satisfy (5.19). According to Lemma 5.2, assuming that Σ_{C} is $(\boldsymbol{Q}_{\mathbf{c}}, \boldsymbol{S}_{\mathbf{c}}, \boldsymbol{R}_{\mathbf{c}})$-dissipative, the unforced origin of nominal closed-loop system $(\Sigma_{\mathrm{P}}, \Sigma_{\mathrm{C}})$, interconnected as depicted in Figure 2.2, is asymptotically stable if (5.14) is satisfied.

According to [178], the reconfigured system $(\Sigma_{\mathrm{P}}, \Sigma_{\mathrm{R}})$, described by (5.12), is $(\boldsymbol{Q}, \boldsymbol{S}, \boldsymbol{R})$-dissipative if and only if the following inequality is satisfied

$$\begin{bmatrix} \mathrm{He}\left\{\boldsymbol{P}\boldsymbol{A}_{\mathrm{R}}\right\} - \boldsymbol{C}_{\mathrm{R}}^{\top}\boldsymbol{Q}\boldsymbol{C}_{\mathrm{R}} & \boldsymbol{P}\boldsymbol{B}_{\mathrm{R}} - \boldsymbol{C}_{\mathrm{R}}^{\top}\boldsymbol{S}^{\top} - \boldsymbol{C}_{\mathrm{R}}^{\top}\boldsymbol{Q}\boldsymbol{D}_{\mathrm{R}} \\ \star & -\boldsymbol{R} - \mathrm{He}\left\{\boldsymbol{D}^{\top}\boldsymbol{S}\right\} - \boldsymbol{D}_{\mathrm{R}}^{\top}\boldsymbol{Q}\boldsymbol{D}_{\mathrm{R}} \end{bmatrix} \preceq 0. \tag{5.21}$$

According to Schur complement lemma, if (5.20) is satisfied, given that $\boldsymbol{Q} \prec 0$, then the following inequality is also satisfied, considering $\boldsymbol{L} \triangleq \begin{bmatrix} \boldsymbol{R}_1\boldsymbol{C}_{\mathrm{f}} & \boldsymbol{R}_2 \end{bmatrix}$:

$$\begin{bmatrix} \boldsymbol{A}_{\mathrm{R}}^{\top}\boldsymbol{P} + \boldsymbol{P}\boldsymbol{A}_{\mathrm{R}} & \boldsymbol{P}\boldsymbol{B}_{\mathrm{f}}\boldsymbol{R}_4 - \boldsymbol{C}_{\mathrm{f}}^{\top}\boldsymbol{R}_1^{\top}\boldsymbol{S}^{\top} \\ \star & -\boldsymbol{R} - \mathrm{He}\left\{\boldsymbol{D}^{\top}\boldsymbol{S}\right\} \end{bmatrix} - \boldsymbol{L}^{\top}\boldsymbol{Q}\boldsymbol{L} \prec 0,$$

that is equivalent to (5.21), *i.e.*, (5.20) is sufficient to $(\Sigma_{\mathrm{P_f}}, \Sigma_{\mathrm{R}})$ be $(\boldsymbol{Q}, \boldsymbol{S}, \boldsymbol{R})$-dissipative. Finally, if (5.14) and (5.20) are satisfied, then the unforced origin of $(\Sigma_{\mathrm{P_f}}, \Sigma_{\mathrm{R}}, \Sigma_{\mathrm{C}})$ is asymptotically stable by fault hiding, and $\Sigma_{\mathrm{P_f}}$ is stable by fault hiding with Σ_{R} described by (5.7). □

Example 5.4. *Consider the aircraft yaw control described in [16], where the following*

simplified and linearized model is considered for the yaw angle ϕ

$$\Sigma_{\mathrm{P}}: \begin{cases} \begin{bmatrix} \dot{x}_R \\ \dot{x}_T \\ \dot{\phi} \end{bmatrix} = \begin{bmatrix} -1 & 0 & 0 \\ 0 & -1 & 0 \\ 0.27 & 0.13 & -10^{-3} \end{bmatrix} \begin{bmatrix} x_R \\ x_T \\ \phi \end{bmatrix} + \begin{bmatrix} 1 & 0 \\ 0 & 1 \\ 0 & 0 \end{bmatrix} \begin{bmatrix} u_R \\ u_T \end{bmatrix}, \\ y_{\mathrm{p}} = \begin{bmatrix} 0 & 0 & 1 \end{bmatrix} \begin{bmatrix} x_R \\ x_T \\ \phi \end{bmatrix} \end{cases},$$

where the rudder and turbine actuation have their own dynamics, which are approximated, as proposed in [16], by first-order models with states variables x_R *and* x_T *and time constants of* 1 *s;* u_R *and* u_T *denote respectively the rudder and differential thrust inputs. The yaw dynamics is controlled by an output feedback controller* Σ_{C} *interconnected as depicted in Figure 2.2*

$$\Sigma_{\mathrm{C}}: \begin{cases} \dot{x}_{\mathrm{c}} = -0.05x_{\mathrm{c}} + 0.05y_{\mathrm{r}}, \\ u_{\mathrm{p}} = \begin{bmatrix} 25 \\ 0 \end{bmatrix} x_{\mathrm{c}}, \end{cases}$$

The controller Σ_{C} *is chosen to highlight the efficacy of the proposed fault hiding approach. One can notice that* Σ_{C} *is nominally designed to use only the rudder actuator, as proposed in [16], which is unusual for real applications. However, it serve to the purpose of illustrating the effect of a fault in the rudder controller and the ability of stability recovery provided by the proposed RBs designed following the dissipativity recovery approach presented in this chapter. Figure 5.4 depicts the system response in a 3000 s numerical simulation. It indicates that the output slowly, since in nominal operation, the origin of* $(\Sigma_{\mathrm{P}}, \Sigma_{\mathrm{C}})$ *is asymptotically stable.*

Consider that such system is subject to an actuator fault, such that its matrix $\boldsymbol{B}_{\mathrm{f}}$ *is described as follows*

$$\boldsymbol{B}_{\mathrm{f}} = \begin{bmatrix} 0 & 0 \\ 0 & 1 \\ 0 & 0 \end{bmatrix},$$

that corresponds to loss the rudder actuator.

Two RBs are designed for this fault scenario. The RB Σ_{R}^{p} *is designed for passivity recovery based on Theorem 5.1, and the second one* Σ_{R}^{d} *is designed for dissipativity*

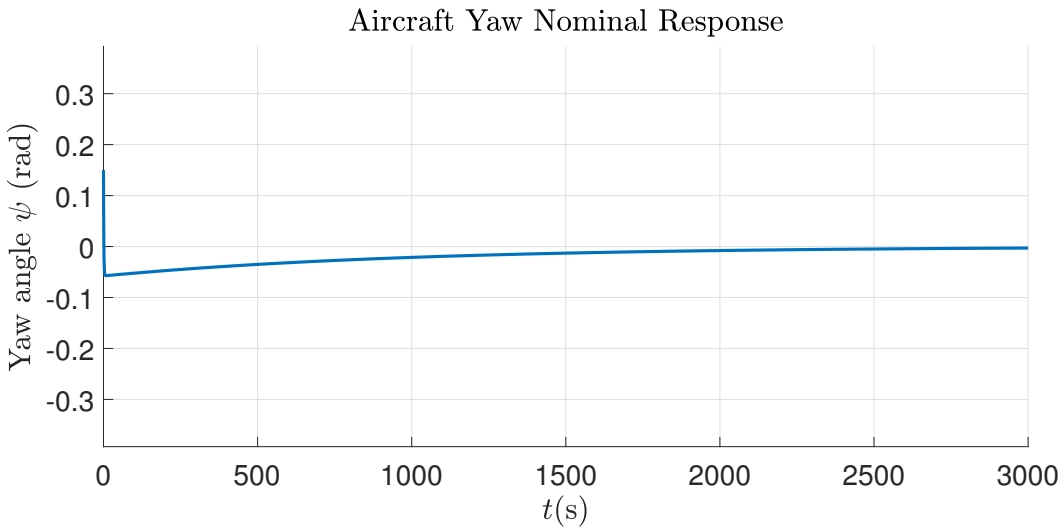

Figure 5.4 – Output response of aircraft yaw control under nominal (fault-free) operation.

recovery based on Theorem 5.2. Their gains are described as follows

$$\boldsymbol{R}_1^p = \begin{bmatrix} 0.6202 & -0.0556 \\ 0.0556 & 2.2842 \end{bmatrix}, \quad \boldsymbol{R}_2^p = \begin{bmatrix} 1.4630 & 0.4650 \\ -0.3470 & 1.5252 \end{bmatrix},$$

$$\boldsymbol{R}_3^p = \begin{bmatrix} 0 & 0 \\ -0.4187 & 0 \end{bmatrix}, \quad \boldsymbol{R}_4^p = \begin{bmatrix} 2.2842 & -0.1227 \\ 0.1227 & 0.8143 \end{bmatrix},$$

$$\boldsymbol{R}_1^d = \begin{bmatrix} 0.5003 & 0 \\ 0 & 5.7735 \times 10^8 \end{bmatrix}, \quad \boldsymbol{R}_2^d = \begin{bmatrix} 0.4477 & 0.0049 \\ 0 & 0 \end{bmatrix},$$

$$\boldsymbol{R}_3^d = \begin{bmatrix} 0 & 0 \\ -1.0675 & 0 \end{bmatrix}, \quad \boldsymbol{R}_4^d = \begin{bmatrix} 0 & 0 \\ -0.0494 & -0.0028 \end{bmatrix}.$$

The results of the actuator fault simulation comparing the reconfigured systems with Σ_{R}^p, Σ_{R}^d, and without RB are depicted in Figures 5.5–5.7 with initial condition $\begin{bmatrix} -1.25 & 1 & 0.15 \end{bmatrix}^\top$, and the fault occurs from $t = 50$ s. An impulse disturbance is inserted at the output at $t = 65$s.

Figure 5.5 depicts the output signals indicating that the aircraft yaw becomes unstable without reconfiguration, but both, Σ_{R}^p and Σ_{R}^d, recovers the stability after the fault occurrence. Figures 5.6 and 5.7 depict the control efforts during the simulation

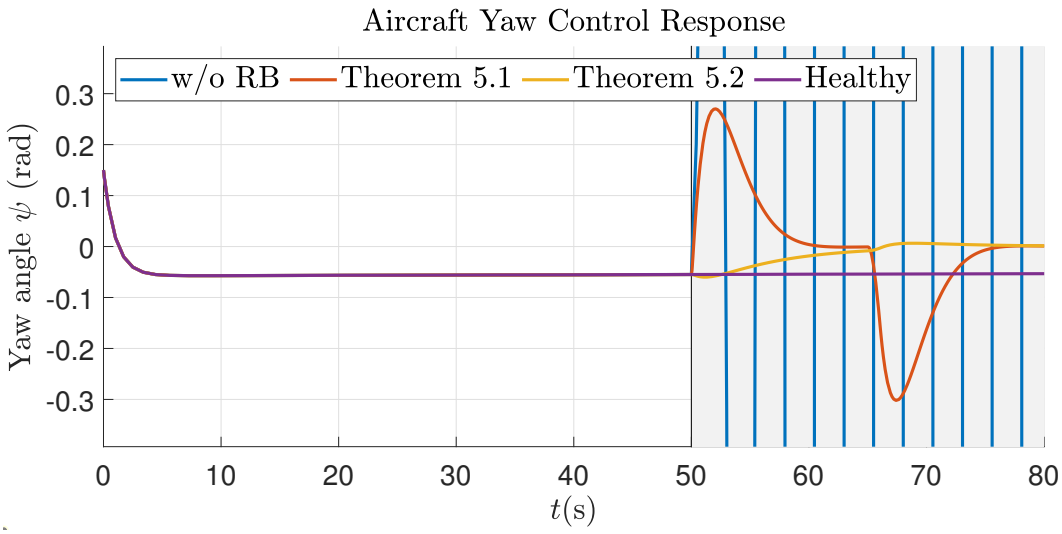

Figure 5.5 – Comparison of the output responses of aircraft yaw control without FTC, with the RBs designed for passivity recovery, with the RBs designed for $(\boldsymbol{Q}, \boldsymbol{S}, \boldsymbol{R})$-dissipativity recovery, and without fault occurrence (healthy).

of the rudder actuator u_R and differential thrust u_T, respectively. Since the controller Σ_{C} initially does not use the differential thrust, when the fault occurs the u_R tends to increase and becomes unstable when there is not an RB. However, Figures 5.6 and 5.7 indicate that the RBs perform a control reallocation using the other actuator to compensate for the fault and recover the aircraft yaw dynamics stability.

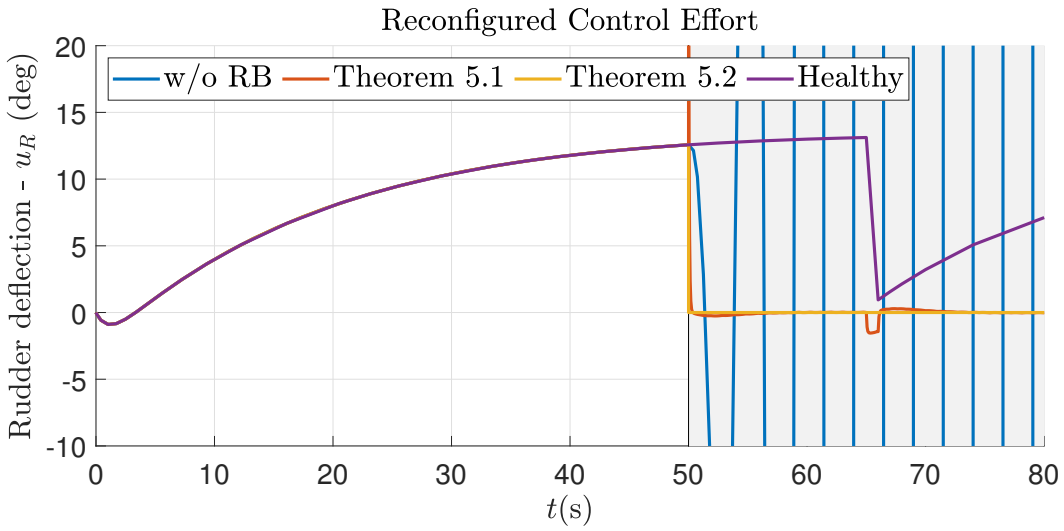

Figure 5.6 – Comparison of reconfigured control signals of the rudder actuator u_R of aircraft yaw control system without FTC, with the RBs designed for passivity recovery, with the RBs designed for $(\boldsymbol{Q}, \boldsymbol{S}, \boldsymbol{R})$-dissipativity recovery, and without fault occurrence (healthy).

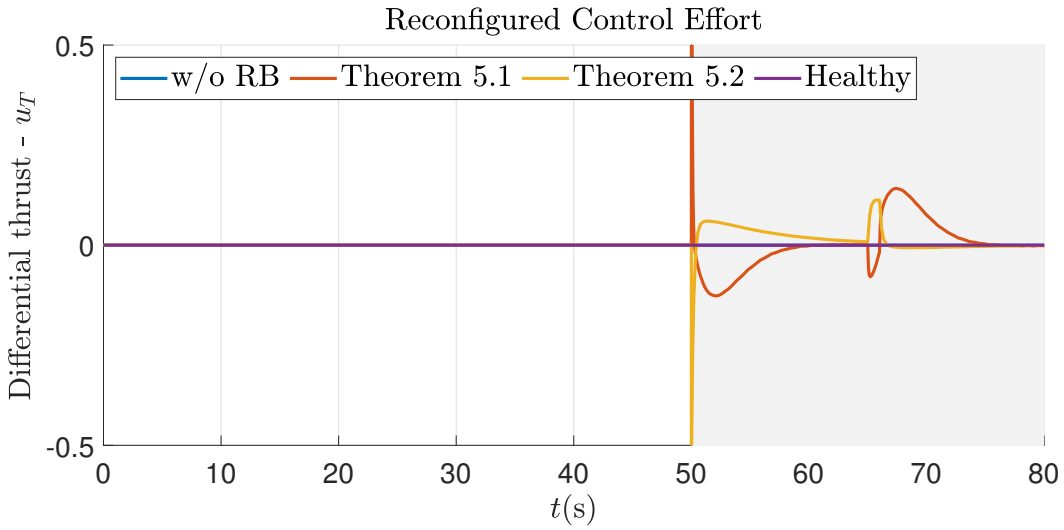

Figure 5.7 – Comparison of reconfigured control signals of the differential thrust u_T of aircraft yaw control system without FTC, with the RBs designed for passivity recovery, with the RBs designed for $(\boldsymbol{Q}, \boldsymbol{S}, \boldsymbol{R})$-dissipativity recovery, and without fault occurrence (healthy).

6 PASSIVATION-BASED FAULT HIDING OF NONLINEAR SYSTEMS

Dissipativity and passivity theory and their relation with input-output stability is an important paradigm of dynamical system analysis and synthesis [178, 250]. Dissipativity and passivity-based approaches are established on a generalized notion of energy balance for dynamical systems considering the supplied and stored energy from the perspective of input and output signals. In this context, the passivity indices [242] and passivation techniques [243, 244] have been studied for obtaining closed-loop systems with desired passivity properties. Passivation is the use of controllers in order to ensure that a closed-loop system will present some desired dissipation or passivity properties.

In this work, a novel RB called PB is presented. It can be generically used for actuator and sensor faults and to perform simultaneously series, feedback and feedfoward passivation of the controller for mitigation of fault effects. In addition, LMI-based conditions are obtained for designing the PB to ensure asymptotic stability of the reconfigured system based on dissipativity theory. Unlike previous approaches, the proposed PB is suitable for different classes of nonlinear systems since their passivity indices can be determined. In summary, the main contributions of this chapter are:

a) the concept of PB for FTC of nonlinear systems is introduced and compared to other passivation strategy for fault mitigation in [200];

b) a $(\boldsymbol{Q}, \boldsymbol{S}, \boldsymbol{R})$-dissipativity and passivity indices analysis for the interconnection between faulty plant, controller, and PB is presented;

c) it is shown that the proposed PB structure generalizes the VAs and VSs for linear systems, although it can also be used for nonlinear systems;

d) new LMI-based stability recovery conditions after sensor or actuator fault occurrence are established.

The remainder of this chapter is organized as follows: Section 6.1 presents the problem of stability recovery by fault hiding based on passivity indices; Section 6.2 presents the concept of PB; Section 6.3 provides the condition for asymptotic stability recovery with PBs; and Section 6.4 presents numerical simulation results.

6.1 Preliminaries

6.1.1 Dissipativity and Passivity Indices

Consider the nonlinear system Σ described as follows

$$\Sigma : \begin{cases} \dot{\boldsymbol{x}}(t) = \boldsymbol{f}\left(\boldsymbol{x}(t)\right) + \boldsymbol{g}\left(\boldsymbol{x}(t), \boldsymbol{u}(t)\right), \\ \boldsymbol{y}(t) = \boldsymbol{h}\left(\boldsymbol{x}(t)\right) + \boldsymbol{j}\left(\boldsymbol{x}(t), \boldsymbol{u}(t)\right), \end{cases} \tag{6.1}$$

where $\boldsymbol{x}(t) \in \mathbb{R}^n$, $\boldsymbol{u}(t) \in \mathbb{R}^m$, and $\boldsymbol{y}(t) \in \mathbb{R}^m$ are, respectively, the state, input and output vectors, and the maps $\boldsymbol{f}$, $\boldsymbol{g}$, $\boldsymbol{h}$, and $\boldsymbol{j}$ satisfy Assumption 6.1. Assume also that Σ is ZSD [19].

Assumption 6.1. *The maps $\boldsymbol{f}$, $\boldsymbol{g}$, $\boldsymbol{h}$, and $\boldsymbol{j}$ are sufficiently smooth to ensure that* (6.1) *is well defined, i.e., for any $x\left(t_0\right)$ and admissible $\boldsymbol{u}(t)$, there exists a unique solution for $t \geq t_0$ such that $\boldsymbol{y}(t)$ is locally integrable. Furthermore, $\boldsymbol{f}(0) = 0$ and $\boldsymbol{h}(0) = 0$.*

Remark 6.1. *For the concept of passivity indices that is discussed in the following, it is required that the number of inputs is equal to the number of outputs. If it is not possible to have the same number of inputs and outputs, it is still possible to extend $\boldsymbol{u}(t)$ or $\boldsymbol{y}(t)$ by adding virtual inputs/output that are negligible in the system dynamics.*

The system Σ is dissipative if its stored energy, represented by the time derivative of a non-negative continuously differentiable function $V(\boldsymbol{x}(t))$, is always less than or equal to the supplied energy, represented by a supply rate function $(\boldsymbol{u}(t), \boldsymbol{y}(t))$. A special case of dissipativity is the $(\boldsymbol{Q}, \boldsymbol{S}, \boldsymbol{R})$-dissipativity introduced in Definition 5.2.

Passivity is a special case of dissipativity, i.e., a system is said to be passive if it is dissipative with respect to the supply rate $(\boldsymbol{u}(t), \boldsymbol{y}(t)) = \boldsymbol{u}(t)^\top \boldsymbol{y}(t)$. In particular, the framework of passivity indices is useful to obtain an indication of the passivity degree [178] as shown in Definition 6.1 and to develop passivation strategies [200]. To this purpose, the concept of IF-OFP systems is provided as follows.

Definition 6.1. ***[200]*** *The system Σ described in* (6.1) *is input feedforward output feedback passive (IF-OFP) if for some $\nu, \rho \in \mathbb{R}$ it is dissipative with respect to*

$$(\boldsymbol{u}(t), \boldsymbol{y}(t)) = \boldsymbol{u}(t)^\top \boldsymbol{y}(t) - \nu \boldsymbol{u}(t)^\top \boldsymbol{u}(t) - \rho \boldsymbol{y}(t)^\top \boldsymbol{y}(t). \tag{6.2}$$

In this case, Σ is denominated IF-OFP(ν, ρ), where ν and ρ are called input feedforward and output feedback passivity indices, respectively, which correspond to the excess of passivity of Σ. If Σ is IF-OFP(ν, ρ) with $\nu > 0$ and $\rho > 0$, then it is said VSP.

Particular cases of Definition 6.1 are used to describe IFP and OFP by removing, respectively, the terms of $\rho \boldsymbol{y}(t)^\top \boldsymbol{y}(t)$ and $\nu \boldsymbol{u}(t)^\top \boldsymbol{u}(t)$ respectively. The passivity indices provide intuitiveness to the dissipativity framework because they are related to the concept of lack (or excess) of passivity of a system. This means that ν indicates how much feedfoward gain can be inserted preserving Σ stability given the excess of input passivity $\nu \boldsymbol{u}(t)^\top \boldsymbol{u}(t)$ and, similarly, ρ indicates how much feedback gain can be inserted to preserve Σ stability given the excess of output passivity $\rho \boldsymbol{y}(t)^\top \boldsymbol{y}(t)$. In this sense, every system is IF-OFP(ν, ρ) for some ν and ρ, but the maximum value that ν and ρ can assume are indicators of the stability margins of that system. For instance, if the maximum ρ that can be assigned for a system Σ is negative, then it is possible to ensure that Σ is open-loop unstable and requires a negative feedback action to compensate for such lack of passivity that results in the instability. Based on that, the following fact is considered regarding the framework of passivity indices.

Lemma 6.1. *If Σ is IF-OFP(ν, ρ) for some scalars ν and ρ, then Σ is also IF-OFP$(\nu^\star, \rho^\star)$ for any $\nu^\star \leq \nu$ and $\rho^\star \leq \rho$.*

Proof. Defining

$$
\begin{aligned}
(\boldsymbol{u}(t), \boldsymbol{y}(t)) &= \boldsymbol{u}(t)^\top \boldsymbol{y}(t) - \nu \boldsymbol{u}(t)^\top \boldsymbol{u}(t) - \rho \boldsymbol{y}(t)^\top \boldsymbol{y}(t), \\
\bar{\boldsymbol{S}}(\boldsymbol{u}(t), \boldsymbol{y}(t)) &= \boldsymbol{u}(t)^\top \boldsymbol{y}(t) - \bar{\nu} \boldsymbol{u}(t)^\top \boldsymbol{u}(t) - \bar{\rho} \boldsymbol{y}(t)^\top \boldsymbol{y}(t),
\end{aligned}
$$

it follows that $\bar{\boldsymbol{S}}(\boldsymbol{u}(t), \boldsymbol{y}(t)) \geq (\boldsymbol{u}(t), \boldsymbol{y}(t))$ for any $\bar{\nu} \leq \nu$ and $\bar{\rho} \leq \rho$. Thus, given that Σ is dissipative with respect to $(\boldsymbol{u}(t), \boldsymbol{y}(t))$ it is also dissipative with respect to $\bar{\boldsymbol{S}}(\boldsymbol{u}(t), \boldsymbol{y}(t))$, and therefore Σ is IF-OFP$(\bar{\nu}, \bar{\rho})$. □

The concepts of passivity indices and $(\boldsymbol{Q}, \boldsymbol{S}, \boldsymbol{R})$-dissipativity are closely related. Indeed, it is observed that the supply function (6.2) is a special case of (5.3) by choosing $\boldsymbol{Q} = -\rho \boldsymbol{I}_m$, $\boldsymbol{S} = -\frac{1}{2}\boldsymbol{I}_m$, and $\boldsymbol{R} = -\nu \boldsymbol{I}_m$. Furthermore, the feedback interconnection of IF-OFP systems is $(\boldsymbol{Q}, \boldsymbol{S}, \boldsymbol{R})$-dissipative as stated in Lemma 6.2.

Lemma 6.2. ***[250]*** *Consider the systems Σ_1 and Σ_2 described as in* (6.1) *and interconnected by negative feedback. If Σ_1 and Σ_2 are IF-OFP(ν_1,ρ_1) and IF-OFP(ν_2,ρ_2), respectively, then the interconnected system is ($\bar{\boldsymbol{Q}}$,$\bar{\boldsymbol{S}}$,$\bar{\boldsymbol{R}}$)-dissipative with matrices*

$$\bar{\boldsymbol{Q}} = \begin{bmatrix} -(\rho_1+\nu_2)\boldsymbol{I}_m & \boldsymbol{0}_{m\times m} \\ \boldsymbol{0}_{m\times m} & -(\rho_2+\nu_1)\boldsymbol{I}_m \end{bmatrix}, \tag{6.3}$$

$$\bar{\boldsymbol{S}} = \begin{bmatrix} \frac{1}{2}\boldsymbol{I}_m & \nu_1\boldsymbol{I}_m \\ -\nu_2\boldsymbol{I}_m & \frac{1}{2}\boldsymbol{I}_m \end{bmatrix}, \tag{6.4}$$

$$\bar{\boldsymbol{R}} = \begin{bmatrix} -\nu_1\boldsymbol{I}_m & \boldsymbol{0}_{m\times m} \\ \boldsymbol{0}_{m\times m} & -\nu_2\boldsymbol{I}_m \end{bmatrix}, \tag{6.5}$$

with input $\boldsymbol{w}(t) \triangleq \left[\boldsymbol{w}_1(t)^\top \ \boldsymbol{w}_2(t)^\top\right]^\top$ and output $\boldsymbol{y} \triangleq \left[\boldsymbol{y}_1(t)^\top \ \boldsymbol{y}_2(t)^\top\right]^\top$. In addition, the origin of (Σ_1, Σ_2) is asymptotically stable if $\rho_1+\nu_2>0$ and $\rho_2+\nu_1>0$.

6.1.2 Passivation blocks

However, eventually, the some usual dissipativity and passivity theorems require the specific dissipativity (passivity) properties from the system under analysis. Then, passivation techniques enable the use of these techniques for a wider class of systems. In the literature, feedback, feedfoward and series passivation techniques have been successfully employed to stabilize dynamical systems. In [200], a general passivation technique expressed by a matrix transformation that comprises the feedback, feedforward, and series passivation actions is presented.

Consider the system Σ_{C} and the SRB that performs an input-output linear transformation by means of the matrix $\boldsymbol{M}$ described as follows

$$\Sigma_{\mathrm{R}}: \begin{bmatrix} \boldsymbol{u}_{\mathrm{r}} \\ \boldsymbol{y}_{\mathrm{r}} \end{bmatrix} = \boldsymbol{M} \begin{bmatrix} \boldsymbol{y} \\ \boldsymbol{u}_{\mathrm{c}} \end{bmatrix}, \tag{6.6}$$

such that their interconnection is depicted in Fig. 6.1.

As shown in [200], the matrix transformation M can be expressed as the combination of passivation gains in series, feedfoward, and feedback. In particular, Xia et al. [200] define the matrix M as follows

$$\boldsymbol{M} \triangleq \begin{bmatrix} m_{\mathrm{p}}\boldsymbol{I} & (m_{\mathrm{s}}-m_{\mathrm{p}}m_{\mathrm{f}})\boldsymbol{I} \\ \boldsymbol{I} & -m_{\mathrm{f}}\boldsymbol{I} \end{bmatrix}, \quad m_{\mathrm{s}} \neq m_{\mathrm{p}}m_{\mathrm{f}}, \tag{6.7}$$

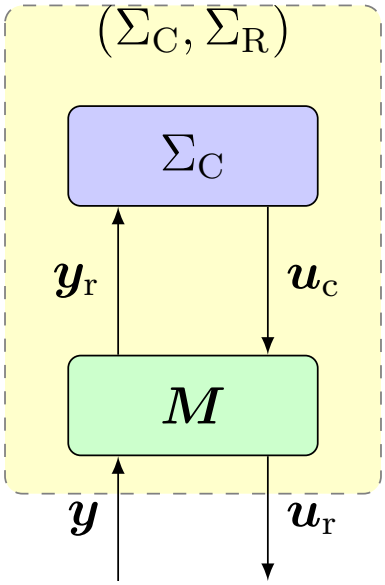

Figure 6.1 – Passivation of Σ_{C}.

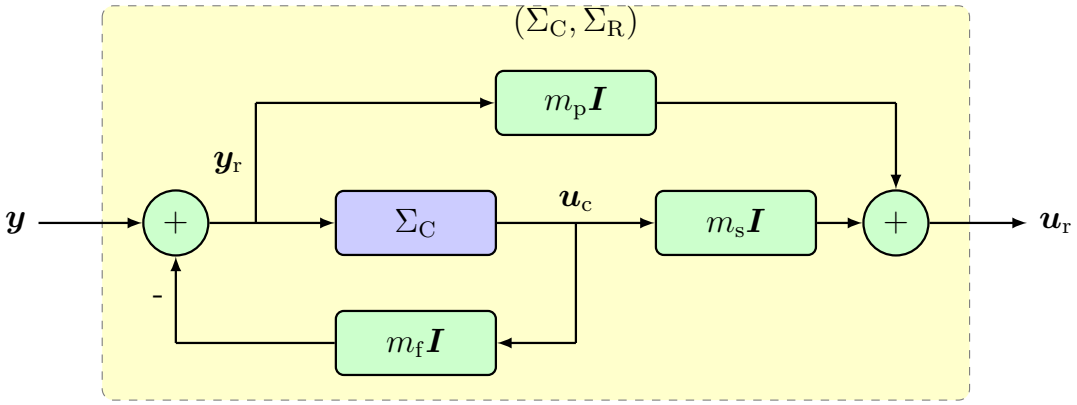

Figure 6.2 – Equivalent interconnection with feedback, series, and feedfoward passivation gains.

where m_{p}, m_{f}, and m_{s} are feedfoward, feedback, and series gains, such that the $(\Sigma_{\mathrm{C}}, \Sigma_{\mathrm{R}})$ is equivalent to the system illustrated in Fig. 6.2.

Lemma 6.3, originally presented in [200], allows to design the matrix $\boldsymbol{M}$ to ensure desired passivity indices for $(\Sigma_{\mathrm{C}}, \Sigma_{\mathrm{R}})$.

Lemma 6.3. ***[200]*** *Let Σ_{C} be finite-gain $\mathcal{L}_2$-stable with gain γ and Σ_{R} described by* (6.6) *and the passivation matrix $\boldsymbol{M}$ given by* (6.7)*. The equivalent system $(\Sigma_{\mathrm{C}}, \Sigma_{\mathrm{R}})$ is*

a) passive if $\boldsymbol{M}$ is chosen such that

$$m_{\mathrm{p}} > 0, \quad m_{\mathrm{s}} = -m_{\mathrm{f}} m_{\mathrm{p}}, \quad 0 < |m_{\mathrm{f}}|\gamma < 1; \tag{6.8}$$

b) $OFP(\rho_{\mathrm{r}})$ with $\rho_{\mathrm{r}} > 0$, such that $\rho_{\mathrm{r}} = \frac{1}{2}(\frac{1}{m_{\mathrm{p}}} + \frac{m_{\mathrm{f}}}{m_{\mathrm{s}}})$, if $\boldsymbol{M}$ is chosen such that

$$m_{\mathrm{p}} \geq m_{\mathrm{s}}\gamma > 0, \quad m_{\mathrm{s}} > m_{\mathrm{f}} m_{\mathrm{p}} > 0; \tag{6.9}$$

c) $IFP(\nu_{\mathrm{r}})$ with $\nu_{\mathrm{r}} > 0$, such that $\nu_{\mathrm{r}} = \frac{1}{2}(m_{\mathrm{p}} + \frac{m_{\mathrm{s}}}{m_{\mathrm{f}}})$, if $\boldsymbol{M}$ is chosen such that

$$1 > m_{\mathrm{f}}\gamma > 0, \quad m_{\mathrm{f}} m_{\mathrm{p}} > m_{\mathrm{s}} > 0; \tag{6.10}$$

d) VSP with indices $\nu_{\mathrm{r}} = \frac{a}{2} m_{\mathrm{p}}$ and $\rho_{\mathrm{r}} = \frac{a}{2}\frac{1}{m_{\mathrm{p}}}$, if $\boldsymbol{M}$ is such that

$$m_{\mathrm{p}} >> 0, \quad m_{\mathrm{s}} = -m_{\mathrm{f}} m_{\mathrm{p}}, \quad m_{\mathrm{f}}^2\gamma^2 \leq \frac{1-a}{1+a}; \tag{6.11}$$

for an arbitrary $0 < a < 1$.

6.1.3 Problem statement

Consider the nominal system Σ_{P} subject to faults whose faulty model is $\Sigma_{\mathrm{P_f}}$ described as follows

$$\Sigma_{\mathrm{P}} : \begin{cases} \dot{\boldsymbol{x}}(t) = \boldsymbol{f}\left(\boldsymbol{x}(t)\right) + \boldsymbol{g}\left(\boldsymbol{x}(t), \boldsymbol{u}_{\mathrm{p}}(t)\right), \\ \boldsymbol{y}_{\mathrm{p}}(t) = \boldsymbol{h}\left(\boldsymbol{x}(t)\right) + \boldsymbol{j}\left(\boldsymbol{x}(t), \boldsymbol{u}_{\mathrm{p}}(t)\right), \end{cases} \tag{6.12}$$

$$\Sigma_{\mathrm{P_f}} : \begin{cases} \dot{\boldsymbol{x}}(t) = \boldsymbol{f}_{\mathrm{f}}\left(\boldsymbol{x}(t)\right) + \boldsymbol{g}_{\mathrm{f}}\left(\boldsymbol{x}(t), \boldsymbol{u}_{\mathrm{p}}(t)\right), \\ \boldsymbol{y}_{\mathrm{p}}(t) = \boldsymbol{h}_{\mathrm{f}}\left(\boldsymbol{x}(t)\right) + \boldsymbol{j}_{\mathrm{f}}\left(\boldsymbol{x}(t), \boldsymbol{u}_{\mathrm{p}}(t)\right), \end{cases} \tag{6.13}$$

where $\boldsymbol{x}(t) \in \mathbb{R}^n$, $\boldsymbol{u}(t) \in \mathbb{R}^m$, and $\boldsymbol{y}(t) \in \mathbb{R}^m$ are, respectively, the vectors of state, input, and output variables; $\boldsymbol{x}_0 = \boldsymbol{x}\left(0\right)$, $\boldsymbol{x}_{\mathrm{f},0} = \boldsymbol{x}\left(t_{\mathrm{f}}\right)$, t_{f} is the time when the fault

begins, and the matrix-valued maps $\boldsymbol{f}$, $\boldsymbol{g}$, $\boldsymbol{h}$, $\boldsymbol{j}$, $\boldsymbol{f}_{\mathrm{f}}$, $\boldsymbol{g}_{\mathrm{f}}$, $\boldsymbol{h}_{\mathrm{f}}$, and $\boldsymbol{j}_{\mathrm{f}}$ are sufficiently smooth with appropriate dimensions under Assumption 6.1.

The plant is interconnected with an output feedback controller Σ_{C} described as follows

$$\Sigma_{\mathrm{C}}: \begin{cases} \dot{\boldsymbol{x}}_{\mathrm{c}}(t) = \boldsymbol{f}_{\mathrm{c}}\left(\boldsymbol{x}_{\mathrm{c}}(t)\right) + \boldsymbol{g}_{\mathrm{c}}\left(\boldsymbol{x}(t)\right)\boldsymbol{y}_{\mathrm{c}}(t), \\ \boldsymbol{u}_{\mathrm{c}}(t) = \boldsymbol{h}_{\mathrm{c}}\left(\boldsymbol{x}(t)\right) + \boldsymbol{j}_{\mathrm{c}}\left(\boldsymbol{x}_{\mathrm{c}}(t)\right)\boldsymbol{y}_{\mathrm{c}}(t). \end{cases} \tag{6.14}$$

where $\boldsymbol{x}_{\mathrm{c}}(t) \in \mathbb{R}^{n_{\mathrm{c}}}$, $\boldsymbol{u}_{\mathrm{c}}(t) \in \mathbb{R}^{m}$, and $\boldsymbol{y}_{\mathrm{c}}(t) \in \mathbb{R}^{m}$ are, respectively, the state, input and output of Σ_{C}, $\boldsymbol{x}_{\mathrm{c},0} = \boldsymbol{x}_{\mathrm{c}}(0)$, the matrix-valued maps $\boldsymbol{f}_{\mathrm{c}}$, $\boldsymbol{g}_{\mathrm{c}}$, $\boldsymbol{h}_{\mathrm{c}}$, and $\boldsymbol{j}_{\mathrm{c}}$ are sufficiently smooth with appropriate dimensions.

As shown in Fig. 6.3, a RB denoted by Σ_{R} is inserted between the faulty plant and the controller to recover the fault-free performance or stability. In this work, Σ_{R} is used as a PB, i.e., Σ_{R} performs series, feedback, and feedfoward passivation on Σ_{C} to ensure that the closed-loop system presents desired dissipativity properties. The concept of passivation for fault mitigation proposed by [200] can be extended to a dynamic structure called dynamic PB (DPB) whose model is described as follows

$$\Sigma_{\mathrm{r}}: \begin{cases} \dot{\boldsymbol{x}}_{\mathrm{r}}(t) = \boldsymbol{A}_{\mathrm{r}}\boldsymbol{x}_{\mathrm{r}}(t) + \boldsymbol{B}_{\mathrm{r,y}}\boldsymbol{y}(t) + \boldsymbol{B}_{\mathrm{r,u}}\boldsymbol{u}_{\mathrm{c}}(t), \\ \boldsymbol{y}_{\mathrm{r}}(t) = \boldsymbol{C}_{\mathrm{r,y}}\boldsymbol{x}_{\mathrm{r}}(t) + \boldsymbol{R}_{1}\boldsymbol{y}(t) + \boldsymbol{R}_{2}\boldsymbol{u}_{\mathrm{c}}(t), \\ \boldsymbol{u}_{\mathrm{r}}(t) = \boldsymbol{C}_{\mathrm{r,u}}\boldsymbol{x}_{\mathrm{r}}(t) + \boldsymbol{R}_{3}\boldsymbol{y}(t) + \boldsymbol{R}_{4}\boldsymbol{u}_{\mathrm{c}}(t), \end{cases} \tag{6.15}$$

with $\boldsymbol{x}_{\mathrm{r}}(t) \in \mathbb{R}^{n_{\mathrm{r}}}$ and gain matrices $\boldsymbol{A}_{\mathrm{r}}$, $\boldsymbol{B}_{\mathrm{r,y}}$, $\boldsymbol{B}_{\mathrm{r,u}}$, $\boldsymbol{C}_{\mathrm{r,y}}$, $\boldsymbol{C}_{\mathrm{r,u}}$ with proper dimensions.

During the fault-free operation, the nominal plant Σ_{P} is connected by feedback to the controller Σ_{C} such that $\boldsymbol{u}_{\mathrm{p}} \leftarrow \boldsymbol{u}_{\mathrm{c}}$ and $\boldsymbol{y}_{\mathrm{c}} \leftarrow \boldsymbol{y}$ (see fault-free system in Fig. 6.3). However, if a fault occurs, the system dynamics is changed and a proper FDI system can indicate the fault occurrence and obtain the passivity indices of $\Sigma_{\mathrm{P_f}}$. Then, Σ_{R} is activated between $\Sigma_{\mathrm{P_f}}$ and Σ_{C} such that $\boldsymbol{u}_{\mathrm{p}} \leftarrow \boldsymbol{u}_{\mathrm{r}}$ and $\boldsymbol{y}_{\mathrm{c}} \leftarrow \boldsymbol{y}_{\mathrm{r}}$ (see reconfigured system in Fig. 6.3).

In this chapter, the exact models of Σ_{P}, $\Sigma_{\mathrm{P_f}}$ and Σ_{C} do not need to be exactly known but only the passivity indices of $\Sigma_{\mathrm{P_f}}$ and Σ_{C} are.

Assumption 6.2. *Assume that Σ_{C} is IF-OFP($\nu_{\mathrm{c}}, \rho_{\mathrm{c}}$) with given ν_{c} and ρ_{c}. In addition, there is no further knowledge about Σ_{P} and Σ_{C} beyond the passivity indices of Σ_{C}.*

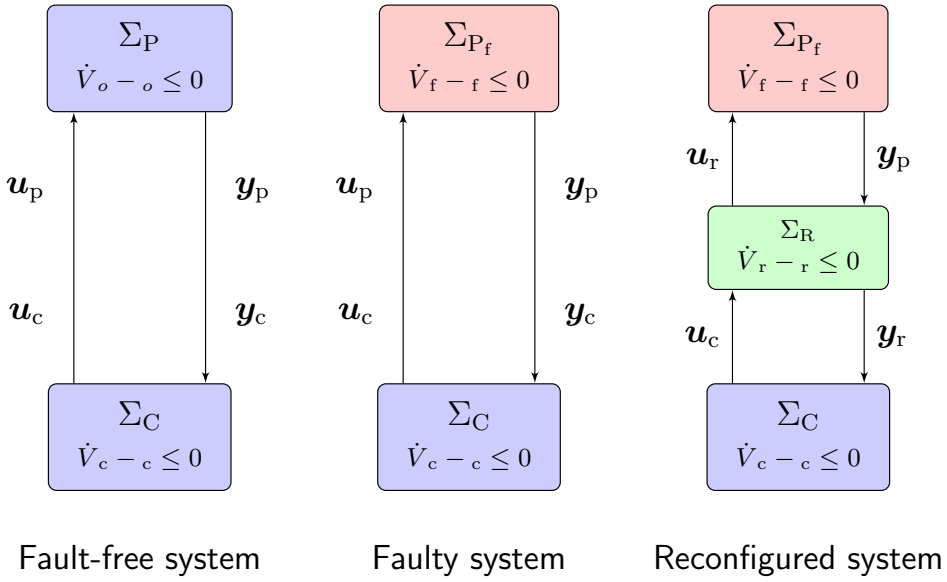

Figure 6.3 – Control reconfiguration by fault hiding.

Assumption 6.3. *It is assumed that $\Sigma_{\mathrm{P_f}}$ is IF-OFP$(\nu_{\mathrm{f}}, \rho_{\mathrm{f}})$ and there exists an FDI system that is able to correctly detect the fault occurrence as soon as it occurs. Furthermore, the FDI system provides the values of ν_{f} and ρ_{f}.*

Remark 6.2. *The results presented in this chapter are based on the knowledge of the dissipative properties of the controller and the estimation of dissipativity properties of the faulty system as stated in Assumptions 6.2 and 6.3. The estimation of dissipativity properties of the faulty system is achieved by means of any efficient FDI strategy (notice that the FDI design is not addressed in this chapter and it is supposed to be available beforehand). The study of fault detection and control reconfiguration is usually separated in the literature on AFTC [261, 136, 18], although both should be implemented together. There are few results on the integrated design AFTC and FDI systems [13]. Although it is still an open issue, the integration between FTC, FDI, and passivity indices estimation is not addressed here.*

Remark 6.3. *The estimation of dissipativity properties is a challenging problem. It is still lacking general procedures for estimating it for different classes of nonlinear systems. There are some available methodologies for estimating dissipativity properties from data [201, 262, 263, 264], although most of them are only applicable for linear time*

invariant systems [262, 263, 264]. There are few results for local dissipativity of nonlinear systems under operational constraints based on polynomial approximations [265] and for dissipativity with respect to a periodic orbit [266].

In the context of dissipativity theory, the following fault hiding problem can be stated.

Problem 6.1. – ***Asymptotic Stability Recovery by Fault Hiding*** – *Let Σ_{P} be a nominal system with fault model $\Sigma_{\mathrm{P_f}}$ and connected to a controller Σ_{C}. Considering Assumptions 6.2 and 6.3, find an RB Σ_{R} such that the origin of $(\Sigma_{\mathrm{P_f}}, \Sigma_{\mathrm{R}}, \Sigma_{\mathrm{C}})$ is asymptotically stable.*

6.2 Passivation blocks for fault hiding

6.2.1 DPB and its relation with RBs

This chapter extends the concept of passivation for fault mitigation proposed by [200] for a DPB described as (6.15) used for solving the FTC Problem 6.1.

The equivalent reconfigured loop obtained by means of the interconnection $(\Sigma_{\mathrm{P_f}}, \Sigma_{\mathrm{R}}, \Sigma_{\mathrm{C}})$ with Σ_{R} described as (6.15) is depicted in Fig. 6.4, where $\boldsymbol{w}_1$, $\boldsymbol{w}_2$, and $\boldsymbol{w}_3$ are external disturbances and r is the reference signal.

Note that the RB proposed in [127] described as

$$\Sigma_{\mathrm{R}} : \begin{bmatrix} \boldsymbol{y}_{\mathrm{r}} \\ \boldsymbol{u}_{\mathrm{r}} \end{bmatrix} = \begin{bmatrix} \boldsymbol{R}_1 & \boldsymbol{R}_2 \\ \boldsymbol{R}_3 & \boldsymbol{R}_4 \end{bmatrix} \begin{bmatrix} \boldsymbol{y} \\ \boldsymbol{u}_{\mathrm{c}} \end{bmatrix}, \tag{6.16}$$

is a particular DPB case obtained from (6.15) if one defines $\boldsymbol{A}_{\mathrm{r}} \triangleq \boldsymbol{0}_{n_{\mathrm{r}} \times n_{\mathrm{r}}}$, $\boldsymbol{B}_{\mathrm{r,y}} \triangleq \boldsymbol{0}_{n_{\mathrm{r}} \times p}$, $\boldsymbol{B}_{\mathrm{r,u}} \triangleq \boldsymbol{0}_{n_{\mathrm{r}} \times m}$, $\boldsymbol{C}_{\mathrm{r,y}} \triangleq \boldsymbol{0}_{p \times n_{\mathrm{r}}}$, $\boldsymbol{C}_{\mathrm{r,u}} \triangleq \boldsymbol{0}_{m \times n_{\mathrm{r}}}$, and $\boldsymbol{x}_{\mathrm{r}}(0) \triangleq \boldsymbol{0}_{n_{\mathrm{r}} \times 1}$.

Comparing (6.7) and (6.16), it is possible to note that M is a particular matrix for Σ_{R}, where $\boldsymbol{R}_1 = \boldsymbol{I}$, $\boldsymbol{R}_2 = -m_{\mathrm{f}}\boldsymbol{I}$, $\boldsymbol{R}_3 = m_{\mathrm{p}}\boldsymbol{I}$, and $\boldsymbol{R}_4 = (m_{\mathrm{s}} - m_{\mathrm{p}}m_{\mathrm{f}})\boldsymbol{I}$. Thus, the RB for passivation purpose is defined as a PB in this work.

Indeed, the PB proposed by [200] is employed in an adaptive control strategy for fault mitigation [201] that is similar to fault hiding. However, the conditions for tuning that kind of PB are too strict and nonconvex, making their design difficult. The PB

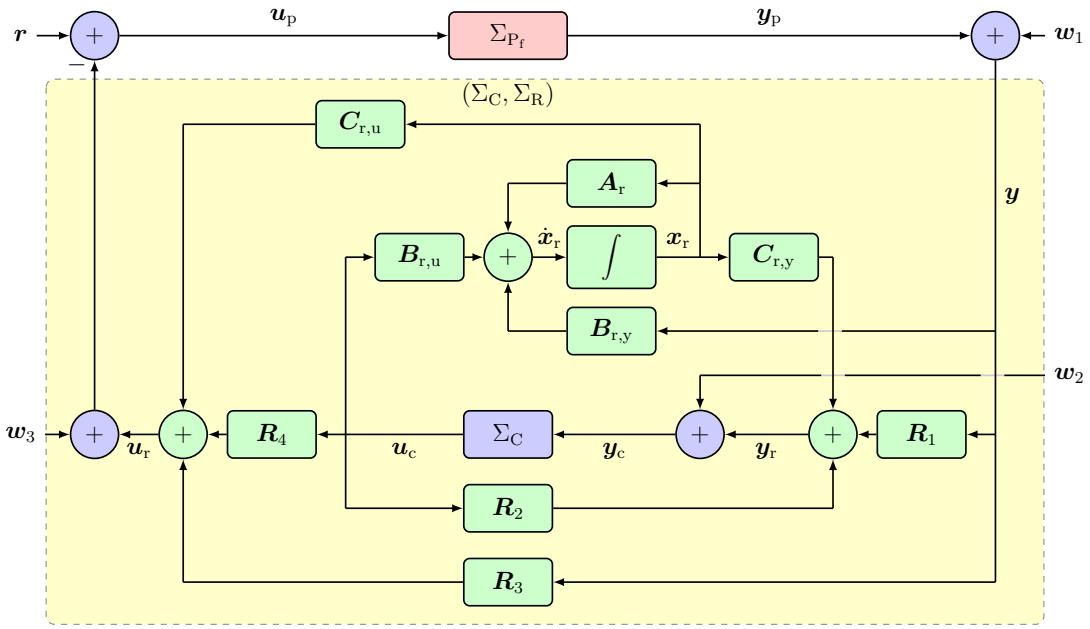

Figure 6.4 – Equivalent interconnection of $(\Sigma_{\mathrm{P_f}}, \Sigma_{\mathrm{R}}, \Sigma_{\mathrm{C}})$ expressed as controller passivation with DPB.

presented in this chapter can be easily obtained by solving a semi-definite programming problem, such that LMI-based conditions are provided. In our numerical simulations, the PB proposed in this thesis is compared to that proposed in [200].

The DPB described as (6.15) also generalizes the existing linear dynamic RBs found in the literature [18]. However, these RBs, namely VSs and VAs, are usually applicable only for linear and polytopic systems and are based on the internal model principle. To show that, consider for the plant the nominal model, given by Σ_{P}, and fault models, given by $\Sigma_{\mathrm{P_f}}$, described as follows

$$\Sigma_{\mathrm{P}} : \begin{cases} \dot{\boldsymbol{x}}(t) = \boldsymbol{A}\boldsymbol{x}(t) + \boldsymbol{B}\boldsymbol{u}_{\mathrm{p}}(t), \\ \boldsymbol{y}_{\mathrm{p}}(t) = \boldsymbol{C}\boldsymbol{x}(t), \end{cases} \tag{6.17}$$

$$\Sigma_{\mathrm{P_f}} : \begin{cases} \dot{\boldsymbol{x}}(t) = \boldsymbol{A}\boldsymbol{x}(t) + \boldsymbol{B}_{\mathrm{f}}\boldsymbol{u}_{\mathrm{p}}(t), \\ \boldsymbol{y}_{\mathrm{p}}(t) = \boldsymbol{C}_{\mathrm{f}}x(t). \end{cases} \tag{6.18}$$

A VS is usually described as follows [18]:

$$\Sigma_{\mathrm{R}} :: \begin{cases} \dot{\boldsymbol{x}}_{\mathrm{r}}(t) = (\boldsymbol{A} - \boldsymbol{L}\boldsymbol{C}_{\mathrm{f}})\boldsymbol{x}_{\mathrm{r}}(t) + \boldsymbol{L}\boldsymbol{y}(t) + \boldsymbol{B}_{\mathrm{f}}\boldsymbol{u}_{\mathrm{c}}(t), \\ \boldsymbol{y}_{\mathrm{r}}(t) = (\boldsymbol{C} - \boldsymbol{J}\boldsymbol{C}_{\mathrm{f}})\boldsymbol{x}_{\mathrm{r}}(t) + \boldsymbol{J}\boldsymbol{y}(t), \\ \boldsymbol{u}_{\mathrm{r}}(t) = \boldsymbol{u}_{\mathrm{c}}(t), \end{cases} \tag{6.19}$$

and it is designed to compensate sensor faults. Note that the VS described in (6.19) is a particular case of (6.15) taking $\boldsymbol{A}_{\mathrm{r}} \triangleq \boldsymbol{A}-\boldsymbol{L}\boldsymbol{C}$, $\boldsymbol{B}_{\mathrm{r,y}} \triangleq \boldsymbol{L}$, $\boldsymbol{B}_{\mathrm{r,u}} \triangleq \boldsymbol{B}_{\mathrm{f}}$, $\boldsymbol{C}_{\mathrm{r,y}} \triangleq \boldsymbol{C}-\boldsymbol{J}\boldsymbol{C}_{\mathrm{f}}$, $\boldsymbol{C}_{\mathrm{r,u}} \triangleq \boldsymbol{0}_{m\times n_{\mathrm{r}}}$, $\boldsymbol{R}_1 \triangleq \boldsymbol{I}_m$, $\boldsymbol{R}_2 \triangleq \boldsymbol{J}$, $\boldsymbol{R}_3 \triangleq \boldsymbol{0}_{m\times p}$, $\boldsymbol{R}_4 \triangleq \boldsymbol{I}_m$ and $\boldsymbol{x}_{\mathrm{r}}(0) \triangleq \boldsymbol{0}_{n_{\mathrm{r}}\times 1}$. On other hand, a VA is described as follows [18]:

$$\Sigma_{\mathrm{R}} : \begin{cases} \dot{\boldsymbol{x}}_{\mathrm{r}}(t) = (\boldsymbol{A} - \boldsymbol{B}_{\mathrm{f}}\boldsymbol{M})\boldsymbol{x}_{\mathrm{r}}(t) + (\boldsymbol{B} - \boldsymbol{B}_{\mathrm{f}}\boldsymbol{N})\boldsymbol{u}_{\mathrm{c}}(t), \\ \boldsymbol{y}_{\mathrm{r}}(t) = \boldsymbol{C}\boldsymbol{x}_{\mathrm{r}}(t) + \boldsymbol{y}(t), \\ \boldsymbol{u}_{\mathrm{r}}(t) = \boldsymbol{M}\boldsymbol{x}_{\mathrm{r}}(t) + \boldsymbol{N}\boldsymbol{u}_{\mathrm{c}}(t), \end{cases} \tag{6.20}$$

and is employed to compensate for actuator faults. The VA in (6.20) is also a particular case of the DPB in (6.15) if one defines $\boldsymbol{A}_{\mathrm{r}} \triangleq \boldsymbol{A} - \boldsymbol{B}_{\mathrm{f}}M$, $\boldsymbol{B}_{\mathrm{r,y}} \triangleq \boldsymbol{0}_{n_{\mathrm{r}}\times p}$, $\boldsymbol{B}_{\mathrm{r,u}} \triangleq \boldsymbol{B} - \boldsymbol{B}_{\mathrm{f}}$, $\boldsymbol{C}_{\mathrm{r,y}} \triangleq \boldsymbol{C}$, $\boldsymbol{C}_{\mathrm{r,u}} \triangleq \boldsymbol{M}$, $\boldsymbol{R}_1 \triangleq \boldsymbol{I}_m$, $\boldsymbol{R}_2 \triangleq \boldsymbol{0}_{p\times m}$, $\boldsymbol{R}_3 \triangleq \boldsymbol{0}_{m\times p}$, $\boldsymbol{R}_4 \triangleq \boldsymbol{N}$ and $\boldsymbol{x}_{\mathrm{r}}(0) \triangleq \boldsymbol{0}_{n_{\mathrm{r}}\times 1}$.

6.3 Dissipativity-based Asymptotic Stability Recovery by Fault Hiding

6.3.1 Stability Recovery with Dynamic Passivation Blocks

In this section, LMI-based conditions for computing the DPB are presented to ensure the asymptotic stability recovery by fault hiding. For this purpose, it is worth to obtain conditions for dissipativity analysis of DPB.

All the results described in this section deal with the reconfigured system $(\Sigma_{\mathrm{P_f}}, \Sigma_{\mathrm{R}}, \Sigma_{\mathrm{C}})$ interconnected as Fig. 6.4, under Assumptions 6.2 and 6.3 where $\Sigma_{\mathrm{P_f}}$, Σ_{C} and Σ_{R} are, respectively, described in (6.1), (6.14) and (6.15).

In particular, Lemma 6.4 provides conditions for Σ_{R} in (6.15) to be IF-OFP(ν_{r},ρ_{r}).

Lemma 6.4. *Σ_{R} is IF-OFP(ν_{r},ρ_{r}) if there exist a matrix $\boldsymbol{P} = \boldsymbol{P}^\top$, and scalars ν_{r} and ρ_{r} such that the following inequalities are satisfied:*

$$\boldsymbol{P} \succ 0 \qquad \boldsymbol{\Theta} \preceq 0 \tag{6.21}$$

with

$$\boldsymbol{\Theta} \triangleq \begin{bmatrix} \mathrm{He}\left\{\boldsymbol{P}\boldsymbol{A}_{\mathrm{r}}\right\} + \boldsymbol{W}_{11} & \boldsymbol{P}\boldsymbol{B}_{\mathrm{r,y}} - \frac{1}{2}\boldsymbol{C}_{\mathrm{r,y}}^{\top} + \boldsymbol{W}_{12} & \boldsymbol{P}\boldsymbol{B}_{\mathrm{r,u}} - \frac{1}{2}\boldsymbol{C}_{\mathrm{r,u}}^{\top} + \boldsymbol{W}_{13} \\ \star & \nu_{\mathrm{r}}\boldsymbol{I}_m - \frac{1}{2}\mathrm{He}\left\{\boldsymbol{R}_1\right\} + \boldsymbol{W}_{22} & -\frac{1}{2}\boldsymbol{R}_2 - \frac{1}{2}\boldsymbol{R}_3^{\top} + \boldsymbol{W}_{23} \\ \star & \star & \nu_{\mathrm{r}}\boldsymbol{I}_m - \frac{1}{2}\mathrm{He}\left\{\boldsymbol{R}_4\right\} + \boldsymbol{W}_{33} \end{bmatrix}$$

$$\boldsymbol{W}_{11} \triangleq \rho_{\mathrm{r}}\boldsymbol{C}_{\mathrm{r,y}}^{\top}\boldsymbol{C}_{\mathrm{r,y}} + \rho_{\mathrm{r}}\boldsymbol{C}_{\mathrm{r,u}}^{\top}\boldsymbol{C}_{\mathrm{r,u}}, \tag{6.22}$$

$$\boldsymbol{W}_{12} \triangleq \rho_{\mathrm{r}}\boldsymbol{C}_{\mathrm{r,y}}^{\top}\boldsymbol{R}_1 + \rho_{\mathrm{r}}\boldsymbol{C}_{\mathrm{r,u}}^{\top}\boldsymbol{R}_3, \tag{6.23}$$

$$\boldsymbol{W}_{13} \triangleq \rho_{\mathrm{r}}\boldsymbol{C}_{\mathrm{r,y}}^{\top}\boldsymbol{R}_2 + \rho_{\mathrm{r}}\boldsymbol{C}_{\mathrm{r,u}}^{\top}\boldsymbol{R}_4, \tag{6.24}$$

$$\boldsymbol{W}_{22} \triangleq \rho_{\mathrm{r}}\boldsymbol{R}_1^{\top}\boldsymbol{R}_1 + \rho_{\mathrm{r}}\boldsymbol{R}_3^{\top}\boldsymbol{R}_3, \tag{6.25}$$

$$\boldsymbol{W}_{23} \triangleq \rho_{\mathrm{r}}\boldsymbol{R}_1^{\top}\boldsymbol{R}_2 + \rho_{\mathrm{r}}\boldsymbol{R}_3^{\top}\boldsymbol{R}_4, \tag{6.26}$$

$$\boldsymbol{W}_{33} \triangleq \rho_{\mathrm{r}}\boldsymbol{R}_2^{\top}\boldsymbol{R}_2 + \rho_{\mathrm{r}}\boldsymbol{R}_4^{\top}\boldsymbol{R}_4. \tag{6.27}$$

Proof. The DPB depicted in Fig. 6.4 and described in (6.15) is represented by using, respectively, augmented input and output vectors: $\bar{\boldsymbol{u}}_{\mathrm{r}}(t) \triangleq \left[\boldsymbol{y}(t)^{\top}\ \boldsymbol{u}_{\mathrm{c}}(t)^{\top}\right]^{\top}$ and $\bar{\boldsymbol{y}}_{\mathrm{r}}(t) \triangleq \left[\boldsymbol{y}_{\mathrm{r}}(t)^{\top}\ \boldsymbol{u}_{\mathrm{r}}(t)^{\top}\right]^{\top}$. Defining $V_{\mathrm{r}}\left(\boldsymbol{x}_{\mathrm{r}}(t)\right) = \boldsymbol{x}_{\mathrm{r}}(t)^{\top}\boldsymbol{P}\boldsymbol{x}_{\mathrm{r}}(t)$ as a storage function, its time derivative is computed as

$$\dot{V}\left(\boldsymbol{x}_{\mathrm{r}}(t)\right) = \mathrm{He}\left\{\boldsymbol{x}_{\mathrm{r}}^{\top}\boldsymbol{P}\boldsymbol{A}_{\mathrm{r}}\boldsymbol{x}_{\mathrm{r}} + \boldsymbol{x}_{\mathrm{r}}^{\top}\boldsymbol{P}\boldsymbol{B}_{\mathrm{r,y}}\boldsymbol{y} + \boldsymbol{x}_{\mathrm{r}}^{\top}\boldsymbol{P}\boldsymbol{B}_{\mathrm{r,u}}\boldsymbol{u}_{\mathrm{c}}\right\}. \tag{6.28}$$

Consider the following supply function for Σ_{R}

$$\left(\bar{\boldsymbol{u}}_{\mathrm{r}}(t), \bar{\boldsymbol{y}}_{\mathrm{r}}(t)\right) = \bar{\boldsymbol{u}}_{\mathrm{r}}^{\top}\bar{\boldsymbol{y}}_{\mathrm{r}} - \nu_{\mathrm{r}}\bar{\boldsymbol{u}}_{\mathrm{r}}^{\top}\bar{\boldsymbol{u}}_{\mathrm{r}} - \rho_{\mathrm{r}}\bar{\boldsymbol{y}}_{\mathrm{r}}^{\top}\bar{\boldsymbol{y}}_{\mathrm{r}}. \tag{6.29}$$

Taking into account that $\boldsymbol{y}_{\mathrm{r}}(t) = \boldsymbol{C}_{\mathrm{r,y}}\boldsymbol{x}_{\mathrm{r}}(t) + \boldsymbol{R}_1\boldsymbol{y}(t) + \boldsymbol{R}_2\boldsymbol{u}_{\mathrm{c}}(t)$ and $\boldsymbol{u}_{\mathrm{r}}(t) = \boldsymbol{C}_{\mathrm{r,u}}\boldsymbol{x}_{\mathrm{r}}(t) + \boldsymbol{R}_3\boldsymbol{y}(t) + \boldsymbol{R}_4\boldsymbol{u}_{\mathrm{c}}(t)$, (6.29) results in

$$\begin{aligned} \left(\bar{\boldsymbol{u}}_{\mathrm{r}}, \bar{\boldsymbol{y}}_{\mathrm{r}}\right) = &- \boldsymbol{x}_{\mathrm{r}}^{\top}\boldsymbol{W}_{11}\boldsymbol{x}_{\mathrm{r}} - \boldsymbol{y}^{\top}\left(-\boldsymbol{R}_1 + \boldsymbol{W}_{22}\right)\boldsymbol{y} - \nu_{\mathrm{r}}\boldsymbol{y}^{\top}\boldsymbol{y} - \boldsymbol{u}_{\mathrm{c}}^{\top}\left(-\boldsymbol{R}_4 + \boldsymbol{W}_{33}\right)\boldsymbol{u}_{\mathrm{c}} \\ &- \nu_{\mathrm{r}}\boldsymbol{u}_{\mathrm{c}}^{\top}\boldsymbol{u}_{\mathrm{c}} + \boldsymbol{y}^{\top}\boldsymbol{C}_{\mathrm{r,y}}\boldsymbol{x}_{\mathrm{r}} - \mathrm{He}\left\{\boldsymbol{x}_{\mathrm{r}}^{\top}\boldsymbol{W}_{12}\boldsymbol{y} + \boldsymbol{x}_{\mathrm{r}}^{\top}\boldsymbol{W}_{13}\boldsymbol{u}_{\mathrm{c}} + \boldsymbol{y}^{\top}\boldsymbol{W}_{23}\boldsymbol{u}_{\mathrm{c}}\right\} \\ &+ \boldsymbol{u}_{\mathrm{c}}^{\top}\boldsymbol{C}_{\mathrm{r,u}}\boldsymbol{x}_{\mathrm{r}} + \boldsymbol{y}^{\top}\boldsymbol{R}_2\boldsymbol{u}_{\mathrm{c}} + \boldsymbol{u}_{\mathrm{c}}^{\top}\boldsymbol{R}_3\boldsymbol{y}. \end{aligned} \tag{6.30}$$

where $\boldsymbol{W}_{ij}$ are defined by (6.22)–(6.27). Based on the identity $\boldsymbol{x}^{\top}\boldsymbol{W}\boldsymbol{y} = \frac{1}{2}\mathrm{He}\left\{\boldsymbol{x}^{\top}\boldsymbol{W}\boldsymbol{y}\right\}$, (6.30) is equivalent to

$$\begin{aligned} \left(\bar{\boldsymbol{u}}_{\mathrm{r}}, \bar{\boldsymbol{y}}_{\mathrm{r}}\right) = &- \boldsymbol{y}^{\top}\left(\nu_{\mathrm{r}}\boldsymbol{I}_m - \tfrac{1}{2}\mathrm{He}\left\{\boldsymbol{R}_1\right\} + \boldsymbol{W}_{22}\right)\boldsymbol{y} - \boldsymbol{u}_{\mathrm{c}}^{\top}\left(\nu_{\mathrm{r}}\boldsymbol{I}_m - \tfrac{1}{2}\mathrm{He}\left\{\boldsymbol{R}_4\right\} + \boldsymbol{W}_{33}\right)\boldsymbol{u}_{\mathrm{c}} \\ &- \boldsymbol{x}_{\mathrm{r}}^{\top}\boldsymbol{W}_{11}\boldsymbol{x}_{\mathrm{r}} - \mathrm{He}\left\{\boldsymbol{x}_{\mathrm{r}}^{\top}\left(-\tfrac{1}{2}\boldsymbol{C}_{\mathrm{r,y}}^{\top} + \boldsymbol{W}_{12}\right)\boldsymbol{y} + \boldsymbol{x}_{\mathrm{r}}^{\top}\left(-\tfrac{1}{2}\boldsymbol{C}_{\mathrm{r,u}}^{\top} + \boldsymbol{W}_{13}\right)\boldsymbol{u}_{\mathrm{c}}\right\} \\ &+ \mathrm{He}\left\{\boldsymbol{y}^{\top}\left(\boldsymbol{R}_2 + \boldsymbol{R}_3^{\top} + \boldsymbol{W}_{23}\right)\boldsymbol{u}_{\mathrm{c}}\right\}. \end{aligned} \tag{6.31}$$

Σ_{R} is dissipative with respect to (6.31) if $\dot{V}\left(\boldsymbol{x}_{\mathrm{r}}(t)\right) - (\bar{\boldsymbol{u}}_{\mathrm{r}}, \bar{\boldsymbol{y}}_{\mathrm{r}}) \leq 0$ or, equivalently, subtracting (6.31) from (6.28) one obtains:

$$\bar{\boldsymbol{x}}_{\mathrm{r}}^{\top} \Theta \bar{\boldsymbol{x}}_{\mathrm{r}} \leq 0 \tag{6.32}$$

with $\bar{\boldsymbol{x}}_{\mathrm{r}} = \left[\boldsymbol{x}_{\mathrm{r}}(t)^{\top}\ \boldsymbol{y}(t)^{\top}\ \boldsymbol{u}_{\mathrm{c}}(t)^{\top}\right]^{\top}$. If (6.21) is satisfied for some ν_{r} and ρ_{r}, then (6.32) is satisfied and Σ_{R} is IF-OFP(ν_{r}, ρ_{r}) according to Definition 6.1. □

The next Lemma presents sufficient conditions for ensuring that the reconfigured system $(\Sigma_{\mathrm{P_f}}, \Sigma_{\mathrm{R}}, \Sigma_{\mathrm{C}})$ is a $(\boldsymbol{Q}, \boldsymbol{S}, \boldsymbol{R})$-dissipative system.

Lemma 6.5. *If $\Sigma_{\mathrm{P_f}}$, Σ_{C}, and Σ_{R} are, respectively, IF-OFP(ν_{f},ρ_{f}), IF-OFP(ν_{c},ρ_{c}), and IF-OFP(ν_{r},ρ_{r}), then the reconfigured system $(\Sigma_{\mathrm{P_f}}, \Sigma_{\mathrm{R}}, \Sigma_{\mathrm{C}})$ is $(\boldsymbol{Q}, \boldsymbol{S}, \boldsymbol{R})$-dissipative with:*

$$\boldsymbol{Q} = \begin{bmatrix} -\left(\rho_{\mathrm{f}} + \nu_{\mathrm{r}}\right)\boldsymbol{I}_m & \boldsymbol{0}_{m\times m} & \frac{1}{2}\boldsymbol{I}_m & \boldsymbol{0}_{m\times m} \\ \star & -\left(\rho_{\mathrm{c}} + \nu_{\mathrm{r}}\right)\boldsymbol{I}_m & \frac{1}{2}\boldsymbol{I}_m & \frac{1}{2}\boldsymbol{I}_m \\ \star & \star & -\left(\nu_{\mathrm{c}} + \rho_{\mathrm{r}}\right)\boldsymbol{I}_m & \boldsymbol{0}_{m\times m} \\ \star & \star & \star & -\left(\nu_{\mathrm{f}} + \rho_{\mathrm{r}}\right)\boldsymbol{I}_m \end{bmatrix}, \tag{6.33}$$

$$\boldsymbol{S} = \begin{bmatrix} \frac{1}{2}\boldsymbol{I}_m & \boldsymbol{0}_{m\times m} & \boldsymbol{0}_{m\times m} & \nu_{\mathrm{f}}\boldsymbol{I}_m \\ -\nu_{\mathrm{r}}\boldsymbol{I}_m & \boldsymbol{0}_{m\times m} & \frac{1}{2}\boldsymbol{I}_m & \boldsymbol{0}_{m\times m} \\ \boldsymbol{0}_{m\times m} & \frac{1}{2}\boldsymbol{I}_m & -\nu_{\mathrm{c}}\boldsymbol{I}_m & \boldsymbol{0}_{m\times m} \\ -\boldsymbol{I}_m & \boldsymbol{0}_{m\times m} & \boldsymbol{0}_{m\times m} & -\nu_{\mathrm{f}}\boldsymbol{I}_m \end{bmatrix}, \tag{6.34}$$

$$\boldsymbol{R} = \begin{bmatrix} -\nu_{\mathrm{f}}\boldsymbol{I}_m & \boldsymbol{0}_{m\times m} & \boldsymbol{0}_{m\times m} & \nu_{\mathrm{f}}\boldsymbol{I}_m \\ \boldsymbol{0}_{m\times m} & -\nu_{\mathrm{r}}\boldsymbol{I}_m & \boldsymbol{0}_{m\times m} & \boldsymbol{0}_{m\times m} \\ \boldsymbol{0}_{m\times m} & \boldsymbol{0}_{m\times m} & -\nu_{\mathrm{c}}\boldsymbol{I}_m & \boldsymbol{0}_{m\times m} \\ \nu_{\mathrm{f}}\boldsymbol{I}_m & \boldsymbol{0}_{m\times m} & \boldsymbol{0}_{m\times m} & -\nu_{\mathrm{f}}\boldsymbol{I}_m \end{bmatrix}. \tag{6.35}$$

Proof. Define

$$\boldsymbol{X}_1 \triangleq \begin{bmatrix} \boldsymbol{I}_m & \boldsymbol{0}_{m\times m} & \boldsymbol{0}_{m\times m} & -\boldsymbol{I}_m \end{bmatrix}, \boldsymbol{X}_2 \triangleq \begin{bmatrix} \boldsymbol{0}_{m\times m} & \boldsymbol{0}_{m\times m} & \boldsymbol{0}_{m\times m} & \boldsymbol{I}_m \end{bmatrix},$$
$$\boldsymbol{X}_3 \triangleq \begin{bmatrix} \boldsymbol{I}_m & \boldsymbol{0}_{m\times m} & \boldsymbol{0}_{m\times m} & \boldsymbol{0}_{m\times m} \end{bmatrix}, \boldsymbol{X}_4 \triangleq \begin{bmatrix} \boldsymbol{0}_{m\times m} & \boldsymbol{I}_m & \boldsymbol{0}_{m\times m} & \boldsymbol{0}_{m\times m} \end{bmatrix},$$
$$\boldsymbol{X}_5 \triangleq \begin{bmatrix} \boldsymbol{0}_{m\times m} & \boldsymbol{0}_{m\times m} & \boldsymbol{I}_m & \boldsymbol{0}_{m\times m} \end{bmatrix}, \bar{w}^{\top} \triangleq \begin{bmatrix} \boldsymbol{r}(t)^{\top} & \boldsymbol{w}_1(t)^{\top} & \boldsymbol{w}_2(t)^{\top} & \boldsymbol{w}_3(t)^{\top} \end{bmatrix},$$
$$\bar{\boldsymbol{y}} \triangleq \begin{bmatrix} \boldsymbol{y}_{\mathrm{p}}(t)^{\top} & \boldsymbol{u}_{\mathrm{c}}(t)^{\top} & \boldsymbol{y}_{\mathrm{r}}(t)^{\top} & \boldsymbol{u}_{\mathrm{r}}(t)^{\top} \end{bmatrix}^{\top}.$$

Considering the equivalent loop in Fig. 6.4, the inputs and outputs of $\Sigma_{\mathrm{P_f}}$, Σ_{C}, and Σ_{R} can be expressed as follows

$$\boldsymbol{u}(t) = \boldsymbol{r}(t) - \boldsymbol{w}_3(t) - \boldsymbol{u}_{\mathrm{r}}(t) = \boldsymbol{X}_1\bar{w} - \boldsymbol{X}_2\bar{\boldsymbol{y}}, \tag{6.36}$$

$$\boldsymbol{y}_{\mathrm{p}}(t) = \boldsymbol{X}_3\bar{\boldsymbol{y}}, \;\; \boldsymbol{u}_{\mathrm{r}}(t) = \boldsymbol{X}_2\bar{\boldsymbol{y}}, \;\; \boldsymbol{y}_{\mathrm{r}}(t) = \boldsymbol{X}_5\bar{\boldsymbol{y}}, \tag{6.37}$$

$$\boldsymbol{y}(t) = \boldsymbol{y}_{\mathrm{p}}(t) + \boldsymbol{w}_1(t) = \boldsymbol{X}_4\bar{\boldsymbol{w}} + \boldsymbol{X}_3\bar{\boldsymbol{y}}, \tag{6.38}$$

$$\boldsymbol{u}_{\mathrm{c}}(t) = \boldsymbol{X}_4\bar{\boldsymbol{y}}, \boldsymbol{y}_{\mathrm{c}}(t) = \boldsymbol{y}_{\mathrm{r}}(t) + \boldsymbol{w}_2(t) = \boldsymbol{X}_5\left(\bar{\boldsymbol{w}} + \bar{\boldsymbol{y}}\right). \tag{6.39}$$

Assuming that $\Sigma_{\mathrm{P_f}}$ is IF-OFP(ν_{f},ρ_{f}), the following inequality holds according to Definition 6.1:

$$\dot{V}_{\mathrm{f}}(\boldsymbol{x}) \leq \boldsymbol{u}_{\mathrm{p}}^{\top}\boldsymbol{y}_{\mathrm{p}} - \nu_{\mathrm{f}}\boldsymbol{u}_{\mathrm{p}}^{\top}\boldsymbol{u}_{\mathrm{p}} - \rho_{\mathrm{f}}\boldsymbol{y}_{\mathrm{p}}^{\top}\boldsymbol{y}_{\mathrm{p}}, \tag{6.40}$$

where V_{f} is a valid storage function for $\Sigma_{\mathrm{P_f}}$. Substituting (6.36) and (6.37) into (6.40), it follows that:

$$\dot{V}_{\mathrm{f}}(\boldsymbol{x}) \leq \bar{\boldsymbol{y}}^{\top}\bar{\boldsymbol{Q}}_{\mathrm{f}}\bar{\boldsymbol{y}} + 2\bar{\boldsymbol{w}}^{\top}\bar{\boldsymbol{S}}_{\mathrm{f}}\bar{\boldsymbol{y}} + \bar{\boldsymbol{w}}^{\top}\bar{\boldsymbol{R}}_{\mathrm{f}}\bar{\boldsymbol{w}}, \tag{6.41}$$

$$\bar{\boldsymbol{Q}}_{\mathrm{f}} = -\nu_{\mathrm{f}}\boldsymbol{X}_2^{\top}\boldsymbol{X}_2 - \rho_{\mathrm{f}}\boldsymbol{X}_3^{\top}\boldsymbol{X}_3, \tag{6.42}$$

$$\boldsymbol{S}_{\mathrm{f}} = \frac{1}{2}\boldsymbol{X}_1^{\top}\boldsymbol{X}_3 - \frac{1}{2}\boldsymbol{X}_2^{\top}\boldsymbol{X}_3 + \nu_{\mathrm{f}}\boldsymbol{X}_1^{\top}\boldsymbol{X}_2, \tag{6.43}$$

$$\bar{\boldsymbol{R}}_{\mathrm{f}} = -\nu_{\mathrm{f}}\boldsymbol{X}_1^{\top}\boldsymbol{X}_1. \tag{6.44}$$

Moreover, given that Σ_{C} is IF-OFP(ν_{c},ρ_{c}), then

$$\dot{V}_{\mathrm{c}}(\boldsymbol{x}_{\mathrm{c}}) \leq \boldsymbol{u}_{\mathrm{c}}^{\top}\boldsymbol{y}_{\mathrm{c}} - \nu_{\mathrm{c}}\boldsymbol{y}_{\mathrm{c}}^{\top}\boldsymbol{y}_{\mathrm{c}} - \rho_{\mathrm{c}}\boldsymbol{u}_{\mathrm{c}}^{\top}\boldsymbol{u}_{\mathrm{c}}, \tag{6.45}$$

where V_{c} is a valid storage function for Σ_{C}. Substituting (6.37) and (6.39) into (6.45), it follows that:

$$\dot{V}_{\mathrm{c}}(\boldsymbol{x}_{\mathrm{c}}) \leq \bar{\boldsymbol{y}}^{\top}\bar{\boldsymbol{Q}}_{\mathrm{c}}\bar{\boldsymbol{y}} + 2\bar{\boldsymbol{w}}^{\top}\bar{\boldsymbol{S}}_{\mathrm{c}}\bar{\boldsymbol{y}} + \bar{\boldsymbol{w}}^{\top}\bar{\boldsymbol{R}}_{\mathrm{c}}\bar{\boldsymbol{w}}, \tag{6.46}$$

$$\bar{\boldsymbol{Q}}_{\mathrm{c}} = \boldsymbol{X}_5^{\top}\boldsymbol{X}_4 - \nu_{\mathrm{c}}\boldsymbol{X}_5^{\top}\boldsymbol{X}_5 - \rho_{\mathrm{c}}\boldsymbol{X}_4^{\top}\boldsymbol{X}_4, \tag{6.47}$$

$$\bar{\boldsymbol{Q}}_{\mathrm{c}} = \boldsymbol{X}_5^{\top}\boldsymbol{X}_4 - \nu_{\mathrm{c}}\boldsymbol{X}_5^{\top}\boldsymbol{X}_5 - \rho_{\mathrm{c}}\boldsymbol{X}_4^{\top}\boldsymbol{X}_4, \tag{6.48}$$

$$\bar{\boldsymbol{R}}_{\mathrm{c}} = -\nu_{\mathrm{c}}\boldsymbol{X}_5^{\top}\boldsymbol{X}_5. \tag{6.49}$$

Similarly, assuming that Σ_{R} is IF-OFP(ν_{r},ρ_{r}) and

$$\bar{\boldsymbol{w}}_{\mathrm{r}} \triangleq \begin{bmatrix} \boldsymbol{y} \\ \boldsymbol{u}_{\mathrm{c}} \end{bmatrix} = \begin{bmatrix} \boldsymbol{X}_4 \\ \boldsymbol{0}_{m\times 4m} \end{bmatrix}\bar{\boldsymbol{w}} + \begin{bmatrix} \boldsymbol{X}_3 \\ \boldsymbol{X}_4 \end{bmatrix}\bar{\boldsymbol{y}}, \tag{6.50}$$

$$\bar{\boldsymbol{y}}_{\mathrm{r}} \triangleq \begin{bmatrix} \boldsymbol{y}_{\mathrm{r}} \\ \boldsymbol{u}_{\mathrm{r}} \end{bmatrix} = \begin{bmatrix} \boldsymbol{X}_5 \\ \boldsymbol{X}_2 \end{bmatrix}\bar{\boldsymbol{y}}, \tag{6.51}$$

it follows that

$$\dot{V}_{\mathrm{r}}(\boldsymbol{x}_{\mathrm{r}}) \leq \bar{\boldsymbol{w}}_{\mathrm{r}}^{\top}\bar{\boldsymbol{y}}_{\mathrm{r}} - \nu_{\mathrm{r}}\bar{\boldsymbol{u}}_{\mathrm{r}}^{\top}\bar{\boldsymbol{u}}_{\mathrm{r}} - \rho_{\mathrm{r}}\bar{\boldsymbol{y}}_{\mathrm{r}}^{\top}\bar{\boldsymbol{y}}_{\mathrm{r}}, \tag{6.52}$$

where V_{r} is a valid storage function for Σ_{R}. Substituting (6.50) and (6.51) into (6.52), it is equivalent to

$$\begin{aligned}
\dot{V}_{\mathrm{r}}(\boldsymbol{x}_{\mathrm{r}}) \leq & \bar{\boldsymbol{y}}^{\top}\bar{\boldsymbol{Q}}_{\mathrm{r}}\bar{\boldsymbol{y}} + 2\bar{\boldsymbol{w}}^{\top}\bar{\boldsymbol{S}}_{\mathrm{r}}\bar{\boldsymbol{y}} + \bar{\boldsymbol{w}}^{\top}\bar{\boldsymbol{R}}_{\mathrm{r}}\bar{\boldsymbol{w}}, & (6.53)\\
\bar{\boldsymbol{Q}}_{\mathrm{r}} = & \boldsymbol{X}_3^{\top}\boldsymbol{X}_5 + \boldsymbol{X}_4^{\top}\boldsymbol{X}_2 - \nu_{\mathrm{r}}\left(\boldsymbol{X}_3^{\top}\boldsymbol{X}_3 + \boldsymbol{X}_4^{\top}\boldsymbol{X}_4\right) \\
& - \rho_{\mathrm{r}}\left(\boldsymbol{X}_5^{\top}\boldsymbol{X}_5 + \boldsymbol{X}_2^{\top}\boldsymbol{X}_2\right), & (6.54)\\
\bar{\boldsymbol{S}}_{\mathrm{r}} = & \frac{1}{2}\boldsymbol{X}_4^{\top}\boldsymbol{X}_5 - \nu_{\mathrm{r}}\boldsymbol{X}_4^{\top}\boldsymbol{X}_3, & (6.55)\\
\bar{\boldsymbol{R}}_{\mathrm{r}} = & -\nu_{\mathrm{r}}\boldsymbol{X}_4^{\top}\boldsymbol{X}_4. & (6.56)
\end{aligned}$$

Thus, adopting the storage function $\bar{V}(\boldsymbol{x}, \boldsymbol{x}_{\mathrm{r}}, \boldsymbol{x}_{\mathrm{c}}) \triangleq \dot{V}_{\mathrm{f}}(\boldsymbol{x}) + \dot{V}_{\mathrm{r}}(\boldsymbol{x}_{\mathrm{r}}) + \dot{V}_{\mathrm{c}}(\boldsymbol{x}_{\mathrm{c}})$ for the reconfigured system $(\Sigma_{\mathrm{P_f}}, \Sigma_{\mathrm{R}}, \Sigma_{\mathrm{C}})$, the following inequality can be obtained by summing the inequalities (6.41), (6.46) and (6.53)

$$\bar{V}(\boldsymbol{x}, \boldsymbol{x}_{\mathrm{r}}, \boldsymbol{x}_{\mathrm{c}}) \leq \bar{\boldsymbol{y}}^{\top}\left(\bar{\boldsymbol{Q}}_{\mathrm{f}} + \bar{\boldsymbol{Q}}_{\mathrm{r}} + \bar{\boldsymbol{Q}}_{\mathrm{c}}\right)\bar{\boldsymbol{y}} + 2\bar{\boldsymbol{w}}^{\top}\left(\bar{\boldsymbol{S}}_{\mathrm{f}} + \bar{\boldsymbol{S}}_{\mathrm{r}} + \bar{\boldsymbol{S}}_{\mathrm{c}}\right)\bar{\boldsymbol{y}} + \bar{\boldsymbol{w}}^{\top}\left(\bar{\boldsymbol{R}}_{\mathrm{f}} + \bar{\boldsymbol{R}}_{\mathrm{r}} + \bar{\boldsymbol{R}}_{\mathrm{c}}\right)\bar{\boldsymbol{w}}.$$

It is straightforwardly obtained that $\boldsymbol{S} = \bar{\boldsymbol{S}}_{\mathrm{f}} + \bar{\boldsymbol{S}}_{\mathrm{r}} + \bar{\boldsymbol{S}}_{\mathrm{c}}$ and $\boldsymbol{R} = \bar{\boldsymbol{R}}_{\mathrm{f}} + \bar{\boldsymbol{R}}_{\mathrm{r}} + \bar{\boldsymbol{R}}_{\mathrm{c}}$ are, respectively, equivalent to (6.34) and (6.35). In addition,

$$\bar{\boldsymbol{Q}}_{\mathrm{f}} + \bar{\boldsymbol{Q}}_{\mathrm{r}} + \bar{\boldsymbol{Q}}_{\mathrm{c}} = \boldsymbol{X}^{\top}\boldsymbol{\Gamma}\boldsymbol{X} \tag{6.57}$$

where $\boldsymbol{X} \triangleq \begin{bmatrix} \boldsymbol{X}_3^{\top} & \boldsymbol{X}_4^{\top} & \boldsymbol{X}_5^{\top} & \boldsymbol{X}_2^{\top} \end{bmatrix}^{\top}$ and

$$\boldsymbol{\Gamma} \triangleq \begin{bmatrix} -\left(\rho_{\mathrm{f}} + \nu_{\mathrm{r}}\right)\boldsymbol{I}_m & \boldsymbol{0}_{m\times m} & \frac{1}{2}\boldsymbol{I}_m & \boldsymbol{0}_{m\times m} \\ \star & -\left(\rho_{\mathrm{c}} + \nu_{\mathrm{r}}\right)\boldsymbol{I}_m & \frac{1}{2}\boldsymbol{I}_m & \frac{1}{2}\boldsymbol{I}_m \\ \star & \star & -\left(\nu_{\mathrm{c}} + \rho_{\mathrm{r}}\right)\boldsymbol{I}_m & \boldsymbol{0}_{m\times m} \\ \star & \star & \star & -\left(\nu_{\mathrm{f}} + \rho_{\mathrm{r}}\right)\boldsymbol{I}_m \end{bmatrix}.$$

Note that since X is an identity matrix then (6.57) is equivalent to $\boldsymbol{Q} = \bar{\boldsymbol{Q}}_{\mathrm{f}} + \bar{\boldsymbol{Q}}_{\mathrm{r}} + \bar{\boldsymbol{Q}}_{\mathrm{c}}$ which results in (6.33). Therefore, $(\Sigma_{\mathrm{P_f}}, \Sigma_{\mathrm{R}}, \Sigma_{\mathrm{C}})$ is $(\boldsymbol{Q}, \boldsymbol{S}, \boldsymbol{R})$-dissipative with $\boldsymbol{Q}$, $\boldsymbol{S}$ and $\boldsymbol{R}$ defined by (6.33)–(6.35), respectively. □

Based on Lemma 6.5, the next Theorem provides sufficient conditions to ensure the stabilization of faulty systems by means of DPB and based on passivity indices.

Theorem 6.1. *Assume that $\Sigma_{\mathrm{P_f}}$ is IF-OFP(ν_{f}, ρ_{f}) and Σ_{C} is IF-OFP(ν_{c},ρ_{c}) for given ν_{f}, ρ_{f}, ν_{c}, and ρ_{c}. The origin of reconfigured system $(\Sigma_{\mathrm{P_f}}, \Sigma_{\mathrm{R}}, \Sigma_{\mathrm{C}})$ is asymptotically stable if there exist scalars γ_1, γ_2, γ_3, γ_4, ν_{r} and μ_{r}, and matrices $\boldsymbol{P} = \boldsymbol{P}^\top$, $\boldsymbol{Z}_1$, $\boldsymbol{Z}_2$, $\boldsymbol{Z}_3$, $\boldsymbol{C}_{\mathrm{r,y}}$, $\boldsymbol{C}_{\mathrm{r,u}}$, $\boldsymbol{R}_1$, $\boldsymbol{R}_2$, $\boldsymbol{R}_3$ and $\boldsymbol{R}_4$ that satisfy the following inequalities:*

$$\begin{aligned} &\boldsymbol{P} \succ 0, \\ &\gamma_1^{-1} \leq \nu_{\mathrm{f}}^{-1}, \quad \gamma_2^{-1} \leq \nu_{\mathrm{c}}^{-1}, \quad \gamma_3 \leq \rho_{\mathrm{f}}, \quad \gamma_4 \leq \rho_{\mathrm{c}}, \end{aligned} \tag{6.58}$$

$$\begin{bmatrix} -\mu_{\mathrm{r}}\boldsymbol{I}_m & \boldsymbol{0}_{m\times m} & \boldsymbol{C}_{\mathrm{r,y}} & \boldsymbol{R}_1 & \boldsymbol{R}_2 \\ \star & -\mu_{\mathrm{r}}\boldsymbol{I}_m & \boldsymbol{C}_{\mathrm{r,u}} & \boldsymbol{R}_3 & \boldsymbol{R}_4 \\ \star & \star & \mathrm{He}\left\{\boldsymbol{P}+\boldsymbol{Z}_1\right\} & \boldsymbol{Z}_2 - \frac{1}{2}\boldsymbol{C}_{\mathrm{r,y}}^\top & \boldsymbol{Z}_3 - \frac{1}{2}\boldsymbol{C}_{\mathrm{r,u}}^\top \\ \star & \star & \star & \nu_{\mathrm{r}}\boldsymbol{I}_m - \frac{1}{2}\mathrm{He}\left\{\boldsymbol{R}_1\right\} & -\frac{1}{2}\boldsymbol{R}_2 - \frac{1}{2}\boldsymbol{R}_3^\top \\ \star & \star & \star & \star & \nu_{\mathrm{r}}\boldsymbol{I}_m - \frac{1}{2}\mathrm{He}\left\{\boldsymbol{R}_4\right\} \end{bmatrix} \prec 0, \tag{6.59}$$

$$\begin{bmatrix} -(\gamma_3+\nu_{\mathrm{r}}) & 0 & \frac{1}{2}\mu_{\mathrm{r}} & 0 & 0 & 0 \\ \star & -(\gamma_4+\nu_{\mathrm{r}}) & \frac{1}{2}\mu_{\mathrm{r}} & \frac{1}{2}\mu_{\mathrm{r}} & 0 & 0 \\ \star & \star & -\mu_{\mathrm{r}} & 0 & -\mu_{\mathrm{r}} & 0 \\ \star & \star & \star & -\mu_{\mathrm{r}} & 0 & \mu_{\mathrm{r}} \\ \star & \star & \star & \star & \gamma_1 & 0 \\ \star & \star & \star & \star & \star & \gamma_2 \end{bmatrix} \prec 0. \tag{6.60}$$

In this case, the gains $\boldsymbol{A}_{\mathrm{r}}$, $\boldsymbol{B}_{\mathrm{r,y}}$, and $\boldsymbol{B}_{\mathrm{r,u}}$ of (6.15) *are given by $\boldsymbol{A}_{\mathrm{r}} = \boldsymbol{I}_n + \boldsymbol{P}^{-1}\boldsymbol{Z}_1$, $\boldsymbol{B}_{\mathrm{r,y}} = \boldsymbol{P}^{-1}\boldsymbol{Z}_2$, and $\boldsymbol{B}_{\mathrm{r,u}} = \boldsymbol{P}^{-1}\boldsymbol{Z}_3$.*

Proof. Using a Schur's complement argument, for $\mu_{\mathrm{r}} > 0$ given, if (6.59) is satisfied then

$$\begin{bmatrix} \mathrm{He}\left\{\boldsymbol{P}+\boldsymbol{Z}_1\right\} & \boldsymbol{Z}_2 - \frac{1}{2}\boldsymbol{C}_{\mathrm{r,y}}^\top & \boldsymbol{Z}_3 - \frac{1}{2}\boldsymbol{C}_{\mathrm{r,u}}^\top \\ \star & \nu_{\mathrm{r}}\boldsymbol{I}_m - \frac{1}{2}\mathrm{He}\left\{\boldsymbol{R}_1\right\} & -\frac{1}{2}\boldsymbol{R}_2 - \frac{1}{2}\boldsymbol{R}_3^\top \\ \star & \star & \nu_{\mathrm{r}}\boldsymbol{I}_m - \frac{1}{2}\mathrm{He}\left\{\boldsymbol{R}_4\right\} \end{bmatrix} + \mu_{\mathrm{r}}^{-1}\boldsymbol{T}_1^\top\boldsymbol{T}_1 \prec 0, \tag{6.61}$$

where

$$\boldsymbol{T}_1 \triangleq \begin{bmatrix} \boldsymbol{C}_{\mathrm{r,y}} & \boldsymbol{R}_1 & \boldsymbol{R}_2 \\ \boldsymbol{C}_{\mathrm{r,u}} & \boldsymbol{R}_3 & \boldsymbol{R}_4 \end{bmatrix}.$$

Furthermore, define

$$\boldsymbol{W} \triangleq \begin{bmatrix} \boldsymbol{W}_{11} & \boldsymbol{W}_{12} & \boldsymbol{W}_{13} \\ \star & \boldsymbol{W}_{22} & \boldsymbol{W}_{23} \\ \star & \star & \boldsymbol{W}_{33} \end{bmatrix},$$

where $\boldsymbol{W}_{ij}$ are defined as in (6.22)–(6.27), $i, j = 1, 2, 3$. Defining $\rho_{\mathrm{r}} \triangleq \mu_{\mathrm{r}}^{-1}$, it follows that

$$\boldsymbol{W} = \mu_{\mathrm{r}}^{-1} \boldsymbol{T}_1^{\top} \boldsymbol{T}_1.$$

Defining $\boldsymbol{Z}_1 \triangleq \boldsymbol{P}\boldsymbol{A}_{\mathrm{r}} - \boldsymbol{P}$, $\boldsymbol{Z}_2 \triangleq \boldsymbol{P}\boldsymbol{B}_{\mathrm{r,y}}$, and $\boldsymbol{Z}_3 \triangleq \boldsymbol{P}\boldsymbol{B}_{\mathrm{r,u}}$, (6.61) is equivalent to (6.21). Thus, according to Lemma 6.4, if (6.59) is satisfied for some $\mu_{\mathrm{r}} > 0$, then (6.21) is also satisfied and Σ_{R} is IF-OFP(ν_{r},ρ_{r}). Lemma 6.5 ensures that if $\Sigma_{\mathrm{P_f}}$, Σ_{C} and Σ_{R} are, respectively, IF-OFP(ν_{f}, ρ_{f}), IF-OFP(ν_{r},ρ_{r}) and IF-OFP(ν_{c},ρ_{c}), then $(\Sigma_{\mathrm{P_f}}, \Sigma_{\mathrm{R}}, \Sigma_{\mathrm{C}})$ is $(\boldsymbol{Q}, \boldsymbol{S}, \boldsymbol{R})$-dissipative with Q, S and R defined, respectively, by (6.33), (6.34), and (6.35). Using the Schur's complement Lemma, if (6.60) is satisfied then

$$\begin{bmatrix} -(\gamma_3 + \nu_{\mathrm{r}}) & 0 & \frac{1}{2}\mu_{\mathrm{r}} & 0 \\ \star & -(\gamma_4 + \nu_{\mathrm{r}}) & \frac{1}{2}\mu_{\mathrm{r}} & \frac{1}{2}\mu_{\mathrm{r}} \\ \star & \star & -\mu_{\mathrm{r}} & 0 \\ \star & \star & \star & -\mu_{\mathrm{r}} \end{bmatrix} - \boldsymbol{T}_2^{\top} \boldsymbol{Y}_1 \boldsymbol{T}_2 \prec 0. \tag{6.62}$$

is also satisfied for $\boldsymbol{T}_2 \triangleq [\boldsymbol{0}_{2\times 2}\ \mu_{\mathrm{r}} \boldsymbol{I}_2]$ and $\boldsymbol{Y}_1^{-1} \triangleq \mathrm{diag}\,\{\gamma_2, \gamma_1\}$. Thus (6.62) is equivalent to

$$\boldsymbol{Y}_2 \triangleq \begin{bmatrix} -(\gamma_3 + \nu_{\mathrm{r}}) & 0 & \frac{1}{2}\mu_{\mathrm{r}} & 0 \\ \star & -(\gamma_4 + \nu_{\mathrm{r}}) & \frac{1}{2}\mu_{\mathrm{r}} & \frac{1}{2}\mu_{\mathrm{r}} \\ \star & \star & -\mu_{\mathrm{r}} - \mu_{\mathrm{r}}^2\gamma_2 & 0 \\ \star & \star & \star & -\mu_{\mathrm{r}} - \mu_{\mathrm{r}}^2\gamma_1 \end{bmatrix} \prec 0. \tag{6.63}$$

Considering (6.58) and Lemma 6.1, it is clear that $\Sigma_{\mathrm{P_f}}$ and Σ_{C} are, respectively, IF-OFP(γ_1^{-1}, γ_3) and IF-OFP(γ_2^{-1}, γ_4). Adopting the congruence transformation $\boldsymbol{T}_3^{\top}\boldsymbol{Y}_2\boldsymbol{T}_3$ with $\boldsymbol{T}_3 \triangleq \mathrm{diag}\,\{1, 1, \mu_{\mathrm{r}}^{-1}, \mu_{\mathrm{r}}^{-1}\}$ and $\mu_{\mathrm{r}}^{-1} = \rho_{\mathrm{r}}$, then notice that $\boldsymbol{T}_3^{\top}\boldsymbol{Y}_2\boldsymbol{T}_3 \succeq \boldsymbol{Q}$ with $\boldsymbol{Q}$ defined by (6.33). Thus, it demonstrates that (6.60) implies that $\boldsymbol{Q} \prec 0$, which it is sufficient to ensure the asymptotic stability of $(\Sigma_{\mathrm{P_f}}, \Sigma_{\mathrm{R}}, \Sigma_{\mathrm{C}})$ according to Lemma 5.1. Finally, any Σ_{R} described as (6.15) with matrix gains that satisfy (6.58)–(6.60) with $\boldsymbol{P} \succ 0$ ensures the asymptotic stability of $(\Sigma_{\mathrm{P_f}}, \Sigma_{\mathrm{R}}, \Sigma_{\mathrm{C}})$ and this concludes the proof. □

Remark 6.4. *The key result of this chapter is provided by Theorem 6.1 for passivation-based fault hiding. The main advantage is that it allows to decouple the analysis of the subsystems based on dissipativity theory that allows to design RBs that ensure dissipativity properties for the global system. Although it focuses on the problem of FTC for nonlinear systems with multiplicative faults, it can be also applied to other problems, for example systems with unknown control directions [267] and variable structure systems [268], possibly with system's order modifications.*

6.3.2 DPB as virtual sensors and actuators

Note that in the literature, VS and VA are usually used as dynamic RBs. It is shown in [18] that a sufficient condition for ensuring the stability recovery after sensor (actuator) faults occurrence by means of a VS (VA) is that $\boldsymbol{A} - \boldsymbol{L}\boldsymbol{C}_{\mathrm{f}}$ $(\boldsymbol{A} - \boldsymbol{B}_{\mathrm{f}}\boldsymbol{M})$ is Hurwitz.

Note that the proof of Theorem 6.1 implies that the DPB Σ_{R} satisfies (6.21) with $\rho > 0$, and consequently

$$\mathrm{He}\left\{\boldsymbol{P}\boldsymbol{A}_{\mathrm{r}}\right\} + \boldsymbol{W}_{11} \prec 0.$$

Considering that $\boldsymbol{W}_{11} \succ 0$ for any $\rho > 0$, then the above inequality implies that $\mathrm{He}\left\{\boldsymbol{P}\boldsymbol{A}_{\mathrm{r}}\right\} \prec 0$ that is sufficient for $\boldsymbol{A}_{\mathrm{r}}$ being Hurwitz. In Subsection 6.2.1, it is shown that the VS and VA are particular cases of the DPB where $\boldsymbol{A}_{\mathrm{r}} \triangleq \boldsymbol{A} - \boldsymbol{L}\boldsymbol{C}_{\mathrm{f}}$ and $\boldsymbol{A}_{\mathrm{r}} \triangleq \boldsymbol{A} - \boldsymbol{B}_{\mathrm{f}}\boldsymbol{M}$ respectively. Therefore, any VS or VA that satisfy Theorem 6.1 also satisfies the stabilization conditions in the literature.

6.4 Numerical example

Consider the following nonlinear faulty system $\Sigma_{\mathrm{P_f}}$:

$$\Sigma_{\mathrm{P_f}} : \begin{cases} \dot{x}_1 = -0.5x_1^3 + 0.5x_2 \\ \dot{x}_2 = -0.5x_1 - 1.25x_2 - 4f_{\mathrm{a}}\boldsymbol{u}_{\mathrm{p}} \\ \boldsymbol{y}_{\mathrm{p}} = -f_{\mathrm{s}}x_2 - 0.5f_{\mathrm{s}}\boldsymbol{u}_{\mathrm{p}} \end{cases} \tag{6.64}$$

where the signals f_{a} and f_{s} denote, respectively, actuator and sensor multiplicative faults such that $f_{\mathrm{a}} = 1$ and $f_{\mathrm{s}} = 1$ represent the fault-free operation.

Let $V(x_1, x_2) = \frac{1}{2}x_1^2 + \frac{1}{2}x_2^2$ be a storage function for $\Sigma_{\mathrm{P_f}}$. Taking its time-derivative, it follows that:

$$\dot{V}(x_1, x_2) = -0.5x_1^4 - 1.25x_2^2 - 4f_{\mathrm{a}}\boldsymbol{u}_{\mathrm{p}}x_2. \tag{6.65}$$

Furthermore, given that $\Sigma_{\mathrm{P_f}}$ is IF-OFP(ν_{f},ρ_{f}), $(\boldsymbol{u}, \boldsymbol{y})$ is the supply rate function in (6.2) for (6.64):

$$(\boldsymbol{u}_{\mathrm{p}}, \boldsymbol{y}_{\mathrm{p}}) = -\left(\frac{1}{2}f_{\mathrm{s}}f_{\mathrm{a}} + f_{\mathrm{a}}^2\nu_{\mathrm{f}} + \frac{1}{4}f_{\mathrm{s}}\rho_{\mathrm{f}}\right)\boldsymbol{u}_{\mathrm{p}}^2 - \left(f_{\mathrm{s}}f_{\mathrm{a}} + f_{\mathrm{s}}\rho_{\mathrm{f}}\right)\boldsymbol{u}_{\mathrm{p}}x_2 - f_{\mathrm{s}}\rho_{\mathrm{f}}x_2^2. \tag{6.66}$$

Disregarding the negative term $-0.5x_1^4$ in (6.65), the following condition, obtained from (6.65) and (6.66), is sufficient to ensure that the passivation indices satisfy $\dot{V}(x_1, x_2) - (\boldsymbol{u}_{\mathrm{p}}, \boldsymbol{y}_{\mathrm{p}}) \leq 0$

$$\begin{bmatrix} x_2 \\ \boldsymbol{u}_{\mathrm{p}} \end{bmatrix}^{\top} \begin{bmatrix} -1.25 + f_{\mathrm{s}}\rho_{\mathrm{f}} & \frac{1}{2}\left(f_{\mathrm{s}}f_{\mathrm{a}} + f_{\mathrm{s}}\rho_{\mathrm{f}} - 4f_{\mathrm{a}}\right) \\ \star & \frac{1}{2}f_{\mathrm{s}}f_{\mathrm{a}} + f_{\mathrm{a}}^2\nu_{\mathrm{f}} + \frac{1}{4}f_{\mathrm{s}}\rho_{\mathrm{f}} \end{bmatrix} \begin{bmatrix} x_2 \\ \boldsymbol{u}_{\mathrm{p}} \end{bmatrix} \leq 0 \tag{6.67}$$

Thus, the above condition allows computing ρ_{f} and ν_{f} by means of semi-definite programming (SDP) for both the fault-free and faulty operation modes since the fault estimates f_{s} and f_{a} are known (cf. Assumption 6.3). To test different fault scenarios (fault-free; actuator, sensor or simultaneous faults), f_{s} and f_{a} are chosen as follows:

$$f_{\mathrm{s}} = \begin{cases} 0.75, & \text{if } 10 < t \leq 85, \\ 1, & \text{otherwise} \end{cases}, \qquad f_{\mathrm{a}} = \begin{cases} 1, & \text{if } t \leq 55, \\ -0.2, & \text{if } t > 55 \end{cases}.$$

Notice that the fault-free operation happens until $t = 10$s, when a sensor attenuation fault starts. While the sensor fault still is present, an actuator fault with $f_{\mathrm{a}} = -0.2$ starts at $t = 10$s. For $t > 85$s, the sensor fault is no longer occurring but only the actuator fault affects the system. The passivity indices are computed solving the maximization of the cost $J = \rho_{\mathrm{f}} + \nu_{\mathrm{f}}$ with constraint (6.67). Then, the passivity indices

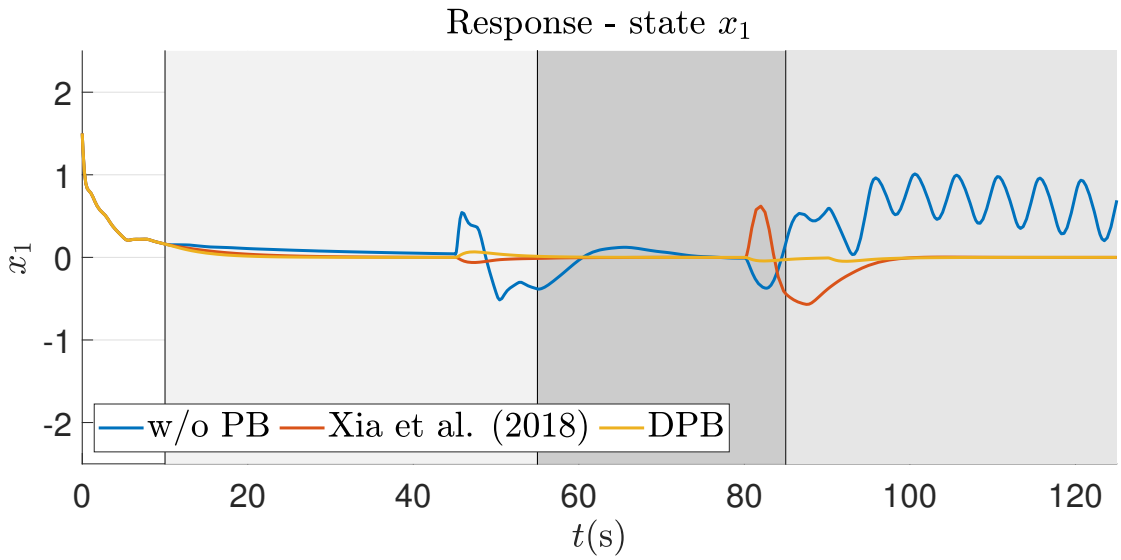

Figure 6.5 – Comparison between the trajectories of the state x_1 with the proposed DPB and the PB in [200] for the nonlinear system.

are:

$$\nu_{\mathrm{f}} = \begin{cases} -2.563, & \text{if } t \leq 10, \\ -0.249, & \text{if } 10 < t \leq 55, \\ -2.843, & \text{if } 55 < t \leq 85, \\ 0.686, & \text{if } t > 85, \end{cases}$$

$$\rho_{\mathrm{f}} = \begin{cases} 0.375, & \text{if } t \leq 10, \\ 0.512, & \text{if } 10 < t \leq 55, \\ 0.001, & \text{if } t > 55. \end{cases}$$

For simulation purposes, a controller Σ_{C} (that is IF-OFP(-0.25,2.75)) is used to stabilization and disturbance rejection for the fault-free system. It is given by:

$$\Sigma_{\mathrm{C}} : \begin{cases} \dot{x}_{\mathrm{c}} = -3.517 x_{\mathrm{c}} - 4.5 \boldsymbol{y}_{\mathrm{c}} \\ \boldsymbol{u}_{\mathrm{c}} = x_{\mathrm{c}} + 0.2045 \boldsymbol{y}_{\mathrm{c}} \end{cases} \tag{6.68}$$

The proposed DPB described in (6.15) is designed based on Theorem 6.1 by using the LMILAB. The computed gains of the Dynamic Passivation Blocks (DPBs) Σ_{R}^{i}

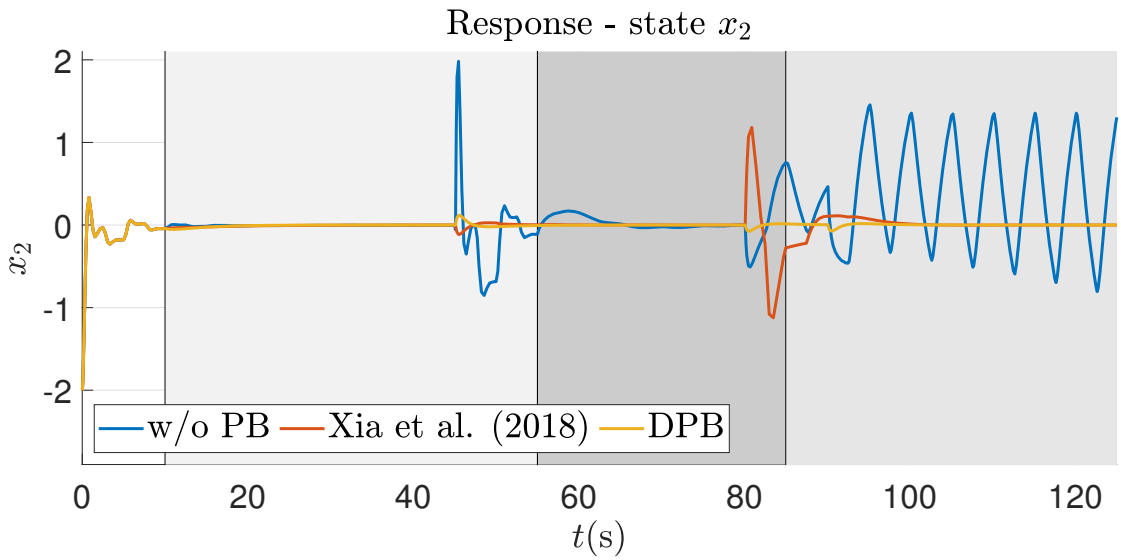

Figure 6.6 – Comparison between the trajectories of the state x_2 with the proposed DPB and the PB in [200] for the nonlinear system.

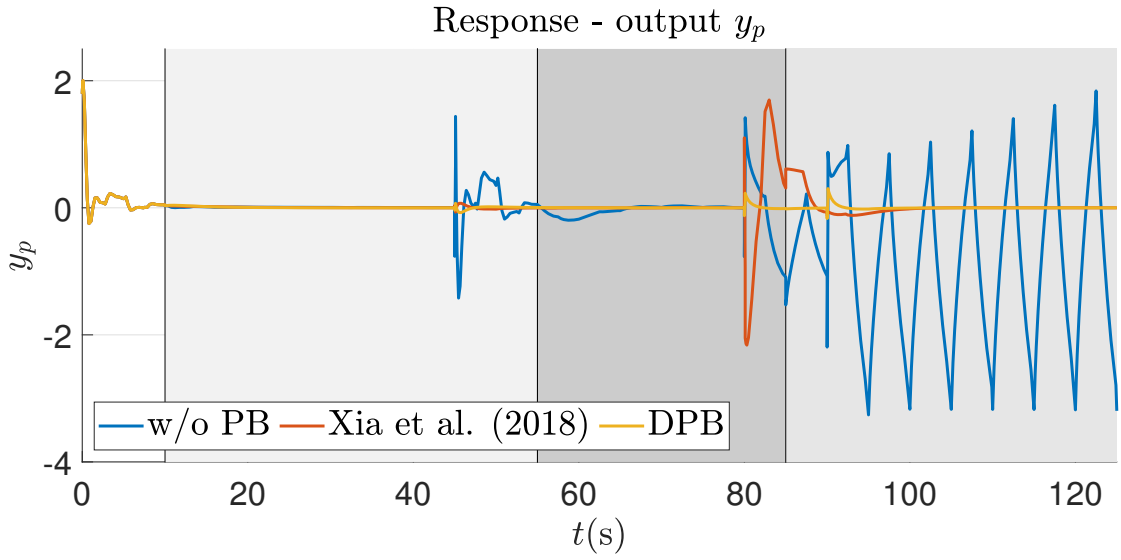

Figure 6.7 – Comparison between the trajectories of the output with the proposed DPB and the PB in [200] for the nonlinear system.

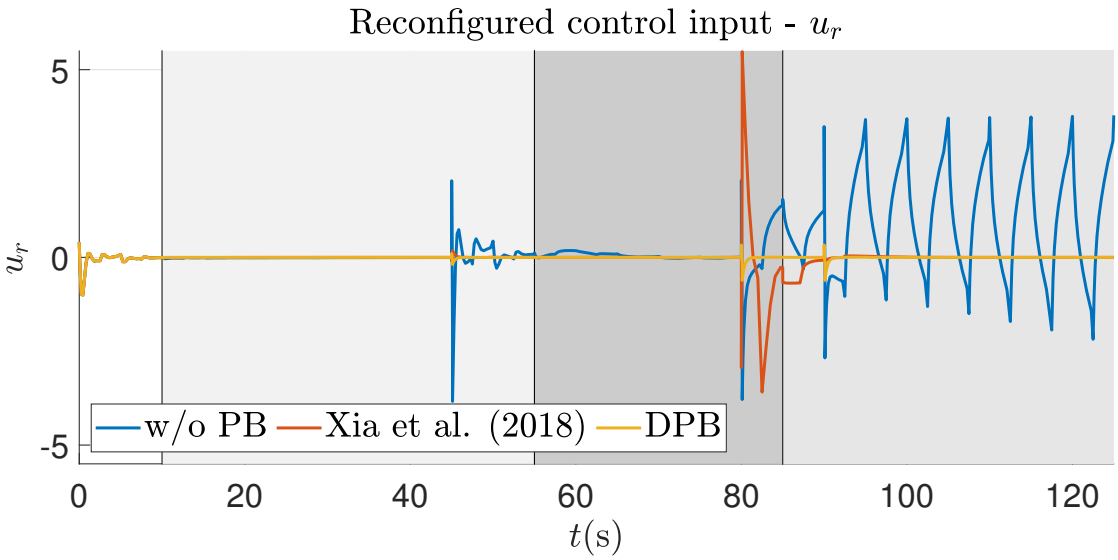

Figure 6.8 – Comparison between the trajectories of the reconfigured input injected into the plant with the proposed DPB and the PB in [200] for the nonlinear system.

for the scenarios $i = 1, 2, 3$ are presented in the sequel. Notice that Scenario 1 denotes the case when only the sensor fault occurs ($10 < t \leq 55$s). Scenario 2 corresponds to the case when only the actuator fault occurs ($t \geq 85$s). And Scenario 3 is the case when both sensor and actuator faults occur simultaneously ($55 < t \leq 85$s). The superscript indices in the matrices indicate the scenario

$$
\begin{aligned}
&\boldsymbol{A}_{\mathrm{r}}^{1} = \begin{bmatrix} -0.5 & 0 \\ 0 & -0.5 \end{bmatrix}, \quad \boldsymbol{A}_{\mathrm{r}}^{2} = \boldsymbol{A}_{\mathrm{r}}^{3} = \begin{bmatrix} -1.4142 & 0 \\ 0 & -1.4142 \end{bmatrix}, \\
&\boldsymbol{B}_{\mathrm{r,u}}^{1} = \boldsymbol{B}_{\mathrm{r,u}}^{2} = \boldsymbol{B}_{\mathrm{r,u}}^{3} = \boldsymbol{B}_{\mathrm{r,y}}^{1} = \boldsymbol{B}_{\mathrm{r,y}}^{2} = \boldsymbol{B}_{\mathrm{r,y}}^{3} = \begin{bmatrix} 0 & 0 \end{bmatrix}^{\top}, \\
&\boldsymbol{C}_{\mathrm{r,u}}^{1} = \boldsymbol{C}_{\mathrm{r,u}}^{2} = \boldsymbol{C}_{\mathrm{r,u}}^{3} = \boldsymbol{C}_{\mathrm{r,y}}^{1} = \boldsymbol{C}_{\mathrm{r,y}}^{2} = \boldsymbol{C}_{\mathrm{r,y}}^{3} = \begin{bmatrix} 0 & 0 \end{bmatrix}, \\
&\boldsymbol{R}_{1}^{1} = \boldsymbol{R}_{4}^{1} = 0.126, \quad \boldsymbol{R}_{1}^{2} = \boldsymbol{R}_{4}^{2} = 0.0181, \\
&\boldsymbol{R}_{1}^{3} = \boldsymbol{R}_{4}^{3} = 0.0207, \quad \boldsymbol{R}_{2}^{1} = \boldsymbol{R}_{3}^{1} = \boldsymbol{R}_{2}^{2} = \boldsymbol{R}_{3}^{2} = \boldsymbol{R}_{2}^{3} = \boldsymbol{R}_{3}^{3} = 0,
\end{aligned}
$$

The procedure proposed in [201] and the PB in (6.6) proposed by [200] can also be employed to recover the stability of the reconfigured system. For this purpose, Lemma 6.2 indicates that the passivation controller must be OFP(ρ_{r}) with $\rho_{\mathrm{r}} > -\nu_{\mathrm{f}}$ for Scenarios 1 and 3. In the Scenario 2, it is sufficient $(\Sigma_{\mathrm{C}}, \Sigma_{\mathrm{R}})$ to be passive since $\nu_{\mathrm{f}} > 0$ and $\rho_{\mathrm{f}} > 0$. According to Lemma 6.3, given that Σ_{C} is finite gain $\mathcal{L}_2$-stable

with gain $\gamma = 0.9688$, the passivation gains may be chosen as

$$\begin{aligned} m_{\mathrm{p}}^1 &= 0.25, \quad m_{\mathrm{f}}^1 = 0.2, \quad m_{\mathrm{s}}^1 = 0.1, \\ m_{\mathrm{p}}^2 &= 2, \quad m_{\mathrm{f}}^2 = 0.5, \quad m_{\mathrm{s}}^2 = -1, \\ m_{\mathrm{p}}^3 &= 0.3, \quad m_{\mathrm{f}}^3 = 0.25, \quad m_{\mathrm{s}}^3 = 0.05. \end{aligned}$$

The numerical simulation results are depicted in Figs. 6.5–6.8 and compare the faulty system response with the reconfigured system responses with the PB proposed by [200] and with the proposed DPB designed based on Theorem 6.1. Disturbances $\boldsymbol{w}_3 = 10$ are added in the system output at $t = 45$ s, $t = 80$ s and $t = 90$ s with duration of 0.1 s. The initial states are $x_1(0) = 1.5$ and $x_2(0) = -2$. The results illustrate that the proposed DPB is able to recover the stability in all the fault scenarios and presents good disturbance rejection action without requiring much control effort. Otherwise, the system without PB became oscillatory in Scenario 2 and unstable in Scenario 3. The PB proposed by [200] also recovers the stability, but it became too sensitive to the disturbance when both faults are occurring (Scenario 2).

7 CONCLUSIONS

7.1 Summary

This thesis addressed the problem of fault-tolerant control based on the fault hiding approach using novel RBs structures. The fault hiding approach consists of inserting an RB between the faulty plant and the nominal controller, which remains unaltered. In the literature, the RBs are usually described as VSs, for dealing with sensor faults, and VAs for dealing with actuator faults, and their structures are based on the internal model principle to enable their design by stabilizing the error dynamics between the plant and the RBs states. Although effective, those structures are too sensitive to FDI uncertainties and model uncertainties. Moreover, there are still few methodologies available to deal with fault hiding of nonlinear systems. In this regard, this thesis contributed to the fault hiding literature by providing novel RB structures and design methodologies that allow the stability recovery by fault hiding of nonlinear systems. In short, this thesis provided the following original contributions.

a) **Nonlinear fault hiding.** This thesis presented novel methodologies for fault hiding of plants represented by nonlinear models, such as systems with input saturation (cf. chapter 3), NT-S fuzzy models (cf. chapter 4), distributed NT-S fuzzy models (cf. chapter 4), and input affine systems (cf. chapter 5 and chapter 6).

b) **Novel RB structures.** This thesis presented alternative RB structures which can substitute the VAs and VSs and not incorporating the fault model parameters in its gains. In particular, this thesis presented SRBs (cf. chapter 3 and chapter 5), fuzzy SRBs (cf. chapter 4), fuzzy distributed SRBs (cf. chapter 4), and PBs (cf. chapter 6). All those blocks can be used for dealing with both sensor and actuator faults simultaneously.

c) **Design methodologies.** This thesis presented three main novel design methodologies for fault hiding of nonlinear systems by means of the new RBs proposed and concerning: *i)* Lyapunov-based stability recovery (cf. chapter 3 and chapter 4), wherein an analysis condition is used to obtain a

Lyapunov function which certifies the stability of the nominal closed-loop system, and also the same Lyapunov function is used to synthesize the RB for the reconfigured system to recover the stability property after the fault occurrence; *ii)* dissipativity recovery (cf. chapter 5), wherein the same idea is applied to obtain the storage and the supply rate functions in the analysis step used to synthesize RBs which recover the system's passivity, dissipativity and stability; and *iii)* passivation-based fault hiding which designs PBs with sufficient passivity indices to compensate for the fault effects in the energy balance of the closed-loop system. For all those methodologies, constructive LMI-based sufficient design conditions are provided.

7.2 Related publications

The content of this thesis is mainly based on results presented in the publications [129, 127, 106, 226, 269]. In particular, [226] proposes the SRB structure which is used in chapter 3 and chapter 5, and presents the results for fault hiding of linear systems with input saturation which are described in chapter 3. In [127], this concept is extended to nonlinear systems represented by NT-S fuzzy models by using centralized and distributed fuzzy SRBs as presented in chapter 4. In [106], the concept of dissipativity and passivity recovery by fault hiding is proposed as presented in chapter 5. Finally, in [129, 269], the concept of PBs, their relation with the canonical RBs, and the passivation-based fault hiding are presented and their content is the basis of chapter 6.

7.3 Parallel and ongoing works

During the doctoral term to which this thesis refers to, some other related topics were investigated, and some results obtained in collaboration with other members of the D!FCOM (Federal University of Minas Gerais) and SAC (Polytechnic University of Catalonia) laboratories, but they were kept apart this thesis for the sake of brevity and cohesion. In this subsection, these parallel researches will be briefly discussed.

During the doctoral studies, the concept of RBs was extended to other applications without the scope of FTC. In [214], the RBs are employed in a cyber-secure

dual-rate control framework with active cyber-attack detection based on watermarking injection. Indeed, the active attack detection methods (inspired by the active fault detection methods) are the most effective way to detect stealthy attacks, however, the signal injection degrades the system performance. In this framework, the RBs are used to mitigate the degradation effect of the watermarking without compromising the attack detection. Moreover, the RBs are also employed in damping control of DC microgrids in [270], where their ability of compensating disturbances is explored to improve the converter stability and damping ability under abrupt power variations in Constant Power Loads (CPLs).

In particular, several collaborations have been established on the broad topic of supervision and safety of systems which, in addition to FTC, includes fault detection, and PHM. As a consequence, the following papers were published or submitted within this scope of: fault hiding [128], fault detection [271], and PHM [272, 273, 274, 275]. Part of the doctoral studies were also interested in the problem of cyber-security of control systems, whose techniques are close to the FTC techniques. Those studies resulted in the following publications and submissions [214, 276, 277, 278].

In addition, since the initial idea of this thesis was related to reduce the dependence of FTC techniques on physical models, the problems of learning-based modeling and control were also investigated during this doctoral term, and resulted in the following published and submitted papers [279, 280, 281, 282]. Finally, within the scope of nonlinear control and estimation, some researches were conduct in collaboration with D!FCOM team resulting in the following publications and submissions [231, 283, 284, 285].

7.4 Future research directions

This section discusses some possibilities of further research directions related to the fault hiding of nonlinear systems and some other emerging applications for RBs which extrapolate the domain of of FTC.

7.4.1 Tolerance to FDI imperfections

Although most of the fault hiding approaches in the literature assume the existence of a perfect FDI system, recent results consider the integration between FDI and fault hiding systems. However, the FDI system is also subject to failures, which are usually ignored in the literature.

In practical applications may be impossible to perform the online design of RBs. In this sense, two options are possible to enable the online fault hiding: i) employing banks of RBs, where there is one pre-designed RB for each possible fault scenario; ii) using RBs whose parameters are able to be updated by the fault estimates, such as adaptive [47, 48, 49, 53, 52, 50, 54, 51] and robust [128, 105] blocks. Within the fault hiding framework, the integration with FDI systems must be able to perform the following tasks

a) **Fault classification** for indicating if it is an actuator or sensor fault and, particularly, what is the actuator/sensor affected by the fault.

b) **Fault estimation** which provides an estimate of the fault magnitude.

c) **Loop reconfiguration** to insert the RB in the control loop.

On the one hand, fault classification and estimation tasks may fail in two ways: inaccuracy and time delay. But on the other hand, the loop reconfiguration may also induce additional delays in addition to harmful consequences of consecutive switching operations. An inaccurate fault classification may lead to a wrong loop reconfiguration command, whose consequences can be fatal since most of the fault hiding approaches are unable to guarantee stability using wrong RB for a given fault. Indeed, the inaccurate fault classification is rarely addressed in fault hiding literature, and the proposed approaches, such as establishing dwell-time conditions [191] or checking the classification sanity, are not able to formally guarantee the safe reconfiguration. Due to the inherent robustness, some inaccuracies in fault estimates should be tolerated, however, their effects must be adequately quantified and analyzed to guarantee the safety of the reconfiguration operation. Similarly, all the delays induced by classification, estimation, and reconfiguration tasks may be somehow tolerated, but it requires rigorous analysis. In general, the analysis of the tolerance and the effects of delays and fault estimation errors are performed by computing positively invariant sets for which

the reconfigured system convergence is ensured despite delays [123] and estimation errors [189].

Although there are sparse solutions that deal with the FDI delays, fault estimation error and fault misclassification, they are still incipient which results in conservative conditions and the inability to deal simultaneously with all those failures. Based on the discussion presented above, the following open challenge related to the tolerance to FDI imperfections is identified.

Research Direction 1. *To develop FTC frameworks that integrate fault diagnosis, estimation, and hiding considering FDI and reconfiguration delays, reconfiguration switching, fault estimation errors, and fault misclassification.*

In particular, the fault hiding approaches for polytopic differential inclusions, whose representation validity is typically local, must consider the inclusion of those invariant sets within the domain of validity of the differential inclusions. Unfortunately, that issue has not been considered in the fault hiding literature yet. In this sense, the following challenge can be also considered.

Research Direction 2. *For plant models which are only locally valid, obtain design conditions for fault hiding with local guarantees considering FDI, reconfiguration delays and fault estimation errors.*

During the doctoral studies to which this thesis is related, some results were obtained for fault hiding approaches robust with respect to a range of fault indications [128]. Those results can be combined with the RBs indpendent of internal model principle, which were investigated in this thesis, to develop robust fault hiding approaches with respect to FDI failures.

7.4.2 Reduce the model dependence

In general, the fault hiding approaches reported in the literature are based on mathematical models. The dependence occurs in two ways: first, the design methodologies require the healthy and faulty plant models to design the RBs gains which guarantee the fault hiding objectives; second, most of the RBs are based on the internal model principle, therefore those structures embed the plant parameters when

they are implemented for online use. However, these models are not always available and sometimes they are not reliable or are too complex to allow the use of existing control techniques. Indeed, this is the main motivation for developing data-driven and model-free methods. Although data-driven FTC and FDI become popular, there are still no data-drive fault hiding approaches proposed in the literature. It is worth mentioning that the concept of data-driven VSs has already been proposed out of the fault hiding context. For example, data-driven VSs are learned from data based on system identification, machine learning or digital twins techniques to solve problems related to: estimation of immeasurable parameter [286]; fault diagnosis [287]; fault detection [288, 289]; fault prognostics [184]; and fault accommodation [290]. Moreover, the VAs designed as fuzzy expert systems also indicate a way for achieving data-driven fault hiding design approaches in the future.

Research Direction 3. *To develop data-driven fault hiding approaches for dealing with plants with unknown dynamics subject to faults whose modeling is uncertain and estimates are inaccurate.*

The results presented in chapter 6 and published in [129, 269] indicates a way to reduce the dependence on models. It can be extended by using some results for data-driven input-output properties as those described in [291, 292, 201, 262, 263, 264]. Moreover, learning-based fuzzy modeling can be adapted to obtain polytopic differential inclusions which eases the estimation of dissipativity properties based on sum of squares or LMIs. Indeed, during the doctoral studies to which this thesis is related, some relevant results were obtained and published related to evolving fuzzy modeling [281] and its application to ETC [280], fuzzy control [282], fault prognostics [273, 275, 274, 272], and fault diagnostics [271]. Those evolving fuzzy modeling are polytopic differential inclusions which can be also applied to the problem of data-driven estimation of dissipativity properties for developing passivation-based data-driven fault hiding.

Since most of the fault hiding approaches are based on the internal model principle, the additional issue to reduce the dependence on models is the sensitivity of those RB structures concerning the fault estimation error. It occurs because the effective faulty model parameters are obtained from the fault estimator, which may not be reliable as discussed in subsection 7.4.1. Even for a good fault estimator, the

estimates take some time to converge, and even a small estimation error should result in a block whose guarantees do not cover the real fault scenario. Therefore, obtaining design methodologies for RBs independent of the internal model principle is also an open challenge.

Research Direction 4. *To develop design methodologies for fault hiding approaches based on RBs independent of the internal model principle.*

In this regard, some recent advances are presented in this thesis and the publications [127, 106], related to this thesis, which propose RBs structures independent of the internal model principle for stability and dissipativity recovery by fault hiding. To design them, procedures consisting of two steps are proposed - first, an analysis step is used to obtain valid storage or Lyapunov functions and, second, a synthesis step is performed based on the function obtained previously. Further works may include less conservative approaches without using the same Lyapunov functions in the second step. Those further approaches can be inspired by design conditions used to obtain SOF controllers, for example, those provided in [231].

Moreover, the PBs are also presented in [129] which may be independent of the internal model principle and generalizes the canonical RBs (VSs and VAs) as indicated in [269]. Indeed, those blocks are designed to perform the passivation of the faulty system without requiring an explicit fault model, but only the faulty system's passivity indices.

7.4.3 Safety constraints

For several applications, the states and inputs of the system are not allowed to violate some boundaries, usually called safety constraints. While most of the fault hiding approaches are concerned with recovering desired stability, tracking, and performance properties, there are few results concerning the maintenance of safety constraints. In particular, the reconfiguration delays and the switching usually lead the reconfigured system to overshoot and high control efforts required from the remaining actuators. In this sense, safety constraints might be violated even when the stability and performance are asymptotically recovered. Indeed, the approach proposed in this thesis and in the related publication [226] is able to deal with input saturation, which is a way to address

the problem of input constraints. Moreover, to deal with safety constraints, MPC-based fault hiding approaches have been recently proposed [211, 130, 131, 227], however, they do not consider the design of the MPC ingredients to guarantee the stability [293]. Therefore to deal simultaneously with the conventional fault hiding objectives and safety constraints is also an open challenge.

Research Direction 5. *To develop fault hiding approaches which are able to recover nominal properties while deal with safety constraints after the control reconfiguration.*

7.4.4 Emerging Applications

In addition to the fault hiding, RBs have been recently applied to solve other problems in the spirit of hiding disturbance effect and improve the system dynamics without modifying the pre-designed controllers. Therefore, these applications are discussed below.

7.4.4.1 Cyber-secure control

With the advances in communication networks, the resilience of dynamic systems against cyber-attacks is attracting interest from academia and industry. To address that issue, cyber-secure control systems are proposed. Most of the results in this regard are inspired by FTC techniques, due to the similarities between the effects of faults and cyber-attacks in dynamic systems.

In this sense, denial-of-service attacks in the controller to the actuator channel can be represented as an efficiency loss of the actuator. In [212], VAs are used to mitigate the effects of those denial-of-service attacks. In addition, for DC microgrids subject to sensor deception attacks, the use of VSs is proposed to recover the correct measurements in [294]. For MASs wherein some agents are subject to attack, a virtual network block is proposed in [295] for hiding the attack effect from the other agents in the network. Moreover, an effective way to detect cyber-attack occurrence is by injecting watermarking signals. However, the signal injection also has disruptive effects. For handling those effects, RBs are used to attenuate the nocive effects of the watermarking signal injection in [213, 214].

Given those recent advances, the application of RBs and fault hiding techniques for cyber-secure control seem to be promising and additional efforts are welcome to develop those ideas.

7.4.4.2 Stabilizing and Damping Control

In power systems, supplementary control loops (e.g., power system stabilizers and power oscillation damping controllers) are usually employed to improve the performance and oscillation damping and guarantee stability. In particular, to deal with the negative impedance effect of CPLs in microgrids, virtual elements are commonly employed, such as virtual impedance [296, 297], inductance [95, 298, 299], capacitance [96], and inertia [300, 301]. Moreover, the performance improvement in power system networks is also obtained by inserting supplementary control loops in a retrofit control scheme in [84, 85, 86, 87, 88], whose similarities with the fault hiding are already discussed in section 2.3.

For load frequency fault-tolerant control, VAs are already used and their effectiveness for damping the frequency oscillations is indicated by the results in [210, 179]. Indeed, RBs are suitable for the context of power systems and microgrids in which highly distributed systems with complex multi-loop control schemes are found. In particular, the possibility of employing RBs that allow the recovery and performance improvement in part of the grids, without changing the baseline controllers or affecting the properties of the remainder of the network, is very attractive and motivates further studies on the application of RBs for stabilizing and damping control of power systems.

7.4.4.3 Networked Control Systems

The absolute majority of fault hiding approaches are designed in continuous-time or discrete-time systems, for which traditional time-triggered sampling and transmissions are employed. However, in NCSs [283], the use of resource-aware control methods is usual, including ETC methods in opposition to the traditional time-triggered methods. Some exceptions are the approaches in [187, 188] that consider the design of RBs for fault-hiding of NCSs that consider varying-rate control schemes. Therefore, it is still necessary to develop effective fault hiding approaches applicable to ETC schemes.

In addition, the RBs may play an alternative role in NCSs [302]. Although the ETC schemes are usually designed by emulation (the event generators design is independent of the controllers' design) or co-design (the event generators and controller are designed simultaneously) methods, in [303] a different approach is proposed. In this paper, given the event generators and the system (plant and controller) models, static PBs are designed to guarantee the stability of the network (considering delays and quantization) without modifying the controllers or the event generators. In general, the co-design conditions are less conservative and lead to better performance in terms of reduction of the number of transmissions but it requires the design of a new controller with the event generator. Otherwise, the approach proposed by [303] designs an additional block to guarantee closed-loop properties and improve its performance without re-design the controller but providing some degrees of freedom to the design process. Indeed, RBs can be useful to achieve novel design methods for NCS and ETC schemes.

7.5 Publication list

7.5.1 Published or Accepted Papers

a) **I. Bessa**, V. Puig, and R. M. Palhares. "Passivation blocks for fault tolerant control of nonlinear systems." In: Automatica 125 (Mar. 2021), p. 109450. doi: 10.1016/j.automatica.2020.109450.

b) I. Bessa, V. Puig, and R. M. Palhares. "TS fuzzy reconfiguration blocks for fault tolerant control of nonlinear systems." In: Journal of the Franklin Institute 357.8 (May 2020), pp. 4592–4623. doi: 10.1016/j.jfranklin.2020.02.002.

c) I. Bessa, M. O. Camargos, V. Puig, and R. M. Palhares. "Dissipativity and Stability Recovery by Fault Hiding." In: IFAC-PapersOnLine 53.2 (2020). 21st IFAC World Congress, pp. 4121–4126. doi: 10.1016/j.ifacol.2020.12.2445.

d) I. Bessa and R. M. Palhares. "Novas Condições para Recuperação de Estabilidade com Atuadores Virtuais Estáticos." In: Anais do 14º Simpósio Brasileiro de Automação Inteligente. Galoa, 2019. doi: 10.17648/sbai-2019-111185.

e) I. Bessa, V. Puig, and R. M. Palhares. "Passivation-based Control Reconfiguration with Virtual Actuators." In: 11th IFAC Symposium on Fault Detection, Supervision and Safety for Technical Processes - SAFEPROCESS. To appear. 2022.

f) I. Bessa, C. Trapiello, V. Puig, and R. M. Palhares. "Dual-Rate Control Framework With Safe Watermarking Against Deception Attacks." In: IEEE Transactions on Systems, Man, and Cybernetics: Systems (2022). Early Access, pp. 1–13. doi: 10.1109/tsmc.2022.3160791.

g) M. M. Quadros, I. V. de Bessa, V. J. Leite, and R. M. Palhares. "Fault tolerant control for linear parameter varying systems: An improved robust virtual actuator and sensor approach." In: ISA Transactions 104 (Sept. 2020), pp. 356–369. doi: 10.1016/j.isatra.2020.05.010.

h) L. A. Q. C. Júnior, P. H. Coutinho, I. Bessa, M. O. Camargos, and R. M. Palhares. "Análise de Compromisso entre Granularidade e Interpretabilidade em Sistemas Granulares Evolutivos." In: Anais do 14º Simpósio Brasileiro de Automação Inteligente. Galoa, 2019. doi: 10.17648/sbai-2019-111316.

i) M. O. Camargos, I. Bessa, M. F. S. V. D'Angelo, and R. M. Palhares. "Fault Prognostics of Rolling Bearings Using a Hybrid Approach." In: IFAC-PapersOnLine 53.2 (2020). 21st IFAC World Congress, pp. 4082–4087. doi: 10.1016/j.ifacol.2020.12.2435.

j) M. O. Camargos, I. Bessa, M. F. S. V. D'Angelo, L. B. Cosme, and R. M. Palhares. "Data-driven prognostics of rolling element bearings using a novel Error Based Evolving Takagi–Sugeno Fuzzy Model." In: Applied Soft Computing 96 (Nov. 2020), p. 106628. doi: 10.1016/j.asoc.2020.106628.

k) M. Camargos, I. Bessa, L. A. Q. C. Junior, P. Coutinho, D. F. Leite, and R. M. Palhares. "Evolving Fuzzy System Applied to Battery Charge Capacity Prediction for Fault Prognostics." In: Atlantis Studies in Uncertainty Modelling. Atlantis Press, 2021. doi: 10.2991/asum.k.210827.010.

l) K. Boutrous, I. Bessa, V. Puig, F. Nejjari, and R. M. Palhares. "Data-driven Prognostics based on Evolving Fuzzy Degradation Models for Power

Semiconductor Devices." In: 7th European Conference of the PHM Society. To appear. 2022.

m) L. A. Q. Cordovil, P. H. S. Coutinho, I. Bessa, M. L. C. Peixoto, and R. M. Palhares. "Learning event-triggered control based on evolving data-driven fuzzy granular models." In: International Journal of Robust and Nonlinear Control 32.5 (Jan. 2022), pp. 2805–2827. doi: 10.1002/rnc.6024.

n) L. A. Q. Cordovil, P. H. S. Coutinho, I. V. de Bessa, M. F. S. V. D'Angelo, and R. M. Palhares. "Uncertain Data Modeling Based on Evolving Ellipsoidal Fuzzy Information Granules." In: IEEE Transactions on Fuzzy Systems 28.10 (Oct. 2020), pp. 2427–2436. doi: 10.1109/tfuzz.2019.2937052.

o) D. Leite, P. Coutinho, I. Bessa, M. Camargos, L. A. Q. C. Junior., and R. Palhares. "Incremental Learning and State-Space Evolving Fuzzy Control of Nonlinear Time-Varying Systems with Unknown Model." In: Atlantis Studies in Uncertainty Modelling. Atlantis Press, 2021. doi: 10.2991/a-sum.k.210827.011.

p) M. L. C. Peixoto, P. H. S. Coutinho, I. Bessa, and R. M. Palhares. "Static output feedback stabilization of discrete-time linear parameter-varying systems under actuator saturation." In: International Journal of Robust and Nonlinear Control (2022). Early Access. doi: 10.1002/rnc.6106.

q) P. H. Coutinho, M. L. Peixoto, I. Bessa, and R. M. Palhares. "Dynamic event-triggered gain-scheduling control of discrete-time quasi-LPV systems." In: Automatica 141 (July 2022), p. 110292. doi: 10.1016/j.automatica.2022.110292.

7.5.2 Submitted Papers

a) I. Bessa, P. H. S. Coutinho, I. V. Bessa, R. L. P. Mendeiros, and R. M. Palhares. "Estabilizadores Virtuais para Conversores CC-CC com Cargas de Potência Constante."

b) M. L. C. Peixoto, P. S. P. Pessim, P. H. S. Coutinho, I. Bessa, and R. M. Palhares. "Controle em Rede com Acionamento por Eventos para Sistemas Sujeitos a Ataques Cibernéticos."

c) P. H. S. Coutinho, I. Bessa, M. L. C. Peixoto, P. S. P. Pessim, P. O. F. Pires, and R. M. Palhares. "Controle com Acionamento por Eventos Resiliente a Ataques de Negação de Serviço."

d) M. L. C. Peixoto, P. S. P. Pessim, P. H. S. Coutinho, I. Bessa, and R. M. Palhares. "Local Event-Triggered Control of Takagi-Sugeno Fuzzy Systems under Deception Attacks."

e) E. Alcalá, I. Bessa, V. Puig, O. Sename, and R. M. Palhares. "MPC using an on-line TS fuzzy learning approach with application to autonomous driving."

f) P. H. S. Coutinho, I. Bessa, W.-B. Xie, A.-T. Nguyen, and R. M. Palhares. "A Sufficient Condition to Design Unknown Input Observers for Nonlinear Systems with Arbitrary Relative Degree."

g) P. S. P. Pessim, P. H. S. Coutinho, I. Bessa, M. L. C. Peixoto, M. Lacerda, and R. M. Palhares. "Controle Distribuído para Sistemas Não Lineares Interconectados Sujeitos a Retardos Variantes no Tempo nas Interconexões."

BIBLIOGRAPHY

[1] ISERMANN, Rolf. Model-based fault-detection and diagnosis – status and applications. **Annual Reviews in Control**, v. 29, n. 1, p. 71 – 85, 2005. ISSN 1367-5788. Page 21.

[2] ISERMANN, Rolf. **Fault-Diagnosis Systems: An Introduction from Fault Detection to Fault Tolerance**. Berlin, Heidelberg: Springer, 2006. ISBN 9783540303688. Page 21.

[3] YIN, Shen; DING, Steven X.; XIE, Xiaochen; LUO, Hao. A review on basic data-driven approaches for industrial process monitoring. **IEEE Transactions on Industrial Electronics**, v. 61, n. 11, p. 6418–6428, Nov 2014. Page 21.

[4] GAO, Zhiwei; CECATI, Carlo; DING, Steven X. A survey of fault diagnosis and fault-tolerant techniques—part i: Fault diagnosis with model-based and signal-based approaches. **IEEE Transactions on Industrial Electronics**, v. 62, n. 6, p. 3757–3767, June 2015. Page 21.

[5] GAO, Zhiwei; CECATI, Carlo; DING, Steven X. A survey of fault diagnosis and fault-tolerant techniques—part ii: Fault diagnosis with knowledge-based and hybrid/active approaches. **IEEE Transactions on Industrial Electronics**, v. 62, n. 6, p. 3768–3774, June 2015. Page 21.

[6] BESSA, Iury; PALHARES, Reinaldo Martínez; D'ÂNGELO, Marcos Flávio Silveira Vasconcelos; CHAVES FILHO, Jo ao Edgar. Data-driven fault detection and isolation scheme for a wind turbine benchmark. **Renewable Energy**, v. 87, p. 634 – 645, 2016. ISSN 0960-1481. Page 21.

[7] BLANKE, Mogens; KINNAERT, Michel; LUNZE, Jan; STAROSWIECKI, Marcel. **Diagnosis and Fault-Tolerant Control**. 2. ed. Berlin, Heidelberg: Springer, 2006. ISBN 978-3-540-35652-3. Pages 21, 36, 42, 44, and 66.

[8] ZHANG, Youmin; JIANG, Jin. Bibliographical review on reconfigurable fault-tolerant control systems. **Annual Reviews in Control**, v. 32, n. 2, p. 229 – 252, 2008. ISSN 1367-5788. Pages 21 and 33.

[9] MOOR, Thomas. A discussion of fault-tolerant supervisory control in terms of formal languages. **Annual Reviews in Control**, v. 41, p. 159 – 169, 2016. ISSN 1367-5788. Page 21.

[10] JIANG, Jin; YU, Xiang. Fault-tolerant control systems: A comparative study between active and passive approaches. **Annual Reviews in Control**, v. 36, n. 1, p. 60 – 72, 2012. ISSN 1367-5788. Pages 21 and 22.

[11] STEFANOVSKI, Jovan D. Passive fault tolerant perfect tracking with additive faults. **Automatica**, v. 87, p. 432 – 436, 2018. ISSN 0005-1098. Page 22.

[12] LEE, Seung Woo; YOO, Sung Jin. Robust approximation-free design for tracking and fault tolerance in the presence of arbitrarily switched unknown nonlinearities. **Journal of the Franklin Institute**, v. 354, n. 5, p. 2183 – 2198, 2017. ISSN 0016-0032. Page 22.

[13] LAN, Jianglin; J.PATTON, Ron. A new strategy for integration of fault estimation within fault-tolerant control. **Automatica**, v. 69, p. 48 – 59, 2016. ISSN 0005-1098. Pages 22 and 153.

[14] ZHANG, Youmin; JIANG, Jin. Active fault-tolerant control system against partial actuator failures. **IEE Proceedings - Control Theory and Applications**, v. 149, n. 1, p. 95–104, Jan 2002. Page 22.

[15] JIANG, Bin; STAROSWIECKI, Marcel; COCQUEMPOT, Vincent. Fault accommodation for nonlinear dynamic systems. **IEEE Transactions on Automatic Control**, v. 51, n. 9, p. 1578–1583, Sep. 2006. Page 22.

[16] LUNZE, Jan; RICHTER, Jan H. Reconfigurable fault-tolerant control: A tutorial introduction. **European Journal of Control**, v. 14, n. 5, p. 359 – 386, 2008. ISSN 0947-3580. Pages 22, 32, 36, 39, 43, 44, 66, 141, and 142.

[17] STEFFEN, Thomas. **Control Reconfiguration of Dynamical Systems: Linear Approaches and Structural Tests**. Berlin, Heidelberg: Springer, 2005. (Lecture Notes in Control and Information Sciences). ISBN 9783540257301. Pages 22, 32, 36, 39, 42, 44, 52, 53, 62, 66, and 69.

[18] RICHTER, Jan H. **Reconfigurable Control of Nonlinear Dynamical Systems: A fault-hiding Approach**. Berlin, Heidelberg: Springer, 2011. (Lecture Notes in Control and Information Sciences). ISBN 9783642176272. Pages 22, 32, 36, 39, 40, 43, 45, 46, 53, 56, 57, 62, 63, 66, 70, 79, 153, 155, 156, and 163.

[19] HILL, David; MOYLAN, Peter. The stability of nonlinear dissipative systems. **IEEE Transactions on Automatic Control**, v. 21, n. 5, p. 708–711, October 1976. ISSN 0018-9286. Pages 28, 129, 130, and 147.

[20] TANAKA, K.; WANG, H.O. **Fuzzy Control Systems Design and Analysis: A Linear Matrix Inequality Approach**. New York, NY: Wiley, 2004. ISBN 9780471465225. Pages 29, 41, 45, and 96.

[21] BERNAL, Miguel; SALA, Antonio; LENDEK, Zsófia; GUERRA, Thierry Marie. **Analysis and Synthesis of Nonlinear Control Systems**. Cham: Springer International Publishing, 2022. Pages 29, 41, and 46.

[22] LUO, Ren C.; CHOU, Ying Chih; CHEN, Ogst. Multisensor Fusion and Integration: Algorithms, Applications, and Future Research Directions. In: **International Conference on Mechatronics and Automation**. Harbin, China: IEEE, 2007. v. 2, n. 2, p. 1986–1991. ISBN 978-1-4244-0827-6. Page 33.

[23] KHALEGHI, Bahador; KHAMIS, Alaa; KARRAY, Fakhreddine O.; RAZAVI, Saiedeh N. Multisensor data fusion: A review of the state-of-the-art. **Information Fusion**, Elsevier B.V., v. 14, n. 1, p. 28–44, 2013. ISSN 15662535. Page 33.

[24] NASBURG, R.; MORAVEC, K. Distributed multisensor data fusion. In: **Aircraft Design Systems and Operations Meeting**. San Diego, CA, USA: American Institute of Aeronautics and Astronautics, 1984. p. 1–8. Pages 33 and 43.

[25] NAHIN, Paul; POKOSKI, John. NCTR Plus Sensor Fusion Equals IFFN or can Two Plus Two Equal Five? **IEEE Transactions on Aerospace and Electronic Systems**, AES-16, n. 3, p. 320–337, may 1980. ISSN 0018-9251. Pages 33 and 43.

[26] LUO, R.C.; LIN, M.-H.; SCHERP, R.S. Dynamic multi-sensor data fusion system for intelligent robots. **IEEE Journal on Robotics and Automation**, v. 4, n. 4, p. 386–396, 1988. Page 33.

[27] WALTZ, Edward L.; BUEDE, Dennis M. Data fusion and decision support for command and control. **IEEE Transactions on Systems, Man, and Cybernetics**, v. 16, n. 6, p. 865–879, 1986. Page 33.

[28] MOXON, Bruce C. A Multiprocessor-Based Sensor Fusion Software Architecture. In: AHLERS, Rolf-Juergen; CHEN, Michael J. W. (Ed.). **Proceedings Volume 0849, Automated Inspection and High-Speed Vision Architectures**. Cambridge, CA: SPIE, 1988. p. 72–79. Pages 33 and 43.

[29] MIRABADI, Ahmad; MORT, Neil; SCHMID, Felix. A fault tolerant train navigation system using multisensor, multifilter integration techniques. In: **Proceedings of Fusion-98, First International Conference on Multisource-Multisensor Information Fusion**. Las Vegas, NV, USA: ISIF, 1998. Pages 33 and 43.

[30] MIRABADI, Ahmad; MORT, Neil; SCHMID, Felix. Design of fault tolerant train navigation systems. In: **American Control Conference**. San Diego, CA, USA: IEEE, 1999. v. 1, n. June, p. 104–108. ISBN 0-7803-4990-3. ISSN 07431619. Pages 33 and 43.

[31] MIRABADI, Ahmad; SCHMID, Felix; MORT, Neil. Multisensor Integration Methods in the Development of a Fault-Tolerant Train Navigation System. **Journal of Navigation**, v. 56, n. 3, p. 385–398, sep 2003. ISSN 0373-4633. Page 33.

[32] STOICAN, Florin; OLARU, Sorin; DE DONÁ, José A.; SERON, María M. A discussion on sensor recovery techniques for fault tolerant multisensor schemes. **International Journal of Systems Science**, v. 45, n. 8, p. 1708–1722, aug 2014. ISSN 0020-7721. Page 33.

[33] OLARU, Sorin; DE DONÁ, José A.; SERON, Marí M.; STOICAN, Florin. Positive invariant sets for fault tolerant multisensor control schemes. **International Journal of Control**, v. 83, n. 12, p. 2622–2640, dec 2010. ISSN 0020-7179. Page 33.

[34] MCCLOY, Ryan; DE DONÁ, José; SERON, Marí M. Fault-tolerant fusion-based MPC with sensor recovery for constrained LPV systems. **International Journal of Robust and Nonlinear Control**, John Wiley and Sons Ltd, v. 28, n. 11, p. 3589–3605, jul 2018. ISSN 10991239. Page 33.

[35] CAPRIGLIONE, Domenico; CARRATU, Marco; PIETROSANTO, Antonio; SOMMELLA, Paolo. Soft Sensors for Instrument Fault Accommodation in Semiactive Motorcycle Suspension Systems. **IEEE Transactions on Instrumentation and Measurement**, IEEE, v. 69, n. 5, p. 2367–2376, may 2020. ISSN 0018-9456. Page 33.

[36] BELCHIOR, Carlos Alberto C.; ARAÚJO, Rui Alexandre M.; SOUZA, Francisco Alexandre A.; LANDECK, Jorge Afonso C. Sensor-fault tolerance in a wastewater treatment plant by means of ANFIS-based soft sensor and control reconfiguration. **Neural Computing and Applications**, Springer London, v. 30, n. 10, p. 3265–3276, nov 2018. ISSN 0941-0643. Page 33.

[37] CHEW, P.; MARZULLO, K. Masking failures of multidimensional sensors. In: **Proceedings of Tenth Symposium on Reliable Distributed Systems**. Pisa, Italy: IEEE, 1991. p. 32–41. Page 33.

[38] WU, N. Eva; THAVAMANI, Sudha; ZHANG, Youmin M.; BLANKE, Mogens. Sensor fault masking of a ship propulsion system. **IFAC Proceedings Volumes (IFAC-PapersOnline)**, v. 36, n. 5, p. 417–422, 2003. ISSN 14746670. Pages 33, 42, 43, 63, and 66.

[39] WU, N. Eva; THAVAMANI, Sudha; ZHANG, Youmin M.; BLANKE, Mogens. Sensor fault masking of a ship propulsion system. **Control Engineering Practice**, v. 14, n. 11, p. 1337–1345, 2006. ISSN 09670661. Pages 33, 43, 63, and 66.

[40] TAKIYAMA, Hiroshi; NAKA, Yuji; O'SHIMA, Eiji; ADRIANI, Arif. Sensor-based data reconciliation method and application to the pilot plant. **Journal of Chemical Engineering of Japan**, v. 24, n. 3, p. 339–346, 1991. ISSN 0021-9592. Pages 33, 43, and 60.

[41] ALBUQUERQUE, João S.; BIEGLER, Lorenz T. Data reconciliation and gross-error detection for dynamic systems. **AIChE Journal**, v. 42, n. 10, p. 2841–2856, oct 1996. ISSN 0001-1541. Page 33.

[42] VACHHANI, Pramod; RENGASWAMY, Raghunathan; VENKATASUBRAMANIAN, Venkat. A framework for integrating diagnostic knowledge with nonlinear optimization for data reconciliation and parameter estimation in dynamic systems. **Chemical Engineering Science**, v. 56, n. 6, p. 2133–2148, mar 2001. ISSN 00092509. Page 33.

[43] SARKAR, Palash; KORTELA, Jukka; BORIOUCHKINE, Alexandre; ZATTONI, Elena; JÄMSÄ-JOUNELA, Sirkka-Liisa. Data-Reconciliation Based Fault-Tolerant Model Predictive Control for a Biomass Boiler. **Energies**, v. 10, n. 2, p. 194, feb 2017. ISSN 1996-1073. Page 33.

[44] BEHZAD, Hamid; CASAVOLA, Alessandro; TEDESCO, Francesco; SADRNIA, Mohammad Ali. A fault-tolerant sensor reconciliation scheme based on LPV Unknown Input Observers. In: **55th Conference on Decision and Control**. Las Vegas, NV, USA: IEEE, 2016. p. 2158–2163. ISBN 9781509018376. Pages 33, 43, 46, 51, 60, 63, and 66.

[45] BEHZAD, Hamid; CASAVOLA, Alessandro; TEDESCO, Francesco; SADRNIA, Mohammad Ali. Fault-Tolerant Sensor Reconciliation Schemes via LFT Unknown Input Observers. **IFAC-PapersOnLine**, Elsevier B.V., v. 51, n. 24, p. 874–879, jan 2018. ISSN 24058963. Pages 33, 51, 60, 63, and 66.

[46] BEHZAD, Hamid; CASAVOLA, Alessandro; TEDESCO, Francesco; SADRNIA, Mohammad Ali. Fault-tolerant sensor reconciliation schemes based on unknown input observers. **International Journal of Control**, Taylor & Francis Ltd., v. 93, n. 3, p. 669–679, mar 2020. ISSN 13665820. Pages 33, 51, 60, 63, and 66.

[47] YADEGAR, Meysam; AFSHAR, Ahamad; MESKIN, Nader. Fault-tolerant control of non-linear systems based on adaptive virtual actuator. **IET Control Theory & Applications**, v. 11, n. 9, p. 1371–1379, jun 2017. ISSN 1751-8652. Pages 34, 43, 48, 51, 60, 63, 66, and 172.

[48] YADEGAR, Meysam; MESKIN, Nader; AFSHAR, Ahmad. Fault-tolerant control of multi-agent systems based on adaptive fault hiding framework. **Proceedings of the American Control Conference**, AACC, n. i, p. 4111–4116, may 2017. ISSN 07431619. Pages 34, 43, 48, 49, 51, 60, 63, 66, and 172.

[49] YADEGAR, Meysam; MESKIN, Nader; AFSHAR, Ahmad. Reconfigurable control of linear systems based on state feedback adaptive virtual actuator. **Proceedings of the American Control Conference**, AACC, p. 4123–4128, may 2017. ISSN 07431619. Pages 34, 43, 48, 51, 60, 63, 66, and 172.

[50] YADEGAR, Meysam; MESKIN, Nader. Output Feedback Fault-Tolerant Control of Heterogeneous Multi-Agent Systems. **Asian Journal of Control**, Wiley-Blackwell, v. 23, n. 2, p. 949–961, mar 2021. ISSN 19346093. Pages 34, 48, 49, 51, 63, 66, and 172.

[51] YADEGAR, Meysam; MESKIN, Nader. Fault-Tolerant Control of One-Sided Lipschitz Nonlinear Systems. **IEEE Control Systems Letters**, v. 6, p. 1460–1465, 2022. ISSN 2475-1456. Pages 34, 51, 63, 66, and 172.

[52] YADEGAR, Meysam; MESKIN, Nader. Mission independent fault-tolerant control of heterogeneous linear multiagent systems based on adaptive virtual actuator. **International Journal of Adaptive Control and Signal Processing**, John Wiley and Sons Ltd, v. 35, n. 3, p. 401–419, mar 2021. ISSN 10991115. Pages 34, 48, 49, 51, 63, 66, and 172.

[53] YADEGAR, Meysam; MESKIN, Nader; AFSHAR, Ahmad. Fault-tolerant control of linear systems using adaptive virtual actuator. **International Journal of Control**, Taylor & Francis, v. 92, n. 8, p. 1729–1741, aug 2019. ISSN 13665820. Pages 34, 48, 51, 63, 66, and 172.

[54] YADEGAR, Meysam; MESKIN, Nader. Fault-tolerant control of nonlinear heterogeneous multi-agent systems. **Automatica**, Elsevier Ltd, v. 127, may 2021. ISSN 00051098. Pages 34, 43, 48, 49, 51, 60, 63, 66, and 172.

[55] RICHTER, Jan H.; LUNZE, Jan; STEFFEN, Thomas. The relation between the virtual actuator and the dual observer. **European Journal of Control**, v. 16, n. 5, p. 525 – 531, 2010. ISSN 0947-3580. Pages 34, 44, 54, and 79.

[56] ROSENBROCK, Howard H. Distinctive problems of process control. **Chemical Engineering Progress**, v. 58, n. 9, p. 43–50, 1962. Pages 34, 44, and 54.

[57] DURHAM, Wayne C. Constrained control allocation. **Journal of Guidance, Control, and Dynamics**, v. 16, n. 4, p. 717–725, 1993. ISSN 07315090. Pages 34 and 43.

[58] BUFFINGTON, James M.; ENNS, Dale F.; TEEL, Andrew R. Control allocation and zero dynamics. In: **Guidance, Navigation, and Control Conference and Exhibit**. San Diego, CA, USA: American Institute of Aeronautics and Astronautics, 1996. p. 1–11. Page 34.

[59] BUFFINGTON, James M.; ENNS, Dale F. Lyapunov stability analysis of daisy chain control allocation. **Journal of Guidance, Control, and Dynamics**, American Inst. Aeronautics and Astronautics Inc., v. 19, n. 6, p. 1226–1230, 1996. ISSN 15333884. Page 34.

[60] JOHANSEN, Tor A.; FOSSEN, Thor I. Control allocation—A survey. **Automatica**, Elsevier Ltd, v. 49, n. 5, p. 1087–1103, may 2013. ISSN 00051098. Page 34.

[61] HÄRKEGÅRD, Ola. Dynamic Control Allocation Using Constrained Quadratic Programming. **Journal of Guidance, Control, and Dynamics**, American Institute of Aeronautics and Astronautics Inc., v. 27, n. 6, p. 1028–1034, nov 2004. ISSN 0731-5090. Page 34.

[62] SØRDALEN, Ole J. Optimal thrust allocation for marine vessels. **Control Engineering Practice**, v. 5, n. 9, p. 1223–1231, sep 1997. ISSN 09670661. Page 34.

[63] SHTESSEL, Yuri; BUFFINGTON, James; BANDA, Siva. Tailless aircraft flight control using multiple time scale reconfigurable sliding modes. **IEEE Transactions on Control Systems Technology**, v. 10, n. 2, p. 288–296, mar 2002. ISSN 10636536. Page 34.

[64] BAJPAI, G.; CHANG, B. C.; LAU, A. Reconfiguration of flight control systems for actuator failures. **IEEE Aerospace and Electronic Systems Magazine**, v. 16, n. 9, p. 29–33, sep 2001. ISSN 08858985. Pages 34 and 43.

[65] OMERDIC, Edin; ROBERTS, Geoff. Thruster fault diagnosis and accommodation for open-frame underwater vehicles. **Control Engineering Practice**, v. 12, n. 12 SPEC. ISS., p. 1575–1598, 2004. ISSN 09670661. Page 34.

[66] CALISE, Anthony J.; LEE, Seungjae; SHARMA, Manu. Development of a reconfigurable flight control law for tailless aircraft. **Journal of Guidance, Control, and Dynamics**, v. 24, n. 5, p. 896–902, 2001. ISSN 15333884. Page 34.

[67] ALWI, Halim; EDWARDS, Christopher. Fault tolerant sliding modes control allocation with control surface priority weighting. In: **Conference on Control Applications**. Yokohama, Japan: IEEE, 2010. p. 1057–1062. ISBN 9781424453627. Page 34.

[68] ALWI, Halim; EDWARDS, Christopher. Fault tolerant control using sliding modes with on-line control allocation. **Automatica**, v. 44, n. 7, p. 1859–1866, jul 2008. ISSN 00051098. Page 34.

[69] ALWI, Halim; EDWARDS, Christopher; STROOSMA, Olaf; MULDER, Jan A. Fault tolerant sliding mode control design with piloted simulator evaluation. **Journal**

of Guidance, Control, and Dynamics, American Institute of Aeronautics and Astronautics Inc., v. 31, n. 5, p. 1186–1201, 2008. ISSN 15333884. Page 34.

[70] YU, Xiang; FU, Yu; PENG, Xiaoyan. Fuzzy logic aided fault-tolerant control applied to transport aircraft subject to actuator stuck failures. **IEEE Transactions on Fuzzy Systems**, IEEE, v. 26, n. 4, p. 2050–2061, aug 2018. ISSN 10636706. Page 34.

[71] IJAZ, Salman; CHEN, Fuyang; Tariq Hamayun, Mirza. A new actuator fault-tolerant control for Lipschitz nonlinear system using adaptive sliding mode control strategy. **International Journal of Robust and Nonlinear Control**, John Wiley and Sons Ltd, v. 31, n. 6, p. 2305–2333, apr 2021. ISSN 10991239. Page 34.

[72] FASANO, Antonio; FERRACUTI, Francesco; FREDDI, Alessandro; LONGHI, Sauro; MONTERIÙ, Andrea. A virtual thruster-based failure tolerant control scheme for underwater vehicles. **IFAC-PapersOnLine**, Elsevier B.V., v. 28, n. 16, p. 146–151, oct 2015. ISSN 24058963. Page 34.

[73] YANG, Zhenyu; BLANKE, Mogens; VERHAGEN, Michel. Robust control mixer method for reconfigurable control design using model matching. **IET Control Theory & Applications**, APA, v. 1, n. 1, p. 349–357, jan 2007. ISSN 1751-8644. Page 34.

[74] SANTOS, Carlos Henrique Farias Dos; CARDOZO, Daisy Isabel Kang; REGINATTO, Romeu; PIERI, Edson Roberto De. Bank of controllers and virtual thrusters for fault-tolerant control of autonomous underwater vehicles. **Ocean Engineering**, Elsevier, v. 121, p. 210–223, 2016. ISSN 00298018. Page 34.

[75] HU, Qinglei; LI, Bo; WANG, Danwei; Kee Poh, Eng. Velocity-free fault-tolerant control allocation for flexible spacecraft with redundant thrusters. **International Journal of Systems Science**, v. 46, n. 6, p. 976–992, 2015. ISSN 14645319. Page 34.

[76] FU, Mingyu; NING, Jipeng; WEI, Yushi. Fault-tolerant control of dynamic positioning vessel after thruster failures using disturbance decoupling methods. In: **International Conference on Automation and Logistics**. Chongqing, China: IEEE, 2011. p. 433–437. ISBN 978-1-4577-0301-0. Pages 34, 43, and 66.

[77] FU, Mingyu; NING, Jipeng; WEI, Yushi. Fault-tolerant control of dynamic positioning vessel by means of a virtual thruster. In: **International Conference on Mechatronics and Automation**. Beijing, CHina: IEEE, 2011. p. 1706–1710. ISBN 978-1-4244-8113-2. Pages 34, 43, and 66.

[78] ISHIZAKI, Takayuki; SADAMOTO, Tomonori; IMURA, Jun-ichi; SANDBERG, Henrik; JOHANSSON, Karl Henrik. Retrofit control: Localization of controller design

and implementation. **Automatica**, Elsevier Ltd, v. 95, p. 336–346, sep 2018. ISSN 00051098. Pages 34 and 35.

[79] BOSKOVIC, Jovan D.; MEHRA, Raman K. An adaptive retrofit reconfigurable flight controller. In: **41st Conference on Decision and Control**. Las Vegas, NV, USA: IEEE, 2002. v. 2, n. December, p. 1257–1262. ISBN 0-7803-7516-5. ISSN 01912216. Pages 35 and 43.

[80] BOSKOVIC, Jovan; PRASANTH, Ravi; MEHRA, Raman. Retrofit Reconfigurable Flight Control. In: **AIAA Guidance, Navigation, and Control Conference and Exhibit**. Reston, VA, USA: American Institute of Aeronautics and Astronautics, 2005. p. 1–11. ISBN 978-1-62410-056-7. Page 35.

[81] BOSKOVIC, Jovan D.; PRASANTH, Ravi; MEHRA, Raman K. Retrofit Fault-Tolerant Flight Control Design Under Control Effector Damage. **Journal of Guidance, Control, and Dynamics**, v. 30, n. 3, p. 703–712, may 2007. ISSN 0731-5090. Page 35.

[82] YU, Xiang; ZHENG, Zhiqiang; ZHANG, Youmin; LU, Xingju. Adaptive retrofit fault-tolerant flight controller design. **European Control Conference**, IEEE, p. 1662–1667, 2009. Page 35.

[83] LANGEWIESCHE, William. **What Really Brought Down the Boeing 737 Max?** 2019. Disponível em: <https://www.nytimes.com/2019/09/18/magazine/boeing-737-max-crashes.html>. Page 35.

[84] SADAMOTO, Tomonori; CHAKRABORTTY, Aranya; ISHIZAKI, Takayuki; IMURA, Jun Ichi. A retrofitting-based supplementary controller design for enhancing damping performance of wind power systems. **Proceedings of the American Control Conference**, AACC, p. 2755–2760, 2017. ISSN 07431619. Pages 35 and 177.

[85] SADAMOTO, Tomonori; CHAKRABORTTY, Aranya; ISHIZAKI, Takayuki; IMURA, Jun Ichi. Retrofit Control of Wind-Integrated Power Systems. **IEEE Transactions on Power Systems**, IEEE, v. 33, n. 3, p. 2804–2815, 2018. ISSN 08858950. Pages 35 and 177.

[86] SASAHARA, Hampei; ISHIZAKI, Takayuki; SADAMOTO, Tomonori; MASUTA, Taisuke; UEDA, Yuzuru; SUGIHARA, Hideharu; YAMAGUCHI, Nobuyuki; IMURA, Jun ichi. Damping performance improvement for PV-integrated power grids via retrofit control. **Control Engineering Practice**, Elsevier Ltd, v. 84, n. December 2018, p. 92–101, 2019. ISSN 09670661. Pages 35 and 177.

[87] ISHIZAKI, Takayuki; SASAHARA, Hampei; INOUE, Masaki; KAWAGUCHI, Takahiro; IMURA, Jun Ichi. Modularity in design of dynamical network systems: Retrofit

control approach. **IEEE Transactions on Automatic Control**, IEEE, v. 66, n. 11, p. 5205–5220, 2021. ISSN 15582523. Pages 35 and 177.

[88] NAHARUDINSYAH, Ilham; ISHIZAKI, Takayuki; KAWAGUCHI, Takahiro; IMURA, Jun-ichi. Model Predictive Control Based Data-Driven Retrofit Controller for Network Systems. In: **Conference on Control Technology and Applications (CCTA)**. Hong Kong, China: IEEE, 2019. p. 215–220. ISBN 978-1-7281-2767-5. Pages 35 and 177.

[89] LIU, Zhixiang; YUAN, Chi; YU, Xiang; ZHANG, Youmin. Retrofit fault-tolerant tracking control design of an unmanned quadrotor helicopter considering actuator dynamics. **International Journal of Robust and Nonlinear Control**, v. 29, n. 16, p. 5293–5313, nov 2019. ISSN 1049-8923. Page 35.

[90] SHU, Han; ZHANG, Xuan; LI, Na; PAPACHRISTODOULOU, Antonis. Control Reconfiguration of Dynamical Systems for Improved Performance via Reverse- and Forward-Engineering. **IEEE Transactions on Automatic Control**, v. 67, n. 3, p. 1490–1497, mar 2022. ISSN 0018-9286. Page 35.

[91] LIAO, Jianquan; YOU, Xiaoyao; LIU, Heping; HUANG, Yuansheng. Voltage stability improvement of a bipolar DC system connected with constant power loads. **Electric Power Systems Research**, Elsevier Ltd, v. 201, dec 2021. ISSN 03787796. Page 35.

[92] LI, Chang; YANG, Yaqian; DRAGICEVIC, Tomislav; BLAABJERG, Frede. A New Perspective for Relating Virtual Inertia With Wideband Oscillation of Voltage in Low-Inertia DC Microgrid. **IEEE Transactions on Industrial Electronics**, IEEE, v. 69, n. 7, p. 7029–7039, jul 2022. ISSN 0278-0046. Page 35.

[93] KUMAR, Ramesh; SHARMA, Rahul; KUMAR, Ashwani. Adaptive negative impedance strategy for stability improvement in DC microgrid with constant power loads. **Computers and Electrical Engineering**, Elsevier Ltd, v. 94, sep 2021. ISSN 00457906. Page 35.

[94] PANG, Shengzhao; NAHID-MOBARAKEH, Babak; PIERFEDERICI, Serge; HUANGFU, Yigeng; LUO, Guangzhao; GAO, Fei. Toward Stabilization of Constant Power Loads Using IDA-PBC for Cascaded LC Filter DC/DC Converters. **IEEE Journal of Emerging and Selected Topics in Power Electronics**, IEEE, v. 9, n. 2, p. 1302–1314, apr 2021. ISSN 21686785. Page 35.

[95] CHENG, Zhiping; GONG, Meng; GAO, Jinfeng; LI, Zhongwen; SI, Jikai. Research on virtual inductive control strategy for direct current microgrid with constant power loads. **Applied Sciences (Switzerland)**, MDPI AG, v. 9, 10 2019. ISSN 20763417. Pages 35 and 177.

[96] MAGNE, Pierre; MARX, Didier; NAHID-MOBARAKEH, Babak; PIERFEDERICI, Serge. Large-Signal Stabilization of a DC-Link Supplying a Constant Power Load Using a Virtual Capacitor: Impact on the Domain of Attraction. **IEEE Transactions on Industry Applications**, v. 48, n. 3, p. 878–887, may 2012. ISSN 0093-9994. Pages 35 and 177.

[97] XIAO, Bing; FU, Zhengzhou; YANG, Jia; WU, Chaofan; HUO, Xing. Retrofit reconfigurable fault tolerant control for mechanical systems. **Proceedings of the 11th Conference on Industrial Electronics and Applications, ICIEA 2016**, IEEE, p. 462–467, 2016. Page 35.

[98] ISHIZAKI, Takayuki; KAWAGUCHI, Takahiro; SASAHARA, Hampei; IMURA, Jun ichi. Retrofit control with approximate environment modeling. **Automatica**, Elsevier Ltd, v. 107, p. 442–453, 2019. ISSN 00051098. Page 35.

[99] SASAHARA, Hampei; ISHIZAKI, Takayuki; IMURA, Jun-ichi. Parameterization of All Output-Rectifying Retrofit Controllers. **IEEE Transactions on Automatic Control**, p. 1–7, 2021. ISSN 0018-9286. Early Access. Page 35.

[100] BODENBURG, Sven; VEY, Daniel; LUNZE, Jan. Plug-and-play reconfiguration of decentralised controllers of interconnected systems. **IFAC-PapersOnLine**, Elsevier B.V., v. 28, n. 21, p. 353–359, 2015. ISSN 24058963. Pages 36, 48, and 66.

[101] KHODABANDEH, Sepehr; KHARRATI, Hamed; HASHEMZADEH, Farzad. Control for Leader–Follower Consensus of Multi-agent Systems with Actuator Faults Using Decentralized Robust Fault-tolerant Control. **Iranian Journal of Science and Technology - Transactions of Electrical Engineering**, Springer, 2020. ISSN 23641827. Pages 40 and 66.

[102] RICHTER, Jan H.; LUNZE, Jan. Reconfigurable control of hammerstein systems after actuator failures: stability, tracking, and performance. **International Journal of Control**, Taylor & Francis, v. 83, n. 8, p. 1612–1630, 2010. Pages 40, 45, 57, and 66.

[103] RICHTER, Jan H.; LUNZE, Jan; JAN, Lunze. H_∞-based virtual actuator synthesis for optimal trajectory recovery. **IFAC Proceedings Volumes**, IFAC, v. 42, n. 8, p. 1587–1592, 2009. ISSN 14746670. Pages 40, 44, and 66.

[104] KROKAVEC, Dušan; FILASOVÁ, Anna; SERBÁK, Vladimír; LIŠčINSKý, Pavol. H_∞ Approach to Virtual Actuators Design. In: **Advanced and Intelligent Computations in Diagnosis and Control**. Cham: Springer International Publishing, 2016. p. 209–222. ISBN 9783319231808. Pages 40 and 66.

[105] QUADROS, Mariella Maia; LEITE, Valter J.S.; PALHARES, Reinaldo Martínez. Robust fault hiding approach for T–S fuzzy systems with unmeasured premise variables.

Information Sciences, v. 589, p. 690–715, apr 2022. ISSN 00200255. Pages 40, 43, 46, 47, 50, 51, 62, 63, 66, 69, and 172.

[106] BESSA, Iury; CAMARGOS, Murilo Osorio; PUIG, Vicenç; PALHARES, Reinaldo Martinez. Dissipativity and stability recovery by fault hiding. In: **IFAC-PapersOnLine**. Berlin, Germany: Elsevier B.V., 2020. v. 53, p. 4121–4126. ISSN 24058963. Pages 40, 47, 52, 57, 66, 127, 128, 170, and 175.

[107] ROTONDO, Damiano; PUIG, Vicenç; NEJJARI, Fatiha; WITCZAK, Marcin. Automated generation and comparison of takagi–sugeno and polytopic quasi-LPV models. **Fuzzy Sets and Systems**, Elsevier BV, v. 277, p. 44–64, out. 2015. Page 41.

[108] LUNZE, Jan H.; STEFFEN, Thomas. Control reconfiguration by means of a virtual actuator. **IFAC Proceedings Volumes (IFAC-PapersOnline)**, Elsevier, v. 36, n. 5, p. 131–136, jun 2003. ISSN 14746670. Pages 42, 43, and 66.

[109] LUNZE, Jan; STEFFEN, Thomas. Control reconfiguration after actuator failures using disturbance decoupling methods. **IEEE Transactions on Automatic Control**, v. 51, n. 10, p. 1590–1601, Oct 2006. Pages 43, 44, 53, and 66.

[110] LUNZE, Jan. Control reconfiguration after actuator failures: The generalised virtual actuator. **IFAC Proceedings Volumes (IFAC-PapersOnline)**, IFAC Secretariat, v. 6, n. PART 1, p. 1240–1245, 2006. ISSN 14746670. Pages 43, 44, and 66.

[111] RICHTER, Jan H.; LUNZE, Jan. Reconfigurable Control of Hammerstein Systems after Actuator Faults. **IFAC Proceedings Volumes**, IFAC, v. 41, n. 2, p. 3210–3215, 2008. ISSN 14746670. Pages 43, 44, 45, 57, 63, and 66.

[112] RICHTER, Jan H.; HEEMELS, W. P. M. H.; WOUW, Nathan van de; LUNZE, Jan. Reconfigurable control of PWA systems with actuator and sensor faults: Stability. In: **47th Conference on Decision and Control**. Cancun, Mexico: IEEE, 2008. p. 1060–1065. Pages 43, 44, 45, 57, and 66.

[113] SERON, María M.; DE DONÁ, José A. Fault tolerant control using virtual actuators and invariant-set based fault detection and identification. In: **48th Conference on Decision and Control**. Shangai, China: IEEE, 2009. p. 7801–7806. ISBN 9781424438716. ISSN 01912216. Pages 43, 50, and 66.

[114] OCA, Saúl Montes Saul Montes de; PUIG, Vicenç. Fault-tolerant control design using a virtual sensor for LPV systems. **Conference on Control and Fault-Tolerant Systems, SysTol'10**, IEEE, n. 1, p. 88–93, oct 2010. Pages 43, 45, 46, 53, 63, and 66.

[115] OCA, Saúl Montes de; PUIG, Vicenç. Fault-tolerant control using a virtual actuator using LPV techniques: Application to a two-degree of freedom helicopter. **IFAC Proceedings Volumes (IFAC-PapersOnline)**, v. 18, n. PART 1, p. 416–421, 2010. ISSN 14746670. Pages 43, 46, 63, and 66.

[116] SERON, María M.; DE DONÁ, José A.; RICHTER, Jan H. Bank of virtual actuators for fault tolerant control. **IFAC Proceedings Volumes (IFAC-PapersOnline)**, IFAC, v. 44, n. 1 PART 1, p. 5436–5441, 2011. ISSN 14746670. Pages 43, 50, and 66.

[117] FILASOVÁ, Anna; SERBÁK, Vladimír. Design of Fuzzy Based Virtual Actuator for a Class of Nonlinear Systems. **Advances in Electrical and Electronic Engineering**, v. 10, n. 2, p. 75–80, jun 2012. ISSN 1804-3119. Pages 43, 46, and 66.

[118] RICHTER, Jan H.; SERON, María M.; DE DONÁ, José A. Virtual actuator for Lure systems with Lipschitz-continuous nonlinearity. **IFAC Proceedings Volumes (IFAC-PapersOnline)**, IFAC, v. 8, n. PART 1, p. 222–227, 2012. ISSN 14746670. Pages 43, 45, 56, 57, and 66.

[119] ROTONDO, Damiano; PUIG, Vicenç; Acevedo Valle, Juan M.; NEJJARI, Fatiha. FTC of LPV systems using a bank of virtual sensors: Application to wind turbines. In: **Conference on Control and Fault-Tolerant Systems (SysTol)**. Nice, France: IEEE, 2013. p. 492–497. ISBN 978-1-4799-2855-2. ISSN 21621195. Pages 43, 46, 50, 53, 63, and 66.

[120] ROTONDO, Damiano; NEJJARI, Fatiha; PUIG, Vicenç. A virtual actuator and sensor approach for fault tolerant control of LPV systems. **Journal of Process Control**, v. 24, n. 3, p. 203–222, 2014. ISSN 0959-1524. Pages 43, 46, 53, 63, and 66.

[121] TABATABAEIPOUR, S. Mojtaba; GALEAZZI, Roberto. Reconfigurable control of input affine nonlinear systems under actuator fault. **IFAC-PapersOnLine**, Elsevier B.V., v. 28, n. 21, p. 345–352, sep 2015. ISSN 24058963. Pages 43, 47, 56, 57, 63, and 66.

[122] VEY, D.; LUNZE, J.; ŽÁCEKOVÁ, E.; PCOLKA, M.; ŠEBEK, M. Control reconfiguration of full-state linearizable systems by a virtual actuator. **IFAC-PapersOnLine**, v. 28, n. 21, p. 339–344, sep 2015. ISSN 24058963. Pages 43, 47, 63, and 66.

[123] ROTONDO, Damiano; PONSART, Jean-Christophe; THEILLIOL, Didier; NEJJARI, Fatiha; PUIG, Vicenç. A virtual actuator approach for the fault tolerant control of unstable linear systems subject to actuator saturation and fault isolation delay. **Annual Reviews in Control**, v. 39, p. 68 – 80, 2015. ISSN 1367-5788. Pages 43, 51, 66, 69, 79, and 173.

[124] KROKAVEC, D.; FILASOVâ, A.; SERBáK, V. FTC structures with virtual actuators and dynamic output controllers. **IFAC-PapersOnLine**, v. 28, n. 21, p. 511–516, sep 2015. ISSN 24058963. Page 43.

[125] MCCLOY, Ryan J.; DE DONÁ, José A.; SERON, María M. Sensor reintegration in the fault tolerant control of linear parameter varying systems. **Australian Control Conference**, p. 294–299, 2015. Pages 43 and 46.

[126] WANG, Ye; ROTONDO, Damiano; PUIG, Vicenç; CEMBRANO, Gabriela; ZHAO, Yuxin. Fault-tolerant Control of Discrete-time Descriptor Systems using Virtual Actuators. In: **4th Conference on Control and Fault Tolerant Systems (SysTol)**. Casablanca, Morocco: IEEE, 2019. p. 147–152. ISBN 978-1-7281-0380-8. Pages 43, 60, and 66.

[127] BESSA, Iury; PUIG, Vicenç; PALHARES, Reinaldo Martinez. TS fuzzy reconfiguration blocks for fault tolerant control of nonlinear systems. **Journal of the Franklin Institute**, Elsevier Ltd, v. 357, n. 8, p. 4592–4623, may 2020. ISSN 00160032. Pages 43, 46, 48, 49, 52, 59, 64, 66, 88, 154, 170, and 175.

[128] QUADROS, Mariella Maia; BESSA, Iury de; LEITE, Valter J.S.; PALHARES, Reinaldo Mart'ıinez. Fault tolerant control for linear parameter varying systems: An improved robust virtual actuator and sensor approach. **ISA Transactions**, ISA - Instrumentation, Systems, and Automation Society, v. 104, p. 356–369, sep 2020. ISSN 00190578. Pages 43, 46, 50, 63, 66, 69, 171, 172, and 173.

[129] BESSA, Iury; PUIG, Vicenç; PALHARES, Reinaldo Martínez. Passivation blocks for fault tolerant control of nonlinear systems. **Automatica**, Elsevier Ltd, v. 125, p. 109450, mar 2021. ISSN 00051098. Pages 43, 47, 48, 52, 58, 64, 66, 170, 174, and 175.

[130] REZENDE, Pedro Henrique V.; SENCIO, Rafael R.; COSTA, Thiago V. Fault-tolerant control and interval operability for non-square faulty systems. **Brazilian Journal of Chemical Engineering**, Springer International Publishing, v. 38, n. 4, p. 763–775, 2021. ISSN 01046632. Pages 43, 44, 60, 63, 66, and 176.

[131] COSTA, Thiago V.; SENCIO, Rafael R.; OLIVEIRA-LOPES, Luís Cláudio; SILVA, Flávio V. Fault-tolerant control by means of moving horizon virtual actuators: Concepts and experimental investigation. **Control Engineering Practice**, Elsevier Ltd, v. 107, feb 2021. ISSN 09670661. Pages 43, 44, 60, 63, 66, and 176.

[132] RICHTER, Jan H.; SCHLAGE, T.; LUNZE, Jan. Control reconfiguration of a thermofluid process by means of a virtual actuator. **IET Control Theory and Applications**, v. 1, n. 6, p. 1606–1620, 2007. ISSN 17518644. Pages 44 and 66.

[133] RICHTER, Jan H.; LUNZE, Jan; SCHLAGE, Thorsten. Control reconfiguration after actuator failures by Markov parameter matching. **International Journal of Control**, v. 81, n. 9, p. 1382–1398, sep 2008. ISSN 00207179. Pages 44 and 66.

[134] RICHTER, Jan H.; WEILAND, Siep; HEEMELS, W. P.M.H. M. H.; LUNZE, Jan. Decoupling-based reconfigurable control of linear systems after actuator faults. **European Control Conference**, IEEE, p. 2512–2517, aug 2009. Pages 44 and 66.

[135] MORADI AMANI, Ali; AFSHAR, Ahmad; MENHAJ, Mohamad Bagher. Fault tolerant control of networked control system in presence of actuator failure using predictive reconfiguration. In: **International Conference on Control and Automation**. Christchurch, New Zealand: IEEE, 2009. p. 477–482. ISBN 978-1-4244-4706-0. Pages 44, 49, 59, and 66.

[136] RICHTER, Jan H.; HEEMELS, W.P.M.H.; WOUW, N.; LUNZE, Jan. Reconfigurable control of piecewise affine systems with actuator and sensor faults: Stability and tracking. **Automatica**, v. 47, n. 4, p. 678–691, 2011. ISSN 0005-1098. Pages 45, 57, 66, and 153.

[137] BOYD, Stephen; GHAOUI, Laurent El; FERON, Eric; BALAKRISHNAN, Venkataramanan. **Linear matrix inequalities in system and control theory**. Philadelphia, PA: SIAM, 1994. Page 45.

[138] COUTINHO, Pedro Henrique S.; LAUBER, Jimmy; BERNAL, Miguel; PALHARES, Reinaldo M. Efficient LMI Conditions for Enhanced Stabilization of Discrete-Time Takagi–Sugeno Models via Delayed Nonquadratic Lyapunov Functions. **IEEE Transactions on Fuzzy Systems**, v. 27, n. 9, p. 1833–1843, 2019. Page 45.

[139] KHALIL, H.K. **Nonlinear Systems**. Upper Saddle River, NJ: Prentice Hall, 2000. ISBN 9780131227408. Pages 45, 71, 73, 89, 127, and 130.

[140] KHOSROWJERDI, M. J.; BARZEGARY, S. Reconfigurable control of nonlinear Lipschitz systems after actuator faults. **Proceedings of 2nd International Conference on Control, Instrumentation and Automation**, IEEE, p. 715–720, dec 2011. Pages 45, 57, and 66.

[141] KHOSROWJERDI, Mohammad; BARZEGARY, Soheila. Fault tolerant control using virtual actuator for continuous–time lipschitz nonlinear systems. **International Journal of Robust and Nonlinear Control**, v. 24, n. 16, p. 2597–2607, 2014. ISSN 1099-1239. Pages 45, 57, and 66.

[142] PEDERSEN, Andreas S.; RICHTER, Jan H.; TABATABAEIPOUR, Mojtaba; JÓHANNSSON, Hjörtur; BLANKE, Mogens. Stabiliser fault emergency control using reconfiguration to preserve power system stability. **IFAC Proceedings Volumes**

(IFAC-PapersOnline), v. 19, n. 11, p. 9093–9098, 2014. ISSN 14746670. Pages 45, 48, 49, 57, and 66.

[143] PEDERSEN, Andreas; RICHTER, Jan; TABATABAEIPOUR, Mojtaba; JÓHANNSSON, Hjörtur; BLANKE, Mogens. Fault tolerant emergency control to preserve power system stability. **Control Engineering Practice**, v. 53, p. 151–159, 2016. ISSN 0967-0661. Pages 45, 48, 49, 57, and 66.

[144] TABATABAEIPOUR, S. M.; STOUSTRUP, J.; BAK, T. Reconfigurable control of input affine nonlinear systems under actuator fault. **IFAC-PapersOnLine**, Elsevier B.V., v. 45, n. 20 PART 1, p. 818–823, 2012. ISSN 14746670. Pages 46 and 66.

[145] TABATABAEIPOUR, Mojtaba S; STOUSTRUP, Jakob; BAK, Thomas. Fault-tolerant control of discrete-time LPV systems using virtual actuators and sensors. **International Journal of Robust and Nonlinear Control**, v. 25, n. 5, p. 707–734, 2015. ISSN 1049-8923. Pages 46, 47, 53, 63, and 66.

[146] ROTONDO, Damiano; PUIG, Vicenç; NEJJARI, Fatiha; ROMERA, Juli. A Fault-Hiding approach for the switching Quasi-LPV Fault-Tolerant control of a Four-Wheeled omnidirectional mobile robot. **IEEE Transactions on Industrial Electronics**, v. 62, n. 6, p. 3932–3944, 2015. ISSN 0278-0046. Pages 46, 51, 60, 63, and 66.

[147] OCA, Saúl; PUIG, Vicenç; WITCZAK, Marcin; DZIEKAN, Łukasz. Fault-tolerant control strategy for actuator faults using LPV techniques: Application to a two degree of freedom helicopter. **International Journal of Applied Mathematics and Computer Science**, n. 1, p. 161–171, 2012. ISSN 1641-876X. Pages 46, 52, 63, and 66.

[148] ROTONDO, Damiano; NEJJARI, Fatiha; PUIG, Vicenç; BLESA, Joaquim. Model reference FTC for LPV systems using virtual actuators and set-membership fault estimation. **International Journal of Robust and Nonlinear Control**, v. 25, n. 5, p. 735–760, 2015. ISSN 1099-1239. Pages 46, 51, and 66.

[149] ROTONDO, Damiano; NEJJARI, Fatiha; PUIG, Vicenç. Fault estimation and virtual actuator FTC approach for LPV systems. **IFAC Proceedings Volumes (IFAC-PapersOnline)**, IFAC Secretariat, v. 8, n. PART 1, p. 824–829, 2012. ISSN 14746670. Pages 46, 51, and 66.

[150] NAZARI, Raheleh; SERON, María M.; DE DONÁ, José A. Fault-tolerant control of systems with convex polytopic linear parameter varying model uncertainty using virtual-sensor-based controller reconfiguration. **Annual Reviews in Control**, Elsevier Ltd, v. 37, n. 1, p. 146–153, apr 2013. ISSN 13675788. Pages 46 and 66.

[151] NAZARI, Raheleh; SERON, María M.; DE DONÁ, José A. On virtual actuators for LPV systems under errors in the measurement of the varying parameter. **Australian Control Conference**, n. 1, p. 148–152, 2015. Pages 46 and 47.

[152] NAZARI, Raheleh; SERON, María M.; DE DONÁ, José A. Set-based fault-tolerant control of convex polytopic LPV systems using a bank of virtual actuators. **IFAC Proceedings Volumes (IFAC-PapersOnline)**, v. 19, n. 3, p. 6722–6727, 2014. ISSN 14746670. Pages 46, 50, and 66.

[153] ROTONDO, Damiano; PUIG, Vicenç; NEJJARI, Fatiha. A bank of virtual sensors for active Fault Tolerant Control of LPV systems. IEEE, p. 252–257, jun 2014. Pages 46, 50, 53, and 66.

[154] ROTONDO, Damiano; PUIG, Vicenç; NEJJARI, Fatiha. Fault tolerant control of a PEM fuel cell using qLPV virtual actuators. **IFAC-PapersOnLine**, v. 28, n. 21, p. 271–276, sep 2015. ISSN 24058963. Pages 46, 63, and 66.

[155] ROTONDO, Damiano; PONSART, Jean Christophe; THEILLIOL, Didier; NEJJARI, Fatiha; PUIG, Vicenç. Fault tolerant control of unstable LPV systems subject to actuator saturations using virtual actuators. **IFAC-PapersOnLine**, v. 28, n. 21, p. 18–23, sep 2015. ISSN 24058963. Pages 46 and 66.

[156] LUZAR, Marcel; WITCZAK, Marcin. Fault-tolerant control and diagnosis for LPV system with H-infinity virtual sensor. **Conference on Control and Fault-Tolerant Systems**, IEEE, v. 2016-Novem, p. 825–830, sep 2016. ISSN 21621209. Pages 46, 53, and 66.

[157] ROTONDO, Damiano; PONSART, Jean-Christophe Christophe; NEJJARI, Fatiha; THEILLIOL, Didier; PUIG, Vicenç. Virtual actuator-based FTC for LPV systems with saturating actuators and FDI delays. **Conference on Control and Fault-Tolerant Systems, SysTol**, IEEE, v. 2016-Novem, p. 831–837, sep 2016. ISSN 21621209. Pages 46, 51, and 66.

[158] BEHZAD, Hamid; CASAVOLA, Alessandro; TEDESCO, Francesco; SADRNIA, Mohammad Ali; GAGLIARDI, Gianfranco. A fault-tolerant sensor reconciliation scheme based on self-tuning LPV observers. In: **15th International Conference on Informatics in Control, Automation and Robotics**. Porto, Portugal: SciTePress, 2018. v. 1, p. 111–118. ISBN 9789897583216. Pages 46, 51, 63, and 66.

[159] BEHZAD, Hamid; CASAVOLA, Alessandro; TEDESCO, Francesco; SADRNIA, Mohammad Ali. Use of LPV-LFT Unknown Input Observers for the Design of Fault Tolerant Sensor Reconciliation Schemes. In: **Iranian Conference on Electrical Engineering**. Mashhad, Iran: IEEE, 2018. p. 899–905. ISBN 978-1-5386-4914-5. Pages 46, 51, 63, and 66.

[160] CHOUIREF, Houda; BOUSSAID, Boumedyen; ABDELKRIM, Mohamed Naceur; PUIG, Vicenç; AUBRUN, Christophe. Integrated FDI/FTC approach for wind turbines

using a LPV interval predictor subspace approach and virtual sensors/actuators. **Proceedings of the Institution of Mechanical Engineers, Part A: Journal of Power and Energy**, SAGE Publications Ltd, v. 235, n. 6, p. 1527–1543, sep 2021. ISSN 20412967. Pages 46, 50, and 66.

[161] MA, Yan-Hua; DU, Xian; SUN, Xi-Ming; ZHAO, Fang-Jiao. Active fault tolerant tracking control of turbofan engine based on virtual actuator. **ISA Transactions**, Elsevier BV, v. 122, p. 247–259, mar. 2022. Pages 46 and 66.

[162] ROTONDO, Damiano; NEJJARI, Fatiha; PUIG, Vicenç. Fault tolerant control of a proton exchange membrane fuel cell using Takagi–Sugeno virtual actuators. **Journal of Process Control**, v. 45, p. 12–29, 2016. ISSN 0959-1524. Pages 12, 46, 53, 63, 66, 105, 106, 107, 108, 109, 110, 111, and 112.

[163] KROKAVEC, Dušan; FILASOVÁ, Anna; LIŠčINSKý, Pavol. PI fuzzy virtual actuator design for Takagi-Sugeno systems. **Proceedings of the 2016 17th International Carpathian Control Conference, ICCC 2016**, IEEE, n. 4, p. 390–395, may 2016. Pages 46, 53, 60, and 66.

[164] FILASOVÁ, Anna; KROKAVEC, Dušan; LIŠčINSKý, Pavol. Relaxed formulation of the design conditions for Takagi–Sugeno fuzzy virtual actuators. **Archives of Control Sciences**, v. 26, n. 2, p. 199–221, 2016. Pages 46 and 66.

[165] KROKAVEC, Dušan; FILASOVá, Anna; SERBáK, Vladimír. Virtual actuator based fault tolerant control design for Takagi-Sugeno fuzzy systems. **14th International Symposium on Applied Machine Intelligence and Informatics**, IEEE, p. 63–68, jan 2016. Pages 46 and 66.

[166] GALAVIZH, Alireza; HASSANABADI, Amir Hossein. Designing Fuzzy Fault Tolerant Controller for a DC Microgrid Based on Virtual Sensor. In: **7th International Conference on Control, Instrumentation and Automation**. Tabriz, Iran: IEEE, 2021. p. 1–6. ISBN 978-1-6654-0350-4. Pages 46 and 66.

[167] DZIEKAN, Ł.; WITCZAK, M.; KORBICZ, J. Active fault-tolerant control design for Takagi-Sugeno fuzzy systems. **Bulletin of the Polish Academy of Sciences: Technical Sciences**, v. 59, n. 1, p. 93–102, mar 2011. ISSN 0239-7528. Pages 46 and 66.

[168] FILASOVÁ, Anna; KROKAVEC, Dušan; SERBÁK, Vladim'ır. Design of FTC structures with PI virtual actuators. **Journal of Physics: Conference Series**, v. 659, n. 1, p. 012007, 2015. Pages 46, 60, and 66.

[169] YONEYAMA, Jun; NISHIKAWA, Masahiro; KATAYAMA, Hitoshi; ICHIKAWA, Akira. h_∞ control for takagi–sugeno fuzzy systems. **International Journal of Systems Science**, Taylor & Francis, v. 32, n. 7, p. 915–924, jan. 2001. Page 46.

[170] YONEYAMA, Jun. h_∞ filtering for fuzzy systems with immeasurable premise variables: An uncertain system approach. **Fuzzy Sets and Systems**, Elsevier BV, v. 160, n. 12, p. 1738–1748, jun. 2009. Page 46.

[171] ICHALAL, D.; MARX, B.; RAGOT, J.; MAQUIN, D. State estimation of Takagi–Sugeno systems with unmeasurable premise variables. **IET Control Theory & Applications**, Institution of Engineering and Technology (IET), v. 4, n. 5, p. 897–908, maio 2010. Page 46.

[172] NGUANG, Sing Kiong; SHI, Peng. H_∞ fuzzy output feedback control design for nonlinear systems: an LMI approach. **IEEE Transactions on Fuzzy Systems**, IEEE, v. 11, n. 3, p. 331–340, jun. 2003. Page 46.

[173] GHORBEL, H.; HAJJAJI, A. El; SOUISSI, M.; CHAABANE, M. Fault–tolerant trajectory tracking control for takagi–sugeno systems with unmeasurable premise variables: Descriptor approach. **Circuits, Systems, and Signal Processing**, Springer Science and Business Media LLC, v. 33, n. 6, p. 1763–1781, jan. 2014. Page 47.

[174] AOUAOUDA, S.; CHADLI, M.; KHADIR, M. Tarek; BOUARAR, T. Robust fault tolerant tracking controller design for unknown inputs T–S models with unmeasurable premise variables. **Journal of Process Control**, Elsevier BV, v. 22, n. 5, p. 861–872, jun. 2012. Page 47.

[175] EL-MADBOULY, Essam I; HAMEED, Ibrahim A; ABDO, Mohamed I. Reconfigurable adaptive fuzzy fault-hiding control for greenhouse climate control system. **Int. J. Automation and Control**, v. 11, n. 2, p. 164–187, 2017. Pages 47, 64, and 66.

[176] STETTER, Ralf. A Virtual Fuzzy Actuator for the Fault-tolerant Control of a Rescue Vehicle. In: **International Conference on Fuzzy Systems (FUZZ-IEEE)**. Glasgow, UK: IEEE, 2020. p. 1–8. ISBN 978-1-7281-6932-3. Pages 47, 64, and 66.

[177] STETTER, Ralf. A fuzzy virtual actuator for automated guided vehicles. **Sensors (Switzerland)**, MDPI AG, v. 20, n. 15, p. 1–23, aug 2020. ISSN 14248220. Pages 47, 64, and 66.

[178] KOTTENSTETTE, Nicholas; MCCOURT, Michael J.; XIA, M.; GUPTA, Vijay; ANTSAKLIS, Panos J. On relationships among passivity, positive realness, and dissipativity in linear systems. **Automatica**, v. 50, n. 4, p. 1003 – 1016, 2014. ISSN 0005-1098. Pages 48, 127, 130, 141, 146, and 147.

[179] MORADI AMANI, Ali; POORJANDAGHI, Seyyed Saeed; AFSHAR, Ahmad; MENHAJ, Mohamad Bagher. Fault tolerant control of large-scale systems subject to actuator fault using a cooperative approach. **Proceedings of the Institution of Mechanical Engineers, Part I: Journal of Systems and Control Engineering**,

SAGE Publications Ltd, v. 228, n. 2, p. 63–77, feb 2014. ISSN 0959-6518. Pages 48, 66, and 177.

[180] VEY, D.; HÜGGING, S.; BODENBURG, S.; LUNZE, J. Control reconfiguration of physically interconnected systems by decentralized virtual actuators. **IFAC-PapersOnLine**, v. 28, n. 21, p. 360–367, sep 2015. ISSN 24058963. Pages 48, 60, and 66.

[181] FURNO, Lidia; NIELSEN, Mikkel Cornelius; BLANKE, Mogens. Centralised versus decentralised control reconfiguration for collaborating underwater robots. **IFAC-PapersOnLine**, Elsevier B.V., v. 28, n. 21, p. 732–739, sep 2015. ISSN 24058963. Pages 48 and 60.

[182] SCHENK, Kai; LUNZE, Jan. Fault-tolerant control in networked systems: A two-layer approach. In: **56th Annual Conference on Decision and Control**. Melbourne, VIC, Australia: IEEE, 2017. p. 6370–6376. ISBN 978-1-5090-2873-3. Pages 48, 49, and 66.

[183] ZHOU, Fujiao; CAO, Kecai. Formation Fault Tolerant Control of Multi-UAV Based on Virtual Actuator. **Proceedings of 5th International Conference on Cloud Computing and Intelligence Systems**, IEEE, p. 28–32, nov 2018. Pages 48 and 66.

[184] TARPØ, Marius; AMADOR, Sandro; KATSANOS, Evangelos; SKOG, Mattias; GJØDVAD, Johan; BRINCKER, Rune. Data-driven virtual sensing and dynamic strain estimation for fatigue analysis of offshore wind turbine using principal component analysis. **Wind Energy**, v. 25, n. 3, p. 505–516, mar 2022. ISSN 1095-4244. Pages 48, 66, and 174.

[185] RAOUFAT, M. Ehsan; TOMSOVIC, Kevin; DJOUADI, Seddik M. Virtual Actuators for Wide-Area Damping Control of Power Systems. **IEEE Transactions on Power Systems**, IEEE, v. 31, n. 6, p. 4703–4711, nov 2016. ISSN 08858950. Pages 49 and 66.

[186] MORADI AMANI, Ali; AFSHAR, Ahmad; MENHAJ, Mohamad Bagher. Fault Tolerant Networked Control Systems subject to actuator failure using virtual actuator technique. **IFAC Proceedings Volumes (IFAC-PapersOnline)**, IFAC, v. 44, n. 1 PART 1, p. 5465–5470, 2011. ISSN 14746670. Pages 49 and 66.

[187] OSELLA, Esteban; HAIMOVICH, Hernan; SERON, Maria M. Fault-tolerant control under controller-driven sampling using a virtual actuator strategy. **3rd Australian Control Conference (AUCC)**, Engineers Australia, p. 289–294, nov 2013. Pages 49, 66, and 177.

[188] OSELLA, Esteban N.; HAIMOVICH, Hernan; SERON, María M. Integration of invariant-set-based FDI with varying sampling rate virtual actuator and controller. **International Journal of Adaptive Control and Signal Processing**, John Wiley and Sons Ltd, v. 30, n. 2, p. 393–411, feb 2016. ISSN 08906327. Pages 49, 50, 60, 66, and 177.

[189] SERON, María M.; DE DONÁ, José A.; RICHTER, Jan. Fault tolerant control using virtual actuators and set-separation detection principles. **International Journal of Robust and Nonlinear Control**, v. 22, n. 7, p. 709–742, may 2012. ISSN 10498923. Pages 50, 66, and 173.

[190] SERON, María M.; DE DONÁ, José A.; RICHTER, Jan H. Integrated sensor and actuator fault-tolerant control. **International Journal of Control**, v. 86, n. 4, p. 689–708, apr 2013. ISSN 00207179. Page 50.

[191] CIESLAK, J.; HENRY, D. A Switching Fault-Hiding Mechanism based on Virtual Actuators and Dwell-Time Conditions. **IFAC-PapersOnLine**, Elsevier B.V., v. 51, n. 24, p. 703–708, jan 2018. ISSN 24058963. Pages 50, 66, and 172.

[192] ZHOU, Meng; QI, Juntong; WANG, Zhenhua; SHEN, Yi. Fault diagnosis and robust fault-tolerant control for linear over-actuated systems. **Proceedings of the Institution of Mechanical Engineers, Part G: Journal of Aerospace Engineering**, v. 230, n. 5, p. 832–844, apr 2016. ISSN 0954-4100. Pages 51 and 66.

[193] QI, Juntong; WANG, Zhenhua; SHEN, Yi. Fault-tolerant control and optimal fault hiding for discrete-time linear systems. In: **International Conference on Cyber Technology in Automation, Control, and Intelligent Systems (CYBER)**. Shenyang, China: IEEE, 2015. p. 1368–1373. ISBN 978-1-4799-8728-3. Pages 51 and 66.

[194] ROTONDO, Damiano; CRISTOFARO, Andrea; JOHANSEN, Tor. Fault tolerant control of uncertain dynamical systems using interval virtual actuators. **International Journal of Robust and Nonlinear Control**, v. 28, n. 2, p. 611–624, 2018. ISSN 1099-1239. Pages 51 and 66.

[195] KROKAVEC, Dušan; FILASOVÁ, Anna. Virtual Actuator Design for Uncertain Metzler Systems. **Frontiers in Control Engineering**, v. 2, n. November, p. 1–13, 2021. Pages 51 and 66.

[196] CIESLAK, J.; STEFANO, M. de; OTT, C.; REINER, M.; JAWORSKI, J.; PAPADOPOULOS, E.; VISENTIN, G.; ANKERSEN, F.; FERNANDEZ, J.G.; HENRY, D.; COLMENAREJO, P.; BRANCO, J.; SANTOS, N.; SERRA, P.; TELAAR, J.; STRAUCH, H.; GIORDANO, A.M. Assessment of a Supervisory Fault-Hiding Scheme in a Classical

Guidance, Navigation and Control Setup: the e.Deorbit mission. In: **4th Conference on Control and Fault Tolerant Systems (SysTol)**. Casablanca, Morocco: IEEE, 2019. p. 7–12. ISBN 978-1-7281-0380-8. Pages 52 and 66.

[197] GAO, Zhiqiang; ANTSAKLIS, Panos J. Stability of the pseudo-inverse method for reconfigurable control systems. **International Journal of Control**, Taylor & Francis, v. 53, n. 3, p. 717–729, 1991. Page 52.

[198] HANENE, Chalandi; YOSRA, Hammi; MOUFIDA, Ksouri. Fault Tolerant Control with Hammerstein virtual actuator "DC motor example". In: **15th International Conference on Sciences and Techniques of Automatic Control and Computer Engineering (STA)**. Hammamet, Tunisia: IEEE, 2014. p. 32–37. ISBN 978-1-4799-5907-5. Pages 57 and 66.

[199] PERODOU, Arthur; COMBASTEL, Christophe; ZOLGHADRI, Ali. Towards Anomaly-Tolerant Systems by Dissipation Block Synthesis. In: **5th International Conference on Control and Fault-Tolerant Systems (SysTol)**. Saint-Raphael, France: IEEE, 2021. v. 2021-Septe, p. 19–24. ISBN 978-1-6654-3159-0. ISSN 21621209. Pages 58, 64, and 66.

[200] XIA, Meng; RAHNAMA, Arash; WANG, Shige; ANTSAKLIS, Panos J. Control design using passivation for stability and performance. **IEEE Transactions on Automatic Control**, v. 63, n. 9, p. 2987–2993, Sept 2018. ISSN 0018-9286. Pages 14, 59, 127, 146, 147, 149, 151, 152, 154, 155, 165, 166, 167, and 168.

[201] ZAKERI, Hasan; ANTSAKLIS, Panos J. A data-driven adaptive controller reconfiguration for fault mitigation: A passivity approach. In: **27th Mediterranean Conference on Control and Automation**. Akko, Israel: IEEE, 2019. p. 25–30. ISSN 2473-3504. Pages 59, 153, 154, 167, and 174.

[202] WITTMANN, Th; RICHTER, Jan H.; MOOR, T. Fault-hiding control reconguration for a class of discrete event systems. **IFAC Proceedings Volumes (IFAC-PapersOnline)**, v. 46, n. 22 PART 1, p. 49–54, 2013. ISSN 14746670. Page 59.

[203] VEY, Daniel; LUNZE, Jan. Towards a reduced virtual actuator: A graph-theoretic approach. **European Control Conference (ECC)**, IEEE, p. 1915–1921, jun 2016. Pages 60 and 66.

[204] WANG, Ye; ROTONDO, Damiano; PUIG, Vicenç; CEMBRANO, Gabriela. Fault-Tolerant Control Based on Virtual Actuator and Sensor for Discrete-Time Descriptor Systems. **IEEE Transactions on Circuits and Systems I: Regular Papers**, IEEE, v. 67, n. 12, p. 5316–5325, dec 2020. ISSN 15580806. Pages 60 and 66.

[205] LI, Mingyang; XIE, Wenbo; ZHANG, Jian. Anti-windup reconfigurable control for dynamic positioning vessel with thruster faults. **Transactions of the Institute of Measurement and Control**, SAGE Publications Ltd, v. 42, n. 16, p. 3216–3224, dec 2020. ISSN 01423312. Pages 60 and 66.

[206] LIU, He; LI, Xiao-Jian. Novel geometric and adaptive approaches to fault-tolerant control for linear systems. In: **40th Chinese Control Conference (CCC)**. Shangai, China: IEEE, 2021. v. 2021-July, p. 4597–4602. ISBN 978-9-8815-6380-4. ISSN 21612927. Pages 60 and 66.

[207] THEILLIOL, Didier; PONSART, Jean-Christophe; MAHFOUF, Mahdi; SAUTER, Dominique. Active Fault Tolerant Control design for an experimental hot rolling mill - A case study. **IFAC Proceedings Volumes**, IFAC, v. 40, n. 11, p. 113–118, 2007. ISSN 14746670. Pages 63 and 66.

[208] PONSART, Jean-Christophe; THEILLIOL, Didier. Sensor Fault Tolerant Control design applied to a winding machine. **IFAC Proceedings Volumes**, IFAC, v. 40, n. 11, p. 311–318, 2007. ISSN 14746670. Pages 63 and 66.

[209] MORADI AMANI, A.; AFSHAR, A.; MENHAJ, M. B. Reconfiguration-Based Fault Tolerant Control of Dynamical Systems: A Control Reallocation Approach. **IEICE Transactions on Information and Systems**, Institute of Electronics, Information and Communication, Engineers, IEICE, E95.D, n. 4, p. 1074–1083, 2012. ISSN 0916-8532. Pages 63 and 66.

[210] MORADI AMANI, Ali; GAEINI, Nozhatalzaman; AFSHAR, Ahamad; MENHAJ, Mohamad Bagher. A New Approach to Reconfigurable Load Frequency Control of Power Systems in Emergency Conditions. **IFAC Proceedings Volumes**, IFAC, v. 46, n. 13, p. 526–531, 2013. ISSN 14746670. Pages 63, 66, and 177.

[211] HASHEMI, Seyed Mohammad; MENHAJ, Mohammad Bagher; MORADI AMANI, Ali. Reconfigurable Fault-Tolerant control by linear quadratic virtual actuator under control signal constraint. **Journal of Engineering and Applied Sciences**, v. 11, n. 3, p. 1998–2004, 2016. ISSN 1819-6608. Pages 63, 66, and 176.

[212] ROTONDO, Damiano; SÁNCHEZ, Helem Sabina; PUIG, Vicenç; ESCOBET, Teresa; QUEVEDO, Joseba. A virtual actuator approach for the secure control of networked LPV systems under pulse-width modulated DoS attacks. **Neurocomputing**, v. 365, p. 21 – 30, 2019. ISSN 0925-2312. Pages 65 and 176.

[213] TRAPIELLO, Carlos; PUIG, Vicenç. Set-based replay attack detection in closed-loop systems using a plug play watermarking approach. In: **Conference on Control and Fault-Tolerant Systems (SysTol)**. Casablanca, Morocco: IEEE, 2019. p. 330–335. ISBN 9781728103808. ISSN 21621209. Pages 65 and 176.

[214] BESSA, Iury; TRAPIELLO, Carlos; PUIG, Vicenç; PALHARES, Reinaldo Mart'ınez. Dual-Rate Control Framework With Safe Watermarking Against Deception Attacks. **IEEE Transactions on Systems, Man, and Cybernetics: Systems**, p. 1–13, 2022. To appear. Pages 65, 170, 171, and 176.

[215] FARIAS, Arllem O.; QUEIROZ, Gabriel Alisson C.; BESSA, Iury; MEDEIROS, Renan Landau P.; CORDEIRO, Lucas C.; PALHARES, Reinaldo Martínez. Sim3Tanks: A Benchmark Model Simulator for Process Control and Monitoring. **IEEE Access**, IEEE, v. 6, p. 62234–62254, 2018. Page 66.

[216] VEY, Daniel; LUNZE, Jan. Experimental evaluation of an active fault-tolerant control scheme for multirotor UAVs. **Conference on Control and Fault-Tolerant Systems (SysTol)**, IEEE, v. 2016-Novem, p. 125–132, sep 2016. ISSN 21621209. Page 66.

[217] KHAKI, Behnam; KILIC, Heybet; YILMAZ, Musa; SHAFIE-KHAH, Miadreza; LOTFI, Mohamed; CATALAO, Joao P.S. Active Fault Tolerant Control of Grid-Connected DER: Diagnosis and Reconfiguration. In: **45th Annual Conference of the IEEE Industrial Electronics Society (IECON)**. Lisbon, Portugal: IEEE, 2019. v. 2019-Octob, p. 4127–4132. ISBN 978-1-7281-4878-6. Page 66.

[218] KAZEMI, Ali; MENHAJ, Mohammad B.; KARRAI, Mehdi; DANESHNIA, Arash. Control reconfiguration of a boiler-Turbine unit after actuator faults. **4th International Conference on Control, Instrumentation, and Automation, (ICCIA)**, IEEE, n. January, p. 439–444, jan 2016. Page 66.

[219] FILASOVÁ, Anna; SERBÁK, Vladimír; GONTKOVIC, Daniel. Analysis of Reconfigured Control Loop with a Virtual Actuator. **Advances in Electrical and Electronic Engineering**, v. 9, n. 2, p. 1248–1254, jul 2011. ISSN 1804-3119. Page 66.

[220] KROKAVEC, Dušan; FILASOVÁ, Anna; SERBÁK, Vladim'ır. FTC with dynamic virtual actuators: Characterization via dynamic output controllers and H–∞ approach. **Mathematical Problems in Engineering**, v. 2015, p. 1–16, 2015. ISSN 1024-123X. Page 66.

[221] NAIR, D. V.; MURTY, M. S.R. Fault tolerant-based virtual actuator design for wide-area damping control in power system. **Electrical Engineering**, Springer Science and Business Media Deutschland GmbH, v. 103, n. 1, p. 463–477, feb 2021. ISSN 14320487. Page 66.

[222] RASHID, Sara Mahmoudi; SHISHAVAN, Hamed Kharrati; GHIASI, Amir Rikhtehgar. A Fault-Tolerant Control Strategy using Virtual Actuator Approach for Flexible

Robot Links with Hysteresis. In: **7th International Conference on Control, Instrumentation and Automation**. Tabriz, Iran: IEEE, 2021. ISBN 9780738124056. Page 66.

[223] CHO, Seongpil; GAO, Zhen; MOAN, Torgeir. Model-based fault detection, fault isolation and fault-tolerant control of a blade pitch system in floating wind turbines. **Renewable Energy**, Elsevier Ltd, v. 120, p. 306–321, may 2018. ISSN 09601481. Page 66.

[224] HAMEED, Ibrahim; EL-MADBOULY, Esam I; ABDO, Mohamed I. Sensor and Actuator Fault-Hiding Reconfigurable Control Design for a Four-Tank System Benchmark. **International Journal of Innovative Computing, Information and Control**, v. 11, n. 2, p. 679–690, 2015. Page 66.

[225] FILASOVÁ, Anna; KROKAVEC, Dušan; SERBÁK, Vladimír. On virtual observers in fault tolerant control. **20th International Conference on Process Control**, IEEE, v. 2015-July, n. 4, p. 266–271, jun 2015. Page 66.

[226] BESSA, Iury; PALHARES, Reinaldo. Novas condições para recuperação de estabilidade com atuadores virtuais estáticos. In: **Anais do 14º Simpósio Brasileiro de Automação Inteligente**. Ouro Preto, MG, Brazil: Galoa, 2019. Pages 66, 67, 170, and 175.

[227] COSTA, Thiago V.; FILETI, Ana M. Frattini; SILVA, Flávio V.; OLIVEIRA-LOPES, Luís Cláudio. Control reconfiguration of chemical processes subjected to actuator faults: A moving horizon approach. In: **IASTED International Conference Intelligent Systems and Control (ISC)**. Marina del Rey, CA: ACTAPRESS, 2013. Pages 66 and 176.

[228] NAZARI, Raheleh; SERON, Maria; DE DONÁ, José. Actuator fault tolerant control of systems with polytopic uncertainties using set-based diagnosis and virtual-actuator-based reconfiguration. **Automatica**, v. 75, p. 182–190, 2017. ISSN 0005-1098. Page 66.

[229] MA, Yan-Hua; DU, Xian; GOU, Lin-Feng; WEN, Si-Xin. Active fault tolerant control of turbofan engines with actuator faults under disturbances. **International Journal of Turbo & Jet-Engines**, De Gruyter Open Ltd, nov 2020. ISSN 2191-0332. Page 66.

[230] HMIDI, Riadh; BRAHIM, Ali Ben; HMIDA, Faycal Ben; SELLAMI, Anis. Diagnosis for lipschitz nonlinear system with sliding mode observer and virtual sensor. **International Conference on Sciences and Techniques of Automatic Control and Computer Engineering (STA)**, IEEE, p. 1–6, mar 2019. Page 66.

[231] PEIXOTO, Márcia L. C.; COUTINHO, Pedro H. S.; BESSA, Iury; PALHARES, Reinaldo Martínez. Static output-feedback stabilization of discrete-time linear parameter-varying systems under actuator saturation. **International Journal of Robust and Nonlinear Control**, Wiley, 2022. Early Access. Pages 71, 171, and 175.

[232] PALMA, Jonathan M.; MORAIS, Cecília F.; OLIVEIRA, Ricardo C. L. F. Linear matrix inequality-based solution for memory static output-feedback control of discrete-time linear systems affected by time-varying parameters. **International Journal of Robust and Nonlinear Control**, v. 31, n. 9, p. 4324–4336, 2021. ISSN 1049-8923. Page 71.

[233] DONG, Jiuxiang; YANG, Guang-Hong. Robust static output feedback control for linear discrete-time systems with time-varying uncertainties. **Systems & Control Letters**, Elsevier BV, v. 57, n. 2, p. 123–131, fev. 2008. Page 71.

[234] PEIXOTO, M. L. C.; COUTINHO, P. H. S.; PALHARES, R. M. Improved robust gain-scheduling static output-feedback control for discrete-time LPV systems. **European Journal of Control**, v. 58, p. 11–16, 2021. ISSN 09473580. Page 71.

[235] LÖFBERG, Johan. YALMIP : A Toolbox for Modeling and Optimization in MATLAB. In: **CACSD Conference**. Taipei, Taiwan: IEEE, 2004. Pages 75 and 83.

[236] ANDERSEN, Erling D.; ANDERSEN, Knud D. The mosek interior point optimizer for linear programming: An implementation of the homogeneous algorithm. In: **Applied Optimization**. New York, NY, USA: Springer US, 2000. p. 197–232. Pages 75 and 83.

[237] FAN, J. H.; ZHANG, Y. M.; ZHENG, Z. Q. Robust fault-tolerant control against time-varying actuator faults and saturation. **IET Control Theory & Applications**, v. 6, n. 14, p. 2198–2208, September 2012. ISSN 1751-8644. Page 79.

[238] TARBOURIECH, Sophie; GARCIA, Germain; JR, João Manoel Gomes da Silva; QUEINNEC, Isabelle. **Stability and stabilization of linear systems with saturating actuators**. London: Springer Science & Business Media, 2011. Page 79.

[239] DONG, Jiuxiang; WANG, Youyi; YANG, Guang-Hong. Control synthesis of continuous-time T-S fuzzy systems with local nonlinear models. **IEEE Transactions on Systems, Man, and Cybernetics, Part B (Cybernetics)**, v. 39, n. 5, p. 1245–1258, Oct 2009. ISSN 1083-4419. Page 89.

[240] SADEGHI, Mokhtar Sha; VAFAMAND, Navid; KHOOBAN, Mohammad Hassan. LMI-based stability analysis and robust controller design for a class of nonlinear chaotic power systems. **Journal of the Franklin Institute**, v. 353, n. 13, p. 2835 – 2858, 2016. ISSN 0016-0032. Page 104.

[241] BAO, Jie; LEE, Peter L. **Process Control: The Passive Systems Approach**. London: Springer, 2007. (Advances in Industrial Control). ISBN 9781846288937. Pages 127, 129, 136, and 137.

[242] MCCOURT, Michael J.; ANTSAKLIS, Panos J. Control design for switched systems using passivity indices. In: **American Control Conference**. Baltimore, MD, USA: IEEE, 2010. p. 2499–2504. ISSN 2378-5861. Pages 127 and 146.

[243] XIA, Meng; ANTSAKLIS, Panos J.; GUPTA, Vijay; ZHU, Feng. Passivity and dissipativity analysis of a system and its approximation. **IEEE Transactions on Automatic Control**, v. 62, n. 2, p. 620–635, Feb 2017. ISSN 0018-9286. Pages 127 and 146.

[244] ZHU, Feng; XIA, Meng; ANTSAKLIS, Panos J. On passivity analysis and passivation of event-triggered feedback systems using passivity indices. **IEEE Transactions on Automatic Control**, v. 62, n. 3, p. 1397–1402, March 2017. ISSN 0018-9286. Pages 127 and 146.

[245] WU, Ligang; ZHENGA, Wei Xing; GAO, Huijun. Dissipativity-based sliding mode control of switched stochastic systems. **IEEE Transactions on Automatic Control**, v. 58, n. 3, p. 785–791, March 2013. ISSN 0018-9286. Page 127.

[246] LI, Mengmou; SU, Lanlan; CHESI, Graziano. Consensus of heterogeneous multi-agent systems with diffusive couplings via passivity indices. **IEEE Control Systems Letters**, v. 3, n. 2, p. 434–439, April 2019. ISSN 2475-1456. Page 127.

[247] RAJPUROHIT, Tanmay; HADDAD, Wassim M. Dissipativity theory for nonlinear stochastic dynamical systems. **IEEE Transactions on Automatic Control**, v. 62, n. 4, p. 1684–1699, April 2017. ISSN 0018-9286. Page 127.

[248] HIRCHE, Sandra; MATIAKIS, Tilemachos; BUSS, Martin. A distributed controller approach for delay-independent stability of networked control systems. **Automatica**, v. 45, n. 8, p. 1828 – 1836, 2009. ISSN 0005-1098. Page 127.

[249] KHONG, Sei Zhen; VAN DER SCHAFT, Arjan. On the converse of the passivity and small-gain theorems for input—output maps. **Automatica**, v. 97, p. 58 – 63, 2018. ISSN 0005-1098. Page 127.

[250] MADEIRA, Diego de S.; ADAMY, Jurgen. Feedback control of nonlinear systems using passivity indices. In: **Conference on Control Applications**. Sydney, NSW, Australia: IEEE, 2015. p. 263–268. ISSN 1085-1992. Pages 127, 146, and 149.

[251] YANG, Hao; COCQUEMPOT, Vincent; JIANG, Bin. Fault tolerance analysis for switched systems via global passivity. **IEEE Transactions on Circuits and Systems II: Express Briefs**, v. 55, n. 12, p. 1279–1283, Dec 2008. ISSN 1549-7747. Page 127.

[252] LEI, Qingyang; WANG, Ruigang; BAO, Jie. Fault diagnosis based on dissipativity property. **Computers & Chemical Engineering**, v. 108, p. 360 – 371, 2018. ISSN 0098-1354. Page 127.

[253] HU, Q.; SHAO, X. Smooth finite-time fault-tolerant attitude tracking control for rigid spacecraft. **Aerospace Science and Technology**, v. 55, p. 144 – 157, 2016. ISSN 1270-9638. Page 127.

[254] SELVARAJ, Palanisamy; KAVIARASAN, Boomipalagan; SAKTHIVEL, Rathinasamy; KARIMI, Hamid Reza. Fault-tolerant SMC for Takagi-Sugeno fuzzy systems with time-varying delay and actuator saturation. **IET Control Theory & Applications**, v. 11, n. 8, p. 1112–1123, May 2017. ISSN 1751-8644. Page 127.

[255] SAKTHIVEL, Rathinasamy; KARIMI, Hamid Reza; JOBY, Maya; SANTRA, Srimanta. Resilient sampled-data control for markovian jump systems with an adaptive fault-tolerant mechanism. **IEEE Transactions on Circuits and Systems II: Express Briefs**, v. 64, n. 11, p. 1312–1316, Nov 2017. ISSN 1549-7747. Page 127.

[256] SAKTHIVEL, Rathinasamy; SARAVANAKUMAR, Thangavel; KAVIARASAN, Boomipalagan; LIM, Yongdo. Finite-time dissipative based fault-tolerant control of Takagi-–Sugeno fuzzy systems in a network environment. **Journal of the Franklin Institute**, v. 354, n. 8, p. 3430 – 3454, 2017. ISSN 0016-0032. Page 127.

[257] MADEIRA, Diego de S.; ADAMY, Jurgen. Static output feedback: An LMI condition for stabilizability based on passivity indices. In: **Conference on Control Applications**. Buenos Aires, Argentina: IEEE, 2016. Page 130.

[258] MCCOURT, Michael J.; ANTSAKLIS, Panos J. Stability of interconnected switched systems using QSR dissipativity with multiple supply rates. In: **American Control Conference**. Montreal, QC, Canada: IEEE, 2012. Page 130.

[259] ORTEGA, Romeo; VAN DER SCHAFT, Arjan; MASCHKE, Bernhard; ESCOBAR, Gerardo. Interconnection and damping assignment passivity-based control of port-controlled hamiltonian systems. **Automatica**, Elsevier BV, v. 38, n. 4, p. 585–596, abr. 2002. Page 133.

[260] ORTEGA, R.; VAN DER SCHAFT, A.J.; MAREELS, I.; MASCHKE, B. Putting energy back in control. **IEEE Control Systems Magazine**, v. 21, n. 2, p. 18–33, 2001. Page 133.

[261] ARGHA, A.; SU, S. W.; CELLER, B. G. Control allocation-based fault tolerant control. **Automatica**, v. 103, p. 408 – 417, 2019. ISSN 0005-1098. Page 153.

[262] ROMER, Anne; MONTENBRUCK, Jan Maximilian; ALLGÖWER, Frank. Some ideas on sampling strategies for data-driven inference of passivity properties for MIMO systems. In: **American Control Conference**. Milwaukee, WI, USA: IEEE, 2018. p. 6094–6100. ISSN 2378-5861. Pages 153, 154, and 174.

[263] TANEMURA, Masaya; AZUMA, Shun ichi. Efficient data-driven estimation of passivity properties. **IEEE Control Systems Letters**, v. 3, n. 2, p. 398–403, April 2019. ISSN 2475-1456. Pages 153, 154, and 174.

[264] ROMER, Anne; MONTENBRUCK, Jan Maximilian; KÖHLER, Johannes; ALLGÖWER, Frank. One-shot verification of dissipativity properties from input–output data. **IEEE Control Systems Letters**, v. 3, n. 3, p. 709–714, July 2019. Pages 153, 154, and 174.

[265] ZAKERI, Hasan; ANTSAKLIS, Panos J. Passivity and passivity indices of nonlinear systems under operational limitations using approximations. **International Journal of Control**, Informa UK Limited, v. 94, n. 4, p. 1114–1124, jul. 2021. Page 154.

[266] BERBERICH, Julian; KÖHLER, Johannes; ALLGÖWER, Frank; MÜLLER, Matthias A. Dissipativity properties in constrained optimal control: A computational approach. **Automatica**, v. 114, p. 108840, 2020. Page 154.

[267] WU, Jian; CHEN, Weisheng; LI, Jing. Global finite-time adaptive stabilization for nonlinear systems with multiple unknown control directions. **Automatica**, Elsevier BV, v. 69, p. 298–307, jul. 2016. Page 163.

[268] UTKIN, V. Variable structure systems with sliding modes. **IEEE Transactions on Automatic Control**, IEEE, v. 22, n. 2, p. 212–222, abr. 1977. Page 163.

[269] BESSA, Iury; PUIG, Vicenç; PALHARES, Reinaldo Martínez. Passivation-based control reconfiguration with virtual actuators. In: **11th IFAC Symposium on Fault Detection, Supervision and Safety for Technical Processes - SAFEPROCESS**. Pafos, Chipre: Elsevier BV, 2022. To appear. Pages 170, 174, and 175.

[270] BESSA, Iury; COUTINHO, Pedro H. S.; BESSA, Isaías V.; MENDEIROS, Renan L. P.; PALHARES, Reinaldo Martínez. Estabilizadores virtuais para conversores CC-CC com cargas de potência constante. Page 171.

[271] CORDOVIL JÚNIOR, Luiz Alberto Queiroz; COUTINHO, Pedro Henrique; BESSA, Iury; CAMARGOS, Murilo Osorio; PALHARES, Reinaldo Martínez. Análise de compromisso entre granularidade e interpretabilidade em sistemas granulares evolutivos. In: **Anais do 14º Simpósio Brasileiro de Automação Inteligente**. Ouro Preto, MG, Brazil: Galoa, 2019. Pages 171 and 174.

[272] CAMARGOS, Murilo Osorio; BESSA, Iury; D'ANGELO, Marcos Flávio Silveira Vasconcelos; PALHARES, Reinaldo Martinez. Fault prognostics of rolling bearings using a hybrid approach. **IFAC-PapersOnLine**, Elsevier BV, Berlin, v. 53, n. 2, p. 4082–4087, 2020. 21st IFAC World Congress. Pages 171 and 174.

[273] CAMARGOS, Murilo Osorio; BESSA, Iury; D'ANGELO, Marcos Flávio Silveira Vasconcelos; COSME, Luciana Balieiro; PALHARES, Reinaldo Martínez. Data-driven prognostics of rolling element bearings using a novel error based evolving takagi–sugeno fuzzy model. **Applied Soft Computing**, Elsevier BV, v. 96, p. 106628, nov. 2020. Pages 171 and 174.

[274] CAMARGOS, Murilo; BESSA, Iury; CORDOVIL JÚNIOR, Luiz A. Q.; COUTINHO, Pedro; LEITE, Daniel Furtado; PALHARES, Reinaldo Martínez. Evolving fuzzy system applied to battery charge capacity prediction for fault prognostics. In: **Atlantis Studies in Uncertainty Modelling**. Bratislava, Slovakia: Atlantis Press, 2021. Pages 171 and 174.

[275] BOUTROUS, Khoury; BESSA, Iury; PUIG, Vicenç; NEJJARI, Fatiha; PALHARES, Reinaldo Martínez. Data-driven prognostics based on evolving fuzzy degradation models for power semiconductor devices. In: **7th European Conference of the PHM Society**. Turin, Italy: PHM Society, 2022. To appear. Pages 171 and 174.

[276] PEIXOTO, Márcia L. C.; PESSIM, Paulo S. P.; COUTINHO, Pedro H. S.; BESSA, Iury; PALHARES, Reinaldo Martínez. Controle em rede com acionamento por eventos para sistemas sujeitos a ataques cibernéticos. Page 171.

[277] COUTINHO, Pedro H. S.; BESSA, Iury; PEIXOTO, Márcia L. C.; PESSIM, Paulo S. P.; PIRES, Pedro O. F.; PALHARES, Reinaldo Martínez. Controle com acionamento por eventos resiliente a ataques de negação de serviço. Page 171.

[278] PEIXOTO, Márcia L. C.; PESSIM, Paulo S. P.; COUTINHO, Pedro H. S.; BESSA, Iury; PALHARES, Reinaldo Martínez. Local event-triggered control of takagi-sugeno fuzzy systems under deception attacks. Page 171.

[279] ALCALÁ, Eugenio; BESSA, Iury; PUIG, Vicenç; SENAME, Olivier; PALHARES, Reinaldo Martínez. Mpc using an on-line ts fuzzy learning approach with application to autonomous driving. Page 171.

[280] CORDOVIL, Luiz A. Q.; COUTINHO, Pedro H. S.; BESSA, Iury; PEIXOTO, Márcia L. C.; PALHARES, Reinaldo Martínez. Learning event-triggered control based on evolving data-driven fuzzy granular models. **International Journal of Robust and Nonlinear Control**, Wiley, v. 32, n. 5, p. 2805–2827, jan. 2022. Pages 171 and 174.

[281] CORDOVIL, Luiz Alberto Queiroz; COUTINHO, Pedro Henrique Silva; BESSA, Iury; D'ÂNGELO, Marcos Flávio Silveira Vasconcelos; PALHARES, Reinaldo Martínez. Uncertain data modeling based on evolving ellipsoidal fuzzy information granules. **IEEE Transactions on Fuzzy Systems**, IEEE, v. 28, n. 10, p. 2427–2436, out. 2020. Pages 171 and 174.

[282] LEITE, Daniel; COUTINHO, Pedro; BESSA, Iury; CAMARGOS, Murilo; CORDOVIL JÚNIOR., Luiz A. Q.; PALHARES, Reinaldo. Incremental learning and state-space evolving fuzzy control of nonlinear time-varying systems with unknown model. In: **Atlantis Studies in Uncertainty Modelling**. Bratislava, Slovakia: Atlantis Press, 2021. Pages 171 and 174.

[283] COUTINHO, Pedro H.S.; PEIXOTO, Márcia L.C.; BESSA, Iury; PALHARES, Reinaldo Martínez. Dynamic event-triggered gain-scheduling control of discrete-time quasi-LPV systems. **Automatica**, Elsevier BV, v. 141, p. 110292, jul. 2022. Pages 171 and 177.

[284] COUTINHO, Pedro H. S.; BESSA, Iury; XIE, Wen-Bo; NGUYEN, Ahn-Tu; PALHARES, Reinaldo Martínez. A sufficient condition to design unknown input observers for nonlinear systems with arbitrary relative degree. Page 171.

[285] PESSIM, Paulo S. P.; COUTINHO, Pedro H. S.; BESSA, Iury; PEIXOTO, Márcia L. C.; LACERDA, Marcio; PALHARES, Reinaldo Martínez. Controle distribu'ıdo para sistemas não lineares interconectados sujeitos a retardos variantes no tempo nas interconexões. Page 171.

[286] MASTI, Daniele; BERNARDINI, Daniele; BEMPORAD, Alberto. A machine-learning approach to synthesize virtual sensors for parameter-varying systems. **European Journal of Control**, Elsevier Ltd, v. 61, p. 40–49, sep 2021. ISSN 09473580. Page 174.

[287] HOSSEINPOOR, Zahra; AREFI, Mohammad Mehdi; RAZAVI-FAR, Roozbeh; MOZAFARI, Niloofar; HAZBAVI, Saeede. Virtual Sensors for Fault Diagnosis: A Case of Induction Motor Broken Rotor Bar. **IEEE Sensors Journal**, v. 21, n. 4, p. 5044–5051, feb 2021. ISSN 1530-437X. Page 174.

[288] DESTRO, Francesco; FACCO, Pierantonio; García Muñoz, Salvador; BEZZO, Fabrizio; BAROLO, Massimiliano. A hybrid framework for process monitoring: Enhancing data-driven methodologies with state and parameter estimation. **Journal of Process Control**, Elsevier Ltd., v. 92, p. 333–351, aug 2020. ISSN 09591524. Page 174.

[289] YAN, Haodong; WANG, Jun; CHEN, Jinglong; LIU, Zijun; FENG, Yong. Virtual sensor-based imputed graph attention network for anomaly detection of equipment with

incomplete data. **Journal of Manufacturing Systems**, Elsevier Ltd, v. 63, n. March, p. 52–63, apr 2022. ISSN 02786125. Page 174.

[290] DARVISHI, Hossein; CIUONZO, Domenico; EIDE, Eivind Rosón; ROSSI, Pierluigi Salvo. Sensor-Fault Detection, Isolation and Accommodation for Digital Twins via Modular Data-Driven Architecture. **IEEE Sensors Journal**, IEEE, v. 21, n. 4, p. 4827–4838, feb 2021. ISSN 15581748. Page 174.

[291] KOCH, Anne. **Determining input-output properties of linear time-invariant systems from data**. Berlin: Logos Verlag, 2022. ISBN 9783832554460. Page 174.

[292] KOCH, Anne; BERBERICH, Julian; KÖHLER, Johannes; ALLGÖWER, Frank. Determining optimal input–output properties: A data-driven approach. **Automatica**, Elsevier BV, v. 134, p. 109906, dez. 2021. Page 174.

[293] MAYNE, David Q.; RAWLINGS, James B.; RAO, Christopher V.; SCOKAERT, Pierre O.M. Constrained model predictive control: Stability and optimality. **Automatica**, v. 36, n. 6, p. 789–814, 2000. ISSN 00051098. Page 176.

[294] MADICHETTY, Sreedhar; PATRA, Sandipan; BASU, Malabika. Hardware-Based Intrusion Detection in E-LAN based Distributed DC Microgrid: A Virtual Sensor Approach. In: **9th Renewable Power Generation Conference (RPG)**. Online Conference: Institution of Engineering and Technology, 2021. v. 2021, n. CP783, p. 210–215. ISBN 978-1-83953-504-8. Page 176.

[295] KUMAR, Sujeet; KAR, I.N. Virtual network based resilient control of linear multi-agent systems. **IFAC-PapersOnLine**, Elsevier Ltd, v. 53, n. 1, p. 488–493, 2020. ISSN 24058963. Page 176.

[296] HUSSAIN, Mosaddique Nawaz; MISHRA, Rahul; AGARWAL, Vivek. A frequency-dependent virtual impedance for voltage-regulating converters feeding constant power loads in a DC microgrid. **IEEE Transactions on Industry Applications**, IEEE, v. 54, p. 5630–5639, 11 2018. ISSN 00939994. Page 177.

[297] LU, Xiaonan; SUN, Kai; GUERRERO, Josep M.; VASQUEZ, Juan C.; HUANG, Lipei; WANG, Jianhui. Stability enhancement based on virtual impedance for DC microgrids with constant power loads. **IEEE Transactions on Smart Grid**, IEEE, v. 6, p. 2770–2783, 11 2015. ISSN 19493053. Page 177.

[298] LIU, Sheng; SU, Peng; ZHANG, Lanyong. A virtual negative inductor stabilizing strategy for DC microgrid with constant power loads. **IEEE Access**, IEEE, v. 6, p. 59728–59741, 2018. ISSN 21693536. Page 177.

[299] LIU, Sheng; SU, Peng; ZHANG, Lanyong. A nonlinear disturbance observer based virtual negative inductor stabilizing strategy for DC microgrid with constant power loads. **Energies**, MDPI AG, v. 11, 11 2018. ISSN 19961073. Page 177.

[300] LI, Chang; YANG, Yaqian; DRAGICEVIC, Tomislav; BLAABJERG, Frede. A New Perspective for Relating Virtual Inertia With Wideband Oscillation of Voltage in Low-Inertia DC Microgrid. **IEEE Transactions on Industrial Electronics**, IEEE, v. 69, p. 7029–7039, 7 2022. ISSN 0278-0046. Page 177.

[301] KERDPHOL, Thongchart; RAHMAN, Fathin Saifur; WATANABE, Masayuki; MITANI, Yasunori. Robust virtual inertia control of a low inertia microgrid considering frequency measurement effects. **IEEE Access**, v. 7, p. 57550–57560, 2019. Page 177.

[302] ZAKERI, Hasan; ANTSAKLIS, Panos J. Passivity measures in cyberphysical systems design: An overview of recent results and applications. **IEEE Control Systems**, IEEE, v. 42, n. 2, p. 118–130, abr. 2022. Page 178.

[303] RAHNAMA, Arash; XIA, Meng; ANTSAKLIS, Panos J. Passivity-Based Design for Event-Triggered Networked Control Systems. **IEEE Transactions on Automatic Control**, IEEE, v. 63, n. 9, p. 2755–2770, sep 2018. ISSN 0018-9286. Page 178.